AD_____

Award Number: W81XWH-07-1-0181

TITLE: Modulation of Stem Cell Differentiation and Myostatin as an Approach to Counteract Fibrosis in Muscle Dystrophy and Regeneration After Injury

PRINCIPAL INVESTIGATOR: Nestor F. Gonzalez-Cadavid, Ph.D.

CONTRACTING ORGANIZATION: Charles R. Drew University of Medicine and Science
Los Angeles, CA 90059

REPORT DATE: March 2012

TYPE OF REPORT: Addendum to Final

PREPARED FOR: U.S. Army Medical Research and Materiel Command
Fort Detrick, Maryland 21702-5012

REPORT DOCUMENTATION PAGE

Form Approved
OMB No. 0704-0188

1. REPORT DATE	2. REPORT TYPE	3. DATES COVERED
March 2012	Addendum to Final	1 March 2011 - 29 February 2012

4. TITLE AND SUBTITLE Modulation of Stem Cells Differentiation and Myostatin as an approach to Counteract fibrosis in Muscle Dystrophy and Regeration after Injury

5a. CONTRACT NUMBER

5b. GRANT NUMBER
W81XWH-07-1-0181

5c. PROGRAM ELEMENT NUMBER

6. AUTHOR(S)
Nestor F. Gonzalez-Cadavid, Ph.D.

E-Mail: ncadavid@ucla.edu

5d. PROJECT NUMBER

5e. TASK NUMBER

5f. WORK UNIT NUMBER

7. PERFORMING ORGANIZATION NAME(S) AND ADDRESS(ES)
Charles R. Drew University of Medicine and Science
Los Angeles, CA 90059

8. PERFORMING ORGANIZATION REPORT NUMBER

9. SPONSORING / MONITORING AGENCY NAME(S) AND ADDRESS(ES)
U.S. Army Medical Research and Materiel Command
Fort Detrick, Maryland 21702-5012

10. SPONSOR/MONITOR'S ACRONYM(S)

11. SPONSOR/MONITOR'S REPORT NUMBER(S)

12. DISTRIBUTION / AVAILABILITY STATEMENT
Approved for Public Release; Distribution Unlimited

13. SUPPLEMENTARY NOTES

14. ABSTRACT We have investigated in the notexin-injured skeletal muscle of the aged mdx mouse a novel therapeutic approach for Duchenne's muscular dystrophy **(DMD)** based on the implantation of muscle-derived stem cells **(MDSC),** and the putative stimulation of their repair capacity by inhibition of myostatin **(Mst)** expression and/or activity, for the alleviation of fibrotic and fatty degeneration of the notexin-injured dystrophic muscle. MDSC from the wild type mouse **(WT MDSC),** the myostatin knock-out mouse **(Mst KO MDSC),** and the mdx mouse **(mdx MDSC)** were compared. Concurrent pharmacological interventions were also tested with WT MDSC on skeletal muscle, and other tissues. We showed the repair capacity of MDSC to counteract fibrosis and the resulting dysfunction in several non-skeletal muscle tissues in other rat and mouse models, the pro-fibrotic effects of myostatin, and the antifibrotic effects of nitric oxide donors (molsidomine), PDE 5 inhibitors (sildenafil), and antioxidants (allopurinol), alone or in combination with WT MDSC. We found that WT MDSC are considerably myogenic in cell culture and stimulate muscle repair after injury in the aged mdx mouse, but that Mst KO MDSC are unable to form myotubes in vitro. However, their myogenic capacity is recovered in vivo under the influence of the myostatin+ host tissue environment, presumably by reactivation of key genes originally silenced in these cells. Our ongoing studies suggest that although myofibroblast generation may impair muscle tissue repair by WT MDSC, this may be counteracted with molsidomine, but not by antioxidants, and that the MDSC/molsidomine combination stimulates angiogenesis in the severely necrotic muscle of mice with limb ischemia.

15. SUBJECT TERMS
Myostatin, muscle dystrophy, stem cells, myogenesis, Oct-4; Duchenne; fibrosis

16. SECURITY CLASSIFICATION OF:			17. LIMITATION OF ABSTRACT	18. NUMBER OF PAGES	19a. NAME OF RESPONSIBLE PERSON
U					USAMRMC
a. REPORT	b. ABSTRACT	c. THIS PAGE			19b. TELEPHONE NUMBER *(include area code)*
U	U	U	UU	204	

Table of Contents

Page

INTRODUCTION

The **overall objective** of this grant is:

To investigate in the mdx mouse a novel therapeutic approach for Duchenne's muscular dystrophy **(DMD)** based on the inhibition of myostatin **(Mst)** expression and/or activity, for the alleviation of fibrotic and fatty degeneration of the skeletal muscle, that would also facilitate the differentiation of transplanted dystrophin+ **(D+)** muscle-derived stem cells **(MDSC)**, in order to ameliorate disease progression.

This will be achieved by: a) comparing the in vitro myogenic and fibrogenic/adipogenic potential of MDSC from D-/Mst+, D+/Mst+ or D+/Mst- mice; b) blocking myostatin expression by gene transfer of myostatin short hairpin RNA (Mst shRNA), or transplantation of D+ MDSC engineered with Mst shRNA, and measuring the myogenic/fibroadipogenic balance, dystrophin expression, and muscle function; and c) combining this with the inhibition of myostatin activity by follistatin. We named the D+/Mst+ cells as **WT MDSC**, the D+/Mst- cells as **Mst KO MDSC**, and the D-/Mst+ cells as **mdx MDSC**.

BODY

In order to comply with the grant objectives, three courses of action were planned that led to the respective complementary approaches. Approach 1 was to characterize in general the differentiation pattern and tissue repair ability of the implanted WT MDSC in different animal models, tissues, and conditions not directly related to skeletal muscle dystrophy, but having some common features with the cell loss and the key lipofibrotic degeneration occurring in the skeletal muscle in DMD and specifically in the mdx mouse, in order to gain information on their potential for muscle repair, particularly after injury. Approach 2 was to investigate in these settings the possible pharmacological modulation of implanted WT MDSC differentiation using agents known to act as antifibrotic and anti-oxidative stress, that at the same time were assumed to modulate stem cell differentiation in general. Approach 3, the most relevant, was to directly investigate the effects of trying to modulate MDSC differentiation by the genetic inactivation of myostatin both in vitro and on the repair of injured dystrophic skeletal muscle in the aged mdx mouse, and to stimulate these effects by simultaneous pharmacological treatment both in the mdx model and in the necrotic ischemic muscle in a diabetic mouse model.

In the description below we refer to, and cite, in parenthesis some of the papers or scientific communications listed under CUMULATIVE REPORTABLE OUTCOMES. Only some key abstracts are reproduced here for immediate consultation. The remaining abstracts can be obtained from the full papers included in the APPENDIX

Approach 1

Our first investigation of the WT MDSC tissue repair ability was conducted on the fibrotic process occurring during aging in the smooth muscle of the penile corpora cavernosa with some common features to the ones in the dystrophic skeletal muscle **(A-1),** and on a similar process in the injured vagina of the rat **(A-4).**

In synthesis: implantation of WT MDSC corrected or prevented the fibrotic degeneration and apoptotic cell loss in these tissues, and the functional consequences of this tissue damage.

A-1. Nolazco G, Kovanecz I, Vernet D, Gelfand RA, Tsao J, Ferrini MG, Magee T, Rajfer J, Gonzalez-Cadavid NF. Effect of muscle-derived stem cells on the restoration of corpora

cavernosa smooth muscle and erectile function in the aged rat. BJU Int. 2008 May;101(9):1156-64.

OBJECTIVE: To determine whether skeletal muscle-derived stem cells (MDSCs) convert into smooth muscle cells (SMCs) both in vitro and in vivo, and in so doing ameliorate the erectile dysfunction (ED) of aged rats, and whether endogenous stem cells are present in the rat corpora cavernosa.
MATERIALS AND METHODS: MDSCs were obtained from mouse muscle, and shown by immunocytochemistry for alpha-smooth muscle actin (alpha SMA) to originate in vitro in myofibroblasts and SMCs, discriminating SMCs by calponin 1 expression. In vivo these MDSCs, labelled with 4',6-diamidino-2-phenylindole, were implanted into the corpora cavernosa of young adult (5-month old) and aged (20-month old) rats for 2 and 4 weeks. Histological changes were assessed by immunohistochemistry and quantitative Western blot. Functional changes were determined by electrical field stimulation (EFS) of the cavernosal nerve.
RESULTS: The exogenous cells replicated and converted into SMCs, as shown in corporal tissue sections by confocal immunofluorescence microscopy for proliferating cell nuclear antigen (PCNA), alpha SMA, and smoothelin, and also by Western blot for alpha SMA and PCNA. MDSC differentiation was confirmed by the activation of the alpha SMA promoter-linked beta-galactosidase in transfected cells, both in vitro and after implantation in the corpora. Putative endogenous stem cells were shown in corporal tissue sections and Western blots by detecting CD34 and a possible Sca1 variant. EFS showed that implanted MDSCs raised in aged rats the maximal intracavernosal pressure/mean arterial pressure levels above (2
weeks) or up to (4 weeks) those of young adult rats.
CONCLUSIONS: MDSCs implanted into the corpora cavernosa of aged rats converted into SMCs and corrected ED, and endogenous cells expressing stem cell markers were also found in untreated tissue. This suggests that exogenous stem cell implantation and/or endogenous stem cell modulation might be viable therapeutic approaches for ageing-related ED.

A-4. Ho MH, Heydarkhan S, Vernet D, Kovanecz I, Ferrini MG, Bhatia NN, Gonzalez-Cadavid NF. Stimulating vaginal repair in rats through skeletal muscle-derived stem cells seeded on small intestinal submucosal scaffolds. Obstet Gynecol. 2009 Aug;114(2 Pt 1):300-9.

OBJECTIVES: Grafts are used for vaginal repair after prolapse, but their use to carry stem cells to regenerate vaginal tissue has not been reported. In this study, we investigated whether 1) muscle-derived stem cells (MDSC) grown on small intestinal submucosa (SIS) generate smooth-muscle cells (SMC) in vitro and upon implantation in a rat model of vaginal defects; 2) express markers applicable to the in-vivo detection of vaginal endogenous stem cells; and 3) stimulate the repair of the vagina.
METHODS: Mouse MDSC grown on monolayer, SIS, or polymeric mesh, were tested for cell differentiation by immunocytochemistry, Western blot and real-time polymerase chain reaction (PCR). Stem cell markers were screened by DNA microarrays followed by real-time PCR, immunocytochemistry, and Western blot. Rats that underwent hysterectomy and partial vaginectomy were left as such or implanted in the vagina with 4',6-Diamidino-2-Phenylindole (DAPI)-labeled MDSC on SIS, or SIS without MDSC, immunosuppressed, and killed at 2-8 weeks. Immunofluorescence, hematoxylin-eosin, and Masson trichrome were applied to tissue sections.
RESULTS: Muscle-derived stem cell cultures on monolayer and on scaffolds differentiate into SMC, as shown by alpha-smooth muscle actin (ASMA), calponin, and smoothelin markers. Muscle-derived stem cells express embryonic stem cell markers Oct-4 and nanog. Dual

DAPI/ASMA fluorescence indicated MDSC conversion to SMC. Muscle-derived stem cells/SIS stimulated vaginal tissue repair, including keratin-5 positive epithelium formation and prevented fibrosis at 4 and 8 weeks. Oct-4+ putative endogenous stem cells were identified.
CONCLUSION: Muscle-derived stem cells/SIS implants stimulate vaginal tissue repair in the rat, thus autologous MDSC on scaffolds may be a promising approach for the treatment of vaginal repair.

Approach 2

The second approach was based on studying the effects of myostatin, an inhibitor of skeletal muscle mass and putative pro-fibrotic agent, on the development of the in vitro fibrotic conversion of a stem cell line **(A2),** or alternatively in vivo on the severe fibrotic process occurring in the penile tunica albuginea of the rat subsequent to the injection of a member of the myostatin gene family, TGFβ1 **(A3, A5).** This was the basis for subsequently studying the effects of implanted Mst KO MDSC, where myostatin expression is inhibited genetically in these cells, in the dystrophic muscle of the mdx mouse (see third approach).

We also investigated the effects of molsidomine, a long-acting nitric oxide donor, or allopurinol, an inhibitor of xanthine oxidoreductase, on the corpora cavernosa smooth muscle fibrosis and oxidative stress in a mouse model where these processes are severely intensified **(A-6)** as the basis for using these interventions to modulate the WT MDSC in concurrent administrations. We had shown in previous publications that both nitiric oxide (mainly produced from iNOS) and its product cGMP (whose breakdown is protected by PDE5 inhibitors like sildenafil) are antifibrotic and quench reactive oxygen species **(ROS)** when given or are generated in a continuous long term administration. This led to testing the combination of sildenafil with MDSC to counteract corpora cavernosal fibrosis induced by neuropraxia in the rat (nerve damage, also occurring in muscle dystrophy) **(A-9)**, or in the severe fibrosis and apoptotic cardiomyocyte loss subsequent to myocardial infarction, also in a rat model **(A-7).**

In synthesis, these studies confirmed the antifibrotic, antioxidant, and tissue repair effects of WT MDSC, and supported the biological inhibition of myostatin in the MDSC by genetic inactivation, or the similar effects of concurrent molsidomine or antioxidants, although sildenafil supplementation still requires further studies..

A-2. Artaza JN, Singh R, Ferrini MG, Braga M, Tsao J, Gonzalez-Cadavid NF. Myostatin promotes a fibrotic phenotypic switch in multipotent C3H 10T1/2 cells without affecting their differentiation into myofibroblasts. J Endocrinol. 2008 Feb;196(2):235-49.

Tissue fibrosis, the excessive deposition of collagen/extracellular matrix combined with the reduction of the cell compartment, defines fibroproliferative diseases, a major cause of death and a public health burden. Key cellular processes in fibrosis include the generation of myofibroblasts from progenitor cells, and the activation or switch of already differentiated cells to a fibrotic synthetic phenotype. Myostatin, a negative regulator of skeletal muscle mass, is postulated to be involved in muscle fibrosis. We have examined whether myostatin affects the differentiation of a multipotent mesenchymal mouse cell line into myofibroblasts, and/or modulates the fibrotic phenotype and Smad expression of the cell population. In addition, we investigated the role of follistatin in this process. Incubation of cells with recombinant myostatin protein did not affect the proportion of myofibroblasts in the culture, but significantly upregulated the expression of fibrotic markers such as collagen and the key profibrotic factors transforming growth factor-beta1 (TGF-beta1) and plasminogen activator inhibitor (PAI-1), as well as Smad3 and 4, and the pSmad2/3. An antifibrotic process evidenced by the upregulation of follistatin, Smad7, and matrix metalloproteinase 8 accompanied these changes. Follistatin inhibited TGF-

beta1 induction by myostatin. Transfection with a cDNA expressing myostatin upregulated PAI-1, whereas an shRNA against myostatin blocked this effect. In conclusion, myostatin induced a fibrotic phenotype without significantly affecting differentiation into myofibroblasts. The concurrent endogenous antifibrotic reaction confirms the view that phenotypic switches in multipotent and differentiated cells may affect the progress or reversion of fibrosis, and that myostatin pharmacological inactivation may be a novel therapeutic target against fibrosis.

A-3. Cantini LP, Ferrini MG, Vernet D, Magee TR, Qian A, Gelfand RA, Rajfer J, Gonzalez-Cadavid NF Profibrotic role of myostatin in Peyronie's disease. J Sex Med. 2008 Jul;5(7):1607-22.

INTRODUCTION: The primary histologic finding in many urologic disorders, including Peyronie's disease (PD), is fibrosis, mainly mediated by the transforming growth factor beta1 (TGFbeta1).
AIM: To determine whether another member of the TGFbeta family, myostatin, (i) is expressed in the human PD plaque and normal tunica albuginea (TA), their cell cultures, and the TGFbeta1-induced PD lesion in the rat model; (ii) is responsible for myofibroblast generation, collagen deposition, and plaque formation; and (iii) mediates the profibrotic effects of TGFbeta1 in PD.
METHODS: Human TA and PD tissue sections, and cell cultures from both tissues incubated with myostatin and TGFbeta1 were subjected to immunocytochemistry for myostatin and alpha-smooth muscle actin (ASMA). The cells were assayed by western blot, Real time-Polymerase chain reaction (RT-PCR), and ribonuclease protection. Myostatin cDNA and shRNA were injected, with or without TGFbeta1, in the rat penile TA, and plaque size was estimated by Masson.
MAIN OUTCOME MEASURES: Myostatin expression in the human TA, the PD plaque, and their cell cultures, and myostatin effects on the PD-like plaque in the rat.
RESULTS: A threefold overexpression of myostatin was found in the PD plaque as compared with the TA. In PD cells, myostatin expression was mainly in the myofibroblasts, and in the TA cells, it increased upon passage paralleling myofibroblast differentiation and was up-regulated by TGFbeta1. Myostatin or its cDNA construct increased the myofibroblast number and collagen in TA cells. Myostatin was detected in the TGFbeta1-induced PD-like plaque of the rat partly in the myofibroblasts, and in the TA. Myostatin cDNA injected in the TA induced a plaque and intensified the TGFbeta1 lesion, which was not reduced by myostatin shRNA.
CONCLUSIONS: Myostatin is overexpressed in the PD plaque, partly because of myofibroblast generation. Although myostatin induces a plaque in the rat TA, it does not appear to mediate the one triggered by TGFbeta1, thus suggesting that both proteins act concurrently and that therapy should target their common downstream effectors.

A-6. Ferrini MG, Moon J, Rivera S, Rajfer J, Gonzalez-Cadavid NF. Amelioration of diabetes-induced cavernosal fibrosis by antioxidant and anti-transforming growth factor-β1 therapies in inducible nitric oxide synthase-deficient mice. BJU Int. 2012 Feb; 109(4):586-93.

OBJECTIVE. To investigate whether sustained long-term separate treatments of diabetic inducible nitric oxide synthase knockout (iNOSKo) mice with allopurinol, an antioxidant inhibiting xanthine oxidoreductase, decorin, a transforming growth factor-β1 (TGFβ1) -binding antagonist, and molsidomine, a long-life nitric oxide donor, prevent the processes of diabetes-induced cavernosal fibrosis.

MATERIALS AND METHODS: Eight week old male iNOS knock out (iNOSKo) mice were made diabetic by injecting 150 mg/kg B.W Streptozotocin (1P) with were either left untreated or treated with the oral antioxidant allopurinol (40 mg/kg/day), Glycemia or decoin (50 mg, 1P, twice), as an anti-TGFβ1 agent (n = 8/group). and oxidative stress markers were determined in blood and urine. Paraffin-embedded tissue sections from the penile shaft were subjected to Masson trichrome staining for the smooth muscle (smc)/collagen ratio, and imunostaining for smc content, profibrotic factors, oxidative stress, cell replication and cell death markers followed by quantitative image analysis.

RESULTS: Eight-week treatment with either allopurinol or decorin counteracted the decrease in smooth muscle cells and the increase in apoptosis and local Decorin but not allopurinol oxidative stress within the corpora tissue. increased the smooth muscle cell/collagen ratio, whereas allopurinol but not Molsidomine was effective in decorin inhibited systemic oxidative stress. reducing both local and systemic oxidative stress, but did not prevent corporal fibrosis.

CONCLUSION: Both allopurinol and decorin appear as promising approaches either as a single or a combined pharmacological modality for protecting the diabetic corpora from undergoing apoptosis and fibrosis although their functional effects still need to be defined.

A-7. Wang JSC, Kovanecz I, Vernet D, Nolazco G, Kopchok GE, Chow SL, White RA, Gonzalez-Cadavid NF. Effects of sildenafil and/or muscle-derived stem cells on myocardial infarction. J Transl Medic, 2012, preliminary acceptance

Background: Previous studies have shown that long-term oral daily PDE 5 inhibitors (PDE5i) counteract fibrosis, cell loss, and the resulting dysfunction in tissues of various rat organs and that implantation of skeletal muscle-derived stem cells (MDSC) exerts some of these effects. PDE5i and stem cells in combination were found to be more effective in non-MI cardiac repair than each treatment separately. We have now investigated whether sildenafil at lower doses and MDSC, alone or in combination are effective to attenuate LV remodeling after MI in rats.

Methods: MI was induced in rats by ligature of the left anterior descending coronary artery. Treatment groups were: “Series A”: 1) untreated; 2) oral sildenafil 3 mg/kg/day from day 1; and “Series B”: intracardiac injection at day 7 of: 3) saline; 4) rat MDSC (10^6 cells); 5) as #4, with sildenafil as in #2. Before surgery, and at 1 and 4 weeks, the left ventricle ejection fraction **(LVEF)** was measured. LV sections were stained for collagen**,** myofibroblasts, apoptosis, cardiomyocytes, and iNOS, followed by quantitative image analysis**.** Western blots estimated angiogenesis and myofibroblast accumulation, as well as potential sildenafil tachyphylaxis by PDE 5 expression. Zymography estimated MMPs 2 and 9 in serum.

Results: As compared to untreated MI rats, sildenafil improved LVEF, reduced collagen, myofibroblasts, and circulating MMPs, and increased cardiac troponin T. MDSC replicated most of these effects and stimulated cardiac angiogenesis. Concurrent MDSC/sildenafil counteracted cardiomyocyte and endothelial cells loss, but did not improve LVEF or angiogenesis, and increased myofibroblasts and upregulated PDE 5.

Conclusions: Long-term oral sildenafil, or MDSC given separately, reduce the MI fibrotic scar and improve left ventricular function in this rat model. The failure of the treatment combination may be due to inducing overexpression of PDE5 and some MDSC differentiation into myofibroblasts.

A-9. Kovanecz I, Rivera S, Nolazco G, Vernet D, Segura D, Gharib S, Rajfer J, Gonzalez-Cadavid NF. Separate or combined treatments with muscle derived stem cells, daily sildenafil, or molsidomine prevent erectile dysfunction in a rat model of cavernosal nerve damage. J Sex Medic, 2012, submitted

Objectives. Long-term daily administration of PDE5 inhibitors **(PDE5i)** in the rat prevents or reverses corporal smooth muscle cell **(SMC)** loss, fibrosis and the resulting CVOD in both aging and bilateral cavernosal nerve resection **(BCNR)** models for erectile dysfunction **(ED)**. In the aging rat model, corporal implantation of skeletal muscle derived stem cells **(MDSC)** reverses CVOD. Nitric oxide **(NO)** and cGMP can modulate stem cell lineage. We have now investigated in the BCNR model the effects of sildenafil **(S)** at different doses, alone or in combination with MDSC or the NO donor molsidomine, on CVOD and the underlying corporal histopathology,
Methods. Rats subjected to BCNR were maintained for 45 days either untreated or given sildenafil in the drinking water at 10, 2.5, and 1.25 mg/kg/day (medium, low, and very low doses), or retrolingually, or with additional intraperitoneal molsidomine as NO donor or MDSC implanted into the corpora cavernosa, or received molsidomine or MDSC alone. Dynamic infusion cavernosometry evaluated CVOD. The underlying histopathology was assesed on penile sections by Masson trichrome, immunohistochemistry for α-smooth muscle actin **(ASMA),** or dual immunofluorescence for nNOS and NF-70, and in fresh tissue by western blot for calponin, SHP-2. Bax, NF70, nNOS, and BDNF, and also by picrosirius red for collagen.
Results. All treatments normalized erectile function (drop rate), and most increased the SMC/ collagen ratio and ASMA expression in corporal tissue sections, and reduced collagen content in the penile shaft tissue (PST). MDSC also increased calponin, nNOS and BDNF in the PST. The combination treatments were not superior to the different agents given alone.
Conclusions. Lowering the dose of a continuous long term sildenafil administration from 10 to 1.25 mg/kg/day still maintained the prevention of CVOD in the BCNR rat previously observed with 20 mg/kg/day, but the prevention of the underlying histopathology was much less effective. As in the aging rat model, MDSC also counteracted CVOD, but supplementation with sildenafil did not improve the outcome.

Approach 3

Finally, the third approach translated all these conclusions into a concerted strategy for the injured dystrophic skeletal muscle of the mdx mouse and (in order to confirm some aspects) in a severely necrotic skeletal muscle in a diabetic model of critical limb ischemia **(CLI).** The completed studies conducted in the mdx mouse were the subject of a manuscript under review **(A-8)**. This is an expanded and extensively revised version of a previously submitted paper that had been objected by the reviewers on the main basis that it compiled too much information on three types of cells (WT MDSC, Mst KO MDSC, and mdx MDSC), and that some in vitro results were confusing and partially contradicted the prevalent view on the role of myostatin in myogenesis. Some of these comments reflected an inadequate knowledge by some of the reviewers on the satellite/MDSC relationship, and a rigid view that would doubt the validity of our in vitro results (the inability of Mst KO MDSC and mdx MDSC to form myotubes in vitro, and their resistance, as well as the WT MDSC robust generation of myotubes, to the putative usual modulators) because so far there is not a clear explanation on the mechanism. This, even if the results were not objected per se, or there was no prior conflicting literature in this respect.

Reluctantly, we decided to eliminate the substantial data on the mdx MDSC and on the WT MDSC-Oct 4 Pr-gfp from the previous manuscript, take out also most of the modulation experiments trying to stimulate Mst KO MDSC and mdx MDSC myogenic differentiation in vitro, carry out a comparative flow cytometry demonstration of the essential stem cell marker similarity between WT MDSC and Mst KO MDSC, and completely re-write the paper in the form of the version that is currently under review in *Stem Cell Res Ther*. If it fails to be accepted, we will continue modifying the paper and re-submitting until it is published, because we trust our results and believe they are very valuable, even if the interpretation is controversial. The remaining data deleted from this version will be used to merge with other studies for potential submission.

A-8. Tsao J, Vernet D, Gelfand R, Kovanecz I, Nolazco G, Bruhn KW, Gonzalez-Cadavid NF. Myostatin genetic inactivation inhibits myogenesis by muscle derived stem cells in vitro but not when implanted in the mdx mouse muscle. Stem Cell Res Ther, 2012, submitted

Introduction: Stimulating the commitment of implanted dystrophin+ muscle derived stem cells (MDSC) into myogenic, as opposed to lipofibrogenic lineages, is a promising therapeutic strategy for Duchenne muscular dystrophy (DMD).
Methods: To examine whether counteracting myostatin, a negative regulator of muscle mass and a pro-lipofibrotic factor, would help this process, we compared the in vitro myogenic and fibrogenic capacity of MDSC from wild type (WT) and myostatin knockout (Mst KO) mice under various modulators, the expression of key stem cell and myogenic genes, and the capacity of these MDSC to repair the injured gastrocnemius in aged dystrophic mdx mice with exacerbated lipofibrosis.
Results: Surprisingly, the potent in vitro myotube formation by WT MDSC was refractory to modulators of myostatin expression or activity, and the Mst KO MDSC failed to form myotubes under various conditions, despite both MDSC expressed Oct-4 and various stem cell genes and differentiated into non-myogenic lineages. The genetic inactivation of myostatin in MDSC was associated with silencing of critical genes for early myogenesis (Actc1, Acta1, and MyoD). WT MDSC implanted into the injured gastrocnemius of aged mdx mice significantly improved myofiber repair and reduced fat deposition and, to a lesser extent, fibrosis. In contrast to their in vitro behavior, Mst KO MDSC in vivo also significantly improved myofiber repair, but had little effects on lipofibrotic degeneration.
Conclusions: While WT MDSC are considerably myogenic in culture and stimulate muscle repair after injury in the aged mdx mouse, myostatin genetic inactivation blocks myotube formation in vitro but the myogenic capacity is recovered in vivo under the influence of the myostatin+ host tissue environment, presumably by reactivation of key genes originally silenced in the Mst KO MDSC.

As a result of the unexpected results obtained in vitro with the WT MDSC that failed to respond to all the tested modulators for myotube formation and the inability of the genetic inactivation of myostatin to stimulate muscle repair in vivo over the WT MDSC, we reported in Year 4 that we would investigate other types of modulators. They were molsidomine, allopurinol, and potentially sildenafil, based on the results reported by us in other tissues and conditions, that were discussed under Approach 2. These ongoing studies will lead to two papers, one in the mdx mouse, and the other in the db/db mouse with CLI **(A-10, A-11)**

<u>Effects of molsidomine and antioxidants on the myogenic, antifibrotic, and angiogenic repair capacity of muscle derived stem cells implanted in the injured muscle of aged mdx mice.</u>

As planned in the no-cost extension, six groups of aged (10 months old) male mdx mice (n=6 each) were injected with notexin into the surgically exposed gastrocnemius muscle as previously **(A-8).** Two days later one group was injected into the muscle with saline as vehicle and remained untreated until sacrifice **(UT)**. Three groups were implanted into the muscle with the WT MDSC (10^6 cells) in saline, of which one group did not receive further treatment **(SC)**, one was treated with intraperitoneal molsidomine as nitric oxide donor at 5 mg/kg/day **(SC+Mol)**, or with an antioxidant mixture of allopurinol (inhibitor of xanthine oxidoreductase) and apocynin (inhibitor of NADPH oxidase), at 10 and 100 mg/kg/day, respectively **(SC+AO).** The MDSC were tagged with DAPI to detect them in the skeletal muscle**.** The last two groups of the notexin-injected mice which had not been implanted with MDSC were treated with either molsidomine **(Mol)** or antioxidant mix **(AO)** as above.

Three weeks later (with no deaths recorded) the mice were anesthesized, blood extracted from the heart, the gastrocnemius muscle dissected, and the animals sacrificed. The muscle specimens were divided in two aliquots around the site of the injection, one for paraffin embedding and preparation of 6 um sections, and the other for liquid N2/isopentane cryosectioning, and the residual tissue was used for storage at -80C and western blotting.

The qualitative fluorescent detection of the DAPI-labeled MDSC into the myofibers is ongoing in frozen sections of the SC against UT groups. However, the most precise identification of the MDSC is based on the expression of the stem cell key gene Oct 4 as in our previous paper **(A-8). Fig. 1** shows a western blot of muscle tissue extracts, where some basal expression of Oct 4 was found in the UT group, indicating the presence of endogenous MDSC,

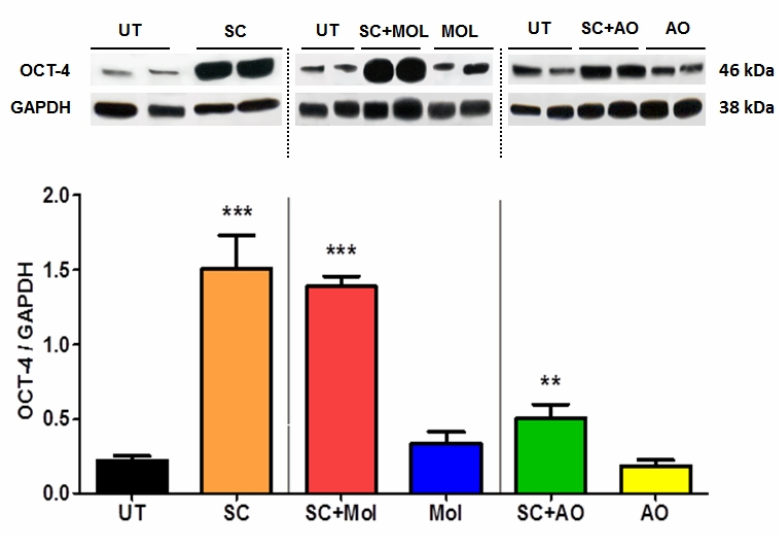

Fig. 1. The implantation of MDSC into the injured muscle of the aged mdx mice led to a considerable expression of the stem cell gene Oct 4, but pharmacological supplementation either failed to upregulate the overall stem cell activation, or even reduced it. Tissue homogenates (n=6) from each group were run against the UT specimens in separate sets of 2 gels ran simultaneously, and western blot analysis was performed, correcting by GAPDH expression. Top: representative lanes for each group. Bottom: Bar graphs of the densitometric ratios. Statistical comparisons were performed by the paired t test for each group against the normalized UT group, and by ANOVA when more than 2 groups were compared. *: p <0.05; **: p <0.01*; ***: p <0.001. For abbreviations see text.

and a remarkable nearly 8-fold increase of Oct 4 in the SC group as a marker of the implanted MDSC, and/or the awakening of the endogenous dormant MDSC by paracrine factors from the implanted MDSC. Daily molsidomine supplementation of the MDSC treatment in the SC+Mol group did not increase further Oct 4 expression, implying that nitric oxide failed to activate the MDSC. Molsidomine alone in the Mol group did not change the basal expression seen in the UT. The antioxidant supplementation in group SC+AO was not only unable to upregulate stem cell activation, but in fact reduced it considerably, and the antioxidant alone did not change the Oct 4 basal expression in the AO group.

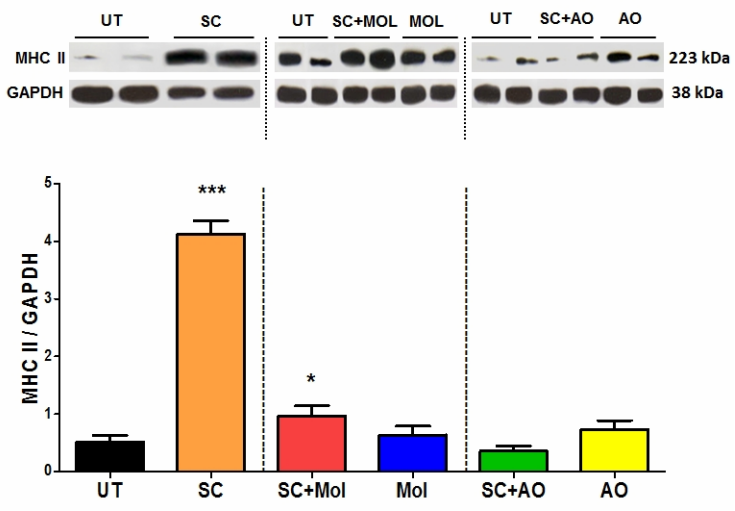

Fig. 2. The implantation of MDSC into the injured muscle of the aged mdx mice led to a considerable expression of the mature myofiber gene MHC-II, but pharmacological supplementation failed to upregulate the overall stem cell activation, and even inhibited it. Western blots were performed as on Fig. 1. Top: representative lanes for each group. Bottom: Bar graphs of the densitometric ratios. Statistical comparisons were performed by the paired t test for each group against the normalized UT group, and by ANOVA when more than 2 groups were compared. *: p <0.05; **: p <0.01*; ***: p <0.001. For abbreviations see text.

The overall stem cell activation observed after MDSC implantation into the skeletal muscle was paralleled by a similar upregulation of MHC-II, a marker of myofiber formation in the SC group **(Fig. 2)**. However, in this case the Mol supplementation in the SC+Mol reduced considerably this up-regulation albeit the MHC-II expression was still higher than in the UT group. As in the case of Oct 4, the supplementation of MDSC treatment with antioxidant abolished the upegulation of MHC-II in the SC+AO group, and antioxidant alone was virtually

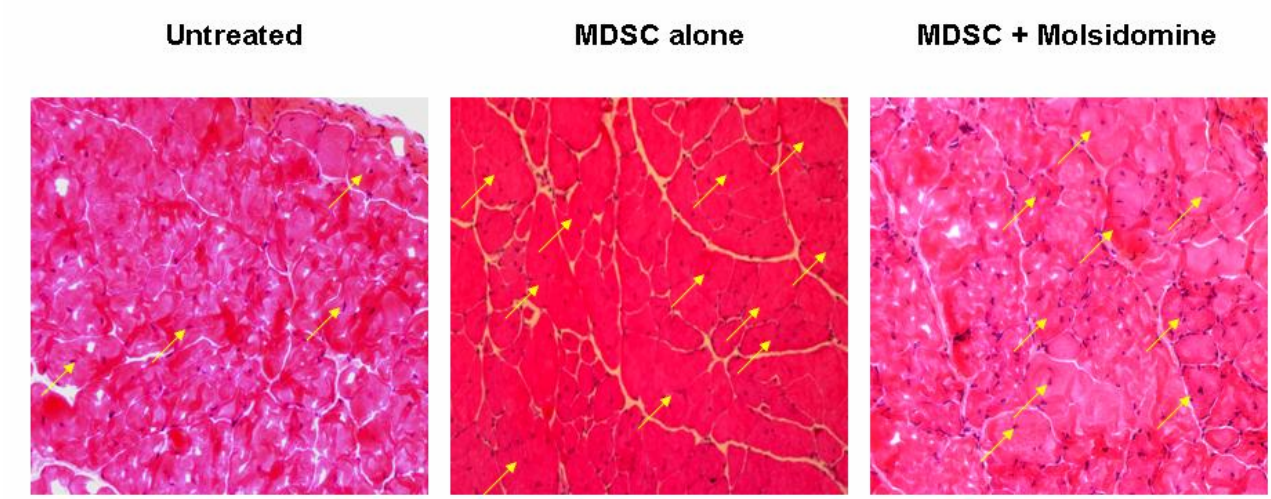

Fig. 3. The implantation of MDSC into the injured muscle of the aged mdx mice led to a considerable increase in central nuclei in the regenerating myofibers, and molsidomine supplementation appears to have upregulated the overall stem cell activation. Representative HE sections. 200X

ineffective in the AO group.

The effect of MDSC alone on MHC-II expression is in agreement with the first images we are collecting on the increase of central nuclei as indicator of muscle repair observed in the SC group in comparison to the UT group, in frozen tissue sections stained with hematoxylin eosin **(Fig. 3).** Also in agreement with MHC-II expression, the SC+Mol group shows in these specific sections much less stimulation. The quantitative image analysis is ongoing for all animals in only these three groups, since the other ones did not have significant changes. This involves 3 sections/animal and 10 fields/ section for 6 mice/group.

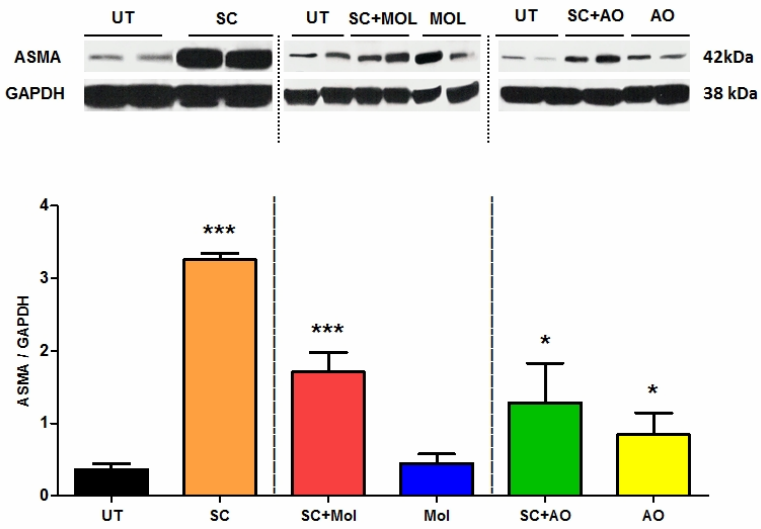

Fig. 4. The implantation of MDSC into the injured muscle of the aged mdx mice led to a considerable expression of ASMA, a myofibroblast and smooth muscle cell marker, but molsidomine and antioxidant supplemention attenuated this expression. Western blots were performed as on Fig. 1. Top: representative lanes for each group. Bottom: Bar graphs of the densitometric ratios. Statistical comparisons were performed by the paired t test for each group against the normalized UT group, and by ANOVA when more than 2 groups were compared. *: p <0.05; **: p <0.01*; ***: p <0.001. For abbreviations see text.

One important feature of muscular dystrophy is lipofibrotic degeneration, and this was investigated first for the fibrosis component by western blot by establishing the ratio between the

expression of α-smooth muscle actin **(ASMA)**, that is a marker of both myofibroblasts and smooth muscle cells **(SMC),** and of calponin 1, that is restricted to SMC. Myofibroblasts are the key cells in wound healing, but also of fibrosis when instead of being eliminated by apoptosis they persist depositing excessive collagen. SMC are an indicator of angiogenesis since they are in the arterial media. **Fig. 4** shows that, surprisingly the SC group had over 7-fold increase in ASMA expression over the UT, and an over 3-fold stimulation was seen with SC+Mol. In the other groups there was a much lower degree of upregulation of ASMA expression.

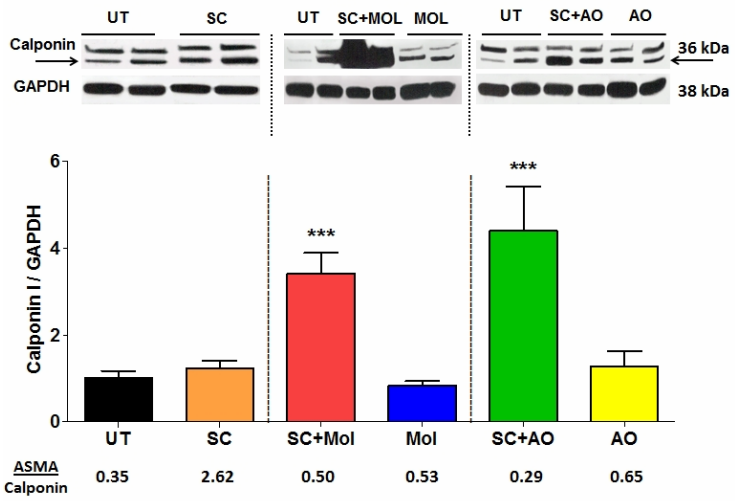

Fig. 5. The implantation of MDSC into the injured muscle of the aged mdx mice did not change the expression of calponin 1, an SMC marker, but molsidomine and antioxidant supplementation considerably increased this expression and reduced the ASMA/calponin ratio. Western blots were performed as on Fig. 1. Top: representative lanes for each group. Bottom: Bar graphs of the densitometric ratios. Statistical comparisons were performed by the paired t test for each group against the normalized UT group, and by ANOVA when more than 2 groups were compared. *: p <0.05; **: p <0.01*; ***: p <0.001. For abbreviations see text.

To assess what proportion of this increase could be ascribed to myofibroblasts and to SMC, respectively, new westerns were carried out for calponin 1.**Fig. 5.** shows virtually no change in the lower band of the doublet, the 38 kDa band, in SC vs UT, which would suggest that the ASMA increase is actually due to myofibroblast accumulation. In contrast, the SC+Mol induced a remarkable upregulation of calponin 1 expression, and the same occurred with the other supplementation, the administration of antioxidant in SC+AO. The ratios of ASMA to calponin 1 depicted at the bottom give a better idea of what can be taken as an indicator of myofibroblasts/ SMC relative ratio (not absolute since these are arbitrary ratios), showing that MDSC has a remarkable 7-fold higher ratio than the UT and 4-5 fold higher that the other groups. This implies that despite being beneficial in terms of increasing Oct 4 and MHC-II expression, may be also differentiating into myofibroblasts and thus contributing to fibrosis, but that supplementation with molsidomine or antioxidant prevents this potentially noxious process. The combination seems to promote angiogenesis, evidenced by generation of SMC

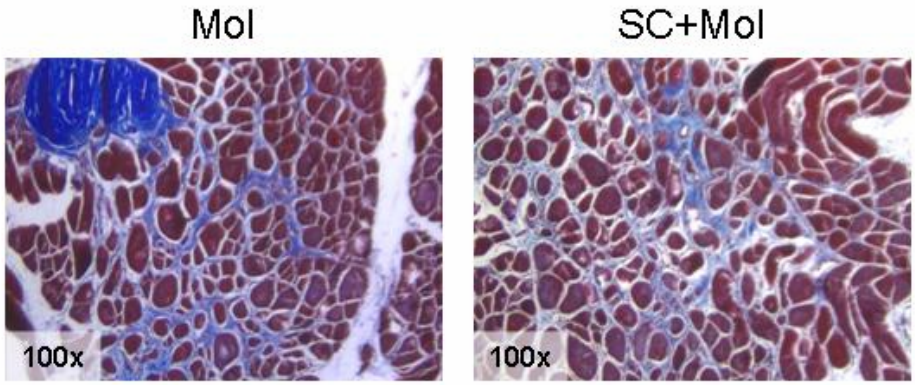

Fig. 6. Representative pictures of Masson trichrome staining to detect the extent of muscle fibrosis in the injured skeletal muscle tissue of the aged mdx mice subjected to the MDSC and molsidomine treatments. Paraffin embedded sections were stained, and quantitative image analysis of the 5 groups is ongoing.

In order to investigate these assumptions, paraffin-embedded sections of muscle tissue were subjected to Masson trichrome staining to evaluate the interstitial collagen content (staining in blue) versus the myofibers (red). Although the quantitative estimation is still ongoing, representative pictures of Mol and SC+Mol **(Fig. 6)** show considerable collagen deposition in the endomysium and perimysium, but since the UT and SC have not been observed yet, any interpretation must wait. A similar situation occurs with ongoing separate dual immunofluorescence staining of UT and SC specimens for ASMA (red) and collagen I (green), and by ASMA (red) and calponin 1 (green), followed in both cases by DAPI staining of nuclei.

One consistent feature in the Masson trichrome pictures is the appearance of small vacuoles that seem to have contained fat globules. To assess the effects of treatments on adipocyte or fat content, frozen sections are being stained with Oil Red O, like in our previous work to compare quantitatively the effects of treatment on lipogeneration.

In a parallel experiment, aged mdx mice (n=5/group) had been subjected to notexin spreading onto half of the diaphragm, leaving the other intact, and received either 10 ul saline as vehicle or saline containing either WT MDSC or Mst KO MDSC ($0.2x10^6$ cells). Because of the difficulty of this experiment and the concerns about survival, no other treatments were performed, but no mice died. Only frozen sections were obtained, which are being subjected to Masson trichrome and Oil red O determinations, to define the impact on the diaphragm, the most sensitive skeletal muscle to the bouts of necrosis occurring in the mdx mouse.

On the other hand, the SMC detection by calponin I in the western blots as a putative indicator of blood vessels and hence of angiogenesis in the gastrocnemius muscle tissue, will soon be complemented by the estimation of endothelium content by quantitative western blot for Von Willebrandt factor or CD31. The final evaluation of the relative repair efficacy of these treatments for angiogenesis will be estimated by the same approach for VEGF, and for neurogenesis or neural repair in the muscle NF70 will be used, as described in the next section.

In summary, the current conclusions, that may be modified as the pending assays are completed, are: 1) confirming our previous data, WT MDSC implantation is effective in repairing skeletal muscle damage even in the severely injured gastrocnemius muscle of the aged mdx mouse; 2) MDSC not only survive but lead to an intense expression of the key stem cell gene, Oct 4, either in the MDSC themselves or by paracrine activation of the endogenous stem cells, but at the cost of a putative generation of myofibroblasts; 3) although molsidomine supplementation of the MDSC treatment does not improve this increased Oct 4 expression and even quenches the MDSC stimulation of myofiber formation shown by MHC-II expression, still it is very effective in stimulating SMC formation (presumably from angiogenesis) and avoiding myofibroblasts generation, as evidenced by the calponin I/ASMA ratio; 4) the antioxidant supplementation of MDSC administration stimulates even better SMC generation, but in contrast with molsidomine, it does not seem to induce skeletal muscle repair or stem cell activation; 5) the treatments with either molsidomine or antioxidant alone are ineffective.

In conclusion: the MDSC tissue repair capacity of the injured dystrophic muscle in the aged mdx mice was confirmed, but we found that myofibroblast generation may complicate this beneficial process. Undesirable myofibroblast accumulation may be counteracted with molsidomine which would still preserve some of the repair capacity of MDSC, but not by antioxidants.

Effects of molsidomine on the myogenic and angiogenic repair capacity of muscle derived stem cells implanted in the skeletal muscle of diabetic mice with necrosis due to critical limb ischemia**.**

In order to determine whether the beneficial effects of WT MDSC alone or supplemented with molsidomine (antioxidant was excluded due to the disappointing results in the mdx mouse) can extend to the repair of a much more damaged muscle tissue than in the mdx dystrophic

mouse, critical limb ischemia **(CLI)** was induced by ligation of the femoral artery irrigating one of the legs in 3 month old male diabetic ob/ob mice. This is a condition that leads to a severe muscle necrosis and even limb loss. Animals (n=8/group) were either left untreated **(UT),** or subjected to MDSC implantation alone **(SC),** or supplemented with molsidomine **(SC+Mol),** or treated with molsidomine alone **(Mol),** as in the mdx mouse study above. A fifth group was normal intact non-diabetic mice left untreated **(ND-UT),** and used as reference. The study was terminated at 3 weeks.

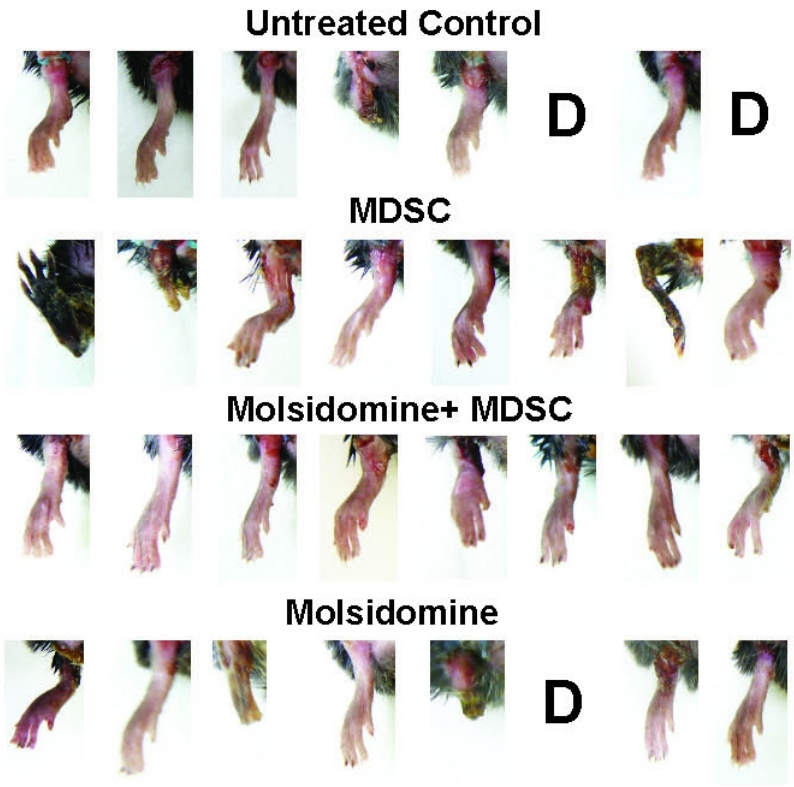

Fig. 7. The treatments with MDSC or molsidomine, alone or in combination, prevented mortality, but improved leg preservation only in combination. D: mouse died in period between 1 and 3 weeks; however, in M it was due to a surgery complication

Blood glucose varied from 308 to 498 mg/dl. **Fig. 7** shows that in the diabetic UT group, 2 animals died, and a third one lost a complete limb, with the rest showing a thin and ischemic leg. Although no deaths were observed in the WT MDSC implanted animals, contrary to expectations two of them had nearly lost the legs and a third one had a very damaged one. No animal died either in the MDSC+Mol group, and the appearance of the legs was better than in the previous groups. In the Mol group, 2 animals lost half of the legs and one died. So, treatments did not visually improve the condition of the mice. The ND-UT was not included since no ischemia had been induced and all legs were normal.

The in vivo assessment of limb function, was based on visual observation according to the following rating from bad to better: 3=dragging of foot, 2=no dragging but no plantar flexion, 1=plantar flexion, and 0=flexing the toes to resist gentle traction on the tail. Semiquantitative measurement of the ischemic damage was also assessed, with rating from moderately bad to worst, based on: 0=no difference from the right hindlimb, 1=mild discoloration, 2=moderate discoloration, 3=severe discoloration or

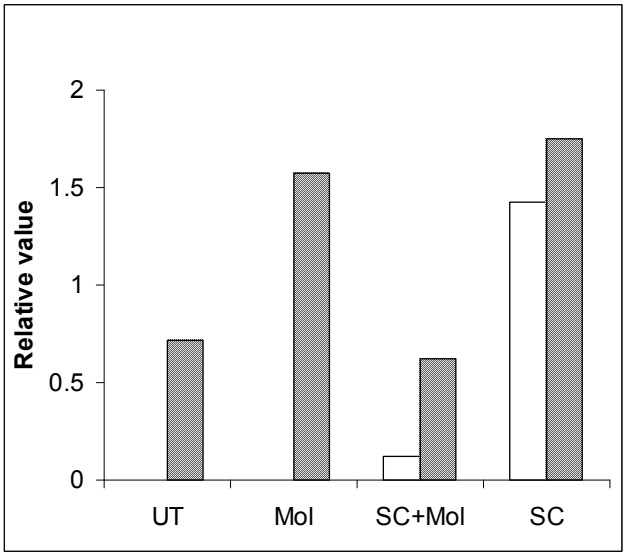

Fig. 8. The combination of molsidomine and MDSC appears to be the more effective treatment for preserving leg function and avoiding ischemia. The number of animals that were used for assessing leg function (blank bars) and ischemic damage (hatched bars) areas follows: UT: 6,7; Mol: 5,7; SC+Mol: 8,8; SC: 6,7

subcutaneous tissue loss or necrosis, and 4=any amputation. **Fig 8** shows that in animals saving their legs, all groups, except paradoxically for some impairment in the SC one, had a virtually normal function. However, both the SC and the Mol exhibited a mild to moderate ischemia, with the SC+Mol showed improvement that agreed with the general appearance of the mice.

The effects of these treatments were also examined by western blot for the markers selected for the previous study in the mdx mouse and additional ones. **Fig. 9** shows for Oct 4 a good agreement with the previous study, with SC considerably stimulating its expression over the UT, and molsidome supplementation in SC+Mol reducing the extent of the up-regulation. Remarkably, and in contrast to our results in the kidney in the diabetic Zucker rat, the expression of Oct 4 in the non-diabetic, non-ischemic control, was much lower than in the UT group, which suggests that in the non-injured normal muscle, the stem cells are dormant.

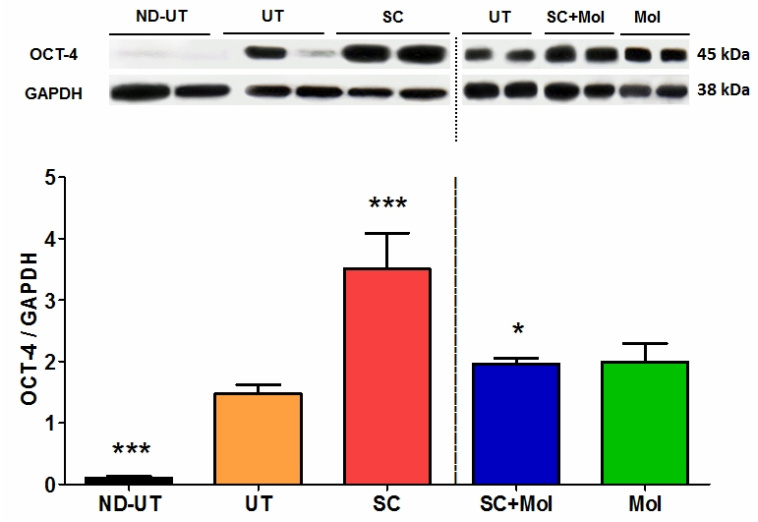

Fig. 9. The implantation of MDSC into the ischemic gastrocnemius of the diabetic db/db mouse led to a considerable expression of the stem cell gene Oct 4, but combination with molsidomine failed to upregulate further the overall stem cell activation. Tissue homogenates (n=6) from each group were run against the UT specimens in separate sets of 2 gels ran simultaneously, and western blot analysis was performed, correcting by GAPDH expression. Top: representative lanes for each group. Bottom: Bar graphs of the densitometric ratios. Statistical comparisons were performed by the paired t test for each group against the normalized UT group, and by ANOVA when more than 2 groups were compared. *: p <0.05; **: p

In contrast, none of the treatments corrected the reduced MHC-II expression in the UT as compared to the ND-UT, as an indicator of myofiber repair, and surprisingly the SC lowered it by a further 25% **(Fig. 10)** The early myogenic marker, MyoD was not changed by any of the treatments excep Mol (not shown).

Where the beneficial effects of treatment were more evident is in the antifibrotic and angiogenic-related effects. **Fig. 11** shows that SC and SC Mol are effective in reducing ASMA expression, although surprisingly ASMA is considerably expressed in the non-diabetic non-ischemic muscle where there should not be any fibrosis. Whether this is due to a phenotypic switch of the SMC to a contractile phenotype, different from

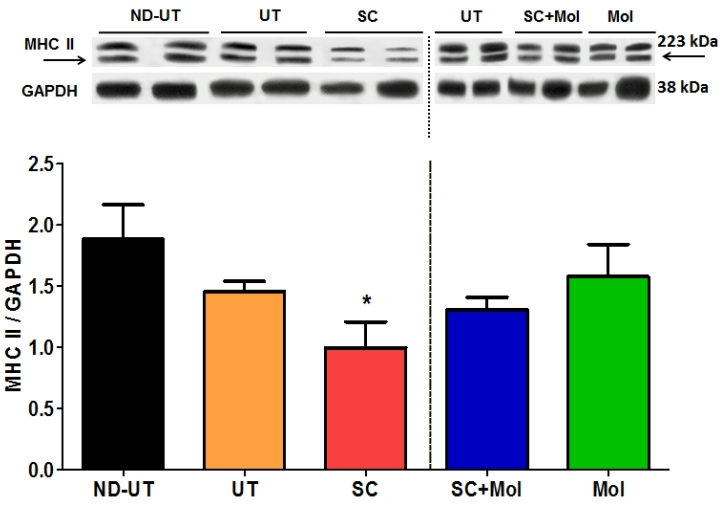

Fig. 10. The implantation of MDSC into the ischemic gastrocnemius of the diabetic db/db mouse led to a reduction in the expression of the myofiber gene MHC-II, and molsidomine also failed to upregulate this expression. Western blots were performed as on Fig. 1. Top: representative lanes for each group. Bottom: Bar graphs of the densitometric ratios. Statistical comparisons were performed by the paired t test for each group against the normalized UT group, and by ANOVA when more than 2 groups were compared. *: p <0.05; **: p <0.01*; ***: p <0.001. For abbreviations see text.

the process operating in the diabetic ischemic muscle setting, is not known. In any case, what is really important is the SC stimulation of calponin 1 expression as a mrker of SMC in the arterial media, and hence of angiogenesis, and the reduction of the ASMA/calponin 1 ratio by both SC and SC+Mol seen in **Fig. 12.**

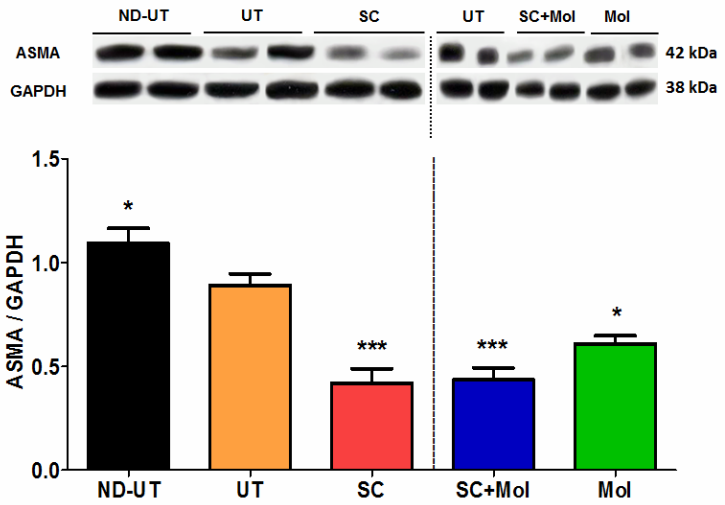

Fig. 11. The implantation of MDSC into the ischemic gastrocnemius of the diabetic db/db mouse led to a considerable reduction of ASMA, a myofibroblast and smooth muscle cell marker, and combination with molsidomine did not reduce it further. Western blots were performed as on Fig. 1. Top: representative lanes for each group. Bottom: Bar graphs of the densitometric ratios. Statistical comparisons were performed by the paired t test for each group against the normalized UT group, and by ANOVA when more than 2 groups were compared. *: p <0.05; **: p <0.01*; ***: p <0.001. For abbreviations see text.

This is accompanied by a stimulation by SC of the expression of von Willebrandt factor, as an endothelial marker, and hence another marker of angiogenesis depicted in **Fig. 13.** However, no significant therapeutic effects were observed in the expression of a neural marker (NF 70).

The effects of treatments on myofiber repair will be better defined by the counting of central nuclei on hematoxylin/eosin stained frozen sections as in Fig 3, and the measurement of apoptotic index on paraffin-embedded sections by TUNEL, that are ongoing. Similarly, the effects on lipofibrotic degeneration are being investigated by quantitative assay of collagen deposition by Masson trichrome staining on paraffin-embedded sections (as in Fig. 6), and of by Oil Red O in frozen sections.

Finally, what is more pertinent is the confirmation of the effects of treatments on angiogenic repair by additional ongoing assays. One is the quantitative immunohistochemistry staining for Pecan (CD31), an endothelial marker, and its confirmation by quantitative western blot. The other, and even more informative is the western blot estimation of VEGF levels, that can be considered as a key angiogenic factor.

In summary, the current conclusions, that may be modified as the pending assays are completed, are: 1) the effects of WT MDSC, and its combination with molsidomine on the necrotic/ischemic skeletal muscle tissue in diabetes-related CLI are as expected in terms of the overall stem cell stimulation in the skeletal muscle, and similar to those

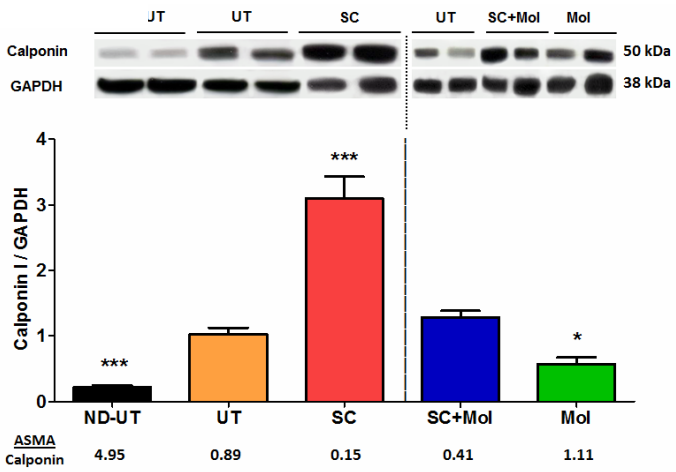

Fig. 12. The implantation of MDSC into the ischemic gastrocnemius of the diabetic db/db mouse led to a considerable upregulation of calponin 1, an SMC marker, and reduction of myofibroblasts as shown by the decreased calponin 1/ASMA ratio Western blots were performed as on Fig. 1. Top: representative lanes for each group. Bottom: Bar graphs of the densitometric ratios. Statistical comparisons were performed by the paired t test for each group against the normalized UT group, and by ANOVA when more than 2 groups were compared. *: p <0.05; **: p <0.01*; ***: p <0.001. For abbreviations see text.

observed in the mdx mouse; 2) this is paralleled by the prevention of CLI-related deaths by the different treatments, and of the leg ischemia by SC+Mol; 3) this is in agreement with the putative stimulation of angiogenesis by SC and SC+Mol, but not of muscle repair, at least as inferred from MHC-II expression.

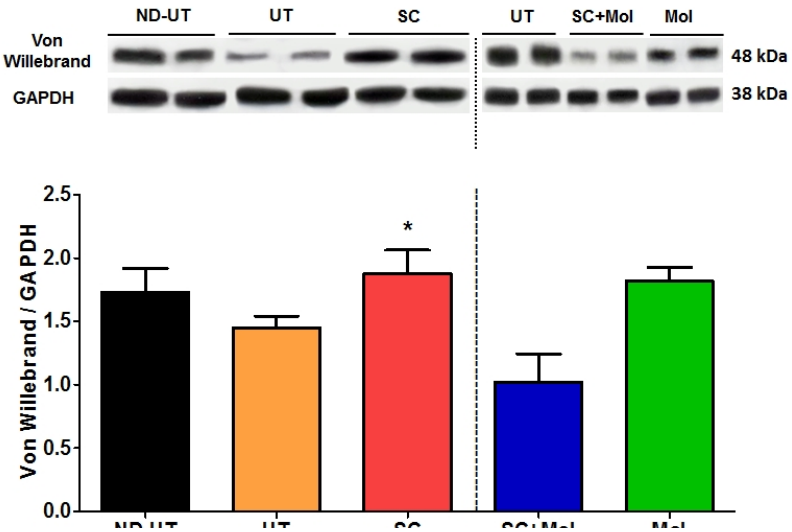

Fig. 13. The implantation of MDSC into the ischemic gastrocnemius of the diabetic db/db mouse led to a moderate upregulation of von Willebrandt factor, an endothelial marker. Western blots were performed as on Fig. 1. Top: representative lanes for each group. Bottom: Bar graphs of the densitometric ratios. Statistical comparisons were performed by the paired t test for each group against the normalized UT group, and by ANOVA when more than 2 groups were compared. *: p <0.05; **: p <0.01*; ***: p <0.001. For abbreviations see text.

In conclusion, so far: the implantation of MDSC into the severely necrotic muscle of mice with critical limb ischemia is effective in stimulating angiogenesis but not myofiber formation, and supplementation with molsidomine does not improve these effects. This encourages further investigation of other potential modulators of both the tissue terrain (antifibrotic, anti-inflammatory, anti-oxidative stress agents), and stem cell differentiation, such as the low dose PPARγ that may be beneficial for both muscular dystrophy and injury in the aged mdx mouse, and muscle necrosis and ischemia in the CLI mouse.

KEY RESEARCH ACCOMPLISHMENTS

They include the demonstration that:

- Muscle derived stem cells (MDSC) without any genetic modification (WT MDSC) are able to exert the repair or prevent cell loss, the appearance of fibrotic tissue, and the resulting dysfunctions upon implantation into smooth muscle-containing tissues as diverse as the penile corpora cavernosa during aging or after nerve damage, the injured vagina, and the heart after myocardial infarction, in their respective rat models, due to their differentiation into multiple cell types and the parallel counteraction of fibrosis

- Myostatin is an inducer of pro-fibrotic phenotype changes in myofibroblasts generated in vitro from stem cell lines, and overexpressing myostatin by gene transfer leads to myofibroblast generation by acting concurrently with TGFbeta1, supporting the view that counteracting myostatin should prevent fibrosis. Similarly, producing nitric oxide through a nitric oxide donor, molsidomine, increasing its product, cGMP, by long-term continuous administration of PDE5 inhibitors, or reducing reactive oxygen species by antioxidants, reduces fibrosis in smooth muscle containing tissues

- The combination of molsidomine or a PDE5 inhibitor (sildenafil) with WT MDSC is more effective than either one alone to prevent fibrosis in the corporal smooth muscle or in the heart in rat models, but this requires fine-tuning of the dosages and times of administration

- In terms of the effects of WT MDSC on skeletal myotube and myofiber generation, while they are considerably myogenic in culture and stimulate muscle repair after injury in the aged mdx mouse, myostatin genetic inactivation blocks myotube formation in vitro but the myogenic capacity is recovered in vivo under the influence of the myostatin+ host tissue environment, presumably by reactivation of key genes originally silenced in the Mst KO MDSC.

- Ongoing studies suggest that although myofibroblast generation may complicate the repair of injured dystrophic muscle in aged mdx mice by MDSC, this may be counteracted with molsidomine while preserving some of their repair capacity, but not by antioxidants.

- Other ongoing studies suggest that the implantation of MDSC into the severely necrotic muscle of mice with critical limb ischemia is effective in stimulating angiogenesis but not myofiber formation, and supplementation with molsidomine does not improve these effects.

CUMULATIVE REPORTABLE OUTCOMES

A. Papers acknowledging this grant (see Appendix for 1-9, and Body for 10,11)

1. Nolazco G, Kovanecz I, Vernet D, Gelfand RA, Tsao J, Ferrini MG, Magee T, Rajfer J, **Gonzalez-Cadavid NF.** Effect of muscle-derived stem cells on the restoration of corpora cavernosa smooth muscle and erectile function in the aged rat. BJU Int. 2008 May;101(9):1156-64

2. Artaza JN, Singh R, Ferrini MG, Braga M, Tsao J, **Gonzalez-Cadavid NF.** Myostatin promotes a fibrotic phenotypic switch in multipotent C3H 10T1/2 cells without affecting their differentiation into myofibroblasts. J Endocrinol. 2008 Feb;196(2):235-49.

3. Cantini LP, Ferrini MG, Vernet D, Magee TR, Qian A, Gelfand RA, Rajfer J, **Gonzalez-Cadavid NF** (2008) Pro-fibrotic role of myostatin in Peyronie's disease. J Sex Med. 2008 Jul;5(7):1607-22.

4. Ho MH, Heydarkhan S, Vernet D, Kovanecz I, Ferrini M, Bhatia NN, **Gonzalez-Cadavid NF,** Stimulating vaginal repair in rats through skeletal muscle-derived stem cells seeded on small intestinal submucosal scaffold. Obstet Gynecol. 2009 Aug;114(2 Pt 1):300-9.

5. **Gonzalez-Cadavid NF**, Rajfer J. Treatment of Peyronie's disease with PDE5 inhibitors: an antifibrotic strategy. Nat Rev Urol. 2010 Apr;7(4):215-21.

6. Ferrini MG, Moon J, Rivera S, Rajfer J, **Gonzalez-Cadavid NF** (2011) Amelioration of diabetes-induced fibrosis by antioxidant and anti-TGFβ1 therapies in the penile corpora cavernosa in the absence of iNOS expression. BJU Int. 2012 Feb;109(4):586-93.

7. Wang JSC, Kovanecz I, Vernet D, Nolazco G, Kopchok GE, Chow SL, White RA, **Gonzalez-Cadavid NF**. Effects of sildenafil and/or muscle-derived stem cells on myocardial infarction. J Transl Medic, 2012, preliminary acceptance

8. Tsao J, Vernet D, Gelfand R, Kovanecz I, Nolazco G, Bruhn KW, **Gonzalez-Cadavid NF**. Myostatin genetic inactivation inhibits myogenesis by muscle derived stem cells in vitro but not when implanted in the mdx mouse muscle. Stem Cell Res Ther, 2012, submitted

9. Kovanecz I, Rivera S, Nolazco G, Vernet D, Segura D, Gharib S, Rajfer J, **Gonzalez-Cadavid NF**. Separate or combined treatments with muscle derived stem cells, daily sildenafil, or molsidomine prevent erectile dysfunction in a rat model of cavernosal nerve damage. J Sex Medic, 2012, submitted

10. Tsao J, Kovanecz I, Agawalla N, Vernet D, Gelfand R, **Gonzalez-Cadavid NF**. Effects of molsidomine and antioxidants on the myogenic, antifibrotic, and angiogenic repair capacity of muscle derived stem cells implanted in the injured muscle of aged mdx mice. Manuscript in preparation, to be submitted in July 2012

11. Tsao J, Kovanecz I, Agawalla N, Vernet D, **Gonzalez-Cadavid NF**. Effects of molsidomine on the myogenic and angiogenic repair capacity of muscle derived stem cells implanted in the the muscle of diabetic mice with critical limb ischemia. Manuscript in preparation, to be submitted in July 2012

B. Abstracts and presentations related to results in the current grant

A-1. J. N. Artaza, **Gonzalez-Cadavid NF** Role of Smad and Wnt signaling pathways in the fibrotic differentiationof C3H 10T (1/2) multipotent cells Induced by Myostatin", Presented at the Western American Federation for Medical Research, January 31-February 3, 2007. Sunset Center Carmel, CA, USA. Winner of the Carmel Scholar Award. Journal of Investigative Medicine, Vol 55, Issue 01, January 2007. Abstract # 61.

A-2. Ferrini MG, Cantini LP, Vernet D, Magee TR, Qian A, Gelfand RA, Rajfer J, **Gonzalez-Cadavid NF** Pro-fibrotic role of myostatin in Peyronie's disease. American Urological Association May 17-22, 2008, Orlando, FL

A-3. Ho MH, Heydarkhan S, Vernet D, Kovanecz I, Ferrini MG, Bathia NN, **Gonzalez-Cadavid NF.** Skeletal muscle-derived stem cells (MDSC) seeded on small intestinal submucosal (SIS) scaffolds stimulate vaginal repair in the rat. American Urological Association May 17-22, 2008, Orlando, FL

A-4. Nolazco G, Kovanecz I, Vernet D, Ferrini MG, Gelfand R, Tsao J, Magee T, Rajfer J, **Gonzalez- Cadavid NF**. Effect of muscle derived stem cells on the restoration of corpora cavernosa smooth muscle and erectile function in the aged rat. American Urological Association May 17-22, 2008, Orlando, FL

A-5. Gonzalez-Cadavid NF. Molecular basis of Peyronie's disease. Ann Meet SMSNA, Orlando, Fl, May 2008

A-6. Wang, S-C, Nolazco G, Kopchock G, Kovanecz I, White R, **Gonzalez-Cadavid NF**. Pharmacological stimulation of NO/cGMP levels as a novel therapeutic approach for myocardial infarction in a rat model**.**

A-7. Nolazco G, Toblli J, Kovanecz I, Gelfand R, Lue Y-H, **Gonzalez-Cadavid NF** (2009) Activation of the Oct-4 gene identifies stem cells in the kidney that are reduced by type 2 diabetes mellitus in a process counteracted by a PPARγ ligand independently from glycemic control. Endocrine Soc Meet, Washington DC

A-8. Vernet D, Heydarkhan S, Kovanecz I, Lue Y-H, Rajfer J, **Gonzalez-Cadavid NF** (2009). Characterization of endogenous stem cells from the mouse penis that express an embryonic stem cell gene and undergo differentiation into several cell lineages. Am Urol Assoc Meet, Chicago, IL, J Urol,

A-9. Gonzalez-Cadavid NF, Tsao J, Vernet D, Gelfand R, Nolazco G (2009) Modulation of cell lineage commitment by skeletal muscle derived stem cells, MDSC, from mdx and myostatin knockout mice Military Health Research Forum 2009, Kansas City, Missouri

A-10. Chow SL CA, Kovancz I, Wang JSC, Vernet D, Kopchock G, White RA, **Gonzalez-Cadavid NF** (2010). Inflammatory Biomarkers in Left Ventricular Remodeling under Stem Cell and Pharmacological Treatment in a Rat Model of Myocardial Infarction. Heart Failure Society of America (HFSA); September 14, 2010; San Diego, CA2010. p. S33.

A-11. Wang JS KI, Vernat D, Nolazco G, Kopchock G, Chow SL, White RA, **Gonzalez-Cadavid N.** . Effects of long-term continuous treatment with sildenafil alone or combined with muscle derived stem cells (MDSC) on myocardial infarction in a rat model. American Heart Association BCVS and American Heart Association Scientific Sessions; July, 19, 2010 and November 15, 2010; Rancho Mirage, CA and Chicago, IL.

A-12.. **Gonzalez-Cadavid NF** , Kovanecz I, Rivera S, Nolazco G, Vernet D, Rajfer J (2011) Long-term, continuous administration of PDE5 inhibitors alone or combined with implantation of stem cells in the penile corpora cavernosa, prevents erectile dysfunction in a rat model of cavernosal nerve damage after radical prostatectomy. DOD-PCRP “Impact “conference, Orlando, Fl

A-13. Kovanecz I, Rivera S, Nolazco G, Vernet D, Rajfer J, **Gonzalez-Cadavid NF** (2011) Long term daily molsidomine and low dose sildenafil, and corporal implantation of muscle derived stem cells (MDSC), alone or in combination, prevent corporal venooclusive dysfunction (CVOD) in a rat model of cavernosal nerve damage Am Urol Assoc (AUA) Annual Meet, Washington, DC

A-14. **Gonzalez-Cadavid NF** (2011) Stem cells and iPS as novel potential therapies for erectile dysfunction (2011) Invited speaker. 5th Guandong Society of Andrology conference (Annual Conference 2011) Guangzhou, China

A-15. Tsao J, Kovanecz I, Agawalla N, Vernet D, Gelfand R, **Gonzalez-Cadavid NF** (2012). Effects of molsidomine and antioxidants on the myogenic, antifibrotic, and angiogenic repair capacity of muscle derived stem cells implanted in the injured muscle of aged mdx mice. 8th Ann World Stem cell Summit, Palm Beach, FA, Dec 2012.

A-16. Tsao J, Kovanecz I, Agawalla N, Vernet D, **Gonzalez-Cadavid NF** (2012). Effects of molsidomine on the myogenic and angiogenic repair capacity of muscle derived stem cells implanted in the the muscle of diabetic mice with critical limb ischemia. Int Meet Health Disparities, Puerto Rico, Nov 2012

C. Grant submissions that partially used results from current grant (MDSC, other stem cells, fibrosis)

A. Funded

1. Gonzalez-Cadavid NF (PI and mentor); one year student training grant: J. Wang: #0543-38F). NIH GCRC at Harbor-UCLA.. Nitric oxide/cGMP modulation of skeletal muscle stem cell differentiation in myocardial infarction in the mouse. 2007-2008

2. **Gonzalez-Cadavid NF (Mentor);** PI: Ho, M; 2 years). Jahnigen Career Development Scholars Award, American Geriatrics Society. Regeneration of Skeletal and Smooth Muscles by Muscle-Derived Stem Cells for the Treatment of Aging Female Pelvic Floor Disorders 2008-2009

3. Gonzalez-Cadavid NF (PI, pilot grant) U54-RR026138-02 (Norris K, Program Director) Therapy of diabetes-related critical limb ischemia with muscle derived stem cells and NO donors. 03/01/11-06/30/12

4. Gonzalez-Cadavid (PI, pilot grant) U54 CA14393-01 (Vadgama J, Program Director) Potential oncogenic effects of alcohol on breast stem cells 01/01/10-08/31/12

5. **Gonzalez-Cadavid NF (PI)** NIH 1R21DK089996-02 Human iPS in erectile dysfunction after radical prostatectomy in rat models 07/01/12-06/30/14. Score: 20 (fundable; goes to Council in late May)

B. Pending

6. 1-12-BS-60. American Diabetes Association **(PI: Gonzalez-Cadavid)** 07/01/12-06/30/15
Pharmacological stem cell modulation for treating erectile dysfunction in type 2 diabetes
Notified that advanced for final review

C. Not funded

6. Modulation of stem cell differentiation in diabetes-related erectile dysfunction **(PI: Gonzalez-Cadavid NF**; 5 years). Submitted on 03/17/08 as main research grant in the O'Brien Urology Center at LABioMed Harbor-UCLA, to NIH-NIDDK in response to RFA.

7. Therapy of penile corporal fibrosis and erectile dysfunction in a rat model of type 2 diabetes by nitric oxide/cGMP modulation of stem cell differentiation **(Co-PI: Gonzalez-Cadavid, NF**; 3 years). RAICES International Cooperation Program, Argentina FONCYT.

8. Modulation of skeletal muscle stem cell differentiation into cardiomyocytes (Mentor: **Gonzalez-Cadavid, NF,** PI: Artaza J; 4 years). Within G12RR030262 NIH RCMI Infrastructure Development grant renewal (PI: Kelly, Baker; NGC: Core Director). Submitted February 2008.

9. Molecular Medicine and Stem Cells Research Core **(Director: Gonzalez-Cadavid NF**; PI: Kelly S/Baker R; 5 years), G12RR030262 NIH/RCMI Infrastructure Development grant Submitted February 2008.

10. **PI: Gonzalez-Cadavid NF** (2009). Modulation of human iPS differentiation in radical prostatectomy-related erectile dysfunction in rat models. NIH Recovery Challenge Grants.

11. **PI: Gonzalez-Cadavid NF** (2009). Erectile Dysfunction and Nitric Oxide Synthase in Aging. RO1 DK53069-07 (resubmission).

12. **PI: Gonzalez-Cadavid NF** (2009) Nitric oxide and cGMP modulation of Oct-4 renal stem cells in diabetic nephropathy . R21 DK085411-01

13. **PI: Gonzalez-Cadavid NF (**2009) Modulation of human iPS differentiation in diabetic nephropathy in rat models NIH Recovery Challenge Grants.

14. **Pending. PI: Gonzalez-Cadavid NF** (2009) PPAR gamma modulation of Oct-4 renal stem cells in diabetic nephropathy R21 DK085413-01

15. Nicholas S/**Gonzalez-Cadavid NF (Co-PIs)(**2011) NIH NIDDK R21 Effects of diabetes on stem cell cross talk in renal tissue repair.

16. **Gonzalez-Cadavid NF** (PI) (2010) Animal Models of Diabetes Complications Consortium. A diabetes mouse model for studying endogenous/exogenous stem cell interaction.

17. NIH NIEHS R21 **(PI: Gonzalez-Cadavid)** (2012) Bisphenol A effects on stem cell lineage commitment affecting penile erection

18. **PI: Gonzalez-Cadavid NF** DOD Prostate Cancer Research Prevention and reversion of erectile dysfunction caused by prostate cancer treatment, by a novel combined stem cell/pharmacological approach (2012)

D. Unrelated grants, funded

19. NIH/NIEHS R21ES019465-01 **(PI: Gonzalez-Cadavid)** 09/01/10-08/31/12
Bisphenol A effects on the peripheral mechanisms of penile erection
Also, administrative minority supplement

20. NIH/NIEHS 1U01ES020887-01 **(PI: Gonzalez-Cadavid)** 10/01/11-09/30/15
Cellular-molecular signature and mechanism of BPA effects on penile erection

CONCLUSIONS

In the case of our initial hypothesis, it is clear through the study of the injured dystrophic muscle in the mdx mouse that although WT MDSC may constitute a general valid approach for potential treatments of DMD, since they improved muscle repair even in these severe conditions, the counteraction of myostatin by using MDSC with myostatin genetic inactivation (Mst KO MDSC) has failed to exert any further improvement, contrary to our expectations. This, combined with the failure to modulate the formation of myotubes in vitro by WT MDSC mainly through myostatin regulating agents, led us to postpone our approach to exert a general pharmacological or biological inhibition of myostatin in the mdx mouse. This may be re-examined once we acquire a better idea of the mechanism of this failure through new grants. If we eventually get funded, we will try to explore the follistatin long-term in vivo approach that we could not pursued because of its excessive cost

To resolve this problem, we reported in Year 4 that we would use other alternatives, such as pharmacological modulation with nitric oxide donors, PDE5 inhibitors, and antioxidants, some of them with FDA approval for other conditions, and hence of potential clinical translation. So far, we have shown that although antioxidants so far were not effective, the first two classes are promising, and we intend to explore them more in depth through the completion of the ongoing studies. But, in addition we intend to test for skeletal muscle repair other approaches that we demonstrated were effective to prevent or ameliorate smooth muscle loss, fibrosis, and oxidative stress. In this sense, the injured skeletal muscle in the aged mdx mouse (for muscular dystrophy and wound healing), and the necrotic ischemic muscle (for critical limb ischemia in diabetes), are good models that we intend to continue using for these new studies.

An important result of this grant is that it led to our recent interaction with two biotechnology industries located in Southern California. We are planning cooperative studies with them that will offer us the possibility of carrying out a series of preclinical and clinical studies, and extensive talks on a series of activities and fund-raising are being conducted. Their products: a stem cell with IND recently issued by FDA for CLI, and an electronic device promoting survival and differentiation, can also be combined with any of our own suggested pharmacological approaches.

At this stage we plan to apply to the Department of Defense AFIRM II for extremity regeneration by regenerative medicine technologies and associated sciences, using these products, and potentially on the CLI model that may mimic the severe necrosis, ischemia and neuropathic damage occurring in combat-related injuries. The advantage of the CLI model is that it is easier to conduct a phase 1 clinical trial within the capabilities of our associated surgical group at Harbor-UCLA Medical Center (Rodney White MD) who are capable to enroll the sufficient number of CLI patients for a phase 1 study. Also, since CLI affects predominantly disadvantaged populations, we will respond to an NIH RFA for Health disparities, and to a CIRM call for projects.

However, DMD continues to be a priority for us and therefore we are discussing a couple of NIH SBIRs, with one of them focusing on DMD by using the repair of muscle injury in the aged mdx mouse as a model, as with our DOD-supported studies on WT MDSC. This may extend to the new CIRM (California Institute of Regenerative Medicine) RFA 12-05 CIRM Strategic Partnership I Awards, since the IND is issued for the proprietary stem cells but the problem will be to find a clinical partner with DMD patients. We will explore this possibility with other centers.

PAID PERSONNEL IN THIS PROJECT

Gonzalez-Cadavid, Nestor F, PhD	PI
Ferrini, Monica G, PhD	LABioMed at Harbor-UCLA site PI Years 1-3
Gelfand, Robert, PhD	Research Associate
Kovanecz, Istvan, PhD	LABioMed at Harbor-UCLA site PI Year 4/no cost ext.
Nolazco, Gaby, MS	Research Assistant
Tsao, James, MD	Research Associate
Vernet, Dolores, PhD	Research Associate

REFERENCES

See references in papers in the Appendix

Effect of muscle-derived stem cells on the restoration of corpora cavernosa smooth muscle and erectile function in the aged rat

Gaby Nolazco*, Istvan Kovanecz*, Dolores Vernet*, Robert A. Gelfand*, James Tsao¶, Monica G. Ferrini*ǂ, Thomas Magee*ǂ§, Jacob Rajfer*ǂ§ and Nestor F. Gonzalez-Cadavid*ǂ§¶

**Los Angeles Biomedical Research Institute at Harbor-UCLA Medical Center, Urology Research Laboratory, §Division of Urology, Harbor-UCLA Medical Center, Torrance, CA, ǂDepartment of Urology, David Geffen School of Medicine at UCLA, Los Angeles, CA, and ¶Department of Internal Medicine, Division of Endocrinology, Charles R Drew University, Los Angeles, CA, USA*

Accepted for publication 18 October 2007

OBJECTIVE

To determine whether skeletal muscle-derived stem cells (MDSCs) convert into smooth muscle cells (SMCs) both *in vitro* and *in vivo*, and in so doing ameliorate the erectile dysfunction (ED) of aged rats, and whether endogenous stem cells are present in the rat corpora cavernosa.

MATERIALS AND METHODS

MDSCs were obtained from mouse muscle, and shown by immunocytochemistry for α-smooth muscle actin (αSMA) to originate *in vitro* in myofibroblasts and SMCs, discriminating SMCs by calponin 1 expression. *In vivo* these MDSCs, labelled with 4′,6-diamidino-2-phenylindole, were implanted into the corpora cavernosa of young adult (5-month old) and aged (20-month old) rats for 2 and 4 weeks. Histological changes were assessed by immunohistochemistry and quantitative Western blot. Functional changes were determined by electrical field stimulation (EFS) of the cavernosal nerve.

RESULTS

The exogenous cells replicated and converted into SMCs, as shown in corporal tissue sections by confocal immunofluorescence microscopy for proliferating cell nuclear antigen (PCNA), αSMA, and smoothelin, and also by Western blot for αSMA and PCNA. MDSC differentiation was confirmed by the activation of the αSMA promoter-linked β-galactosidase in transfected cells, both *in vitro* and after implantation in the corpora. Putative endogenous stem cells were shown in corporal tissue sections and Western blots by detecting CD34 and a possible Sca1 variant. EFS showed that implanted MDSCs raised in aged rats the maximal intracavernosal pressure/mean arterial pressure levels above (2 weeks) or up to (4 weeks) those of young adult rats.

CONCLUSIONS

MDSCs implanted into the corpora cavernosa of aged rats converted into SMCs and corrected ED, and endogenous cells expressing stem cell markers were also found in untreated tissue. This suggests that exogenous stem cell implantation and/or endogenous stem cell modulation might be viable therapeutic approaches for ageing-related ED.

KEYWORDS

erectile dysfunction, corporal fibrosis, corporal veno-occlusive dysfunction

INTRODUCTION

Ageing-related erectile dysfunction (ED) is primarily due to corporal veno-occlusive dysfunction (CVOD) [1,2], as a result of a loss of the corporal smooth muscle cells (SMCs) together with excessive collagen deposition within the corpora, as shown both in man [3–5] and rat models [6–14]. It has been hypothesized that this histological alteration is due to oxidative stress triggered by the release of profibrotic factors such as reactive oxygen species, TGF-β_1, plasminogen activator inhibitor-1, and others, that not only lead to collagen accumulation but also to an increase in apoptosis and a reduction in corporal SMC proliferation [6–14]. As such, it appears as if the ideal way to treat this ageing-related ED would be to reverse or prevent these changes, because such an approach has the potential to become a curative rather than a palliative intervention for this form of ED.

Recently, it was shown experimentally in the aged rat that the long-term and sustained administration of phosphodiesterase-5 (PDE-5) inhibitors not only increases the SMC to collagen ratio within the corpora cavernosa but also improves the underlying CVOD [6]. Such a pharmacological approach has been used successfully in both the rat and man with another form of ED, the post-prostatectomy animal model and the post-prostatectomy patient [4,9,15,16]. In both species, the long-term administration of PDE-5 inhibitors resulted in preservation of the normal SMC to collagen ratio within the corpora.

While it is possible that pharmacological therapy, or even gene therapy [17], may one day prove to be efficacious in reversing ageing-related and other forms of ED in the human, it has recently been reported that the

therapeutic applications of stem cells [18,19] might extend to the replenishment of the corporal SMC population that is impacted by the ageing process. To date, only a few studies of stem cell implantation in experimental models of ED, to repair either nerves or smooth muscle in the corpora, have been conducted [20–23], although stem cells are also being investigated for the repair of other urogenital organs, such as the bladder, urethra, and kidney [24–27]. The first study in the penis [20] was based on the injection of rat embryonic stem cells modified *ex vivo* to express brain-derived nerve growth factor into the corpora cavernosa in a rat model of cavernosal nerve damage. Although there was an improvement in erectile function and neurofilament staining even at 3 months after injection of the stem cells, no surviving stem cells were found nor were any SMC markers investigated, as the primary objective of that study was to achieve nerve regeneration. A more recent report did claim that implantation of human bone marrow mesenchymal stem cells into the normal rat corpora resulted at 2 weeks in the differentiation of these stem cells into both endothelial and SMCs, but retrovirus-immortalized cells and not truly self-replicating cells were used [21]. A more convincing study was performed with native rat bone marrow mesenchymal stem cells engineered to express endothelial nitric oxide synthase, where these stem cells were injected into the corpora cavernosa of aged rats [22]. Not only was ED corrected, but SMC markers were expressed at 3 weeks after implantation.

Stem cells isolated from adult skeletal muscle, or 'muscle-derived stem cells' (MDSCs), have been investigated extensively because of their active prolonged proliferation, low immunogenicity, and ability to convert into several cell lineages after implantation into different organs [28]. MDSCs are not to be confused with regular myoblast or 'satellite cell' preparations. These types of cells are not pluripotent but have been used in clinical trials for treating heart disease as satellite cells may generate active syncitia with cardiomyocytes, or even new cardiomyocytes [29]. MDSCs can be prepared from skeletal muscle biopsies, more accessible for autologous transplants than bone marrow, and as such do not pose the immunogenic risks of embryonic stem cells [28]. MDSCs have been claimed to generate SMCs *in vitro* [30], albeit the SMC characterization was not performed with true SMC markers, such as calponin or smoothelin and particularly *in vivo* after implantation in the urethra in a rat model of stress urinary incontinence [26,31]. Intrapenile injection of MDSCs also improved erectile function in a bilateral cavernosal nerve resection rat model of ED [23], but as the objective was to improve nerve regeneration after bilateral cavernosal nerve resection, no studies on MDSC differentiation into corporal SMCs were performed.

From the above it follows that MDSCs might be preferable to other stem cells for potential clinical applications aimed at restoring functional SMCs in the corpora cavernosa, particularly in ageing-related ED where, as stated, CVOD is the main manifestation. However, the MDSC to SMC differentiation in this context requires further biological characterization and the demonstration that it is functionally effective in a related animal model. Moreover, as we previously characterized stem cells in the human penile tunica albuginea that were able to generate SMCs [32], it is important to determine whether stem cells are also detectable among the SMCs in the corpora cavernosa itself, which could potentially be activated by the paracrine effects of an exogenous implant, or by pharmacological interventions. In the present work we have implanted MDSCs into the corpora in the aged rat model, and studied both their effects on the erectile response to electrical field stimulation (EFS) of the cavernosal nerve, and on their replicative and differentiation ability utilizing immunoblotting, confocal microscopy, and activation of a gene promoter for a SMC marker. We also investigated whether endogenous stem cells are present in the rat penis, specifically in the corpora cavernosa.

MATERIALS AND METHODS

Skeletal muscles were obtained from the hind limb of C57BL/6 mice and MDSCs were isolated applying the pre-plating procedure [33]. The mouse skeletal muscle was preferred because these MDSCs are the only ones prepared by this method that have been extensively characterized as stem cells [28], whereas isolating them from rat skeletal muscle would require us to validate this procedure on the rat cells. Briefly, tissues were dissociated using sequentially collagenase XI, dispase and trypsin, and after filtration through a 60-μm nylon mesh, and pelleting, the released cells were suspended in GM-20, Dulbecco's Modified Eagle's Medium (DMEM)/20% fetal bovine serum (FBS). Cells were then plated onto collagen I-coated flasks for 2 h (pre-plate 1 or pP1), followed by a series of sequential daily decantation of floating cells and platings for 2–6 days, until pP6. The latter is the cell population containing the MDSCs. Fibroblasts are concentrated in the pP2 fraction while satellite cells are essentially in the pP3 and pP4 fractions. Cells were counted in each supernatant. In general, cells were maintained in DMEM/20% FBS on regular culture flasks (no coating) and used in the 15–20th passage, as MDSCs from mouse muscle were properly characterized with stem cell markers have been maintained in our laboratory for at least 40 generations with the same, or even increasing, growth rate. The absence of SMCs in these enriched stem cells was verified at the initial passages by immunocytochemistry and Western blot for αSMC actin (αSMA).

For the *in vitro* experiments involving the activation of the αSMA gene promoter to detect SMC generation, MDSCs were grown onto six-well plates and transfected at 80% confluence with a construct expressing the β-galactosidase gene under this promoter (αSMA Pr-β-gal). The construct was prepared by substituting the rat αSMA 764 bp promoter region [34] (GenBank S76011.1), modified to include Eco RI and Asc I restriction sites at its 5′ end and a Xho I site at its 3′ end, for the cytomegalovirus (CMV) promoter of the pCMVβ plasmid (Clontech, Mountain View, CA, USA) upstream from the full length *E. coli* β-galactosidase gene. On the following day, cells were transferred to DMEM with 2.5% FBS and TGF-β_1 at 5 ng/mL to induce differentiation, and maintained for 6 days. Cells were then fixed with 1% glutaraldehyde, stained with 5-bromo-4-chloro-3-indolyl-β-D-galactopyranoside (X-gal) [35], and counterstained with Fast Red. For *in vivo* implantation, the MDSCs were transfected similarly and cultured for 7 days in DMEM/20% FBS.

Male Fisher 344 rats (Harlan Sprague-Dawley Inc., San Diego, CA, USA), of 20 months of age ('aged') were used for EFS determinations and some histological/biochemical detections (eight/group/period), while we used 5-month-old rats ('young adult') only for some preliminary non-EFS assays (four/period). The rats were treated according to National Institutes of Health (NIH)

regulations with an Institutional Animal Care and Use Committee-approved protocol. The MDSCs ($0.5–1.0 \times 10^6$ cells/50 μL Hanks) were labelled with the nuclear fluorescent stain 4′,6-diamidino-2-phenylindole (DAPI) and implanted aseptically into two different sites in the mid-part of the shaft in anaesthetized rats. Tacrolimus was given daily (1 mg/kg, s.c.) to avoid immuno-rejection of the mouse stem cells. At 1, 2, and 4 weeks after implantation, rats were either killed (1, 2, 4 weeks, young adult rats only), or underwent EFS and then killed (2 and 4 weeks, aged rats only). An additional group of four young adult rats was similarly implanted with MDSCs transfected with the αSMA-β galactosidase construct and killed at 5 and 10 days. For tissue excision, rats were perfused with saline under anaesthesia, killed, then the penises were excised and denuded, and small portions of the penile shaft tissue were cryoprotected in 25% sucrose, immersed in OCT, and cryosectioned (5 μm for regular microscope, or 20–30 μm for confocal microscope) with no fixation. The remainder of the penile shaft tissue was frozen in liquid nitrogen and stored at −80 °C.

Cells on collagen-coated eight-well removable chambers and frozen tissue sections, were reacted [8–10,15,16,32] with some of the following primary antibodies against: (i) human myosin heavy chain type II (MHC-II; monoclonal, 1:200 Vector Laboratories, Burlingame, CA, USA), a marker for skeletal myotubes; (ii) human αSMA (mouse monoclonal in Sigma kit, 1:2, Sigma Chemical, St Louis, MO, USA), a marker for both SMC and myofibroblasts; (iii) human calponin-1 (basic mouse monoclonal, 1:25, Novocastra, Burlingame, CA, USA) and (iv) chicken smoothelin (mouse monoclonal, 1:100, Abcam, Cambridge, MS, USA), two exclusive markers for SMCs; (v) proliferating cellular nuclear antigen (PCNA) (mouse monoclonal, 1:100, Chemicon, Temecula, CA, USA) a marker for replicating cells; (vi) human CD34 (rabbit polyclonal, 1:200, Santa Cruz Biotechnology, Santa Cruz, CA, USA), a stem cell marker; and (vii) mouse Sca1 (rat monoclonal, 1:200, BD Pharmigen, Franklin Lake, NJ, USA) another stem cell marker.

For cells not previously labelled with DAPI, cultures or tissue sections were subjected to immunohistochemical detection by quenching in 0.3% H_2O_2-PBS, blocking with goat (or corresponding serum), and incubated overnight at 4 °C with the primary antibody. This was followed by biotinylated anti-mouse IgG (Vector Laboratories), respectively, for 30 min, the ABC complex containing avidin-linked horseradish peroxidase (1:100; Vector Laboratories), 3,3′ diaminobenzidine, and counterstaining with haematoxylin, or no counterstaining.

For cells labelled with DAPI, fluorescent detection techniques were used. The secondary anti-mouse IgG antibody was biotinylated (goat, 1:200, Vector Laboratories) and this complex was detected with streptavidin-Texas Red. For the CD34 detection we used a biotinylated anti-rabbit IgG (goat, 1:200, Vector Laboratories). After washing with PBS, the sections were mounted with Prolong antifade (Molecular Probes, Carlsbad, CA, USA). Negative controls in all cases omitted the first antibodies or were replaced by IgG isotype.

The sections were viewed under an Olympus BH2 fluorescent microscope or in a confocal using blue and/or red filters and overlay. Confocal fluorescence images were taken with a confocal microscope (Leica TCS-SP, Heidelberg, Germany), equipped with an argon laser (488 nm blue excitation: JDS Uniphase), a diode laser (DPSS; 561 nm, yellow-green excitation: Melles Griot), a helium-neon laser (633 nm, red). Spectral emission filters were set at 500–550 nm for green fluorescence and 580–700 nm for red fluorescence. Cytochemistry for alkaline phosphatase to detect osteoblasts *in vitro* was performed as described previously [32]. For quantitative image analysis, staining intensity was determined by computerized densitometry using the ImagePro Plus 5.1 program (Media Cybernetics, Silver Spring, MD, USA), coupled to the Olympus BH2 microscope with a Spot RT colour digital camera (Diagnostic Instruments Inc., Sterling Heights, MI, USA). The number of positive cells was expressed as a percentage of the total cells. In all cases, five non-overlapping fields were screened per well.

For Western blots [8–10,15,32], cell homogenates were obtained in boiling lysis buffer (1% SDS, 1 mM sodium orthovanadate, 10 mM Tris pH 7.4 and protease inhibitors: 3 μM leupeptin, 1 μM pepstatin A, 1 mM phenylmethylsulphonyl fluoride), and centrifuging at 16 000***g*** for 5 min, 30 μg of protein were run on 7.5% or 10% polyacrylamide gels, and submitted to Western blot and immunodetection with the antibodies against PCNA, CD34, and Sca1 described above, or with an antibody against human αSMA (monoclonal, 1:1000, Calbiochem, La Jolla, CA, USA). Membranes were incubated with a secondary polyclonal horse anti-mouse IgG linked to horseradish peroxidase (1:2000; BD Transduction Laboratories, Franklin Lakes, NJ, USA, or 1:5000, Amersham GE, Pittsburgh, PA, USA) and bands were visualized with luminol (Pierce, Rockford, IL, USA). In the case of Sca1, the secondary peroxidase-linked antibody was anti-rat IgG (rabbit, 1:2000, Sigma Chemical). For the negative controls the primary antibody was omitted.

EFS in the rat was performed as described previously [36,37]. Briefly, under anaesthesia, the cavernosal nerve was exposed, and hooked by a bipolar platinum electrode. Systemic arterial and intracavernosal pressure measurements were obtained by simultaneous intrafemoral artery and cavernosal catheterization, respectively. EFS was applied at 10 V and a frequency of 15 Hz for pulses of 60 s, separated by 2-min intervals, with a Grass Stimulator (Grass Instruments Co., Quincy, MA, USA). A data acquisition system (Biopac Systems, Santa Barbara, CA, USA) simultaneously recorded arterial blood and intracavernosal pressure, and values were expressed in mmHg. The ratio between the maximal intracavernosal pressure (MIP) and the mean arterial pressure (MAP) at the peak of erectile response were calculated, to normalize for variations in blood pressure.

Values are expressed as the mean (SEM). The normality distribution of the data was established using the Wilk–Shapiro test. Multiple comparisons were analysed by a single factor ANOVA, followed by *post hoc* comparisons with the Newman–Keuls test. Differences among groups were considered statistically significant at $P < 0.05$.

RESULTS

The mouse MDSCs obtained by the pre-plate procedure were ≈1% of the original mononucleated cell population extracted from the normal mouse skeletal muscle and ≈60% bound to Sca1-coated magnetic beads, indicating that this cell fraction expressed the stem cell marker Sca1 (not shown). When the total non-Sca1-selected MDSCs were incubated for 3 weeks in myogenic differentiation medium, they underwent

FIG. 1. MDSCs incubated in vitro generated myotubes, myofibroblasts, osteoblasts, and SMCs. MDSCs were incubated in myogenic medium for 3 weeks (A), fibrogenic medium for 2 weeks (B), osteogenic medium for 4 weeks (C), and regular medium at low serum/rapamycin [38] for 4 weeks (D), and differentiation was assayed by immunocytochemistry for MHC-II (A), αSMA (B), calponin (D), or histochemistry for alkaline phosphatase (AP; C), on six-well plates and transferred to eight-well removable chambers before staining. Quantitative image analysis was applied on B and C (Bar graphs). A, D: ×200; B, C: ×400.

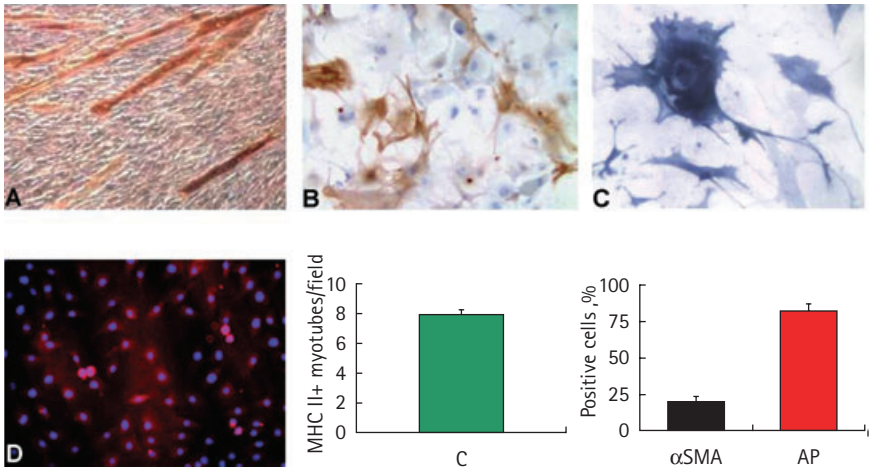

FIG. 2. MDSCs implanted into the rat corpora cavernosa remained proliferating after 2 weeks of implantation. DAPI-labelled MDSCs (0.8×10^6 cells) were injected into the corpora cavernosa of young adult rats, and frozen penile sections were stained with propidium iodide (top panels), or with biotinylated antibody for PCNA detecting with streptavidin-Texas Red (bottom panels). Images were obtained with blue (A, D) and red (B, E) filters in a regular fluorescent microscope and merged (C, F). Top: ×100, bottom: ×200.

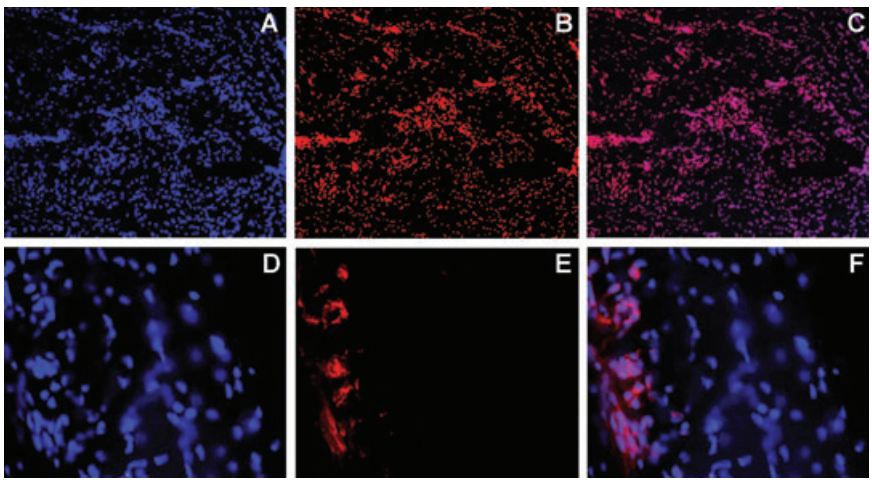

conversion into multinucleated skeletal myotubes that expressed MHC-II and are equivalent to the skeletal myofibers (Fig. 1A). The myogenically committed precursors, the satellite cells [28], were excluded in the initial platings by their faster adhesion to the culture flasks. The MDSCs were also able to convert into myofibroblasts and osteoblasts when they were incubated, respectively, in fibrogenic medium, containing TGF-β_1 for 2 weeks, as detected by αSMA (which also is expressed in SMCs) combined with the typical morphology for the actin filaments (Fig. 1B), or in osteogenic medium for 4 weeks, as detected by alkaline phosphatase (Fig. 1C). The MDSC conversion into SMCs was assessed for 4 weeks in DMEM-2.5% FBS and 20 nM rapamycin to enhance the contractile phenotype [38] by another SMC marker that is not expressed in myofibroblasts, namely calponin. In this case, the MDSCs were labelled with DAPI and calponin identified by immunodetection with Texas Red fluorescence, observing the positive cells in magenta colour in the overlay of the blue and red filters (Fig. 1D). Although only a few cells per field intensively expressed calponin, many others had a faint or moderate expression. Quantitative image analysis (Fig. 1E) showed substantial skeletal myotube formation by the MDSCs (≈eight per field), as well as a 20% conversion into myofibroblasts and/or SMCs, and 80% into osteoblasts. The SMCs were not quantified because of the variable levels of calponin expression in the fields.

The MDSC were then labelled with DAPI, and injected into the corpora cavernosa of young adult rats, that were immunosuppressed with tacrolimus to prevent a potential inter-species immunorejection, and killed at 1, 2, and 4 weeks after implantation. Representative pictures of cryosections around the site of injection at 2 weeks showed the presence of abundant DAPI-labelled MDSCs around the corpora cavernosa cisternae that were inserted in between endogenous cells whose nuclei were propidium iodide positive but DAPI negative (Fig. 2A vs B). The merge (overlay) of both images shows in magenta the implanted MDSC nuclei (Fig. 2C). In other fields (not shown), a much lower fraction of the MDSC nuclei were present (DAPI+) among the propidium iodide labelled total nuclei. Not all the implanted MDSCs were in active replication, as indicated by the comparison of DAPI-stained nuclei (Fig. 2D) with cells immunostained for PCNA, a marker of proliferation, that were concentrated in a certain region (Fig. 2E,F). Essentially the same was observed at 1 week, and replicative cells were also seen at 4 weeks (not shown).

The conversion of the implanted MDSCs into SMCs that line up the corpora cavernosa cisternae was suggested by αSMA staining, using a fluorescent confocal microscope that produces optical sections of ≤0.5 μm thickness. This allowed colocalization of the implanted nuclei after a longer period (4 weeks) (Fig. 3, top A,C) with the αSMA positive cells (Fig. 3B), thus eliminating potential artifacts from overlapping planes. Confirmation was obtained by immunofluorescence staining with smoothelin, a specific SMC marker, which in addition to calponin is not expressed in myofibroblasts that showed many magenta

cells concentrated around the cisternae in the overlay (Fig. 3, top D, F vs E). MDSC implantation increased the αSMA content of the penile shaft tissue, assayed by Western blot, as compared with penises that were not implanted with cells (Fig. 3, bottom), although a larger *n* is required to confirm this visual assessment. However, there was no stimulation of cell proliferation in the injected tissues, as indicated by PCNA.

MDSC conversion into SMCs involves transcriptional activation of genes related to the contractile phenotype, such as αSMA, and this process is a direct indicator of the generation of SMCs and potentially of myofibroblasts. We constructed a plasmid expressing a reporter gene (β-galactosidase) under the control of the αSMA promoter, and transfected separately cultures of rat SMCs (Fig. 4A) and of mouse MDSCs (Fig. 4B), which were then incubated for 7 days with TGF-β_1, as a differentiation factor [39,40]. β-galactosidase was detected histochemically in blue staining, and all nuclei were identified by Fast Red counterstain. Only a small fraction of morphologically distinctive SMCs exhibited activation of the αSMA promoter, probably as a reflection of most cells being already in the contractile phenotype, with little *de novo* αSMA activation (Fig. 4A). In the case of the MDSCs, as only a fraction of cells were expected to differentiate, and the period of incubation was short, αSMA activation was confined therefore to even fewer cells (Fig. 4B). *In vivo,* the injection of DAPI-labelled MDSCs into the corpora cavernosa for 5 and 10 days, identified by blue fluorescent nuclei (Fig. 4C), was accompanied by the appearance of some histochemically detected blue cells in the smooth muscle region of the corpora (Fig. 4D). In this case, no overlay was possible, as the glutaraldehyde fixation or the β-galactosidase histochemical staining quenches DAPI. Therefore, images are from the same well/section but not from identical sites.

The ability of the corpora cavernosal tissue to stimulate the differentiation of exogenous stem cells, such as the MDSCs, suggests that this could also be the case with endogenous stem cells that may be present in the adult penis, and that might be activated for a differentiation process by the paracrine effects of exogenous MDSCs. We have previously identified stem cells in fibroblast cultures from the human tunica albuginea, which generated SMCs *in vitro* [32]. Sca1 and

FIG. 3. Confocal microscopy confirmed the expression of SMC markers in DAPI-labelled MDSCs implanted into the corpora cavernosa, and the subsequent increase of corporal SMCs was revealed by Western blot. Frozen sections adjacent to those examined in Fig. 2 were immunostained for αSMA (top micrographs) or smoothelin (bottom micrographs) and examined in optical sections of 0.5 μm using a confocal microscopy. Bottom: the remaining tissues from penises injected with MDSCs and control penile tissue that was not implanted with cells were homogenized and subjected to Western blot for αSMA and PCNA loading equal amounts of protein (all ×200).

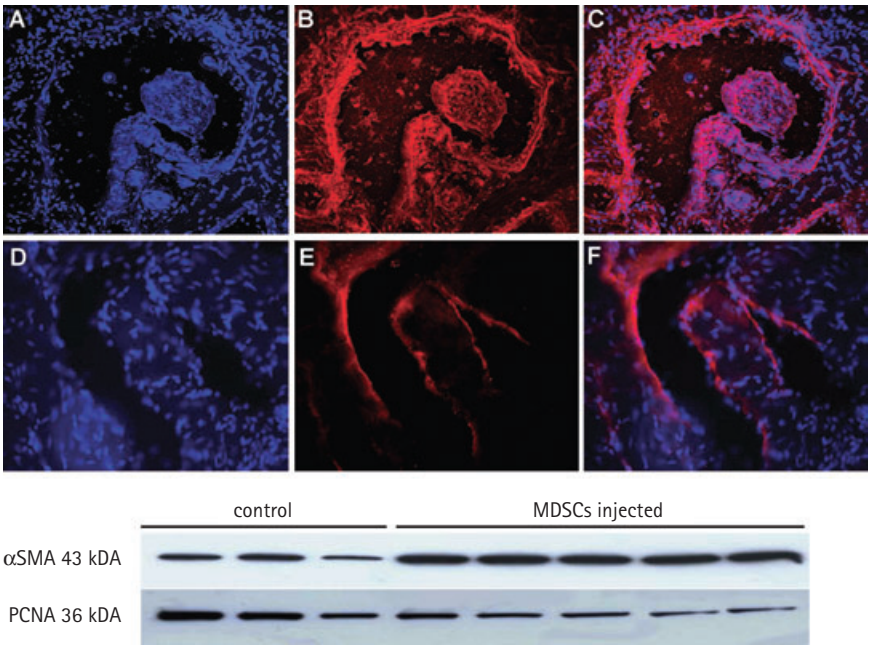

CD34, two markers expressed in MDSCs, with the latter also previously detected in tunical multipotent cells [33], were also detected in corpora cavernosa tissue sections obtained from young rat penises that were not implanted with MDSCs. This was shown first for CD34 by immunohistochemistry, where many positive cells were distributed all along the tunica albuginea (Fig. 5, top left; solid arrows) interspersed with a few CD34 negative cells (broken arrows). They were also identified in scattered clusters in the corpora cavernosa (Fig. 5, top right). Immunofluorescence using a secondary antibody linked to Texas Red confirmed this extensive distribution in the tunica (Fig. 5, middle left) contrasted with only a few in the corpora (Fig. 5, middle right). Western blot analysis of penile tissue homogenates from young and old rats showed the presence of the expected 97 kDa band (Fig. 5, bottom panel).

By contrast, Sca1 was negative in the tunica albuginea and showed some positive cells along the corporal cisternae and the arterial media, both by immunohistochemistry (Fig. 6, top left) and immunofluorescence (Fig. 6, top right). However, the expected 18 kDa Sca1 band was only visible in extracts from low-passage Sca1-positive MDSCs that had been selected with immunobeads carrying the Sca1 antibody. The high-passage nonselected MDSCs used in this work had lost completely this antigen upon culture, as shown by the absence of any band, and remarkably, the penile shaft homogenates, both from young and old rats, displayed an ≈36–38 kDa band assumed to be a dimer of the typical Sca1 protein (Fig. 6, bottom panel).

The therapeutic efficacy of the MDSCs implanted into the corpora was assessed by a functional determination. Aged male rats (20-month-old), that are an accepted model of ED, and specifically CVOD [6,8,36,37], were injected with 0.5–1 × 10^6 MDSCs, and received tacrolimus, as above, for 2 and 4 weeks. Control rats received saline. The measurement of erectile function was conducted by EFS of the cavernosal nerve [36,37]. When compared with the control untreated aged rats (Fig. 7A) the MIP/MAP ratio in the aged rats, 2 weeks after

FIG. 4. MDSCs were able to activate in vitro the αSMA promoter when stimulated with TGF-β1, or when injected in vivo into the corpora cavernosa. Rat corporal SMCs (A) or mouse MDSCs (B) were transfected in vitro with a plasmid expressing β-galactosidase under the αSMA promoter and were incubated for 7 days in the presence of TGF-β1 to induce αSMA expression. Wells were stained with X-gal and Fast Red. DAPI-labelled MDSCs were also injected into the penile corpora cavernosa of adult rats, and the penile tissue was dissected. Frozen-tissue sections obtained for examining DAPI nuclei (C) and then subjected to X-gal staining (D). Micrographs were obtained in the same section but not necessarily the same fields (no overlapping). A, C: ×100, B: ×400, D: ×200.

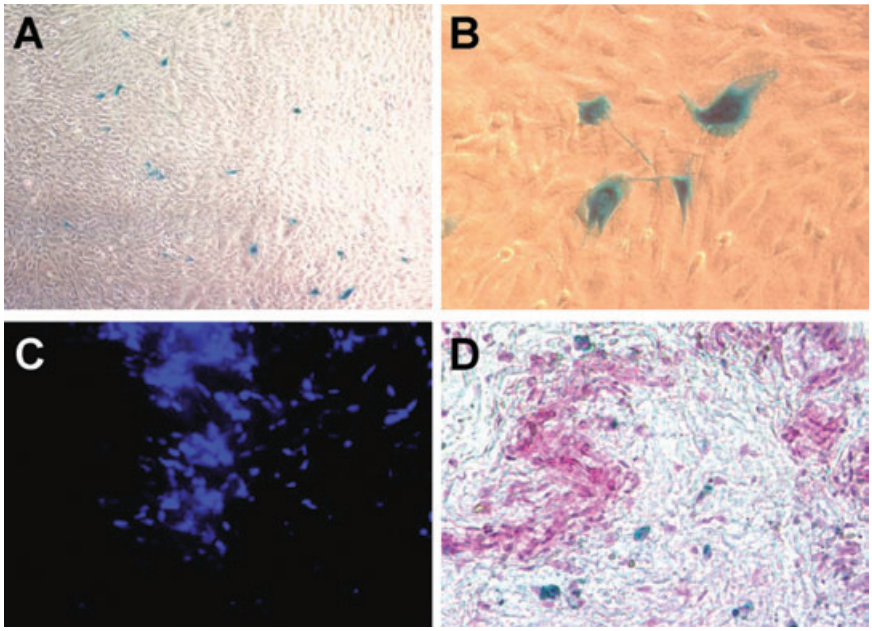

FIG. 5. Stem cell marker CD34 was expressed endogenously in the tunica albuginea and corporal tissue of rats not implanted with MDSCs. Top panels: Tissue sections from penises of young adult rats (not injected with MDSCs) were stained for CD34 using either secondary antibody linked to peroxidase (top) or the fluorescent biotinylated secondary antibody and streptavidin Texas Red (middle), and examined in the tunical and trabecular regions (×400). Bottom panel: Western blot for CD34, conducted in penile tissue homogenates from the same rats, as well as from aged rats.

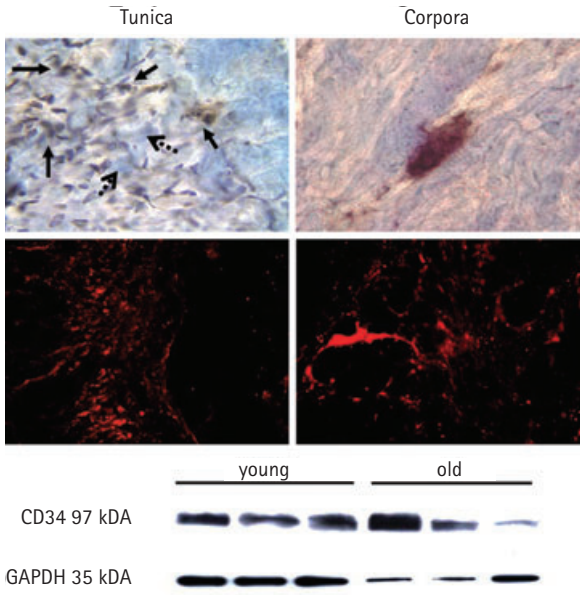

implantation of the MDSCs (Fig. 7B), was significantly increased to 1.13 (0.2), a value above the one usually seen in adult rats 0.8 (0.05) [34,36,37,41–43]. In two of these MDSC-implanted rats, the MIP was up to surprisingly 125 mmHg, a value rarely seen in this species. When another series of rats was tested after 4 weeks of MDSC transplantation (Fig. 7C), although the mean MIP/MAP decreased to 0.72 (0.05), this ratio was still significantly higher than in the untreated aged rats and close to that seen in 5-month-old adult rats. In all these treated aged rats, both at 2 and 4 weeks, DAPI-positive MDSCs were detected in the penile corpora cavernosa, and they were in active replication and differentiating into SMCs (not shown).

DISCUSSION

The present study shows that MDSCs can convert into SMCs when implanted into the rat corpora cavernosa and can correct ageing-related ED for at least several weeks after implantation. The study confirms the potential efficacy of stem cells to replace cavernosal SMCs that are lost or functionally damaged in the penis during the ageing process and by so, it appears to restore the normal compliance of the tissue. These findings agree with those recently reported using bone marrow stem cells and achieved comparable results [22].

The relatively low *in vitro* conversion of the MDSCs into SMCs was compensated by the reasonable differentiation efficacy seen *in vivo*, possibly because of the influence by paracrine factors secreted by the corporal tissue. In addition, as skeletal muscle biopsies are easier to obtain than other sources of stem cells, the present results suggest that they could become an alternative supply of implantable cells more acceptable to patients with ED, if stem cells are eventually used to treat ED, specifically the myopathy that occurs with ageing. Adult autologous stem cells from different sources are already being tested in clinical trials for other conditions (see list under 'stem cells' in http://www.clinicaltrials.gov), and even if they are less efficient than embryonic stem cells, they pose lower immunogenic and carcinogenic risks.

The present results also suggest that endogenous stem cells might be present in the penile corpora cavernosa, thus extending our previous report of these multipotent cells in the human tunica albuginea [32]. We have now seen that many, if not most, cells in the tunica are CD34 positive, which suggests that this marker is also expressed in fibroblasts, the most predominant cell type in this tissue, and possibly in the stem cells previously identified by differentiation assays similar to the ones applied now to MDSCs. Confirming our previous results, no Sca1-positive cells were

FIG. 6. Stem cell marker Sca1 was expressed endogenously in corporal tissue but not in the tunica albuginea (rats not implanted with MDSCs). Top panels: Tissue sections from penises of young adult rats not injected with MDSCs were stained for Sca1 using either secondary antibody linked to peroxidase (top left) or the fluorescent biotinylated secondary antibody and streptavidin Texas Red (top right), and examined in the tunical and trabecular regions (left, ×400; right, ×200). Bottom panel: Western blot for Sca1, conducted in penile tissue homogenates from the same rats, as well as from aged rats. Sca1+, MDSCs selected for Sca1 expression, low passage; NS, nonselected MDSCs at high passage.

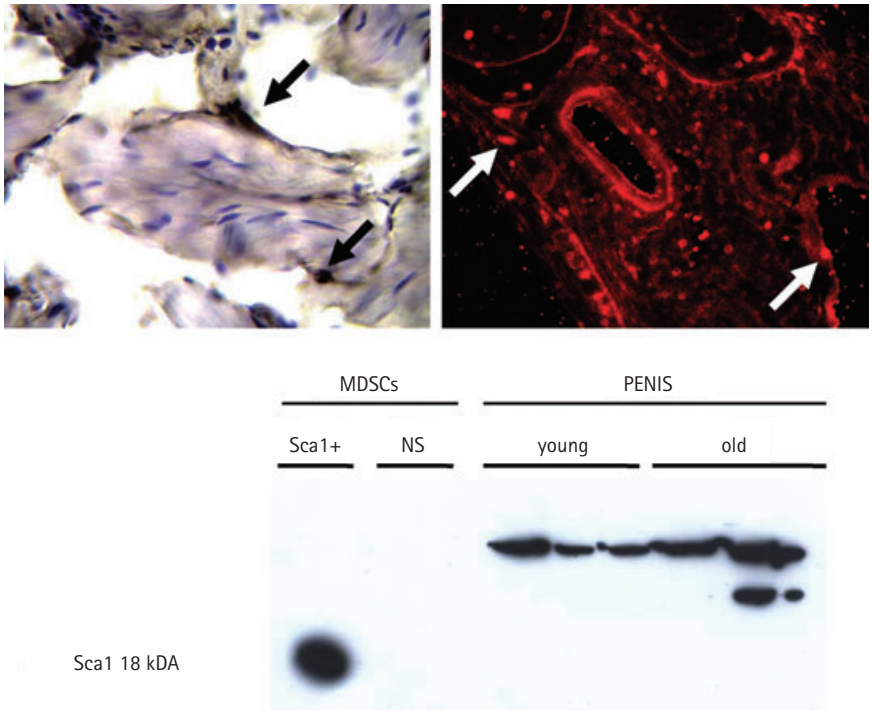

*FIG. 7. MDSC implantation into the corpora cavernosa stimulated the erectile response to EFS in aged rats. 20-month-old rats were injected with MDSCs (B, C) or with saline as controls (A) and subjected to EFS after 2 (B) and 4 weeks (C). *P < 0.05; **P < 0.01.*

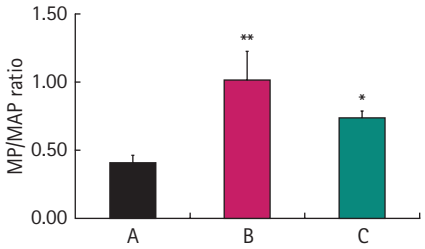

identified in the tunica. However, in the corpora both markers were detected, albeit in just a few cells, and in the case of Sca1 the size of the protein suggests an isoform or dimer. It remains to be established whether both markers in the corpora are expressed in the same cells, like the low-passage MDSCs, and whether cells expressing Sca1 and/or CD34 are indeed multipotent like their tunical counterpart. If they are, this may open up a complementary approach to MDSC implantation, by the potential modulation of endogenous stem cells to achieve similar effects. Interestingly, both nitric oxide and cGMP, physiological mediators of penile erection whose levels can be increased pharmacologically, have been shown to trigger stem cell differentiation [44–46], and therefore they could constitute new approaches to awaken dormant stem cells.

As αSMA is also a marker of myofibroblasts, the use of confocal microscopy, with its ability to discriminate between overlapping planes and thus exclude artefacts, in combination with the detection of calponin and smoothelin as SMC markers, and the *in vitro* and *in vivo* activation of the αSMA promoter in transfected cells, provides a more precise confirmation that the MDSCs convert into SMCs than by simply using αSMA detection and regular microscopy alone. This is important, because by αSMA being also a marker of myofibroblasts, involved in penile fibrosis, the risks of inducing this cell type must be considered [47,48]. Further work is needed to conclusively exclude this possibility *in vivo*. Even with this caveat, the present validation of MDSC conversion into SMCs supports the use of MDSCs for ageing-related ED, in a fashion similar to their postulated use for the regeneration of SMCs in the bladder and urethra [25,26,31], albeit if the latter was essentially based on αSMA detection. The present results appear to be the first to show *in vitro* the conversion of MDSCs into SMCs based on a true SMC marker, as a previous study used only αSMA [30].

The present data, taken together with the previous study with bone marrow stem cells tested in a rat model of ageing-related ED [22], establishes the proof of concept for the efficacy of stem cell therapy in regenerating SMCs that undergo apoptosis in the corpora cavernosa during ageing and other conditions, and thus for ameliorating vasculogenic ED. It may even be assumed that other cell lineages, e.g. nerves, endothelium, might be also generated by the MDSCs, and thus would compensate for the relative loss of nitrergic nerves in the corpora cavernosa [49] and some degree of endothelium damage in this tissue [50] that occurs in the corpora during ageing. The multipotency of the MDSCs could therefore be an asset in certain ED conditions where not only SMCs are lost, but there is nerve damage, such as in rat models of ED in diabetes [10] and after radical prostatectomy [7,9,13–16]. In the latter case, both embryonic stem cells and MDSCs themselves have shown initial promise [20,23].

Despite this encouraging proof of concept, as in the field of gene therapy [17], further animal studies are needed before attempting to transplant stem cells in the clinic, and MDSCs in particular, for the therapy of ED. First, when using the rat as host, a truly allogenic source of MDSCs has to be tested, e.g. rat MDSCs, to eliminate the need for pharmacological immunosuppression or an immunodeficient strain. Second, in the present study, as well as the other parallel work with bone marrow cells [22], the effects were comparatively short-lived, as in our case, the considerable stimulation of erectile function achieved at 2 weeks was reduced at 4 weeks, albeit still remaining at the normal

levels of an adult rat. This reduction in the MIP/MAP ratio over time might be because one rat in this group had evidence of a pre-existent testis tumour and was also adversely affected by tacrolimus. Therefore, new research has to be conducted to improve the survival of these cells and assure that the salutary functional effects can be prolonged for at least 3–6 months to exclude transient amelioration. Third, the detection of donor cells in the corporal tissue at these long-term treatments would require the use of stable markers, such as cells from transgenic rats expressing green fluorescent protein, or selected new exogenous cell markers in lieu of fluorescent tags that are diluted along cell proliferation.

Despite these hurdles, stem cell therapy for ED, specifically with MDSCs, is a promising approach, particularly combined with *ex vivo* gene transfer, as achieved previously with endothelial nitric oxide synthase [22]. The list of potential genes is as extensive as in the case of non cell-mediated gene therapy, but in this case, cell modification may involve strategies to prevent undesirable myofibroblast generation and thus fibrosis. Alternatively, the engineering may aim to intensify the differentiation capacity of stem cells into the main desired cell line, such as SMCs, without reducing their multipotency to form simultaneously ancillary cell types, such as endothelial or neural cells according to needs. Another strategy would involve combined pharmacological, or gene therapy, treatment to enhance stem cell survival, e.g. by stimulating trophic factors and access to nutrients through improving a potentially defective angiogenesis in aged animals [51]. However, perhaps the greatest challenge would be to engineer by gene transfer exogenous stem cells to paracrinely awake the dormant stem cells in the penis and generate damaged or lost differentiated cells, or to directly stimulate pharmacologically a similar commitment for the endogenous stem cells.

ACKNOWLEDGEMENTS

This work was supported by grants NIH R01DK-53069, Department of Defense PC061300 and in certain aspects, NIH G12RR-03026. Dr Ferrini and Dr Magee are also supported by Grant N1 P20 MD000545 from the National Center on Minority Health and Health Disparities, NIH.

CONFLICT OF INTEREST

None declared.

REFERENCES

1 **Rajfer J, Rosciszewski A, Mehringer M.** Prevalence of corporeal venous leakage in impotent men. *J Urol* 1988; **140**: 69–71
2 **Mulhall JP, Slovick R, Hotaling J *et al.*** Erectile dysfunction after radical prostatectomy: hemodynamic profiles and their correlation with the recovery of erectile function. *J Urol* 2002; **167**: 1371–5
3 **Iacono F, Giannella R, Somma P, Manno G, Fusco F, Mirone V.** Histological alterations in cavernous tissue after radical prostatectomy. *J Urol* 2005; **173**: 1673–6
4 **Schwartz EJ, Wong P, Graydon RJ.** Sildenafil preserves intracorporeal smooth muscle after radical retropubic prostatectomy. *J Urol* 2004; **171**: 771–4
5 **Yaman O, Yilmaz E, Bozlu M, Anafarta K.** Alterations of intracorporeal structures in patients with erectile dysfunction. *Urol Int* 2003; **71**: 87–90
6 **Ferrini MG, Kovanecz I, Sanchez S *et al.*** Long-term continuous treatment with sildenafil ameliorates aging-related erectile dysfunction and the underlying corporal fibrosis in the rat. *Biol Reprod* 2007; **76**: 915–23
7 **Podlasek CA, Meroz CL, Tang Y, McKenna KE, McVary KT.** Regulation of cavernous nerve injury-induced apoptosis by sonic hedgehog. *Biol Reprod* 2007; **76**: 19–28
8 **Kovanecz I, Ferrini MG, Vernet D, Nolazco G, Rajfer J, Gonzalez-Cadavid NF.** Ageing-related corpora veno-occlusive dysfunction in the rat is ameliorated by pioglitazone. *BJU Int* 2007; **100**: 867–74
9 **Kovanecz I, Rambhatla A, Ferrini MG *et al.*** Chronic daily tadalafil prevents the corporal fibrosis and veno-occlusive dysfunction (CVOD) that occurs after cavernosal nerve resection. *BJU Int* 2008; **101**: 203–10
10 **Kovanecz I, Ferrini MG, Vernet D, Nolazco G, Rajfer J, Gonzalez-Cadavid NF.** Pioglitazone prevents corporal veno-occlusive dysfunction in a rat model of type 2 diabetes mellitus. *BJU Int* 2006; **98**: 116–24
11 **Jiang R, Chen JH, Jin J, Shen W, Li QM.** Ultrastructural comparison of penile cavernous tissue between hypertensive and normotensive rats. *Int J Impot Res* 2005; **17**: 417–23
12 **Bakircioglu ME, Sievert KD, Nunes L, Lau A, Lin CS, Lue TF.** Decreased trabecular smooth muscle and caveolin-1 expression in the penile tissue of aged rats. *J Urol* 2001; **166**: 734–8
13 **User HM, Hairston JH, Zelner DJ, McKenna KE, McVary KT.** Penile weight and cell subtype specific changes in a post-radical prostatectomy model of erectile dysfunction. *J Urol* 2003; **169**: 1175–9
14 **Leungwattanakij S, Bivalacqua TJ, Usta MF *et al.*** Cavernous neurotomy causes hypoxia and fibrosis in rat corpus cavernosum. *J Androl* 2003; **24**: 239–49
15 **Kovanecz I, Rambhatla A, Ferrini MG *et al.*** Long-term continuous sildenafil treatment ameliorates corporal veno-occlusive dysfunction (CVOD) induced by cavernosal nerve resection in rats. *Int J Impot Res* 2007 September 20 [Epub ahead of print]; doi: 10.1038/sj.ijir.3901612
16 **Ferrini MG, Davila HH, Kovanecz I, Sanchez SP, Gonzalez-Cadavid NF, Rajfer J.** Vardenafil prevents fibrosis and loss of corporal smooth muscle that occurs after bilateral cavernosal nerve resection in the rat. *Urology* 2006; **68**: 429–35
17 **Melman A.** Gene transfer for the therapy of erectile dysfunction: progress in the 21st century. *Int J Impot Res* 2006; **18**: 19–25
18 **Mimeault M, Hauke R, Batra SK.** Stem cells: a revolution in therapeutics-recent advances in stem cell biology and their therapeutic applications in regenerative medicine and cancer therapies. *Clin Pharmacol Ther* 2007; **82**: 252–64
19 **Becker C, Jakse G.** Stem cells for regeneration of urological structures. *Eur Urol* 2007; **51**: 1217–28
20 **Bochinski D, Lin GT, Nunes L *et al.*** The effect of neural embryonic stem cell therapy in a rat model of cavernosal nerve injury. *BJU Int* 2004; **94**: 904–9
21 **Song YS, Lee HJ, Park IH, Kim WK, Ku JH, Kim SU.** Potential differentiation of human mesenchymal stem cell transplanted in rat corpus cavernosum toward endothelial or smooth muscle cells. *In J Impot Res* 2007; **19**: 378–85
22 **Bivalacqua TJ, Deng W, Kendirci M *et al.*** Mesenchymal stem cells alone or *ex vivo* gene modified with endothelial nitric

oxide synthase reverse age-associated erectile dysfunction. *Am J Physiol Heart Circ Physiol* 2007; **292**: H1278–90
23 **Kim Y, de Miguel F, Usiene I *et al.*** Injection of skeletal muscle-derived cells into the penis improves erectile function. *Int J Impot Res* 2006; **18**: 329–34
24 **Mitterberger M, Pinggera GM, Marksteiner R *et al.*** Adult stem cell therapy of female stress urinary incontinence. *Eur Urol* 2008; **53**: 169–75
25 **Frimberger D, Lin HK, Kropp BP.** The use of tissue engineering and stem cells in bladder regeneration. *Regen Med* 2006; **1**: 425–35
26 **Rodriguez LV, Alfonso Z, Zhang R, Leung J, Wu B, Ignarro LJ.** Clonogenic multipotent stem cells in human adipose tissue differentiate into functional smooth muscle cells. *Proc Natl Acad Sci USA* 2006; **103**: 12167–72
27 **Rastogi A, Nissenson AR.** The future of renal replacement therapy. *Adv Chronic Kidney Dis* 2007; **14**: 249–55
28 **Urish K, Kanda Y, Huard J.** Initial failure in myoblast transplantation therapy has led the way toward the isolation of muscle stem cells: potential for tissue regeneration. *Curr Top Dev Biol* 2005; **68**: 263–80
29 **Engelmann MG, Franz WM.** Stem cell therapy after myocardial infarction: ready for clinical application? *Curr Opin Mol Ther* 2006; **8**: 396–414
30 **Hwang JH, Yuk SH, Lee JH *et al.*** Isolation of muscle derived stem cells from rat and its smooth muscle differentiation [corrected]. *Mol Cells* 2004; **17**: 57–61
31 **Kwon D, Kim Y, Pruchnic R *et al.*** Periurethral cellular injection: comparison of muscle-derived progenitor cells and fibroblasts with regard to efficacy and tissue contractility in an animal model of stress urinary incontinence. *Urology* 2006; **68**: 449–54
32 **Vernet D, Nolazco G, Cantini L *et al.*** Evidence that osteogenic progenitor cells in the human tunica albuginea may originate from stem cells: implications for Peyronie's disease. *Biol Reprod* 2005; **73**: 1199–210
33 **Qu-Petersen Z, Deasy B, Jankowski R *et al.*** Identification of a novel population of muscle stem cells in mice: potential for muscle regeneration. *J Cell Biol* 2002; **157**: 851–64
34 **Blank RS, McQuinn TC, Yin KC *et al.*** Elements of the smooth muscle alpha-actin promoter required in cis for transcriptional activation in smooth muscle. Evidence for cell type-specific regulation. *J Biol Chem* 1992; **267**: 984–9
35 **Ma W, Rogers K, Zbar B, Schmidt L.** Effects of different fixatives on beta-galactosidase activity. *J Histochem Cytochem* 2002; **50**: 1421–4
36 **Magee TR, Kovanecz I, Davila HH *et al.*** Antisense and short hairpin RNA (shRNA) constructs targeting PIN (Protein Inhibitor of NOS) ameliorate aging-related erectile dysfunction in the rat. *J Sex Med* 2007; **4**: 633–43
37 **Magee TR, Ferrini M, Garban HJ *et al.*** Gene therapy of erectile dysfunction in the rat with penile neuronal nitric oxide synthase. *Biol Reprod* 2002; **67**: 1033–41
38 **Martin KA, Merenick BL, Ding M *et al.*** Rapamycin promotes vascular smooth muscle cell differentiation through IRS-1/PI 3-Kinase/Akt2 feedback signaling. *J Biol Chem* 2007; **282**: 36112–20
39 **Ross JJ, Hong Z, Willenbring B *et al.*** Cytokine-induced differentiation of multipotent adult progenitor cells into functional smooth muscle cells. *J Clin Invest* 2006; **116**: 3139–49
40 **Sinha S, Hoofnagle MH, Kingston PA, McCanna ME, Owens GK.** Transforming growth factor-beta1 signaling contributes to development of smooth muscle cells from embryonic stem cells. *Am J Physiol Cell Physiol* 2004; **287**: C1560–8
41 **Garban H, Marquez D, Magee T *et al.*** Cloning of rat and human inducible penile nitric oxide synthase. Application for gene therapy of erectile dysfunction. *Biol Reprod* 1997; **56**: 954–63
42 **Garban H, Vernet D, Freedman A, Rajfer J, Gonzalez-Cadavid NF.** Effect of aging on nitric oxide-mediated penile erection in the rat. *Am J Physiol* 1995; **268**: H467–75
43 **Moody JA, Vernet D, Laidlaw S, Rajfer J, Gonzalez-Cadavid NF.** Effects of long-term oral administration of L-arginine on the rat erectile response. *J Urol* 1997; **158**: 942–7
44 **Romagnani P, Lasagni L, Mazzinghi B, Lazzeri E, Romagnani S.** Pharmacological modulation of stem cell function. *Curr Med Chem* 2007; **14**: 1129–39
45 **Madhusoodanan KS, Murad F.** NO-cGMP signaling and regenerative medicine involving stem cells. *Neurochem Res* 2007; **32**: 681–94
46 **Wang L, Gang Zhang Z, Lan Zhang R, Chopp M.** Activation of the PI3-K/Akt pathway mediates cGMP enhanced-neurogenesis in the adult progenitor cells derived from the subventricular zone. *J Cereb Blood Flow Metab* 2005; **25**: 1150–8
47 **Hinz B, Phan SH, Thannickal VJ, Galli A, Bochaton-Piallat ML, Gabbiani G.** The myofibroblast: one function, multiple origins. *Am J Pathol* 2007; **170**: 1807–16
48 **Darby IA, Hewitson TD.** Fibroblast differentiation in wound healing and fibrosis. *Int Rev Cytol* 2007; **257**: 143–79
49 **Carrier S, Nagaraju P, Morgan DM, Baba K, Nunes L, Lue TF.** Age decreases nitric oxide synthase-containing nerve fibers in the rat penis. *J Urol* 1997; **157**: 1088–92
50 **Musicki B, Kramer MF, Becker RE, Burnett AL.** Age-related changes in phosphorylation of endothelial nitric oxide synthase in the rat penis. *J Sex Med* 2005; **2**: 347–57
51 **Hsieh PS, Bochinski DJ, Lin GT, Nunes L, Lin CS, Lue TF.** The effect of vascular endothelial growth factor and brain-derived neurotrophic factor on cavernosal nerve regeneration in a nerve-crush rat model. *BJU Int* 2003; **92**: 470–5

Correspondence: Nestor F. Gonzalez-Cadavid, Harbor-UCLA Medical Center, Urology, Bldg. F-6, 1000 West Carson Street, Torrance, CA 90509, USA.
e-mail: ncadavid@ucla.edu

Abbreviations: **MDSC**, skeletal muscle-derived stem cell; **SMC**, smooth muscle cell; **PDE-5**, phosphodiesterase 5; **ED**, erectile dysfunction; **αSMA**, α-smooth muscle actin; **EFS**, electrical field stimulation of the cavernosal nerve; **PCNA**, proliferating cell nuclear antigen; **CVOD**, corporal veno-occlusive dysfunction; **DMEM**, Dulbecco's Modified Eagle's Medium; **FBS**, fetal bovine serum; **pP(1–6)**, pre-plate fraction (1–6); **αSMA Pr-β-gal**, plasmid construct expressing the *E. coli* β-galactosidase gene under the rat αSMA promoter; **CMV**, cytomegalovirus; **X-gal**, 5-bromo-4-chloro-indolyl-β-D-galactopyranoside; **NIH**, National Institutes of Health; **DAPI**, 4′,6-diamidino-2-phenylindole; **MHC-II**, myosin heavy chain 2; **PCNA**, proliferating cell nuclear antigen; **MIP**, maximal intracavernosal pressure; **MAP**, mean arterial pressure.

Myostatin promotes a fibrotic phenotypic switch in multipotent C3H 10T1/2 cells without affecting their differentiation into myofibroblasts

Jorge N Artaza[1,2], Rajan Singh[1], Monica G Ferrini[2,3], Melissa Braga[1], James Tsao[1] and Nestor F Gonzalez-Cadavid[1,3]

[1]Division of Endocrinology, Metabolism and Molecular Medicine and RCMI Molecular Core, [2]Department of Biomedical Sciences, The Charles R Drew University of Medicine and Science, 1731 East 120th Street, Los Angeles, California 90059, USA

[3]Department of Urology, UCLA David Geffen School of Medicine, Los Angeles, California 90095, USA

(Correspondence should be addressed to J N Artaza at the Division of Endocrinology, Metabolism and Molecular Medicine, Charles Drew University of Medicine and Science; Email: jorgeartaza@cdrewu.edu)

Abstract

Tissue fibrosis, the excessive deposition of collagen/extracellular matrix combined with the reduction of the cell compartment, defines fibroproliferative diseases, a major cause of death and a public health burden. Key cellular processes in fibrosis include the generation of myofibroblasts from progenitor cells, and the activation or switch of already differentiated cells to a fibrotic synthetic phenotype. Myostatin, a negative regulator of skeletal muscle mass, is postulated to be involved in muscle fibrosis. We have examined whether myostatin affects the differentiation of a multipotent mesenchymal mouse cell line into myofibroblasts, and/or modulates the fibrotic phenotype and Smad expression of the cell population. In addition, we investigated the role of follistatin in this process. Incubation of cells with recombinant myostatin protein did not affect the proportion of myofibroblasts in the culture, but significantly upregulated the expression of fibrotic markers such as collagen and the key profibrotic factors transforming growth factor-β1 (TGF-β1) and plasminogen activator inhibitor (PAI-1), as well as Smad3 and 4, and the pSmad2/3. An antifibrotic process evidenced by the upregulation of follistatin, Smad7, and matrix metalloproteinase 8 accompanied these changes. Follistatin inhibited TGF-β1 induction by myostatin. Transfection with a cDNA expressing myostatin upregulated PAI-1, whereas an shRNA against myostatin blocked this effect. In conclusion, myostatin induced a fibrotic phenotype without significantly affecting differentiation into myofibroblasts. The concurrent endogenous antifibrotic reaction confirms the view that phenotypic switches in multipotent and differentiated cells may affect the progress or reversion of fibrosis, and that myostatin pharmacological inactivation may be a novel therapeutic target against fibrosis.

Journal of Endocrinology (2008) **196,** 235–249

Introduction

Progressive scarring (fibrosis) is the main pathological process in fibroproliferative diseases. During advanced stages, these disorders are responsible for close to 45% of all deaths in the developed world (Wynn 2007). They often involve a relative loss of cells essential to normal tissue function. Fibrosis is analogous to abnormal wound healing occurring during tissue response due to chronic and sustained injury, microtrauma, oxidative stress, endogenous or exogenous insults, autoimmunity, and other factors. This process affects multiple organs in localized, multifocal, or disseminated forms, in conditions such as systemic sclerosis, liver cirrhosis, progressive kidney disease, cardiovascular disease, pulmonary fibroses, macular degeneration, and muscle dystrophies (Willis *et al.* 2006, Gharaee-Kermani *et al.* 2007, Henderson & Iredale 2007). Although chronic inflammation usually precedes fibrosis, it is neither necessary nor sufficient to trigger it, and as a result anti-inflammatory agents are usually not effective against fibrosis. In fact, successful antifibrotic treatments are very rare (Wynn 2007).

At the cellular level, one of the main factors of fibrosis is the differentiation of a not well-defined progenitor (local mesenchymal stem cells; fibroblasts; or epithelial, smooth muscle, or stellate cells; or recruited exogenous cells such as perycites or bone marrow fibrocytes) into myofibroblasts, the cells that share a fibroblast/smooth muscle phenotype (Kisseleva & Brenner 2006, Qi *et al.* 2006, Iredale 2007). In fact, myofibroblasts are usually absent from normal tissue. They accumulate after injury or the impact of a noxious factor, and synthesize collagen and extracellular matrix during tissue repair. They then normally disappear by apoptosis when the process is completed. An increase in the differentiation of fibroblasts from their progenitors, or the failure of myofibroblasts to be removed after sufficient collagen has been deposited, is probably the basis of many fibroses (Iredale 2007, Wynn 2007). However, the activation of already differentiated contractile cells – myofibroblasts,

DOI: 10.1677/JOE-07-0408
0022–0795/08/0196–235
Online version via http://www.endocrinology-journals.org

fibroblasts, or smooth muscle cells – to a synthetic phenotype where collagen is produced intensively is also a key step in fibrosis progression. Counteracting this myofibroblast differentiation and/or activation is therefore the primary target of novel therapies, considering that tissue defense mechanisms against these processes may operate in the now accepted concept of spontaneous reversibility of fibrosis, as in cirrhosis of the liver and kidney (Iredale 2007, Wynn 2007).

Many members of the transforming growth factor-β (TGF-β) superfamily, particularly TGF-β1 and activin A, are well-known profibrotic factors that play a role in most of the stages in this process in many organs. This occurs specifically in the stimulation of myofibroblast differentiation, the switch to the synthetic phenotype, and in the inhibition of apoptosis (Sulyok *et al.* 2004, Mauviel 2005, Ruiz-Ortega *et al.* 2007). They upregulate collagen synthesis, the expression of ancillary profibrotic proteins, and of each other, as in the case of PAI-1 or connective tissue growth factor. They also share the downstream Smad signaling pathway.

Smad3 is a well-known profibrotic agent, more than Smad2, whereas Smad6 and 7 are antifibrotic, similar to another upstream member of the TGF-β1 family, bone morphogenic protein 7 (BMP-7; Wang *et al.* 2005, Ask *et al.* 2006, Liu 2006). Moreover, follistatin, a protein that binds and inactivates TGF-β1 and activin A, and downregulates the expression of their mRNAs, is antifibrotic in a number of conditions, namely, lung, liver, and kidney fibrosis (Aoki *et al.* 2005, Patella *et al.* 2006).

Myostatin, the only known negative regulator of skeletal muscle mass, is also a member of the TGF-β superfamily (Lee 2004, Tsuchida 2004). It has been shown to modulate multipotent cell differentiation, specifically in the C3H10T1/2 mouse embryonic cell line of fibroblast origin, where myostatin stimulates adipogenic commitment while inhibiting myogenic lineage, whereas androgens exert the opposite effect (Singh *et al.* 2003, Artaza *et al.* 2005, Jasuja *et al.* 2005, Feldman *et al.* 2006). C3H10T1/2 is a well-known and widely used multipotent mesenchymal cell line that undergoes differentiation into several cell lineages (Taylor & Jones 1979, Atkinson *et al.* 1997, Fischer *et al.* 2002, Wilson & Rotwein 2006).

In addition, myostatin inactivation increases osteogenic differentiation in bone marrow stem cells (Hamrick *et al.* 2007). Recent indirect evidence suggests that myostatin acts in the same way as other members of the TGF-β family, by inducing fibrosis in the skeletal muscle (Engvall & Wewer 2003, McCroskery *et al.* 2005). This is likely to occur via the Smad pathway, since myostatin signals through Smad2–4, and phosphorylates Smad3 (Zhu *et al.* 2004). In addition, it triggers a feedback compensatory mechanism through the inhibitory Smad7 that inactivates myostatin promoter, and counteracts myostatin and TGF-β action (Zhu *et al.* 2004, Forbes *et al.* 2006, Kollias *et al.* 2006). In turn, Smad2–4 upregulate myostatin expression by activating its promoter (Zhu *et al.* 2004).

Similar to TGF-β1 and activin A, myostatin is inhibited by follistatin, and also by the agents that induce follistatin expression, such as deacetylase inhibitors that block myostatin negative action on the muscle (Lee & McPherron 2001, Amthor *et al.* 2004, Iezzi *et al.* 2004, Kocamis *et al.* 2004). However, it is not known whether myostatin's putative profibrotic action is exerted via the stimulation of myofibroblasts differentiation from their progenitor, or by inducing a switch of the differentiated cell to the synthetic phenotype producing extracellular matrix. It is also unclear whether follistatin neutralizes these effects.

In our current work, we examined the effects of recombinant and endogenous myostatin on a) the differentiation of the multipotent C3H10T1/2 cell line into myofibroblasts, b) the regulation of the expression of TGF-β1 and other fibrotic-related genes, and c) proteins involved in the Smad signaling cascade and follistatin. In addition, we investigated whether a) follistatin counteracts the effect of myostatin, b) over-expression of myostatin mRNA mimics the paracrine effects of the exogenous protein, and c) this effect is blocked by the myostatin shRNA.

Materials and Methods

Cell culture

Mouse C3H10T1/2 multipotent cells (ATCC, Manassas, VA, USA) grown in Dulbecco's Modified Eagle's Medium (DMEM) with 10% fetal bovine serum at 37 °C were treated with or without 20 μM 5′-azacytidine (AZCT) for 3 days to induce differentiation (Singh *et al.* 2003, Artaza *et al.* 2005). Cells were split in a 1:2 ratio; allowed to recover for 2 days; seeded onto 60–70% confluence in T75 flasks, eight-well chamber slides or six-well plates; and incubated with 4 μg/ml recombinant 113 amino acid myostatin protein (R-Mst; Artaza *et al.* 2005) in DMEM–10% serum for 0·5, 1, 2, 3, and 24 h and for 3, 4, and 10 days to assess paracrine effects of myostatin (see the section below). Azacytidine-treated cells were also co-transfected at 60% confluence in six-well plates with a) a myostatin cDNA plasmid expressing the full-length 375 amino acid protein (pcDNA-Mst-375; Taylor *et al.* 2001) or b) the silencer RNAs for two different myostatin sequences (pSil-Mstno.4 and 326) (Artaza *et al.* 2005, Magee *et al.* 2006) (see the section below). A pcDNA3.1-EGFP (Invitrogen) was co-transfected separately to evaluate the transfection efficiency.

siRNA myostatin

siRNA myostatin was described by Artaza *et al.* (2005) and Magee *et al.* (2006). To prepare the silencer RNA construct for myostatin, we analyzed the mouse myostatin gene sequence (accession no. NM_010834) using the web-based siRNA target finder and design tool provided in the Ambion website (Ambion Inc., Austin, TX, USA). Five regions were initially targeted for likely inhibitory activity by siRNAs (nucleotide position target no.): 176(no. 4), 207(no. 8), 426(no. 26), 647(no. 45), and

1064(no. 72)). Double-stranded RNAs were transcribed *in vitro* using the Silencer siRNA Construction Kit. In addition, a control siRNA targeting glyceraldehyde-3-phosphate dehydrogenase (GAPDH) and provided with the kit was also synthesized. Each siRNA was tested for inhibitory activity at 1, 10, and 100 nM concentrations by co-transfection of pCDNA3.1-Mst into human embryonic kidney cells (HEK)293 cell cultures using Lipofectamine 2000 (Invitrogen). After 48 h, cell lysates were collected in M-PER (Pierce Biotechnology Inc., Rockford, IL, USA) and western blot analyses were performed. Two siRNAs (growth differentiation factor (GDF)8 siRNA26 and siRNA4) were found to inhibit more than 95% of the myostatin gene expression (Magee *et al.* 2006).

Based on a GenBank Blast search, these sequences have homology not only to mouse but also to human, rat, rabbit, cow, macaque, and baboon. A short hairpin DNA sequence was synthesized and cloned into the pSilencer 2.1-U6 neo (Ambion Inc.), according to the manufacturer's instructions. The DNA sequence consists of a *Bam*HI DNA restriction site, sense strand, nine-nucleotide loop, antisense strand, RNA polymerase III terminator, and *Hin*dIII DNA restriction site 5′ to 3′ (Artaza *et al.* 2005, Magee *et al.* 2006). The pSilencer 2.1-U6 neo-GDF8 siRNA plasmid constructs were transfected (1 μg/well plate, six-well plate) into C3H10T1/2 cell cultures using Lipofectamine 2000 following the manufacturer's instructions as before.

Qualitative and quantitative immunocytochemical analyses

Cells grown in eight-well chamber slides were fixed in 2% *p*-formaldehyde, quenched with H_2O_2, blocked with normal goat or horse serum and incubated with specific antibodies (Artaza *et al.* 2002, Singh *et al.* 2003, 2006, Artaza *et al.* 2005, Jasuja *et al.* 2005). These consisted of a α-smooth muscle actin immunohistology kit (Sigma–Aldrich), and antibodies against pSmad2/3 (1:500); Smad3 (1:500), Smad4 (1:500) and Smad7 (1:500) (Santa Cruz Biotechnology Inc., Santa Cruz, CA, USA); PAI-1 (1:200; Abcam Inc.); TGF-β1 (1:200) (Promega Corporation); collagen I (1:100) and collagen III (1:100; Chemicon International Inc., Temecula, CA, USA).

Detection was based on a secondary biotinylated antibody (1:200), followed by the addition of the streptavidin–horseradish peroxidase ABC complex (1:100), Vectastain (Elite ABC System, Vector Laboratories, Burlingame, CA, USA) and 3,3′-diaminobenzidine and H_2O_2 mixture (Sigma). The cells were counterstained with Mayer's hematoxylin solution (Sigma). In negative controls, we either omitted the first antibody or used a rabbit non-specific IgG.

In all cases, the cytochemical staining was quantitated by image analysis using ImagePro-Plus 5.1 software (Media Cybernetics, Silver Spring, MD, USA) coupled to a Leica digital microscope bright field light fluorescence microscope/VCC video camera. After images were calibrated for background lighting, wherein integrated OD (IOD = area × average intensity) was calculated using at least ten pictures per treatment group per well done in duplicate. These experiments were repeated at least thrice (Singh *et al.* 2003, Artaza *et al.* 2005, Jasuja *et al.* 2005).

Western blot and densitometry analyses

Cell lysates (40–80 μg protein) were subjected to western blot analyses (Artaza *et al.* 2002, Singh *et al.* 2003) by 4–15% Tris–HCl PAGE (Bio-Rad) in running buffer (Tris/glycine/SDS). Proteins were transferred overnight at 4 °C to nitrocellulose membranes in transfer buffer (Tris/glycine/methanol). The next day the non-specific binding was blocked by immersing the membranes in 5% non-fat dried milk and 0·1% (v/v) Tween 20 in PBS for 1 h at room temperature. After several washes with washing buffer (PBS Tween 0·1%), the membranes were incubated with the primary antibodies for 1 h at room temperature. Monoclonal antibodies were as follows: a) α-smooth muscle actin (1:1000; Calbiochem, La Jolla, CA, USA) and b) GAPDH; 1:10 000) (Chemicon International). Polyclonal antibodies were used for a) Smad3 (1:200), b) Smad7 (1:200; Santa Cruz Biotechnology Inc., Santa Cruz, CA, USA), c) TGF-β1 (1:1000; Promega Corporation), and d) myostatin (1:1000) (Chemicon International Inc). The washed membranes were incubated for 1 h at room temperature with 1:3000 dilution (anti-mouse) or 1:2000 dilution (anti-rabbit) of secondary antibody linked to horseradish peroxidase respectively. After several washes, the immunoreactive bands were visualized using the emission of chemiluminescence (ECL) plus Western blotting chemiluminescence detection system (Amersham Biosciences). The densitometry analysis of the bands was done with the Scion Image software beta 4.0.2 (Scion Corp., Frederick, MD, USA).

Recombinant proteins

Myostatin recombinant protein was produced in *Escherichia coli* as a 16 kDa protein containing 113 amino acid residues of the human myostatin protein (BioVendor Laboratory Medicine Inc., Palackeho, Czech Republic). Recombinant follistatin protein was generated in Sf21 cells as a 31 kDa protein containing 289 amino acid residues (R&D Systems, Minneapolis, MN, USA). Recombinant human TGF-β1 was produced in Chinese hamster ovary (CHO) cells as a 25 kDa protein containing 112 amino acid residues (Chemicon International Inc).

Real-time quantitative PCR

Total RNA was extracted using Trizol reagent (Invitrogen) and equal amounts (2 μg) of RNA were reverse transcribed using a RNA PCR kit (Applied Biosystems, Foster City, CA, USA). The locations of forward/reverse PCR primers for real-time RT-PCR are as follows: Smad7 region 575–597/626–641 on BC074818.2 (67 bp); follistatin (Fst; 150 bp), PPM04451A on NM_008046 and GAPDH (152 bp), 606–626/758–738 on BC023196. Mouse gene PCR primer sets (RT2) were purchased from SuperArray Bioscience (Frederick, MD, USA). The Qiagenn Sybr Green

PCR kit with HotStar *Taq* DNA polymerase (Qiagen) was used with i-Cycler PCR thermocycler and fluorescent detector lid (Bio-Rad; Singh *et al.* 2006).

The protocol included melting for 15 min at 95 °C, 40 cycles of three-step PCR including melting for 15 s at 95 °C, annealing for 30 s at 58 °C, elongation for 30 s at 72 °C, with an additional detection step of 15 s at 81 °C, followed by a melting curve from 55 to 95 °C at the rate of 0·5 °C per 10 s. Fst annealing for primers, however, was at 55 °C and detection at 76 °C. We confirmed that inverse derivatives of melting curves show sharp peaks for Smad7 at 82 °C, Fst at 84·5 °C, and GAPDH at 87 °C, indicating the correct products. Samples of 25 ng cDNA were analyzed in quadruplicate in parallel with GAPDH controls; standard curves (threshold cycle versus log pg cDNA) were generated by log dilutions of from 0·1 pg to 100 ng standard cDNA (reverse-transcribed mRNA from C3H10T1/2 cells in AM). Experimental mRNA starting quantities were then calculated from the standard curves and averaged using i-Cycler, iQ software, as described previously (Singh *et al.* 2003). The ratios of marker experimental gene (e.g. follistatin mRNA) to GAPDH mRNA were computed and normalized to control (untreated) samples as 100%.

DNA microarray analysis of TGF-β/BMP target genes

Pools of total cellular RNA from three different T75 flasks for each experimental condition were isolated with Trizol reagent from C3H10T1/2 cells undergoing differentiation with AZCT and treated with or without recombinant myostatin protein (4 μg/ml) for 3 h and 3 days. Isolated RNA was subjected to cDNA gene microarrays (GEArray Q Series, TGF-β/BMP signaling pathway gene array (matrix microarray (MM)-023) and osteogenesis gene array (MM-026) analysis (SuperArray BioScience Corp). The microarray assays were performed in two separate experiments in each case. This series of mice TGF-β/BMP signaling pathway gene arrays are designed to study the genes involved in TGF-β/BMP signaling pathway (MM-023) and the osteogenic array (MM-026) contains collagens of some other fibrotic-related genes. Biotin-labeled cDNA probes were synthesized from total RNA, denatured, and hybridized overnight at 60 °C in GEHybridization solution to membranes spotted with TGF-β/BMP signaling pathway-specific genes, as well as with genes involved in the regulation of osteogenic differentiation. Membranes were then washed, and chemi-luminescent analysis was performed as per the manufacturer's instructions. Raw data were analyzed using GEArray Expression Analysis Suite (SuperArray BioScience Corp). Fold changes in relative gene expression were presented after background correction and normalization with a housekeeping gene.

Confirmation of DNA microarray analysis by RT^2 profiler PCR array analysis of TGF-β/BMP target gene

RT^2 profiler PCR SuperArray analyses of TGF-β/BMP target genes were applied in order to confirm selected genes from the GEArray data. Aliquots of total cellular RNA isolated with Trizol reagent from C3H10T1/2 cells undergoing differentiation with AZCT were treated with or without recombinant myostatin protein (4 μg/ml) for 3 h and 3 days. They were then subjected to reverse transcription, and the resulting cDNA was analyzed by RT^2 profiler PCR mouse TGF-β/BMP signaling pathway (APM-035A) (SuperArray BioScience Corp). This series of mouse TGF-β/BMP signaling pathway gene array is designed to study the genes involved in and downstream of TGF-β/BMP signaling. Each array contains a panel of 84 primer sets related to the TGF-β/BMP signaling genes plus 5 housekeeping genes and two negative controls. Real-time PCRs were performed as follows: a) melting for 10 min at 95 °C, b) 40 cycles of two-step PCR including melting for 15 s at 95 °C, and c) annealing for 1 min at 60 °C. The raw data were analyzed using the $\Delta\Delta C_t$ method following the manufacturer's instructions (SuperArray).

Statistical analysis

All data are presented as mean ± S.E.M., and between-group differences were analyzed using ANOVA. If the overall ANOVA revealed significant differences, then pair-wise comparisons between groups were performed by Newman–Keuls multiple comparison test. All comparisons were two-tailed, and $P<0{\cdot}05$ were considered statistically significant. The *in vitro* experiments were repeated thrice, and data from representative experiments are shown. Specifically, the DNA microarrays tests were done twice and the results confirmed by qRT-PCR in triplicate.

Results

Myofibroblast generation from multipotent C3H10T1/2 cells occurs spontaneously, and is not affected by azacytidine or incubation with exogenous myostatin, but myostatin triggers a fibrotic phenotype associated with transcriptional regulation of fibrotic-related genes and the Smad cascade

C3H10T1/2 cells, treated or non-treated with AZCT, were tested for the presence of myofibroblasts (cells with a fibroblast/smooth muscle cell hybrid phenotype, which play a key role in fibrosis), and also to determine whether myostatin stimulates C3H10T1/2 commitment to this differentiation lineage. The cultures not treated with AZCT had some cells that stained positive for α-smooth muscle actin (ASMA), a marker that is common to myofibroblasts and smooth muscle cells (data not shown). They had the typical appearance of myofibroblasts with prominent actin filaments and lamellipodia. Treatment of these cultures with either AZCT alone or in combination with recombinant myostatin protein did not alter this morphology (data not shown), nor there was any apparent increase from these treatments in terms of myofibroblast number (~8% of the total cell population) as confirmed by quantitative image analysis. Western immunoblot analysis of the cell extracts for ASMA compared with GAPH expression agreed with the qualitative

and quantitative immunocytochemistry observations. In addition, calponin, a marker for smooth muscle cells, which is not expressed in myofibroblasts, was not detected in the extracts (data not shown). This indicates that the $ASMA^+$ cells in the C3H10T1/2 cultures are indeed myofibroblasts.

Although myostatin did not stimulate myofibroblast differentiation in the azacytidine-induced multipotent C3H10T1/2 culture, it switched these cells towards the synthetic fibrotic phenotype, as shown in Fig. 1. Starting with this experiment, cells were always treated with AZCT, even if this drug did not affect the number of myofibroblasts that originated from C3H10T1/2 cells. This was done in order to facilitate comparisons with studies, including our previous results (Singh *et al.* 2003, Artaza *et al.* 2005, Jasuja *et al.* 2005) where azacytidine was routinely employed to stimulate multipotent stem cell differentiation (Schmittwolf *et al.* 2005). Incubation with recombinant myostatin protein clearly stimulated the intensity of immunocytochemical staining for the four selected fibrotic markers PAI-1, TGF-β1, collagen I, and collagen III (Fig. 1A and B, left panels). Most of the cells had a very low basal level of expression in the absence of treatment, but the expression per cell was intensified by myostatin. This is reflected

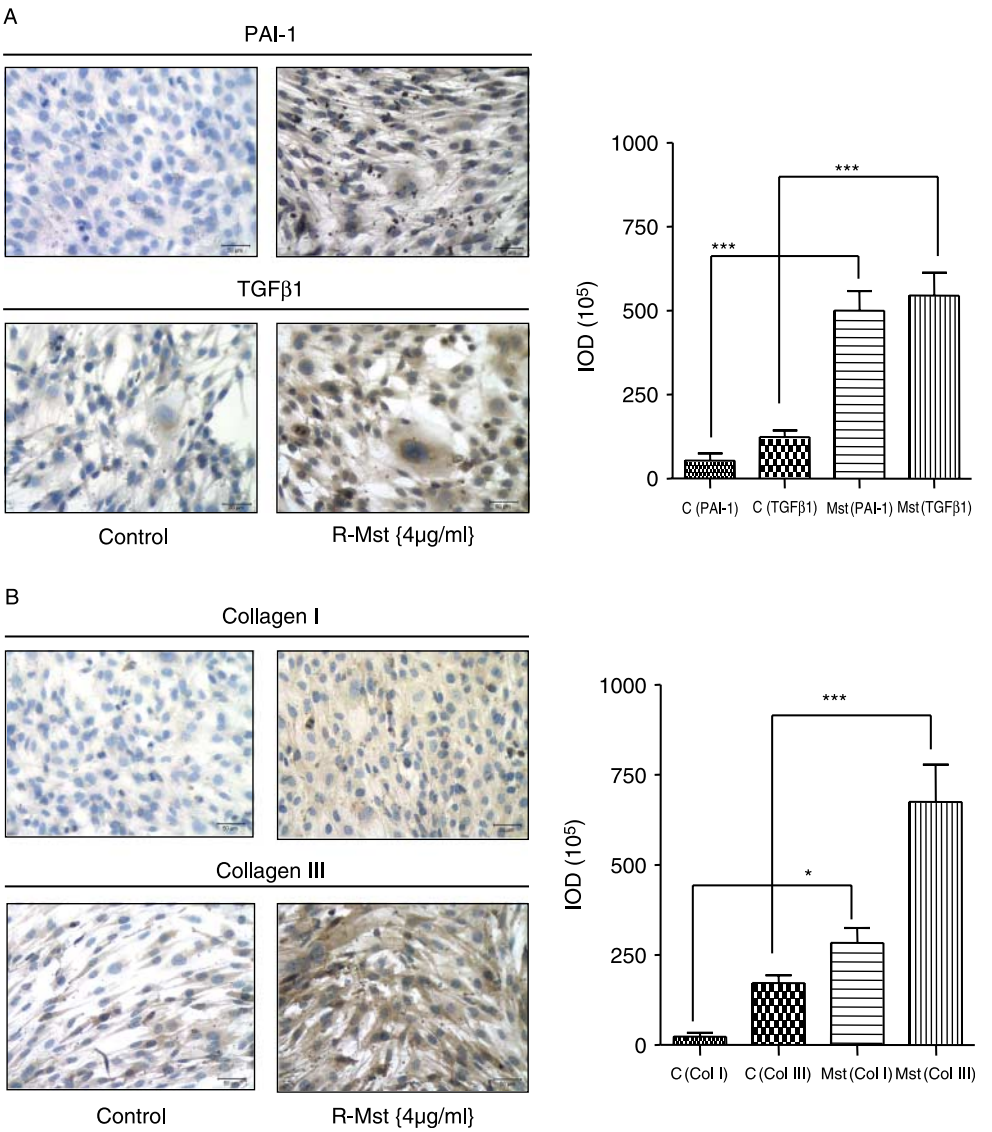

Figure 1 Effects of recombinant myostatin protein on the expression of profibrotic genes and collagen in C3H10T1/2 cells. Representative pictures (200×) of cells treated with azacytidine (20 μM) to induce differentiation and which, 2 days later, received myostatin (4 μg/ml), or no myostatin, on eight-well removable chambers, for 3 days followed by immunostaining (left) with the corresponding antibodies. (A) Profibrotic genes: PAI-1 and TGF-β1 and (B) collagen I and III. Mean ± S.E.M. corresponds to experiments done in triplicate of the integrated optical densities (IOD). $^*P<0{\cdot}05$, $^{***}P<0{\cdot}001$ (200×).

on the quantitative image analysis (Fig. 1A and B, right panels) that shows a statistically significant increase in PAI-1, TGF-β1, collagen I, and collagen III expression after incubation with recombinant myostatin (R-Mst) for 4 days.

The stimulation of fibrotic gene expression in the C3H10T1/2 cells by myostatin was also analyzed at the transcriptional level using mouse osteogenesis gene array (MM-026) and mouse TGF-β/BMP signaling pathway gene array (MM-023) (data not shown).

Figure 2 shows one of the two sets of membranes for DNA mouse osteogenesis gene array assay performed on total RNA extracted from cells subjected for 3 h (2A) and 3 days (2B) of incubation with or without recombinant myostatin. Some of the genes that showed differential RNA expression between the myostatin-treated and -untreated cells are indicated by circles (Fig. 2A and B) and were selected for the table shown in Fig. 2C, where the computer-generated ratios of spot intensities, normalized by housekeeping genes are tabulated for 3 days in the left column. This PCR microarray panel has only some of the fibrotic genes – essentially collagens, BMP members, and all the Smad genes – that transduce signals triggered by the members of the TGF-β1 family. For this reason, other genes selected from the mouse TGF-β/BMP panel are also included. The change of expression of some selected genes at 3 days was ultimately confirmed by real-time PCR using the RT^2 profiler PCR SuperArray set of primers and procedures. The ratios for triplicate determinations are shown on the right column. The agreement between the ratios obtained by DNA microarrays and RT-PCR is in general adequate and provides a reasonable assessment of up- and downregulation. From both the columns and the quantitative microarray data for 3 h (not shown), it was found that the stimulation of the mRNA expression of collagen I α, collagen IX α1, Smad3, 4, and 7, BMP 3, BMP 6, BMP7, and v cam occurred early, whereas it took longer to enhance the levels of the mRNAs for collagen I α1, collagen IV α4, collagen IV α6, and MMP8. The increase in Smad7 mRNA by myostatin remained considerable at 3 days, whereas that for Smad3 and 4 mRNAs was negligible.

The early transcriptional stimulation of Smad3 mRNA expression by myostatin was demonstrated at the protein level by immunocytochemistry, as shown in the time course depicted in Fig. 3A. TGF-β1, the main profibrotic factor and the member of the TGF-β superfamily that includes myostatin, signals through the Smad pathway, and was therefore used as positive control. There was an early and dramatic increase in the intensity of Smad3 staining (Fig. 3A) that peaked at 1 h, and was later downregulated reaching normal values at 24 h. The 3-h expression was confirmed by western blot analysis, which showed that myostatin was nearly as effective as TGF-β1 (Fig. 3B).

The time course of exogenous myostatin induction of Smad proteins shows an early expression and phosphorylation of the Smad2–4 genes followed by a later upregulation of the inhibitory Smad7

Smad3 was not the only Smad protein modulated by myostatin. C3H10T1/2 cells were incubated with recombinant myostatin; a very early stimulation of the phosphorylated Smad2/3 proteins was observed at 30 min, peaking at 1 h. This decayed at 2 h and normalized at 24 h (Fig. 4A). A similar process after 1 h occurred with the expression of Smad4 protein (Fig. 4B).

Consistent with the results shown in Fig. 2, Smad7 was expressed early. However, the immunostaining remained high even at 6 h (Fig. 5A). Western blot analysis confirmed the early Smad7 expression induced by myostatin. This was even higher than that induced by TGF-β1 (Fig. 5B). On the other hand, real-time RT-PCR showed that the stimulation of Smad7 mRNA expression by myostatin persisted even at 3 days, when the other Smad proteins had fallen to negligible levels (Fig. 5C).

Exogenous myostatin upregulates the expression of its inhibitory protein, follistatin, and the addition of follistatin downregulates the myostatin-induced upregulation of TGF-β1

Since the activities of myostatin, TGF-β1, activin, and other members of the TGF-β family are inhibited by follistatin through binding to these proteins, we investigated whether myostatin modulated the expression of follistatin in the cells that were undergoing a fibrotic phenotypic differentiation. Contrary to our initial assumption that follistatin levels would be downregulated by myostatin, and would thus boost myostatin effects, real-time RT-PCR (Fig. 6A) revealed an early threefold stimulation at 3 h of follistatin mRNA levels that remained remarkably high even at 3 days.

To determine whether this was a compensatory mechanism of the C3H10T1/2 cells to counteract the profibrotic effects of myostatin, we tested whether the addition of recombinant follistatin protein would block the myostatin stimulation of the production of profibrotic factors by these cells. We also investigated whether myostatin modulation of the fibrotic phenotypic differentiation is mediated by the upregulation of the expression of TGF-β1, the main profibrotic factor. Figure 6B shows that at 4 days, myostatin stimulated TGF-β1 expression, and that the addition of follistatin (0·5 μg/ml) blocked this stimulation, whereas follistatin *per se* did not affect TGF-β1 expression. These effects were confirmed by western immunoblot (Fig. 6C).

The profibrotic effects of myostatin on C3H10T1/2 cells can also be exerted autocrinely by over-expression of myostatin mRNA, or through the breakdown of myostatin mRNA by its shRNA

The preceding experiments indicated that exogenous myostatin regulated the fibrotic phenotype of C3H10T1/2 cells which contain myofibroblasts that originated from this multipotent cell culture. Questions remained, however, whether endogenously produced myostatin would cause the same effects, and whether blocking its expression at the protein level would inhibit the production of fibrotic factors. Figure 7 shows that transfection of these cells with plasmid constructs expressing myostatin increased myostatin expression, as evidenced by the western blot analysis (Fig. 7B, left) and the corresponding densitometry

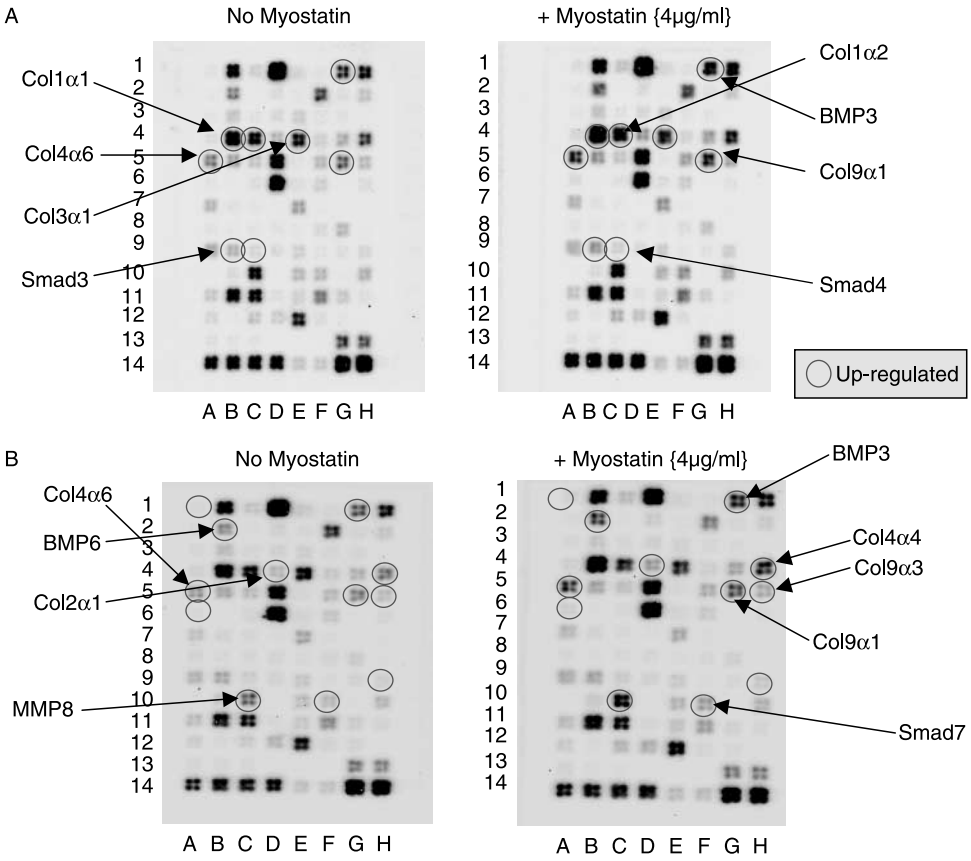

C

Symbol	Description	Microarray Ratios (3 days)	Real time PCR Ratios (3 days)
Bmp3	Bone morphogenetic protein 3	2·8	3·5
Bmp6	Bone morphogenetic protein 6	2·7	3·6
Col1α1	Procollagen, type I, α1	2·8	3·3
Col1α2	Procollagen, type I, α2	2·9	3·5
Col3α1	Procollagen, type III, α1	2·8	3·1
Col2α1	Procollagen, type II, α1	2·7	3·9
Col4α4	Procollagen, type IV, α4	3·2	4·3
Col4α6	Procollagen, type IV, α6	3·1	3·9
Col9α1	Procollagen, type IX, α1	3·4	3·8
Col9α3	Procollagen, type IX,α3	3·2	3·8
Fst	Follistatin	2·4	2·9
Mmp8	Matrix metalloproteinase 8	3·1	3·9
Smad7	Mad homolog 7	2·0	2·5

Figure 2 Effects of recombinant myostatin protein on the transcriptional expression of Smad proteins, collagen, and other fibrotic genes in C3H10T1/2 cells. Cells were treated as shown in Fig. 1, but in 75 cm^2 flasks, for 3 h (A) and 3 days (B). Total RNA was isolated and subjected to DNA microarray analysis for genes related to extracellular matrix represented in the osteogenesis gene array. (A and B) Representative membranes of assays performed in two separate experiments. (C) In parallel reactions, total RNA was subjected to RT-real-time PCR by the RT^2-PCR profiler TGF-β array and the ratio between the myostatin-treated versus myostatin-untreated cells corrected by GAPDH was calculated for the assays performed in triplicate.

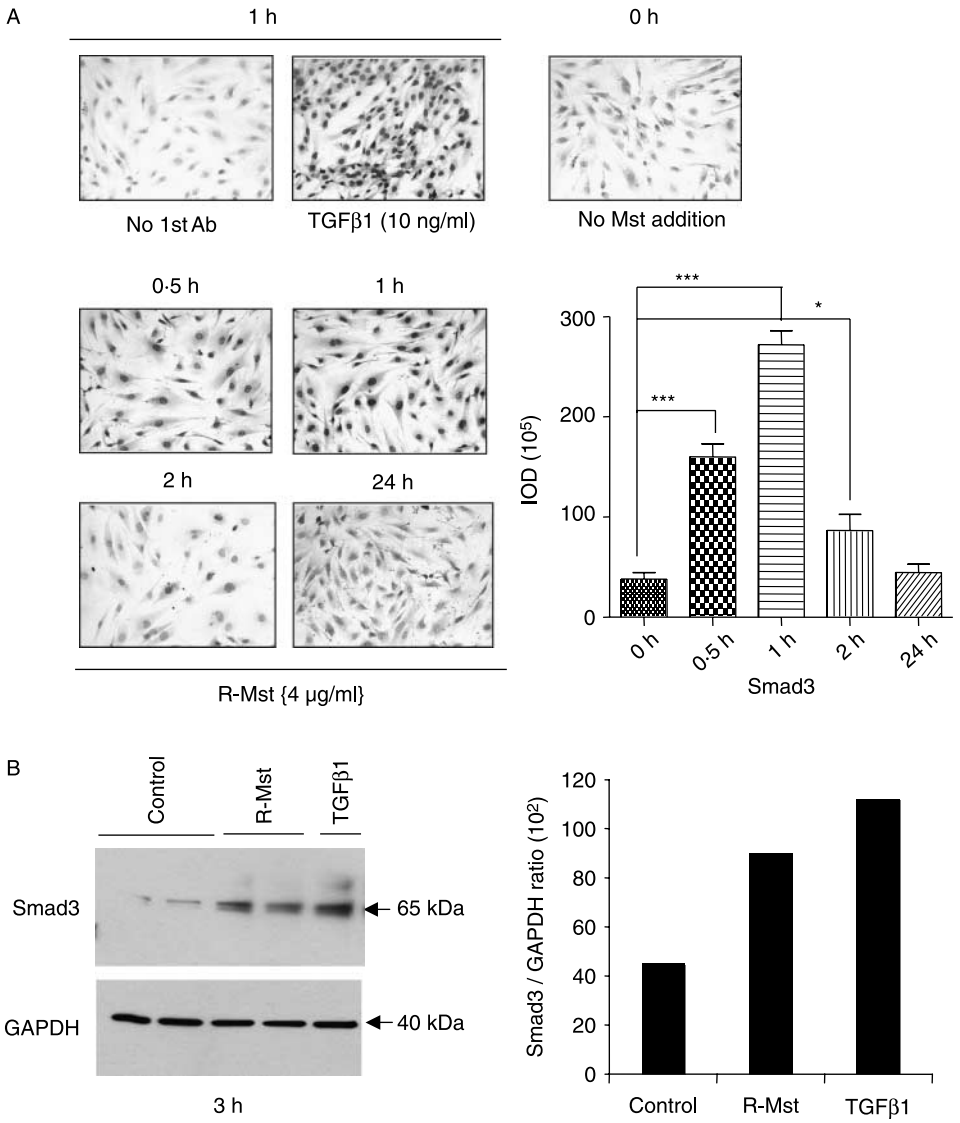

Figure 3 Myostatin stimulates the early expression of Smad3 protein in C3H10T1/2 cells. Azacytidine-treated cells were incubated on eight-well removable chambers in a time course manner and, for the 3 h incubation, on six-well plates, with or without myostatin, for the indicated periods. TGF-β1 was used as positive control. (A) Representative pictures of the immunodetection for Smad3 are presented (left) (200×), as well as the quantitative image analysis (right). (B) Western blot analysis was performed for the extracts from the 3-h incubation (left) and the corresponding densitometry analysis (right). Control; R-Mst, recombinant myostatin protein and TGF-β1 as positive control. Ab, antibody. Mean ± S.E.M. corresponds to experiments done in triplicate. *$P<0{\cdot}05$, ***$P<0{\cdot}001$. (A) 200×.

analysis of the band intensities (Fig. 7B, right). The transfection efficiency was estimated at about 60% by co-transfection of the myostatin construct with a reporter vector, pcDNA-EGFP (Fig. 7A). The two different plasmid constructs for the shRNA against myostatin mRNA decreased the expression of the myostatin band, as evidenced by the western blot analysis and the corresponding densitometry analysis (Fig. 7B). In parallel, there was considerable upregulation of PAI-1, visualized by the western blot analysis, and of the myostatin densitometry analysis, which was also blocked by the myostatin shRNA (Fig. 7C). A random RNA construct corresponding to the shRNA sequences for myostatin had previously been shown by our group to be inactive both *in vitro* (Artaza *et al.* 2005) and *in vivo* (Magee *et al.* 2006). This set of experiments confirmed that endogenous myostatin might act similarly to the exogenous myostatin protein.

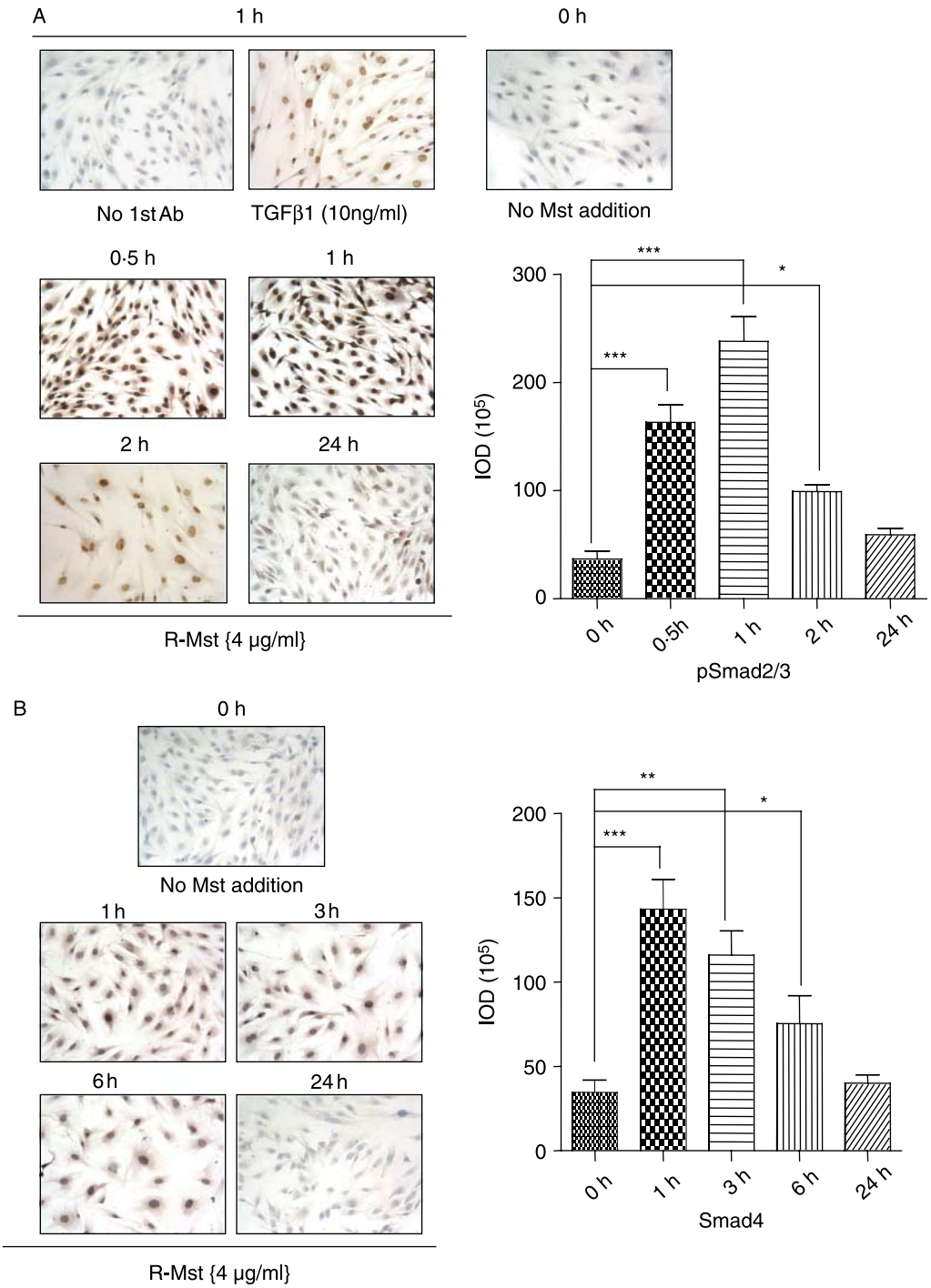

Figure 4 Time course of recombinant myostatin effects on the expression of the phosphorylated form of Smad2/3 protein (pSmad2/3) and Smad4 protein in C3H10T1/2 cells. Azacytidine-treated cells were incubated on eight-well removable chambers with or without myostatin, for the indicated periods. TGF-β1 was used as positive control. Representative pictures of the immunodetection are presented in left panels (200×), as well as the quantitative image analysis in the right panels. (A) pSmad2/3, (B) Smad4. Ab, antibody; R-Mst, recombinant myostatin protein. *$P<0{\cdot}05$, **$P<0{\cdot}01$, ***$P<0{\cdot}001$ (200×).

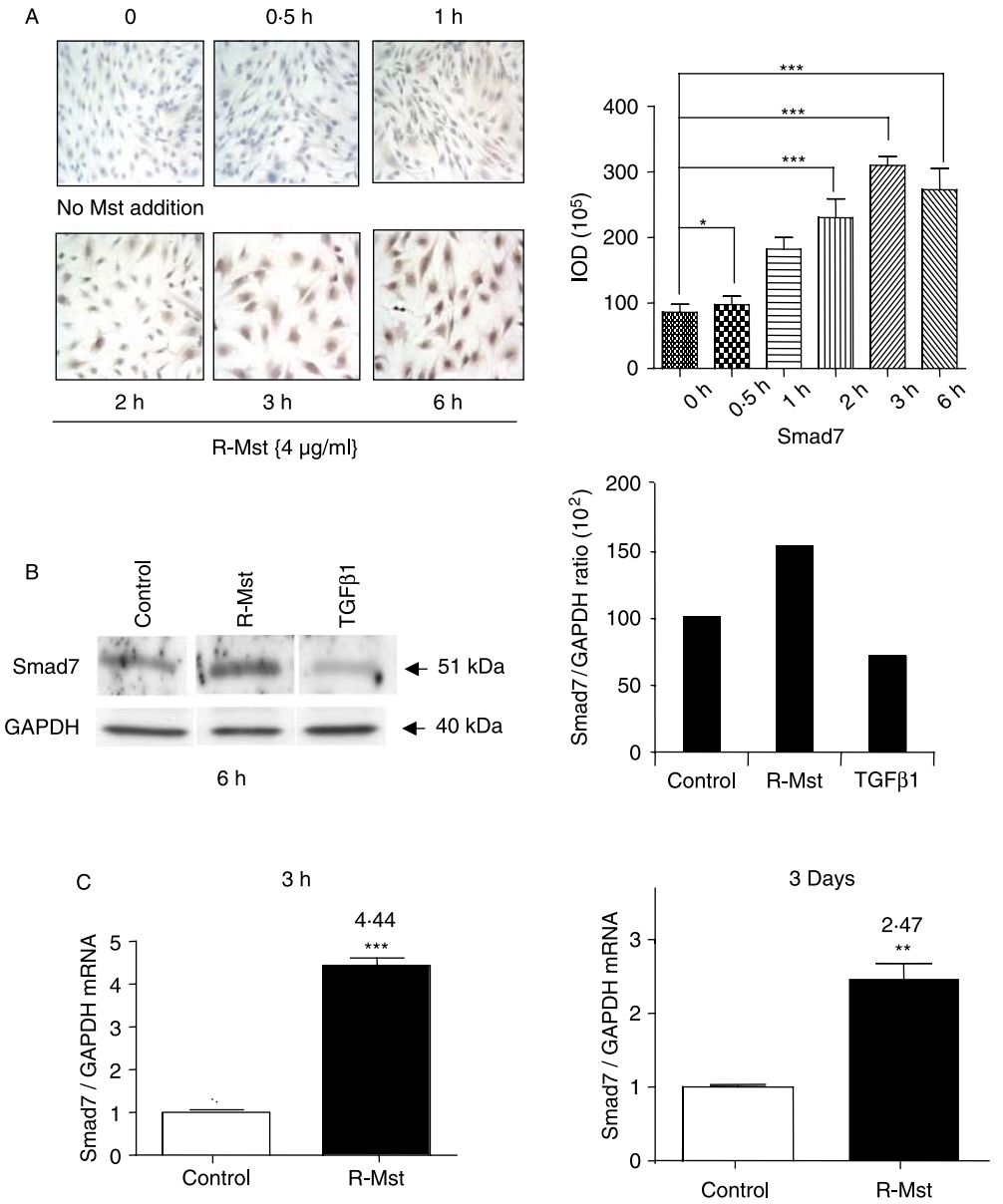

Figure 5 Time course of recombinant myostatin effects on the expression of the Smad7 gene in C3H10T1/2 cells. Azacytidine-treated cells were incubated on eight-well removable chambers in a time course manner, and, for the 3 h, 6 h, and 3 days incubations, on six-well plates, with or without myostatin. TGF-β1 was used as positive control. (A) Representative pictures of the immunodetection are presented (left), as well as the quantitative image analysis (right). (B) Western immunoblot analysis was performed for extracts from the 6-h incubation (left) and the corresponding densitometry analysis (right). (C) Total RNA isolation followed by real-time RT-PCR was applied in other aliquots for the 3-h and 3-day incubations normalized by GAPDH housekeeping gene. Ab, antibody; R-Mst, recombinant myostatin protein. Mean±S.E.M. corresponds to experiments done in triplicate. *$P<0{\cdot}05$, **$P<0{\cdot}01$, ***$P<0{\cdot}001$ (200×).

Discussion

The current study elucidates an important issue in the cell biology effects of myostatin, a protein that, in addition to its well-known role as a negative regulator of skeletal muscle mass and modulator of stem cell differentiation, acts as a profibrotic in this tissue (Engvall & Wewer 2003, McCroskery *et al.* 2005). This is consistent with the effects of other members of the TGF-β family such as activin and TGF-β1 in various tissues (Wada *et al.* 2004, Yamashita *et al.* 2004, Verrechia *et al.* 2006). Using the multipotent mesenchymal embryonic C3H10T1/2 cell line, it was possible in our

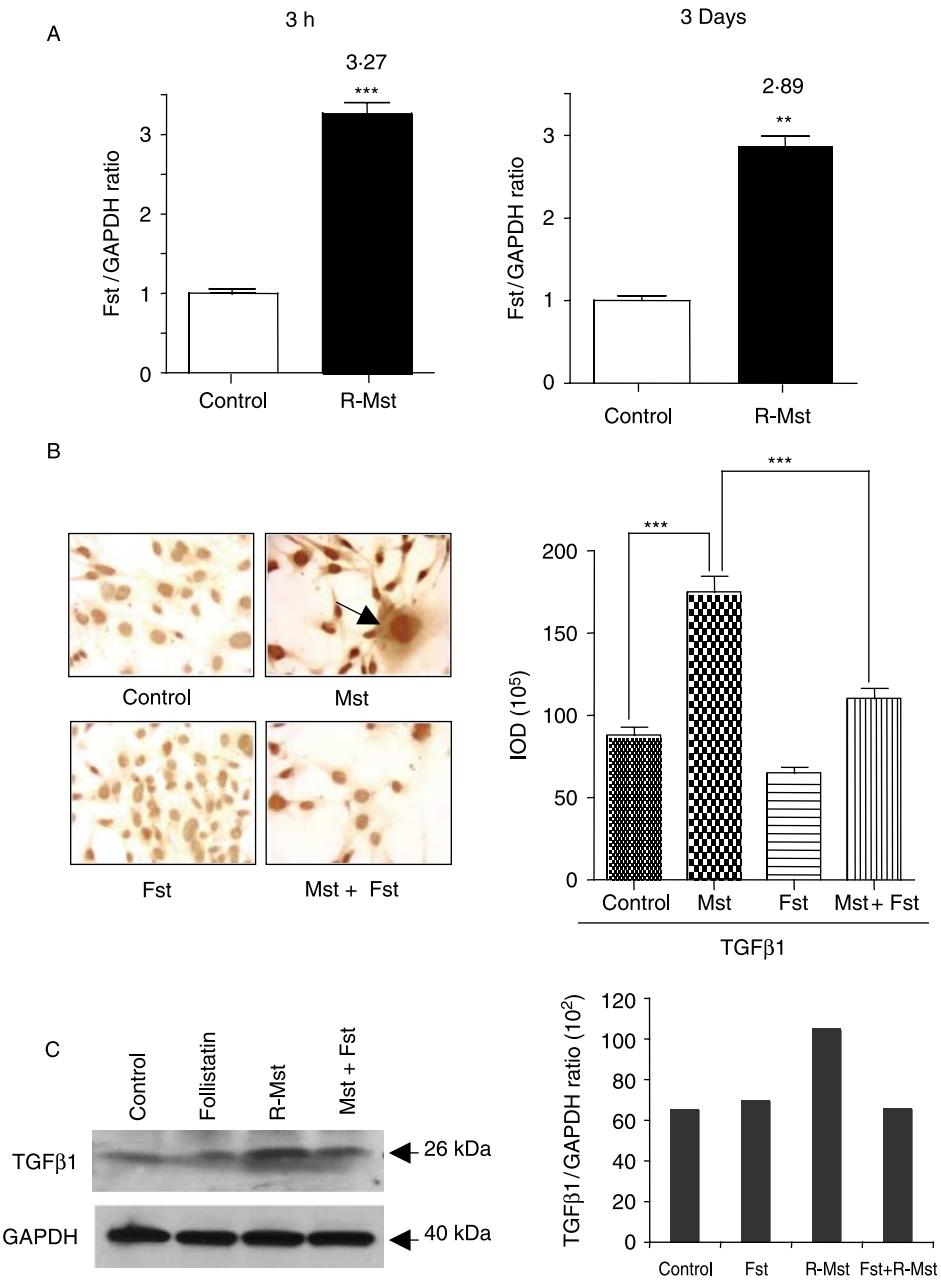

Figure 6 Effects of recombinant myostatin on follistatin and TGF-β1 expression, and modulation by follistatin of TGF-β1 protein expression. (A) Total RNA from the experiment of Fig. 5 was subjected to real-time RT-PCR for follistatin mRNA. (B) In a separate experiment, azacytidine-treated cells were incubated with either recombinant myostatin (4 μg/ml), TGF-β1 (5 ng/ml) or follistatin (0·5 μg/ml), for 4 days and subjected to immunocytochemistry and quantitative image analysis for TGF-β1 (200×). (C) Western immunoblot analysis for TGF-β1: R-Mst, recombinant myostatin protein; Fst, follistatin. $^{**}P<0{\cdot}01$, $^{***}P<0{\cdot}001$.

current work to demonstrate that myostatin did not affect paracrinely the differentiation of these cells into myofibroblasts (the typical fibrotic cells), and did not generate smooth muscle cells that are also potentially involved in extracellular matrix deposition when they switch to a fibrotic phenotype. However, myostatin was found to induce this switch in the overall multipotent and myofibroblast cell populations, as indicated by the stimulation in most cells within the culture of the expression TGF-β1 and another key profibrotic factor, PAI-1 (Eddy & Fogo 2006), and particularly by the ultimate

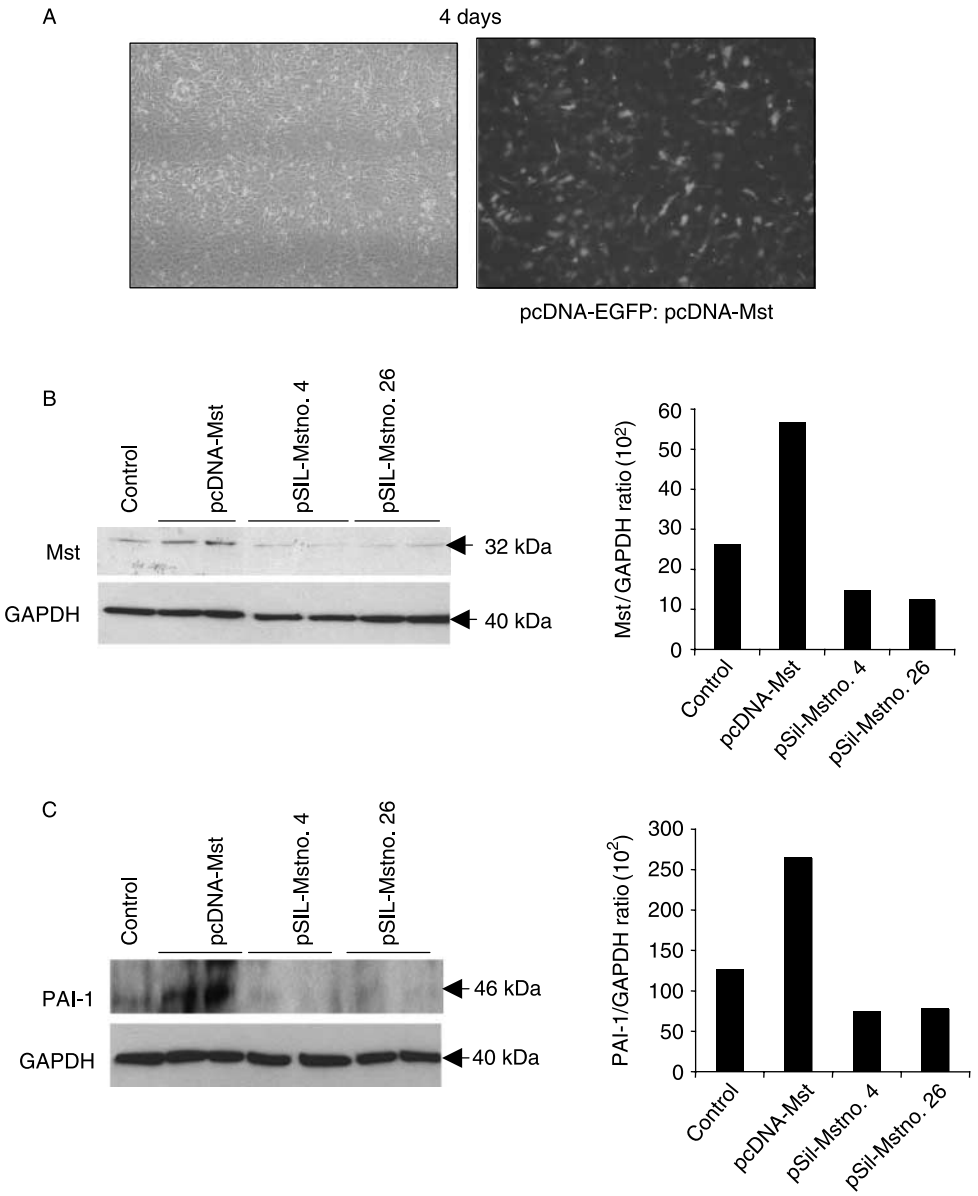

Figure 7 Effect of the modulation of the endogenous expression of myostatin on the expression of PAI-1. C3H10T1/2 cells were grown on six-well plates and transfected with either a reporter gene plasmid construct and a plasmid DNA construct encoding myostatin, or the latter construct or the one for myostatin shRNA, and analyzed after 4 days. (A) Fluorescent microscope, green filter (right), or regular light (left) of cells co-transfected with pcDNA-Mst and pcDNA-EGFP in order to check transfection efficiency (200×). (B) Western blot analysis of myostatin expression, with GAPDH as reference gene of cells transfected with: pcDNA-Mst-375; Mst siRNAs: pSiL-Mstno. 4 and pSiL Mstno. 26 (sequences no. 4 and no. 26) (left), densitometry evaluation of band intensities (right). (C) Western blot analysis of PAI-1 expression, as shown in (B).

products that define fibrosis – collagens I, III, and other isoforms (Bhogal *et al.* 2005, Attallah *et al.* 2007).

These processes were associated with the upregulation of the expression of Smad3 and 4, and the phosphorylation of Smad2 and 3, as expected from a member of the TGF-β family that signals through this pathway (Zhu *et al.* 2004, Kollias *et al.* 2006). An antifibrotic process was simultaneously elicited, as evidenced by the stimulation of the expression of a) the myostatin activity inhibitor, follistatin (Hill *et al.* 2002, Amthor *et al.* 2004, Kocamis *et al.* 2004), b) a Smad signaling inhibitor, Smad7 (Forbes *et al.* 2006), and c) a collagen breakdown inducer, matrix metalloproteinase 8 (MMP-8; Siller-Lopez *et al.* 2004). Follistatin did block the upregulation of TGF-β1 expression by myostatin, as shRNA against myostatin (Magee *et al.* 2006) inhibited the

expression of PAI-1, which in turn was stimulated autocrinely by the forced over-expression of myostatin. It is also well known that PAI-1 expression is upregulated by TGF-β1 (Otsuka *et al.* 2007).

An intriguing aspect of this study is that neither myostatin nor the well-known demethylating agent and differentiation inducer, azacytidine (Singh *et al.* 2003), affected the sizable number of C3H10T1/2 cells (7–8%) that expressed the typical myofibroblast marker ASMA, in the absence of any detectable expression of the smooth muscle cell marker, calponin. Myostatin acted differently from TGF-β1 in this respect, and in its inability to induce (at least in 10 days) the smooth muscle cell lineage, since TGF-β1 stimulates considerably the appearance of smooth muscle markers in this cell line at an earlier stage, acting through the Smad2/3 pathway (Sato *et al.* 2005, Chen *et al.* 2006).

The induction by exogenous recombinant myostatin protein of the expression of collagens I and III mRNA and protein is the hallmark of the acquisition of a fibrotic phenotype. This is likely to be mediated by the ActIIb receptor that binds myostatin and mediates its signaling, and which was detected in C3H10T1/2 cells (Artaza *et al.* 2007). The increase in the mRNA expression of other minor isoforms of collagen, particularly II and IV, and, to a lesser extent, collagen IX, by myostatin, agrees with what occurs in fibrotic conditions (Bhogal *et al.* 2005, Attallah *et al.* 2007). This may be due at least in part to the observed upregulation of TGF-β1 (Liu *et al.* 2006). This factor is known to upregulate myostatin expression (Budasz-Rwiderska *et al.* 2005). Reports are not available on the induction by myostatin of the other main vascular fibrotic factor, PAI-1, and we assume that the considerable upregulation observed may be either a direct effect of myostatin or is mediated by TGF-β1 (Otsuka *et al.* 2007).

In any case, the observed profibrotic effects of myostatin do not seem to be due to the appearance of a new specific cell lineage that would be very active in extracellular matrix deposition, and would differ from the rest of the cell population in this respect. Rather, profibrotic factor expression and collagen deposition may be mediated by the stimulation of the general multipotent fibroblast population to acquire this phenotype, with little conversion into myofibroblasts and none into smooth muscle cells. This would be similar to the differentiated smooth muscle cell transition from a 'contractile' to 'synthetic' phenotype (Budasz-Rwiderska *et al.* 2005). This transition has also been documented on myofibroblast cultures *in vivo* and *in vitro* (Hirose *et al.* 1999, Burstein *et al.* 2007, Darby & Hewitson 2007, Krieg *et al.* 2007), and myostatin should be considered, along with TGF-β1, as a factor eliciting this response.

We believe that the most significant findings of our study are the detection of an early 'antifibrotic' response simultaneous to the profibrotic phenotype induced by myostatin, as evidenced by the observed upregulation of Smad7, follistatin, and MMP8. The upregulation of Smad7 by myostatin was already observed in an elegant study where myostatin induced the expression of Smad7 in C2C12 myoblasts. The latter in turn inhibited myostatin promoter activity, thus suggesting that myostatin autoregulates its expression by feedback loop through Smad7 (Forbes *et al.* 2006), which involves the interaction of Smad2/3 with the Smad7 promoter (Zhu *et al.* 2004). The fact that Smad7 abrogates myostatin – but not TGF-β1-mediated repression of myogenesis (Kollias *et al.* 2007) – raises the question of why myofibroblast differentiation was not triggered by the myostatin-induced TGF-β1 expression in our experiments. It seems that either this expression was too low to trigger C3H10T1/2 cell differentiation, or the Smad7 induction by myostatin was blocked in these cells through counteracting the Smad2/3 upregulation. Myostatin does inhibit myoblast progression into myotubes in C2C12 myoblasts via Smad3 phosphorylation (Langley *et al.* 2002).

The upregulation of follistatin expression by myostatin does not seem to have been reported before, although TGF-β1 through the Smad protein potentiates the stimulatory effects of tumor necrosis factor-α (TNF-α) on the activity of a follistatin-related gene promoter (Bartholin *et al.* 2007), and TNF-α is associated with fibrotic processes (Yoshimura 2006). TGF-β1 also directly upregulates follistatin expression in bovine granulosa cells (Fazzini *et al.* 2006). As stated previously, follistatin in turn inactivates myostatin, and is a well-known antifibrotic agent (Sulyok *et al.* 2004, Wada *et al.* 2004). Our findings are consistent in terms of indicating that treatment with follistatin counteracted the upregulation of TGF-β1 expression exerted by recombinant myostatin in our culture.

Smad7 and follistatin inhibit myostatin signaling and activity respectively, and therefore act as a feedback mechanism against myostatin profibrotic effects, demonstrated by the fact that the C3H10T1/2 cells reacted to myostatin by upregulating MMP-8. This metalloproteinase, like MMP-1 or MMP-13, cleaves collagen at a single site and renders it susceptible to degradation by other MMPs and proteases. An adenoviral construct for a cDNA encoding MMP-8 over-expressed the MMP-8 pro-collagenase in rat models of liver fibrosis, which was then endogenously activated and led to a reversion of the process (Siller-Lopez *et al.* 2004). The MMP-8 upregulation exerted by myostatin in our system therefore appears to be an attempt to degrade collagens I and III deposited as a result of incubation with myostatin. This is sort of a second stage of defense to complement the feedback mechanism that inactivates myostatin.

The interplay of profibrotic and antifibrotic processes observed in the current study with myostatin suggests that counteracting myostatin might be a potentially effective therapy against fibrosis, in addition to that based on the use of decorin (Li *et al.* 2004), Smad7 cDNA (Forbes *et al.* 2006), and follistatin (Aoki *et al.* 2005, Patella *et al.* 2006), against TGF-β1/activin A/Smad signaling, or the use of agents such as deacetylase inhibitors that induce follistatin (Iezzi *et al.* 2004). This approach of targeting myostatin may aim to downregulate myostatin expression, like the shRNA against

myostatin applied in the current *in vitro* study, and that we previously used *in vitro* and *in vivo* to promote myogenesis (Magee *et al*. 2006). Further experimental work is needed on the potential application of these inhibitors to discriminate the relative contribution of myostatin, TGF-β1, and activin to fibrotic processes. It is also important to elucidate whether the Smad pathway is the single downstream signaling for these effectors in the acquisition of the fibrotic phenotype by terminally differentiated cells, and if so, whether Smad7 indeed acts specifically on myostatin in this respect. In addition, despite our results with the C3H10T1/2 cells, it is uncertain whether myostatin *in vivo* triggers the differentiation of endogenous or circulating stem cells to myofibroblasts, as does TGF-β1. If this would be the case, then the anti-myostatin strategy may also block an additional profibrotic mechanism operating through stem cell lineage commitment. However, the fact that myostatin stimulates the switch of myofibroblast to a fibrotic phenotype suggests that this by itself may be the main cellular target for its profibrotic effects, since myofibroblasts play such a fundamental role in fibrosis and scarring (Darby & Hewitson 2007).

Acknowledgements

This work was supported by NIH/MBRS Score Program 3S06-GM068510-02S21 (J A & J T), NIH/NCRR 5U54 RR019234-05 (J A), NIH/National Center on Minority and Health Disparities 1P20 MD000545-02 (J A & M G F), Department of Defense PR064756 (N G C), and NIH/RCMI G12R R003026. The authors declare that there is no conflict of interest that would prejudice the impartiality of this scientific work.

References

Amthor H, Nicholas G, McKinnell I, Kemp CF, Sharma M, Kambadur R & Patel K 2004 Follistatin complexes myostatin and antagonises myostatin-mediated inhibition of myogenesis. *Developmental Biology* **270** 19–30.

Aoki F, Kurabayashi M, Hasegawa Y & Kojima I 2005 Attenuation of bleomycin-induced pulmonary fibrosis by follistatin. *American Journal of Respiratory and Critical Care Medicine* **172** 713–720.

Artaza JN, Bhasin S, Mallidis C, Taylor W, Ma K & Gonzalez-Cadavid NF 2002 Endogenous expression and localization of myostatin and its relation to myosin heavy chain distribution in C2C12 skeletal muscle cells. *Journal of Cellular Physiology* **190** 170–179.

Artaza JN, Bhasin S, Magee TR, Reisz-Porszasz S, Shen R, Groome NP, Meerasahib MF & Gonzalez-Cadavid NF 2005 Myostatin inhibits myogenesis and promotes adipogenesis in C3H 10T(1/2) mesenchymal multipotent cells. *Endocrinology* **146** 3547–3557.

Artaza JN, Reisz-Porszasz S, Dow JS, Kloner RA, Tsao J, Bhasin S & Gonzalez-Cadavid NF 2007 Alterations in myostatin expression are associated with changes in cardiac left ventricular mass but not ejection fraction in the mouse. *Journal of Endocrinology* **194** 63–76.

Ask K, Martin GE, Kolb M & Gauldie J 2006 Targeting genes for treatment in idiopathic pulmonary fibrosis: challenges and opportunities, promises and pitfalls. *Proceedings of the American Thoracic Society* **3** 389–393 (Review).

Atkinson BL, Fantle KS, Benedict JJ, Huffer WE & Gutierrez-Hartmann A 1997 Combination of osteoinductive bone proteins differentiates mesenchymal C3H/10T1/2 cells specifically to the cartilage lineage. *Journal of Cellular Biochemistry* **65** 325–339.

Attallah AM, Mosa TE, Omran MM, Abo-Zeid MM, El-Dosoky I & Shaker YM 2007 Immunodetection of collagen types I, II, III, and IV for differentiation of liver fibrosis stages in patients with chronic HCV. *Journal of Immunoassay and Immunochemistry* **28** 155–168.

Bartholin L, Guindon S, Martel S, Corbo L & Rimokh R 2007 Identification of NF-κB responsive elements in follistatin related gene (FLRG) promoter. *Gene* **393** 153–162.

Bhogal RK, Stoica CM, McGaha TL & Bona CA 2005 Molecular aspects of regulation of collagen gene expression in fibrosis. *Journal of Clinical Immunology* **25** 592–603.

Budasz-Rwiderska M, Jank M & Motyl T 2005 Transforming growth factor-beta1 upregulates myostatin expression in mouse C2C12 myoblasts. *Journal of Physiology and Pharmacology* **56** (Suppl 3) 195–214.

Burstein B, Qi XY, Yeh YH, Calderone A & Nattel S 2007 Atrial cardiomyocyte tachycardia alters cardiac fibroblast function: a novel consideration in atrial remodeling. *Cardiovascular Research* **76** 442–452.

Chen S, Crawford M, Day RM, Briones VR, Leader JE, Jose PA & Lechleider RJ 2006 RhoA modulates Smad signaling during transforming growth factor-beta induced smooth muscle differentiation. *Journal of Biological Chemistry* **281** 1765–1770.

Darby IA & Hewitson TD 2007 Fibroblast differentiation in wound healing and fibrosis. *International Review of Cytology* **257** 143–179.

Eddy AA & Fogo AB 2006 Plasminogen activator inhibitor-1 in chronic kidney disease: evidence and mechanisms of action. *Journal of the American Society of Nephrology* **17** 2999–3012.

Engvall E & Wewer UM 2003 The new frontier in muscular dystrophy research: booster genes. *FASEB Journal* **17** 1579–1584.

Fazzini M, Vallejo G, Colman-Lerner A, Trigo R, Campo S, Baranao JL & Saragueta PE 2006 Transforming growth factor beta1 regulates follistatin mRNA expression during *in vitro* bovine granulosa cell differentiation. *Journal of Celluar Physiology* **207** 40–48.

Feldman BJ, Streeper RS, Farese RV, Jr & Yamamoto KR 2006 Myostatin modulates adipogenesis to generate adipocytes with favorable metabolic effects. *PNAS* **103** 15675–15680.

Fischer L, Boland G & Tuan RS 2002 Wnt-3A enhances bone morphogenetic protein-2-mediated chondrogenesis of murine C3H10T1/2 mesenchymal cells. *Journal of Biological Chemistry* **277** 30870–30878.

Forbes D, Jackman M, Bishop A, Thomas M, Kambadur R & Sharma M 2006 Myostatin auto-regulates its expression by feedback loop through Smad7 dependent mechanism. *Journal of Celluar Physiology* **206** 264–272.

Gharaee-Kermani M, Gyetko MR, Hu B & Phan SH 2007 New insights into the pathogenesis and treatment of idiopathic pulmonary fibrosis: a potential role for stem cells in the lung parenchyma and implications for therapy. *Pharmacological Research* **24** 819–841.

Hamrick MW, Shi X, Zhang W, Pennington C, Thakore H, Haque M, Kang B, Isales CM, Fulzele S & Wenger KH 2007 Loss of myostatin (GDF8) function increases osteogenic differentiation of bone marrow-derived mesenchymal stem cells but the osteogenic effect is ablated with unloading. *Bone* **40** 1544–1553.

Henderson NC & Iredale JP 2007 Liver fibrosis: cellular mechanisms of progression and resolution. *Clinical Science* **112** 265–280.

Hill JJ, Davies MV, Pearson AA, Wang JH, Hewick RM, Wolfman NM & Qiu Y 2002 The myostatin propeptide and the follistatin-related gene are inhibitory binding proteins of myostatin in normal serum. *Journal of Biological Chemistry* **277** 40735–40741.

Hirose M, Kosugi H, Nakazato K & Hayashi T 1999 Restoration to a quiescent and contractile phenotype from a proliferative phenotype of myofibroblast-like human aortic smooth muscle cells by culture on type IV collagen gels. *Journal of Biochemistry* **125** 991–1000.

Iezzi S, Di Padova M, Serra C, Caretti G, Simone C, Maklan E, Minetti G, Zhao P, Hoffman EP, Puri PL *et al*. 2004 Deacetylase inhibitors increase muscle cell size by promoting myoblast recruitment and fusion through induction of follistatin. *Developmental Cell* **6** 673–684.

Iredale JP 2007 Models of liver fibrosis: exploring the dynamic nature of inflammation and repair in a solid organ. *Journal of Clinical Investigation* **117** 539–548.

Jasuja R, Ramaraj P, Mac RP, Singh AB, Storer TW, Artaza J, Miller A, Singh R, Taylor WE, Lee ML *et al.* 2005 Delta-4-androstene-3, 17-dione binds androgen receptor, promotes myogenesis *in vitro*, and increases serum testosterone levels, fat-free mass, and muscle strength in hypogonadal men. *Journal of Clinical Endocrinology and Metabolism* **90** 855–863.

Kisseleva T & Brenner DA 2006 Hepatic stellate cells and the reversal of fibrosis. *Journal of Gastroenterology and Hepatology* **21** (Suppl 3) S84–S87.

Kocamis H, Gulmez N, Aslan S & Nazli M 2004 Follistatin alters myostatin gene expression in C2C12 muscle cells. *Acta Veterinaria Hungarica* **52** 135–141.

Kollias HD, Perry RL, Miyake T, Aziz A & McDermott JC 2006 Smad7 promotes and enhances skeletal muscle differentiation. *Molecular and Cellular Biology* **26** 6248–6260.

Krieg T, Abraham D & Lafyatis R 2007 Fibrosis in connective tissue disease: the role of the myofibroblast and fibroblast–epithelial cell interactions. *Arthritis Research and Therapy* **9** (Suppl 2) S4.

Langley B, Thomas M, Bishop A, Sharma M, Gilmour S & Kambadur R 2002 Myostatin inhibits myoblast differentiation by down-regulating MyoD expression. *Journal of Biological Chemistry* **277** 49831–49840.

Lee SJ 2004 Regulation of muscle mass by myostatin. *Annual Review of Cell and Developmental Biology* **20** 61–86.

Lee SJ & McPherron AC 2001 Regulation of myostatin activity and muscle growth. *PNAS* **98** 9306–9311.

Li Y, Foster W, Deasy BM, Chan Y, Prisk V, Tang Y, Cummins J & Huard J 2004 Transforming growth factor-beta1 induces the differentiation of myogenic cells into fibrotic cells in injured skeletal muscle: a key event in muscle fibrogenesis. *American Journal of Pathology* **164** 1007–1019.

Liu Y 2006 Renal fibrosis: new insights into the pathogenesis and therapeutics. *Kidney International* **69** 213–217.

Liu X, Hu H & Yin JQ 2006 Therapeutic strategies against TGF-β signaling pathway in hepatic fibrosis. *Liver International* **26** 8–22.

Magee TR, Artaza JN, Ferrini MG, Zuniga FI, Cantini L, Reisz-Porszasz S, Rajfer J & Gonzalez-Cadavid NF 2006 Myostatin short interfering hairpin RNA gene transfer increases skeletal muscle mass. *Journal of Gene Medicine* **8** 1171–1181.

Mauviel A 2005 Transforming growth factor-beta: a key mediator of fibrosis. *Methods in Molecular Medicine* **117** 69–80.

McCroskery S, Thomas M, Platt L, Hennebry A, Nishimura T, McLeay L, Sharma M & Kambadur R 2005 Improved muscle healing through enhanced regeneration and reduced fibrosis in myostatin-null mice. *Journal of Cell Science* **118** 3531–3541.

Otsuka G, Stempien-Otero A, Frutkin AD & Dichek DA 2007 Mechanisms of TGF-beta1-induced intimal growth: plasminogen-independent activities of plasminogen activator inhibitor-1 and heterogeneous origin of intimal cells. *Circulation Research* **100** 1300–1307.

Patella S, Phillips DJ, Tchongue J, de Kretser DM & Sievert W 2006 Follistatin attenuates early liver fibrosis: effects on hepatic stellate cell activation and hepatocyte apoptosis. *American Journal of Physiology. Gastrointestinal and Liver Physiology* **290** G137–G144.

Qi W, Chen X, Poronnik P & Pollock CA 2006 The renal cortical fibroblast in renal tubulo interstitial fibrosis. *International Journal of Biochemistry and Cell Biology* **38** 1–5.

Ruiz-Ortega M, Rodriguez-Vita J, Sanchez-Lopez E, Carvajal G & Egido J 2007 TGF-beta signaling in vascular fibrosis. *Cardiovascular Research* **74** 196–206.

Sato M, Kawai-Kowase K, Sato H, Oyama Y, Kanai H, Ohyama Y, Suga T, Maeno T, Aoki Y, Tamura J *et al.* 2005 c-Src and hydrogen peroxide mediate transforming growth factor-beta1-induced smooth muscle cell-gene expression in 10T1/2 cells. *Arteriosclerosis, Thrombosis, and Vascular Biology* **25** 341–347.

Schmittwolf C, Kirchhof N, Jauch A, Dürr M, Harder F, Zenke M & Müller AM 2005 *In vivo* haematopoietic activity is induced in neurosphere cells by chromatin-modifying agents. *EMBO Journal* **24** 554–566.

Siller-Lopez F, Sandoval A, Salgado S, Salazar A, Bueno M, Garcia J, Vera J, Galvez J, Hernandez I, Ramos M *et al.* 2004 Treatment with human metalloproteinase-8 gene delivery ameliorates experimental rat liver cirrhosis. *Gastroenterology* **126** 1122–1133.

Singh R, Artaza JN, Taylor WE, Gonzalez-Cadavid NF & Bhasin S 2003 Androgens stimulate myogenic differentiation and inhibit adipogenesis in C3H 10T1/2 pluripotent cells through an androgen receptor-mediated pathway. *Endocrinology* **144** 5081–5088.

Singh R, Artaza JN, Taylor WE, Braga M, Yuan X, Gonzalez-Cadavid NF & Bhasin S 2006 Testosterone inhibits adipogenic differentiation in 3T3-L1 cells: nuclear translocation of androgen receptor complex with beta-catenin and T-cell factor 4 may bypass canonical Wnt signaling to down-regulate adipogenic transcription factors. *Endocrinology* **147** 141–154.

Sulyok S, Wankell M, Alzheimer C & Werner S 2004 Activin: an important regulator of wound repair, fibrosis, and neuroprotection. *Molecular and Cellular Endocrinology* **225** 127–132.

Taylor SM & Jones PA 1979 Multiple new phenotypes induced in 10T1/2 and 2T3 cells treated with azacytidine. *Cell* **17** 769–779.

Taylor WE, Bhasin S, Artaza J, Byhower F, Azam M, Willard DH Jr, Kull FC Jr & Gonzales-Cadavid N 2001 Myostatin inhibits cell proliferation and protein synthesis in C2C12 muscle cells. *American Journal of Physiology, Endocrinology and Metabolism* **280** E221–E228.

Tsuchida K 2004 Activins, myostatin and related TGF-beta family members as novel therapeutic targets for endocrine, metabolic and immune disorders. *Current Drug Targets. Immune, Endocrine and Metabolic Disorders* **4** 157–166.

Verrecchia F, Mauviel A & Farge D 2006 Transforming growth factor β signaling through the Smad proteins: role in systemic sclerosis. *Autoimmune Reviews* **5** 563–569.

Wada W, Kuwano H, Hasegawa Y & Kojima I 2004 The dependence of transforming growth factor-beta-induced collagen production on autocrine factor activin A in hepatic stellate cells. *Endocrinology* **145** 2753–2759.

Wang W, Koka V & Lan HY 2005 Transforming growth factor-beta and Smad signalling in kidney diseases. *Nephrology* **10** 48–56.

Willis BC, duBois RM & Borok Z 2006 Epithelial origin of myofibroblasts during fibrosis in the lung. *Proceedings of the American Thoracic Society* **3** 377–382.

Wilson EM & Rotwein P 2006 Control of MyoD function during initiation of muscle differentiation by an autocrine signaling pathway activated by insulin-like growth factor-II. *Journal of Biological Chemistry* **281** 62–71.

Wynn TA 2007 Common and unique mechanisms regulate fibrosis in various fibroproliferative diseases. *Journal of Clinical Investigation* **117** 524–529.

Yamashita S, Maeshima A, Kojima I & Nojima Y 2004 Activin A is a potent activator of renal interstitial fibroblasts. *Journal of the American Society of Nephrology* **15** 91–101.

Yoshimura A 2006 Signal transduction of inflammatory cytokines and tumor development. *Cancer Science* **97** 439–447.

Zhu X, Topouzis S, Liang LF & Stotish RL 2004 Myostatin signaling through Smad2, Smad3 and Smad4 is regulated by the inhibitory Smad7 by a negative feedback mechanism. *Cytokine* **26** 262–272.

Received in final form 4 October 2007
Accepted 7 November 2007
Made available online as an Accepted Preprint
7 November 2007

ORIGINAL RESEARCH—BASIC SCIENCE

Profibrotic Role of Myostatin in Peyronie's Disease

Liliana P. Cantini, MSc,*¶ Monica G. Ferrini, MSc, PhD,*‡§ Dolores Vernet, PhD,* Thomas R. Magee, PhD,*‡ Ansha Qian, PhD,* Robert A. Gelfand, PhD,* Jacob Rajfer, MD,*†‡ and Nestor F. Gonzalez-Cadavid, PhD*†‡§

*Los Angeles Biomedical Research Institute at Harbor-UCLA Medical Center, Urology Research Laboratory, Los Angeles, CA, USA; †Division of Urology, Harbor-UCLA Medical Center, Torrance, CA, USA; ‡Department of Urology, David Geffen School of Medicine at UCLA, Los Angeles, CA, USA; §Department of Internal Medicine, The Charles Drew University, Los Angeles, CA, USA; ¶Instituto Venezolano de Investigaciones Científicas, Caracas, Venezuela

DOI: 10.1111/j.1743-6109.2008.00847.x

ABSTRACT

Introduction. The primary histologic finding in many urologic disorders, including Peyronie's disease (PD), is fibrosis, mainly mediated by the transforming growth factor β1 (TGFβ1).

Aim. To determine whether another member of the TGFβ family, myostatin, (i) is expressed in the human PD plaque and normal tunica albuginea (TA), their cell cultures, and the TGFβ1-induced PD lesion in the rat model; (ii) is responsible for myofibroblast generation, collagen deposition, and plaque formation; and (iii) mediates the profibrotic effects of TGFβ1 in PD.

Methods. Human TA and PD tissue sections, and cell cultures from both tissues incubated with myostatin and TGFβ1 were subjected to immunocytochemistry for myostatin and α-smooth muscle actin (ASMA). The cells were assayed by western blot, Real time-Polymerase chain reaction (RT-PCR), and ribonuclease protection. Myostatin cDNA and shRNA were injected, with or without TGFβ1, in the rat penile TA, and plaque size was estimated by Masson.

Main Outcome Measures. Myostatin expression in the human TA, the PD plaque, and their cell cultures, and myostatin effects on the PD-like plaque in the rat.

Results. A threefold overexpression of myostatin was found in the PD plaque as compared with the TA. In PD cells, myostatin expression was mainly in the myofibroblasts, and in the TA cells, it increased upon passage paralleling myofibroblast differentiation and was up-regulated by TGFβ1. Myostatin or its cDNA construct increased the myofibroblast number and collagen in TA cells. Myostatin was detected in the TGFβ1-induced PD-like plaque of the rat partly in the myofibroblasts, and in the TA. Myostatin cDNA injected in the TA induced a plaque and intensified the TGFβ1 lesion, which was not reduced by myostatin shRNA.

Conclusions. Myostatin is overexpressed in the PD plaque, partly because of myofibroblast generation. Although myostatin induces a plaque in the rat TA, it does not appear to mediate the one triggered by TGFβ1, thus suggesting that both proteins act concurrently and that therapy should target their common downstream effectors. **Cantini LP, Ferrini MG, Vernet D, Magee TR, Qian A, Gelfand RA, Rajfer J, and Gonzalez-Cadavid NF. Profibrotic role of myostatin in Peyronie's disease. J Sex Med 2008;5:1607–1622.**

Key Words. Fibrosis; Fibroblasts; Myofibroblasts; TGFβ1; Stem Cells; Penis

Introduction

Fibrosis refers to an excessive deposition of both collagen fibers and extracellular matrix combined with a relative decrease of cell number. This process is now considered to be at the root of many urologic disorders such as erectile dysfunction, specifically corporal veno-occlusive dysfunction [1–6], overactive bladder, and benign prostatic hyperplasia [7–9], as well as certain nephropathies [10,11]. One of the best recognized forms of fibrosis is Peyronie's disease (PD), which is character-

ized by a distinct circumscribed lesion in the penile tunica albuginea (TA) [12,13]. This condition is rather prevalent, impairs the quality of life of both patients and their partners, and is essentially refractory to any medical treatment. It has been hypothesized that the PD plaque results from microtrauma during the sexual act, may cause severe penile curvature and pain upon erection, and is often associated with erectile dysfunction.

One of the fibrotic factors that seems to be involved in PD, as well as other localized and diffuse fibroses, is the transforming growth factor β1 (TGFβ1) [14,15], a cytokine that elicits collagen deposition and the generation of myofibroblasts, the main cell type involved in scarring and fibrosis [16,17]. The expression of TGFβ1 is enhanced in the PD plaque as compared with the normal TA. A widely employed animal model of this condition is based on the injection of this agent into the TA of the rat, leading to the development, after 6–7 weeks, of a lesion that histologically resembles the human plaque in terms of collagen deposition, plasminogen activator inhibitor-1 (PAI-1) expression, oxidative stress, and other fibrotic markers [18–23]. Tunical TGFβ1 is up-regulated in another rat model of PD, where the TA injury is induced by the injection of fibrin into the TA [23–25]. This model reproduces the fibrinogen transvasation that occurs with microtrauma to the TA in human. Conversely, with interventions that reduce the tunical fibrosis in this fibrin-induced model of PD, TGFβ1 is down-regulated [25].

However, TGFβ1 is not the only member of the large TGFβ super family of growth and differentiation factors (GDFs) that have been implicated as fibrotic agents, as activin, inhibin, and some bone morphogenic proteins (BMPs) are known to induce fibrosis, all converging through downstream signaling by the Smad pathway and presumably, also via the connective tissue growth factor (CTGF) [16,26–29]. More recently, another family member, myostatin, also known as the GDF-8, the only well-identified negative regulator of skeletal muscle mass [30–32], has been proposed not only as an inhibitor of myofiber formation but also as an inducer of fibrosis in skeletal muscle [33–36]. Specifically, (i) myostatin stimulates fibroblast proliferation in vitro and induces differentiation of fibroblasts into myofibroblasts; (ii) TGFβ1 and myostatin stimulate each other's expression or secretion in vivo; (iii) myostatin knockout mice develop significantly less fibrosis when compared with wild-type mice following muscle injury; and (iv) both members of the TGFβ family colocalize in myofibers in the early stages of muscle injury [36].

In turn, myostatin intensifies the fibrotic phenotype of myofibroblasts differentiated from a multipotent mouse cell line of embryonic origin, the C3H 10T1/2, but not the preceding stage in its differentiation pathway into myofibroblasts [37]. This contrasts with the fact that myostatin does modulate myogenic and adipogenic differentiation of the parental cell line [38]. Several tools allow to investigate more mechanistically the role of myostatin in fibrosis vis-à-vis TGFβ1: cDNAs encoding the full-length 375 amino acid myostatin protein and its processed 110 amino acid carboxy terminus, as well as the respective recombinant proteins, and an shRNA that breaks down myostatin mRNA and elicits in vivo a functional response by increasing muscle mass [31,37–40].

In the current work, we have studied whether myostatin is expressed in the normal human penile TA, the human PD fibrotic plaque, in their respective cell cultures, and in the corresponding tissues from the rat model for this condition. We have also examined whether myostatin is expressed in human TA and PD myofibroblasts and whether it can induce their generation in vitro, stimulate collagen synthesis, and enhance in vivo the PD-like plaque triggered in the rat TA by TGFβ1, and whether myostatin plays any role in the aforementioned effects of TGFβ1.

Materials and Methods

Human Tissues and Cell Cultures

Tissue sections, and tissue homogenates preserved at –80°C, derived from one of our previous studies [19] were used. Normal TA was obtained from non-PD patients who were undergoing a penectomy because of either penile cancer or penile prosthesis surgery (N = 4), and the PD plaque was harvested from patients with PD (N = 8) who underwent a surgical procedure to remove the plaque. All procedures were institutional review board-approved, and a written informed consent was obtained. Fragments of the tissue had been stored for 24 hours in "RNAlater" (Ambion, Inc., Austin, TX, USA), for RNA analysis, in 4% formalin for histochemistry and immunohistochemistry, or in a culture medium (Dulbecco's modified essential medium [DMEM]/10% fetal calf serum) for protein analysis. Other portions were frozen at –80°C until further use, whereas the fixed tissues were stored at 4°C in phosphate buffered saline (PBS) until paraffin embedding.

Fibroblast primary cultures containing stem cells were originally obtained from another study [41,42] and maintained in our laboratory either under liquid nitrogen or under cell culture passage. These cells were derived from fragments of human TA from non-PD patients (N = 3) undergoing penile prosthesis surgery or from plaque tissue isolated from PD patients (N = 4) as above. A written informed consent was also obtained under IRB approval. Briefly, each specimen was washed in Hanks solution, minced in fibroblast growth medium-2 (FGM; Cambrex Inc., Walkersville, MD, USA) containing 20% fetal bovine serum (FBS), and plated onto a 25-cm^2 culture flask. Fragments were left undisturbed until attachment for about 1 week, and once the monolayer was starting to develop, they were removed. Medium with 10% serum was replaced once a week, and when cells achieved approximately 80% confluence (3–4 weeks), they were trypsinized and split onto three 10-cm plates. The cells were allowed to grow again to 80% confluence, with the medium changed twice weekly. The cells collected from this passage were considered as passage 1. Successive passages were performed at 1:3 split ratio, and the cells were used at passages 1–15. The purity of these cultures was established by immunocytochemistry for the fibroblast marker vimentin, which showed 100% staining as previously described, with virtually no TA cells positive for α-smooth muscle actin (ASMA) [20,41].

For the experiments, after trypsination and centrifugation the cell pellet from one plate was suspended and plated at 25–35% confluence on 8-well removable chamber plates (for immunocytochemistry), 12-well plates (for protein homogenates), or 6-well plates (for RNA isolation) and allowed to grow in either FGM or osteogenic medium (OM) supplemented with 10% FBS [43] for the indicated periods (usually 2 or 4 weeks). OM consisted of DMEM with 0.1 μM dexamethasone, 50 μM ascorbate-2 phosphate, and 10 mM β-glycerophosphate. In certain experiments, TGFβ1 was added at the indicated concentrations. All experiments were in duplicate or triplicate.

Myostatin Protein and Adenoviral cDNA Construct

Two human myostatin recombinant proteins, with identical amino acid sequence to the mouse counterparts, were used for cell incubations. They correspond to the 375 amino acid full sequence (Mst375) and to the 110 amino acid carboxy-terminus cleavage product claimed to be the final processed myostatin protein (Mst110). Each was prepared as described [31,39].

The construction of adenovirus expressing the mouse myostatin full-length cDNA under the CMV promoter (AdV-CMV-Mst375) was carried out as follows: the mouse myostatin cDNA was initially cloned into the donor plasmid pDNR-CMV using the Adeno-X Expression System II Kit (Clontech, Palo Alto, CA, USA). The myostatin sequence was generated by PCR from a previously cloned mouse myostatin plasmid (pcDNA3.1-myostatin) [40], by using primers located at the 5′ and 3′ regions. The 5′ ends of each primer have homology to the pDNR-CMV vector in order to facilitate recombinational cloning into the vector. PCR amplification was done in a reaction mix consisting of 1× HD Advantage polymerase buffer, 0.2 mM deoxyribonucleotide triphosphate (dNTP) mix, 200 pmol of each primer, 50 ng of myostatin plasmid template, and 1 unit of Advantage HD polymerase (Clontech) in a total volume of 25 μL. The reaction consisted of 30 cycles of 94°C for 15 seconds, 60°C for 15 seconds, 72°C for 1 minute, followed by a final 72°C incubation for 10 minutes. PCR fragment was agarose gel purified and then recombined into the pDNR-CMV donor plasmid using the BD In-Fusion cloning kit as per manufacturer's instructions (Clontech). Recombinant plasmids were transformed into DH5-alpha competent *Escherichia coli* and clones verified by DNA restriction enzyme analysis and DNA sequencing resulting in plasmid pDNR-CMV-Mst375.

Then, the Mst375 cDNA was recombined into pLP-Adeno-X-CMV acceptor plasmid using the Adeno-X Expression System II Kit according to the manufacturer's instructions (Clontech). The plasmids were transformed into *E. coli*, screened for correct recombination, and purified using a Qiagen Endo-Free Maxi Kit (Qiagen, Valencia, CA, USA). The adenoviral plasmid was linearized with PacI DNA restriction enzyme and transfected into HEK293 cells in a 6-cm plate using Lipofectamine 2000 (BD Biosciences, Palo Alto, CA, USA) as described previously [40]. Adenovirus infected cells were harvested after 3 days, amplified once, and the resulting viral lysate was used for subsequent infection experiments. The virus was titered by serial dilution and infection of HEK293 cells in 96-well plates as described in the pSilencer adeno 1.0-CMV system kit manual (Ambion). Viral titer is expressed as infective viral units per milliliter (ivu/mL).

Adenoviral Myostatin shRNA

The construction of adenovirus expressing an shRNA, which targets myostatin, was carried out as follows: the shRNA against mouse myostatin had been identified by our group as previously described, with the shRNA inhibiting more than 95% of myostatin gene expression [37,38,40]. Oligonucleotides corresponding to the shRNA were synthesized, annealed, and ligated into the pSilencer adeno 1.0 shuttle vector according to the manufacturer's instructions (pSilencer adeno 1.0-CMV system kit). The top annealing oligonucleotide was 5′-TCGAGGATGACGATTATCACG CTATTCAAGAGATAGCGTGATAATCGTCA TCTTA-3′ and the bottom annealing oligonucleotide was 5′-CTAGTAAGATGACGATTATCA CGCTATCTCTTGAATAGCGTGATAATCGT CATCC-3′. The DNA sequence consists of a XhoI DNA restriction site, sense strand, nine nucleotide loop, antisense strand, and SpeI DNA restriction site 5′ to 3′. In addition, an shRNA "randomer," provided with the pSilencer kit and known not to block any mammalian mRNA, was also prepared. The shRNA plasmid constructs were identified by DNA sequencing. The pSilencer Adeno 1.0-Mst shRNA plasmid and adenoviral vector backbone plasmid were linearized with Pac1 and cotransfected in HEK293 cells using the calcium phosphate transfection method. Virus lysate was isolated, amplified, and titered as described above for the myostatin cDNA adenovirus, yielding a virus named AdV-Mst shRNA.

Both the AdV-CMV-Mst375 and the AdV-Mst shRNA constructs were tested for their ability to express or block the expression of myostatin in HEK293 cells by western blot, and later in the TA cells, as described under the Results section.

Animal Treatments

Male Fisher 344 rats (8–11 months old, NIH/NIA colony Harlan Sprague–Dawley, Inc., San Diego, CA, USA) were maintained under controlled temperature and lighting and treated according to the National Institutes of Health (NIH) regulations with an institutionally approved protocol. The rats (N = 5/group) were anesthetized with isofluorane (IsoFLO, Abbott Labs, North Chicago, IL, USA) by inhalation in an induction chamber at a concentration of 2.3% and injected in the penile TA close to the middle of the penis with either saline or 0.5 μg TGFβ1 (Biotech Diagnostic, Laguna Niguel, CA, USA), as previously described [19]. Other similar groups received either TGFβ1 together with a single injection in the tunica of AdV-CMV-Mst375 (2×10^6 ivu), or alternatively, after 5 weeks, saline and AdV-Mst shRNA (2×10^6 ivu). During the penile injection, anesthesia was maintained with a face mask. At 45 days after the initial injection into the TA, the rats were pretreated with heparin (1,000 UI/kg; intraperitoneal (i.p.). 15 minutes before perfusion, Elkins-Sinn, Cherry Hills, NJ, USA), anesthetized with thiopental (50 mg/g, Abbott Labs), and perfused through the left ventricle with saline followed by 10% formalin, and the penises were excised. The skin was denuded, removing the glans and adhering non-crural tissue, the penile shaft was separated from the crura, and a 2- to 3-mm transversal slice was cut around the site of the saline or TGFβ1 injection. The tissues were postfixed or fixed overnight in 10% formalin, washed in PBS, and stored at 4°C in 70% ethanol.

Quantitative Estimations in Tissue Sections

For histochemistry and immunohistochemistry, 5-μm adjacent tissue sections obtained from the human or rat tissues were used for at least one of these procedures: (i) collagen/smooth muscle cells ratio by Masson trichrome (Sigma Diagnostic, St. Louis, MO, USA) [19–25] and (ii) myostatin detection by immunodetection, using a rabbit polyclonal purified immunoglobulin G (IgG) antibody generated by our group against a 16-amino acid sequence starting at residue 349 (peptide B) common to human and mouse sequences [31]. For myostatin, the sections were quenched in 0.3% H_20_2–PBS, blocked with goat serum (Vector Laboratories, Burlingame, CA, USA), and incubated overnight at 4°C, with the primary antibody at a 1:500 dilution. This was followed by reaction with biotinylated anti-rabbit IgG (Vector Laboratories) for 30 minutes, followed by the Avidin: Biotinylated enzyme Complex (ABC) complex (1:100; Vector Laboratories) and 3,3′ diaminobenzidine. The sections were counterstained with hematoxylin. Negative controls omitted the primary antibodies or replaced them with IgG isotype at the same concentration. All slides were dehydrated and mounted with permount.

Cells grown on eight-well chamber slides were fixed in 4% p-formaldehyde, quenched with H_2O_2, blocked with normal goat or horse serum, and incubated with specific antibodies for (i) myostatin, with antibody as above and (ii) ASMA mouse monoclonal antibody in Sigma kit, $^1/_2$ dilution (Sigma Chemical, St. Louis, MO, USA), as a marker for myofibroblasts.

Tissue staining was quantified by quantitative image analysis (QIA) using the ImagePro 4.01 program (Media Cybernetics, Silver Spring, MD, USA) coupled to an Olympus BHS microscope equipped with a Spot RT color digital camera (Diagnostic Instruments Inc., Sterling Heights, MI, USA) [19–25,37–41]. The PD-like plaque in the rat TA was estimated by Masson trichrome staining within the half section of the corpora cavernosa where the tunical injection was given. The plaque size was expressed as the ratio between the area that stained positive for collagen fibers (blue), divided by the total area of smooth muscle cells (red) plus the remaining lacunar spaces and the cytoplasm of nonstained cells, mainly fibroblasts (white). For myostatin, using a computer-generated grid, the number of positive cells was counted in the TA, and the results were expressed as the number of positive cells per field area, and as the total intensity (optical density) per field area. Five nonoverlapping fields were screened. Six sections per tissue specimen from the groups of eight rats were then used to calculate the mean ± standard error of the mean (SEM).

For nonquantitative dual confocal microscopy, the primary antibodies against myostatin and ASMA were as described above, and the secondary anti-mouse IgG antibody was biotinylated (goat, 1/200, Vector Laboratories). The complex was detected using streptavidin linked to Texas Red (red) or fluorescein (FITC) (green). After washing with PBS, the sections were mounted with Prolong antifade (Molecular Probes, Carlsbad, CA, USA). The negative controls in all cases omitted the first antibodies or they were replaced by IgG isotype. Tissue sections or cells were visualized under a Leica TCS SP (Bannockburn, IL, USA) confocal laser-scanning microscope equipped with argon and HeNe lasers coupled to an acquisition software. Images were imported to Adobe Photoshop 7.0 (San Jose, CA, USA), cropped and adjusted for brightness and contrast only, and saved as tagged image file format (TIFF) files.

Western Blot and Densitometry Analysis

Cell lysates (20–50 μg of protein) were subjected to western blot analyses [31,37–41] by 4–15% Tris-HCl polyacrylamide gel electrophoresis (Bio-Rad, Hercules, CA, USA) in running buffer (Tris/glycine/sodium dodecyl sulfate). Proteins were transferred overnight at 4°C to nitrocellulose membranes in transfer buffer (Tris/glycine/methanol). The next day, nonspecific binding was blocked by immersion of the membranes in 5% nonfat dried milk, 0.1% (v/v) Tween 20 in tris buffered saline (TBS) for 1 hour at room temperature. After several washes with washing buffer (TBS Tween 0.1%), the membranes were incubated with the primary antibodies for 1 hour at room temperature. Monoclonal antibodies were as follows: (i) ASMA, monoclonal (1/1,000) (Calbiochem, La Jolla, CA, USA); (ii) glyceraldehyde-3-phosphate dehydrogenase (GAPDH) (1/10,000) (Chemicon International, Temecula, CA, USA) [41]; and (iii) myostatin, using a mouse monoclonal antibody against the myostatin carboxy-terminal 113 amino acids [38]. In negative controls, we either omitted the first antibody or used a nonimmune IgG. The washed membranes were incubated for 1 hour at room temperature with 1/3,000 dilution of anti-mouse secondary antibody linked to horseradish peroxidase. After several washes, the immunoreactive bands were visualized using the Super Signal West Pico Chemiluminiscent detection system (Pierce, Rockford, IL, USA). The densitometry analysis of the bands was done with the Scion Image software beta 4.0.2 (Scion Corp., Frederick, MD, USA).

RT-PCR and Ribonuclease Protection Assay

Two micrograms of total RNA extracted from human tissues or cultured cells using the Trizol reagent (Invitrogen; Carlsbad, CA, USA) were reverse transcribed, and cDNA was amplified for 35 cycles by PCR at 94°C for 30 seconds, primer annealing at 58°C for 30 seconds, and extension at 72°C for 1 minute [37,38,40]. PCR products were analyzed in 2% agarose gels. In some cases, a multiplex reaction was carried out, using the primers ii, iii, v, vi, and vii, in combination. The sequences of the Mst forward/reverse PCR primers, and the predicted fragment sizes, are as follows: (i) myostatin: forward: 5′-GACAAAACACGAGGTAC TC, reverse: 5′-TGGATTCAGGCTGTTTGA GC (531 bp); (ii) myostatin: forward: 5′-GGAAA CAATCATTACCATGC, reverse: 5′-ATCCATA GT TGGGCCTTTAC (129 bp); (iii) ASMA: forward: 5′-CCGGGACATCAAGGAGAAAC, reverse: 5′-CATAGTGGTGCCCCCTGATA (289 bp); (iv) GAPDH: forward: 5′-ATCACTG CCACC CAGAAGACT, reverse: 5′-CATGCC AGTGAGCTTCCCGTT (152 bp); (v) GAPDH: forward: 5′-CATGGGGAAGGTGAAGGTCG, reverse: 5′-TTACTCCTTGGAGGCCATG (1,009 bp); (vi) collagen I-α: forward: 5′-AGGT GCTACATCTATGTGAT, reverse: 5′-TTCCA CATGCTTTATTCC AG (510 bp); and (vii) BMP-2: forward: 5′-TTGGACACCAGGTTGG

TGAA, reverse: 5′-AGGCGT TTCCGCTGTT TGT (302 bp).

A ribonuclease protection assay [44] was carried out to conclusively determine the presence of the myostatin mRNA. Twenty micrograms of total RNA was used for hybridization based on the manufacturer's protocol (RPA III assay, Ambion). The myostatin probe (80 nucleotides) was in vitro synthesized and radioactively labeled with ^{32}P-UTP using the MaxiScript in vitro transcription kit (Ambion). The probe was DNase treated and ethanol precipitated. Probe (5×10^4 cpm) was coprecipitated with 20-μg nonhomologous RNA overnight, redissolved, denatured, and hybridized to cellular RNA overnight at 42°C. After hybridization, unprotected single-stranded RNA was digested with RNase, which was then inactivated; after which, the protected RNA was precipitated, redissolved, and run on a 5% denaturing polyacrylamide gel. Following electrophoresis, the gels were dried onto filter paper and exposed to X-ray film for 72 hours.

Statistics

The data are expressed as the mean (SEM). The normality of the data distributions was established by the Wilk–Shapiro test, and pairs of groups were compared by the *t*-test. Multiple comparisons among groups were analyzed by one-way analysis of variance, followed by post hoc Student–Neuman–Keuls tests. Differences were considered significant at $P < 0.05$.

Results

Myostatin is Expressed in the Normal Human TA and Overexpressed in PD Fibrotic Plaque, and the Latter Expression Occurs at Least in Part in Myofibroblasts

Paraffin-embedded tissue sections of the human PD plaque and the normal TA, adjacent to those sections used for previous studies [19], were subjected to immunohistochemistry for myostatin. Representative micrographs (Figure 1A, B) show that only a few discrete cells were positive in the normal TA (Figure 1A), whereas a much larger number of cells were intensively stained in the plaque (Figure 1B). QIA (Figure 1, bottom) showed a significant increase in both the number of positive cells (over threefold) and in the intensity of staining in the PD plaque as compared with the normal TA.

The immunohistochemical detection of myostatin was validated by identifying the mRNA for myostatin in three specimens of the PD plaque by RT-PCR, with a set of primers spanning two exons, which rules out any contribution from eventual DNA contamination, that leads to a 510-bp fragment (Figure 2A). The RNA from the normal penile corpora cavernosa generated a much fainter band, suggesting that it stems mainly from the tunica. The band in the positive control skeletal muscle tissue was intense, as expected, and was absent in the negative control reaction of PD plaque RNA in which reverse transcriptase was omitted. A second validation, the confirmation of the expression at the protein level, was obtained by western blot of tissue homogenates from the same PD specimens, showing the 32-kDa putative glycosylated dimer of the 110 amino acid processed protein [31], and the 52-kDa monomeric 375 amino acid full-length protein (Figure 2B).

In the dual fluorescence immunodetection of tissue sections adjacent to the ones examined in Figure 1, virtually all myofibroblasts in the PD plaque (identified in red fluorescence by ASMA immunostaining in Figure 2C, panel A) expressed myostatin (identified in green fluorescence, Figure 2C, panel B), as confirmed by the overlay where positive cells are yellowish (Figure 2C, panel C). However, myostatin was also expressed in cells not positive for ASMA, and hence, not identifiable as myofibroblasts, possibly fibroblasts or stem cells [41,45].

Myostatin is Also Overexpressed in Human PD Plaque Cells, Stimulates Myofibroblast Generation and Collagen Expression in Normal TA Cells, Is Up-Regulated and Translocated by TGFβ1, and Potentiates the Effects of TGFβ1

As the cell cultures obtained from both the normal human TA and the PD plaque are mostly fibroblasts but, in addition, contain both myofibroblasts and stem cells [41,45], we investigated, by RT-PCR, the relationship between the myofibroblast content and myostatin expression at different cell passages. Figure 3A shows that little myostatin mRNA was expressed in the normal tunical cells, but this expression increased with passage number, in parallel to a similar increase in the faint ASMA band, denoting simultaneous myofibroblast generation. In contrast, the PD cells had, from the very early period, much higher levels of myostatin than the tunical cells. This expression in the PD cells remained constant with passage, paralleling robust expression of ASMA, in close correspondence to the situation in vivo. These differences between cultures from the PD plaque and the TA

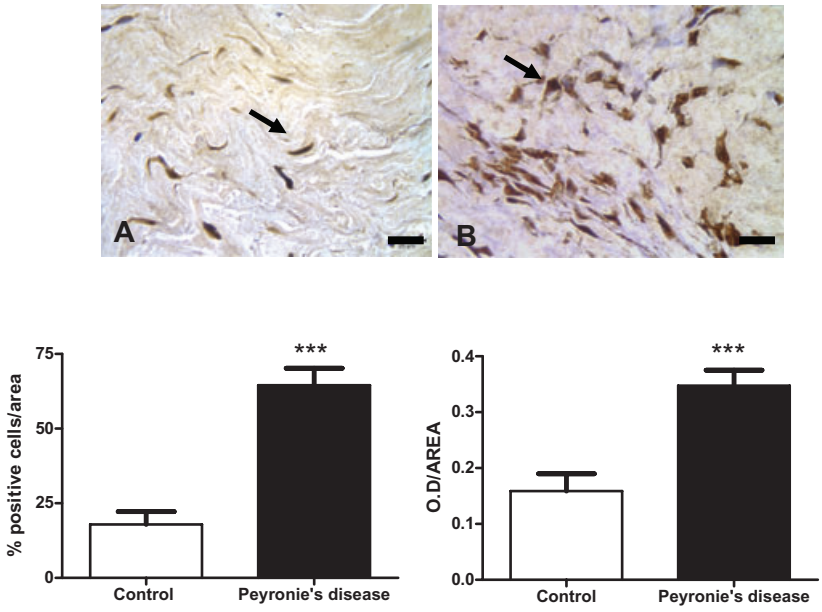

Figure 1 Myostatin is overexpressed in discrete cells in the human Peyronie's disease (PD) plaque, as compared with the normal tunica albuginea. (A, B) Representative micrographs of paraffin-embedded tissue sections stained with myostatin antibody by immunohistochemistry, without counterstain. (A) Tunica albuginea from normal subjects; (B) fibrotic PD plaque. (Bottom) Quantitative image analysis (N = 5/group). ***$P < 0.001$.

would be even more pronounced if the band intensities were normalized for the relatively lower expression in the PD cells of GAPDH.

To exclude any artifact in the detection of myostatin mRNA from the cells, as RT-PCR may pick up even RNA breakdown products or contaminating DNA, we carried out a ribonuclease protection assay to visualize the predicted 225-bp protected fragment that would be a better indication of intact mRNA. Figure 3B shows a clear band in

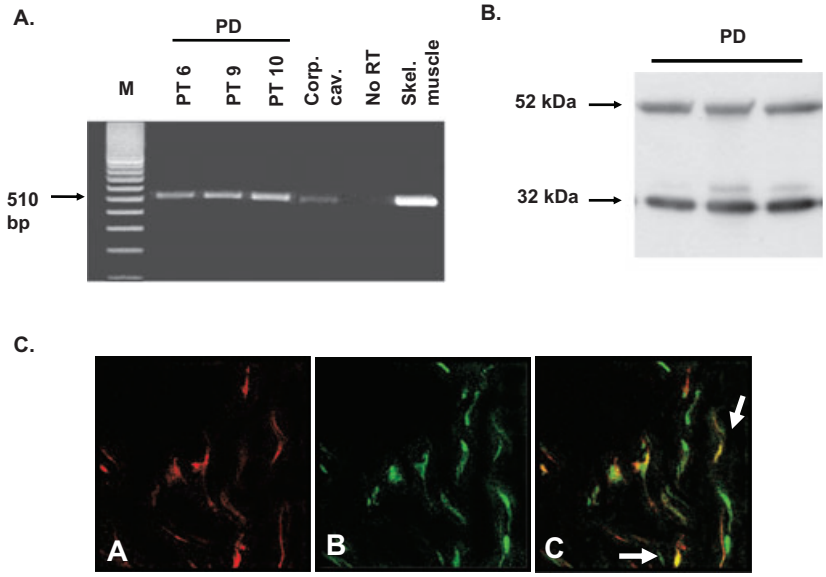

Figure 2 Myostatin expression in the human fibrotic Peyronie's disease (PD) plaque was confirmed by RT-PCR and western blot, and detected in the myofibroblasts by immunofluorescence. (A) RNA was isolated from three specimens of PD plaque, subjected to RT-PCR that yields a 510-bp RNA, and visualized by ethidium bromide staining on agarose gels. (B) Aliquots from the same three specimens of PD plaque were subjected to western blot for myostatin and luminol reaction, identifying two bands of 32 and 52 kDa. (C) Representative micrographs for tissue sections adjacent to those on Figure 1B. The sections were reacted sequentially with α-smooth muscle actin (ASMA) and myostatin primary antibodies, followed by specific secondary antibodies linked to either Texas Red (panel A, ASMA) or biotin and streptavidin-FITC (panel B, myostatin). The sections were examined separately (panels A, B) and after overlay (panel C) under a regular fluorescent microscope. Dual-stained cells are indicated with arrows. Corp. cav. = human corpora cavernosa RNA; no RT = reaction for PT10 RNA conducted without reverse transcriptase; skel. muscle = positive control from human skeletal muscle RNA.

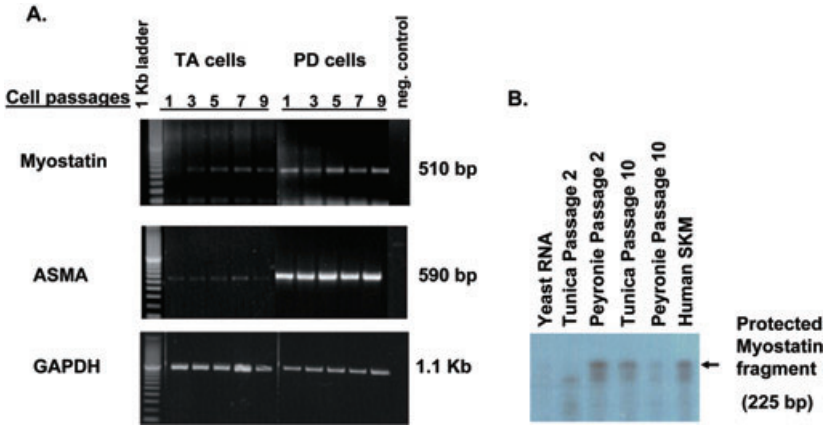

Figure 3 Cell cultures from the human Peyronie's disease (PD) plaque containing myofibroblasts overexpress myostatin, in comparison to cells from the normal tunica albuginea (TA), as determined by RT-PCR and ribonuclease protection assay. (A) RNA was isolated from the cell cultures from the normal TA (TA cells) and PD plaque (PD cells) at passages 1–9, and was subjected to RT-PCR for myostatin as in Figure 2A, for α-smooth muscle actin (ASMA), and for glyceraldehyde-3-phosphate dehydrogenase (GAPDH) as the reporter gene. (B) RNAs between passages 2 and 10, and from the yeast (negative control) and skeletal muscle (SKM) (positive control) were subjected to RNA protection assay and ran on a polyacrylamide gel, detecting the 225-bp protected fragment from the mRNA by hybridization to a cDNA probe.

passage 2 from the human PD plaque cells, which however, was very faint in passage 10, suggesting some degradation. The same band was visible in the RNA from the corresponding tunical passages, and as expected, in the positive control (the human skeletal muscle), and absent in the negative control, yeast. This unequivocally confirmed the expression of myostatin RNA in both the human TA and PD cells.

As TGFβ1 up-regulates ASMA levels in TA cells [41], implying myofibroblast generation, and as TGFβ1 is a key profibrotic factor expressed in the human PD plaque [19,20] and also an inducer of a PD-like plaque in the rat model [19,20,24,35], we next investigated whether TGFβ1 exerted any effect on myostatin localization and content in the TA and PD cells. Myostatin was mainly localized in the nuclei, as shown under high magnification in Figure 4A, and at lower magnification, that incubation with TGFβ1 partially translocated myostatin to the cytoplasm (Figure 4C), in comparison to untreated cells where cytoplasmic myostatin was low (Figure 4B). To determine whether myostatin expression may be a factor in myofibroblast differentiation, human normal TA cells were incubated for 10 days with recombinant human myostatin proteins corresponding to the full-length 375 amino acid (Mst375) (Figure 4E) or the processed carboxy-terminus 110 amino acid (Mst110) (Figure 4F) sequences, or without myostatin (Figure 4D). Both forms of myostatin induced ASMA expression, suggesting that they stimulate myofibroblast generation.

To determine whether myostatin produces a profibrotic effect, we transfected TA cells with an adenoviral construct containing cDNA, encoding the full-length myostatin protein (AdV-CMV-Mst375), and incubated them for 1 week in a medium (OM) that stimulates the fibrogenic and osteogenic differentiation of these cultures [41,43]. Transfected cells were compared with nontransfected controls; RNA was extracted from the cultures and subjected to a simultaneous multiplex RT-PCR analysis for four different genes, using sets of primers that generate DNA fragments that can easily be discriminated by gel electrophoresis (Figure 4, bottom left). In the OM, myostatin RNA expression is virtually negligible, but is significantly expressed after transduction with the myostatin cDNA construct, even at the lower viral load ("1," roughly equivalent to 2–5 ivu). Collagen I-α RNA, a typical end product in the PD plaque, and fibrosis in general, was stimulated in parallel with myostatin. The same result was observed for BMP-2, another TGFβ family member that has not been associated with fibrosis but rather with osteogenesis in general [28] and with PD fibrotic plaque ossification in particular [41]. Densitometric analysis for the expression of each band corrected by GAPDH confirmed this visual evaluation (Figure 4, bottom right).

To confirm the mRNA results at the protein level, normal TA cells were transduced with the AdV-CMV-Mst375 construct and incubated for 10 days. Western blot analysis for myostatin expression shows a substantial dose-dependent overex-

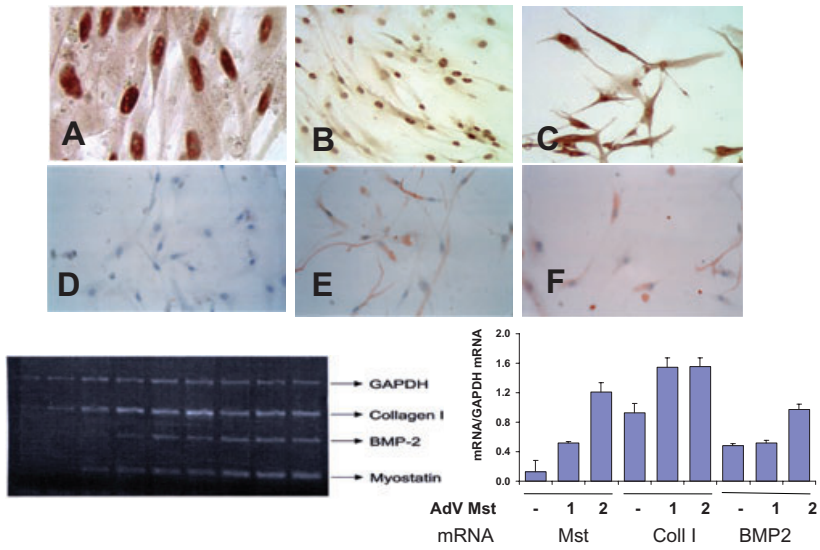

Figure 4 Myostatin mainly localizes in the nuclei of the human Peyronie's disease (PD) plaque cells, translocates upon incubation with the transforming growth factor β1 (TGFβ1), and in the tunica albuginea cells, stimulates α-smooth muscle actin (ASMA) and collagen mRNA expression. (A–C) Representative micrographs of human PD plaque cells were stained with the antibody against myostatin. (A) Control cells (400×); (B) control cells (100×); (C) cells treated with 5 ng/mL TGFβ1 (100×). (D–F) Representative micrographs of human tunica albuginea cells (100×) incubated for 1 week with recombinant human myostatin proteins corresponding to the 110- (F) or the 375-amino acid sequences (E), or without additions (D), and then stained for ASMA. (Bottom left) Ethidium bromide stained agarose gel for multiplex RT-PCR reactions on RNAs from tunical cells incubated for 1 week in special medium, osteogenic medium, that were left untreated or transduced with the adenoviral cDNA construct for Mst375 under the CMV promoter construct at 2 ivu differing by a factor of five. The experiment was carried out in triplicate, as shown. (Bottom right) Densitometric values corrected by glyceraldehyde-3-phosphate dehydrogenase (GAPDH). BMP-2 = bone morphogenic protein-2.

pression induced by the construct, accompanied by a parallel stimulation of ASMA (Figure 5A). The 100% transduction efficiency of this adenoviral vector was confirmed by X-gal staining of cells transduced in parallel with a construct of the same vector expressing β-galactosidase. To assess whether myostatin effects on ASMA expression are additive to those of TGFβ1, the experiment was repeated in the presence and absence of TGFβ1 (5 ng/mL). Figure 5B shows the expected results, namely stimulation of ASMA expression by TGFβ1, potentiated by the adenoviral myostatin construct.

Expression of Myostatin in the Rat TA Is Substantial Despite the Virtual Absence of Myofibroblasts, but Is Not Increased in a TGFβ1-induced PD-like Fibrotic Plaque Where It Is Partially Located in the Myofibroblasts

Myostatin was immunodetected at the site of saline injection in the TA of control rats not injected with TGFβ1. At 45 days after TGFβ1 injection, a surprisingly large level of myostatin expression in discrete cells was observed, nearly as high as in the plaque (Figure 6A, top, a vs. b). QIA (Figure 6A, bottom) confirmed the visual observation. Neither the considerably elevated number of positive cells per unit area in the rat TA (about 60%, well above the 20% in the human TA shown in Figure 1) nor the intensity were significantly different in the TGFβ1-induced plaque. Therefore, endogenous myostatin production in the TA fibroblasts is not by itself sufficient to induce myofibroblast formation or to elicit the fibrotic plaque. As in the case of the human PD plaque, myostatin in the rat counterpart is expressed in myofibroblasts, as shown by double immunofluorescence detection of ASMA and myostatin, analogous to the experiment performed on human tissues (Figure 6B) and also in other cells in the rat PD-like plaque previously identified as fibroblasts by vimentin staining [19,41,42].

Myostatin Can Induce or Stimulate Fibrosis in the Rat TA, and the PD-like Plaque Induced by TGFβ1 Is Enhanced but Does Not Seem to be Mediated by Myostatin

The previous experiment showed that considerable endogenous expression of myostatin occurs in the rat TA, even in the absence of plaque forma-

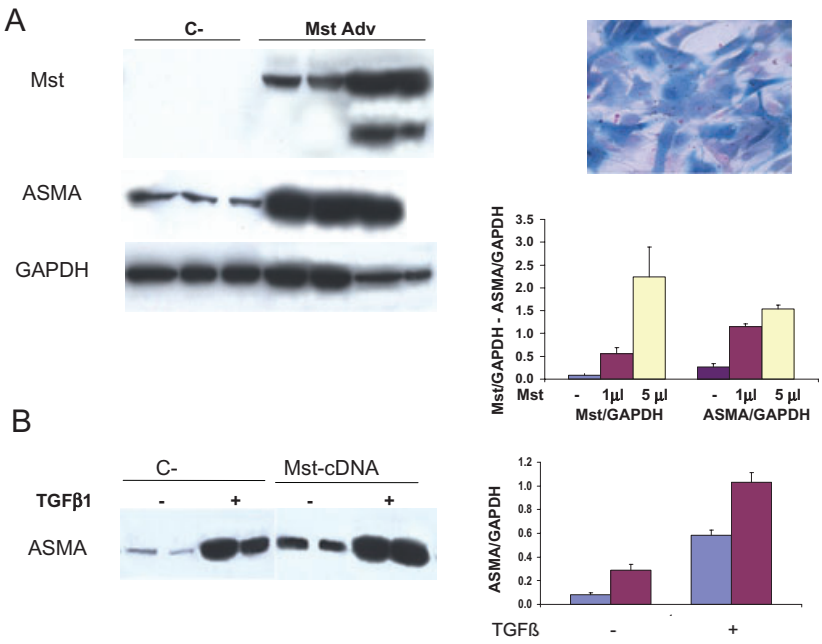

Figure 5 The stimulation of α-smooth muscle actin (ASMA) mRNA expression by myostatin in tunica albuginea cells is also detectable at the protein level and is additive to the transforming growth factor β1 (TGFβ1) effects. (A, left) Representative western blots for tunica albuginea cells left untreated (C) or transduced with 1 or 5 µL of adenoviral cDNA construct for Mst375 under the CMV promoter (Mst AdV) for 10 days, separately probed with antibodies for myostatin, ASMA, and glyceraldehyde-3-phosphate dehydrogenase (GAPDH). (A, top right) Tunica albuginea cells transduced with the corresponding AdV construct expressing β-galactosidase and assayed after 3 days with X-gal. (A, bottom right) Corresponding densitometric analysis of ASMA (38 kDa) and myostatin (50 kDa) band intensities corrected by GAPDH. (B, left) As in A (left) but with cells treated or not with TGFβ1 (5 ng/mL); (B, bottom right) Corresponding densitometric analysis of myostatin band intensities corrected by GAPDH.

tion, whereas in human, it is restricted to the PD plaque itself. To elucidate this apparent discrepancy, we used a more direct approach to determine whether myostatin could induce new plaque development in the rat TA or exacerbate an already preformed plaque. Figure 7 (top) shows the representative micrographs of Masson trichrome staining that detect collagen fibers in blue, and smooth muscle cells in red. The AdV-CMV-Mst375 was injected directly into the TA of the rat, and 45 days later, a PD-like plaque was observable (Figure 7B vs. control in Figure 7A), not significantly different in size from the one induced by TGFβ1 (Figure 7C). When the Adv-Mst construct was injected simultaneously with TGFβ1 (Figure 7D), the plaque was increased in size as compared with the ones generated by TGFβ1 alone. However, the inhibition of myostatin expression with an injection of the corresponding adenoviral anti-myostatin shRNA (AdV-Mst shRNA), that specifically breaks down myostatin mRNA [37,38,40], did not reduce the plaque induced by TGFβ1. This was confirmed by QIA (Figure 7, E). The plasmid construct expressing myostatin shRNA had previously been shown to inhibit myostatin expression in HEK293 cells, 10T1/2 cells, rat cardiomyocytes, and in skeletal muscle [37,38,40]. We confirmed this effect in TA cells by incubation for 3 days with AdV-CMV-Mst375 either alone or in the presence of increasing ratios of AdV-Mst shRNA (Figure 7, bottom right), which showed that the shRNA construct dose dependently inhibited myostatin expression.

Discussion

These results are the first demonstration of the expression of a second TGFβ family member, myostatin, in addition to TGFβ1 itself, in the normal human penile TA and in the human PD fibrotic plaque. In the latter tissue, there is an overexpression of myostatin and this corresponds to what is seen in the cell cultures of the normal human TA and PD plaque. A similar effect was also seen in the corresponding tissues from the experimental rat model of PD, although in the rat tunica, the expression is as high as in the PD-like lesion. The latter tissue resembles the human

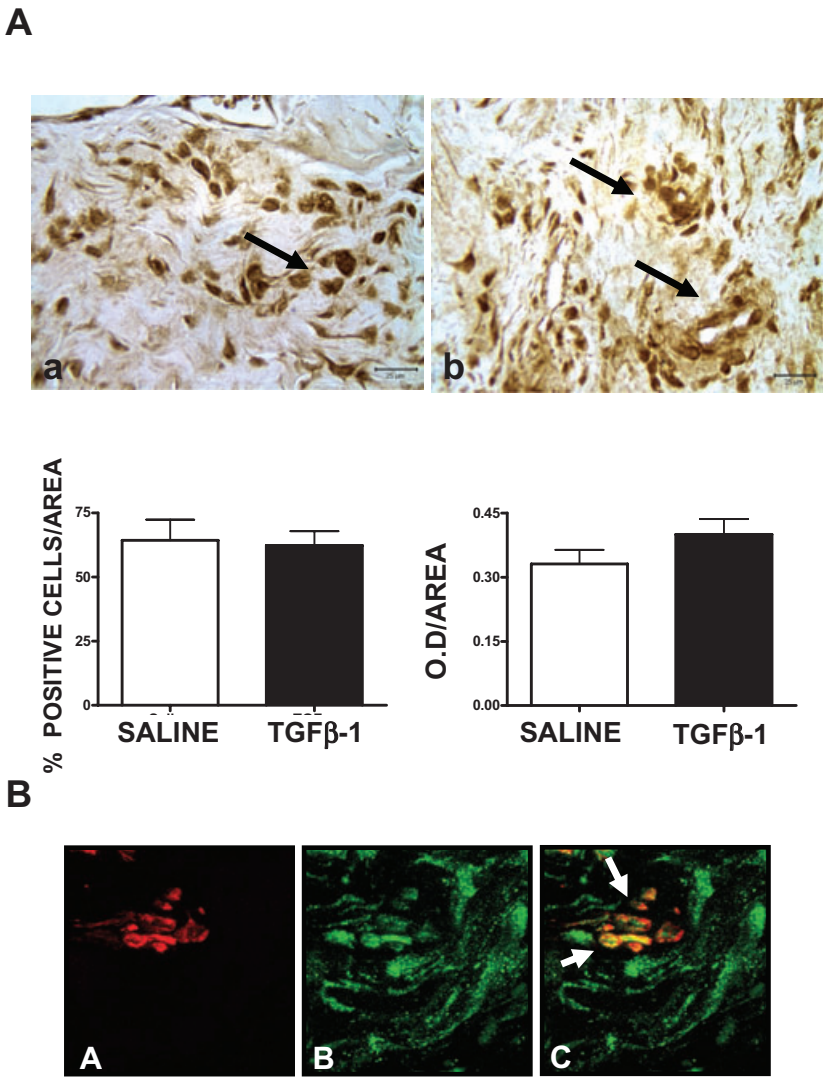

Figure 6 Myostatin is expressed in myofibroblasts in the Peyronie's disease (PD)-like plaque induced by the transforming growth factor β1 (TGFβ1) in the rat tunica albuginea, but in contrast to the human tissue, this does not involve substantial overexpression. (A, top) Representative micrographs (200×, bar = 25 μm) for penile tissue sections around the site of injection from rats treated with either saline (a) or 0.1 μg of TGFβ1 (b) and maintained for 45 days. Immunostaining was performed for myostatin as in Figure 1. (A, bottom) Quantitative image analysis (N = 6/group). (B) Micrographs (200×, bar = 25 μm) for tissue sections adjacent to those in panel A, PD tissue. The sections were stained sequentially by immunofluorescence with α-smooth muscle actin antibody (Texas Red, red fluorescence) and with myostatin antibody (FITC, green fluorescence) as in Figure 2, and examined separately and after overlay under a confocal microscope. Dual-stained cells are indicated with arrows.

plaque in the accumulation and disorganization of collagen fibers, appearance of myofibroblasts, oxidative stress and expression of fibrotic markers, as well as by the induction of the antifibrotic factor inducible nitric oxide synthase. Fibrosis in this rat model is not normally accompanied by chronic inflammation [13,15,18–22]. Although the levels of myostatin in the normal rat tunical fibroblasts are considerable, they are not sufficient to induce myofibroblast formation or fibrosis, and therefore, other ancillary factors may be required for such effects to occur.

Myostatin is expressed both in vivo and in vitro in myofibroblasts, the cells that play a major role in fibrosis. They are characterized by vimentin and ASMA expression, and although the latter marker is also present in smooth muscle cells, their presence was excluded by the absence of smoothelin when the primary cultures were obtained [20,41,42]. In tissue sections, myofibroblasts are

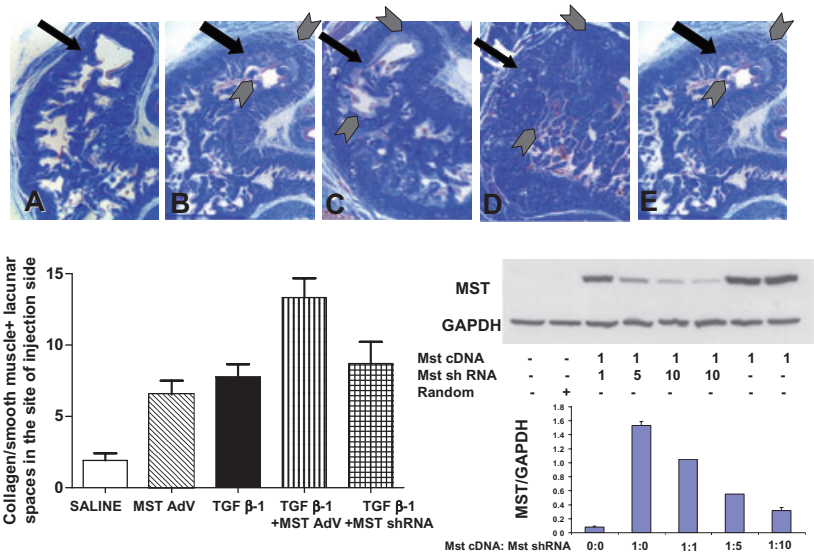

Figure 7 Myostatin overexpression in the rat tunica albuginea induced a small PD like plaque and increased the TGFβ1-induced fibrosis, but myostatin was not necessary for plaque generation. Top: representative micrographs of Masson trichrome-stained tissue sections around the site of intra tunical injection (n = 5/group) with: A: saline; B: AdV-CMV-Mst cDNA (2×10^6 ivu); C: TGFβ1 (0.5 μg); D: AdV-CMV-Mst cDNA and TGFβ1; E: TGF-β1, followed by Adv-CMV-Mst shRNA (2×10^6 ivu) injected 2 weeks before sacrifice. All animals were sacrificed at 45 days from the time of the first injection. Magnification: 40×; Black arrows point to the site of injection; gray arrows show approximately the plaque size. Bottom left: plaque size measured by quantitative image analysis. Bottom right: western blot analysis of the dose dependent inhibition by AdV-CMV-Mst shRNA on the expression of AdV-CMV-Mst cDNA, and quantitative densitometry of bands intensities corrected by GAPDH. TA cells were transfected for 3 days with the indicated constructs. Mst: myostatin; AdV: adenovirus.

easily differentiated from smooth muscle cells by their respective restricted location in the TA and the corpora cavernosa [19,20]. Myostatin expression is seen in the human plaque and in the rat lesion induced by TGFβ1, and in vitro, myostatin triggers the generation of myofibroblasts, presumably from stem cells present in the tunical fibroblast cultures [41,45]. The profibrotic action of myostatin is supported by the finding that in vivo, it can elicit a PD-like plaque in the rat TA and intensify the one triggered by TGFβ1, although the effects of TGFβ1, similar to what occurs in the TA cell cultures, do not seem to require myostatin.

Collectively, the current results extend previous in vitro findings on the intensification by myostatin of the fibrotic phenotype of myofibroblasts derived from the multipotent C3H 10T1/2 cell line [36,37], as well as on the cell lineage differentiation of skeletal muscle fibroblasts [36]. Therefore, myostatin joins not just TGFβ1 but other TGFβ family members such as activin and possibly, BMP-4 [26,28], which have been acknowledged as profibrotic factors, and suggests that antifibrotic therapies aimed at inhibiting common converging downstream effectors for all these proteins would be more effective than trying to block single agents within the family individually.

Myostatin was initially thought to be restricted to skeletal muscle and cultured myotubes [30,31], but subsequently, it was also found to be expressed at low levels in cardiomyocytes [46], differentiating multipotent C3H 10T1/2 cells [37,38], and fibroblasts [36]. This suggests that the role of myostatin was not restricted just to being a negative regulator of skeletal muscle mass, but, in agreement with its original designation as GDF-8, myostatin may also participate in cardiomyocyte, adipocyte, and myofibroblast differentiation [36–38,46]. In contrast to the well-characterized inhibitory action of myostatin on myogenesis, its effects on cardiomyogenesis and adipogenesis are still controversial, but the induction of myofibroblasts and of fibrotic factors by myostatin has been confirmed by at least two groups [36,37]. In an article directly relevant to myofibroblast differentiation, it was shown that myostatin induced in vitro myofibroblast generation from skeletal muscle fibroblasts present in the so-called "PP1" fraction during the muscle derived stem cell (MDSC) PP6 isolation, as indicated by ASMA levels, and that this was accompanied by the deposition of collagen I and III [36].

Our current results in the normal human TA fibroblasts indicate that these profibrotic effects of

myostatin occur in fibroblasts from at least two sources. However, in the human TA cell cultures and rat TA tissue, stem cells have been identified [41,45], and it is not yet clear whether they or the true fibroblasts are the cells undergoing myofibroblast differentiation. We have shown here that myostatin is expressed in TA myofibroblasts and that in vitro, this occurs in the nuclei, in agreement with what has been shown in skeletal muscle fibroblast cultures. This has also been found in another multipotent cell line of fibroblast origin, the mouse C3H 10T1/2 cells, despite the membrane location of its receptor, the activin IIb receptor [46]. Interestingly, the de novo myofibroblast generation induced by myostatin that we have observed was not found in the C3H 10T1/2 cells. Although myostatin is profibrotic in the myofibroblasts themselves, as shown by its effect of switching them to the synthetic phenotype, it does not stimulate stem cell/myofibroblast lineage differentiation per se [37]. The fact that TGFβ1 stimulates myostatin expression, and conversely that myostatin up-regulates TGFβ1 levels, was shown in the case of skeletal muscle fibroblasts [36], and the same observation was also found with the C3H 10T1/2 cells [37]. This mutual interaction between both profibrotic members of the TGFβ family has been confirmed here with TA/PD fibroblast cultures that are known to contain stem cells [41].

It is intriguing that myostatin could induce myofibroblast formation in vitro and a PD-like fibrotic plaque in the rat TA, and stimulate the in vivo plaque induction by TGFβ1, whereas blocking myostatin expression by the shRNA against myostatin did not inhibit plaque formation induced by TGFβ1, and also, endogenous high myostatin expression in the normal rat TA was not associated with fibrosis. It is therefore likely that the myostatin profibrotic effects may proceed mainly via endogenous TGFβ1 induction, as in the case of fibrin [29,30], whereas exogenous TGFβ1 does not seem to require myostatin to act. In fact, decorin, an antifibrotic proteoglycan that binds to and blocks the activity of TGFβ1, neutralizes the effects of myostatin on the fibroblast generation of myofibroblasts [36,47]. However, both decorin [36] and myostatin itself [37] up-regulate the expression of follistatin, an antagonist of these two members of the TGFβ family [48] and also an antagonist to a third member, activin; so, it is difficult to determine whether myostatin can act as a profibrotic agent independently from TGFβ1 secretion. Further studies need to be conducted using a specific blocker of TGFβ1 activity that does not affect myostatin, such as shRNA against TGFβ1.

In earlier experiments, the shRNA construct against myostatin blocked its expression both in vivo in the skeletal muscle [40] and in vitro in several cell cultures [37,38]. In the current study, it was shown to block myostatin expression in tunical cells, but this inhibition did not reduce the PD-like plaque in the rat model. We cannot discard the possibility that the shRNA did not efficiently inhibit myostatin expression in the PD-like plaque, but even if it did, this does not necessarily mean that the profibrotic effects of myostatin are unimportant in the development of the human condition. First, it is quite likely that, as in the skeletal muscle myofibroblasts, there may be a synergistic effect of myostatin and TGFβ1. Second, it is still possible that the TGFβ1-induced plaque in the rat TA does not mimic in this respect the human PD plaque, where TGFβ1 levels may be much lower. Therefore, myostatin would act in that latter setting as a true cofactor in fibrotic induction.

Although anti-TGFβ1 therapeutic strategies have not been tested for PD either experimentally (because the rat lesion requires this agent for the development of PD) or clinically, the potential for intervention against myostatin and other TGFβ family members based on the effects seen in this study, suggests that it would be better to collectively inhibit all these agents rather than focus on inhibiting just one. In this sense, both follistatin and decorin, which have been tested successfully in skeletal muscle fibrosis [47,49], may be worth investigating in rat models of PD, in particular, the model in which the plaque is elicited by fibrin instead of TGFβ1 itself, even if this latter factor is also induced in this type of lesion [24].

Another potential target is the Smad gene set. This acts through a downstream pathway common to TGFβ1, myostatin, and activin, thereby transducing the profibrotic effects of these proteins [27,29]. In this sense, cDNA constructs of the inhibitory Smad7 [50] may be used as a proof of concept, as well as inhibitors of cyclic adenosine monophosphate (cAMP)-dependent phosphodiesterase enzymes (PDEs) such as forskolin or isoproterenol. The latter agents, via the increase of cAMP inhibit TGFβ1-stimulated collagen synthesis and ASMA expression in cardiac fibroblast cultures, in part, by reducing binding of the transcriptional coactivator cAMP response element-binding (CREB)-binding protein 1 to transcriptional complexes containing Smad2, Smad3, and Smad4 [51]. It appears that cAMP-

elevating agents inhibit the profibrotic effects of TGFβ1, partially by reducing the Smad-mediated recruitment of transcriptional coactivators. This would explain our previous results where we observed that a nonspecific PDE inhibitor, pentoxifylline, blocked the development of the TGFβ1-induced fibrotic plaque in the rat TA [22].

On the other hand, BMP-7, a well-known antifibrotic member of the TGFβ family, acting on liver and kidney [52,53], counteracts myofibroblast differentiation and collagen deposition triggered by TGFβ1. This happens in part by inhibition of the expression of its effector, Smad3 [54]. Myostatin increased BMP-7 and Smad7 expression in the multipotent C3H 10T1/2 cells [37]. Independent of the Smad pathway, the relationship of myostatin with the CTGF, an effector for TGFβ1 fibrotic signaling that in part signals through Smad by inhibiting Smad7 and promoting Smad2 [55], needs to be clarified. In conclusion, the multiplicity of TGFβ members that may act as profibrotic agents (particularly TGFβ1 and myostatin) or antifibrotic (BMP-7), their mutual regulatory interaction, their putative synergistic action, and their common signaling pathways should stimulate further studies to clarify their relative contribution to myofibroblast generation and fibrosis development in general, and specifically in PD. This may help to develop novel therapeutic targets for these conditions.

Acknowledgments

This work was supported by grants NIH R01DK-53069, Department of Defense PR064756, and in certain aspects, NIH G12RR-03026. Dr. Ferrini is also supported by Grant N1 P20 MD000545 from the National Center on Minority Health and Health Disparities, NIH.

Corresponding Author: Nestor F. Gonzalez-Cadavid, PhD, LABioMed at Harbor-UCLA Medical Center, Urology, Bldg. F-6, 1124 West Carson Street, Torrance, CA 90502, USA. Tel: (310) 222-3824; Fax: (310) 222-1914; E-mail: ncadavid@ucla.edu

Conflict of Interest: None declared.

Statement of Authorship

Category 1

(a) Conception and Design
Nestor F. Gonzalez-Cadavid

(b) Acquisition of Data
Liliana P. Cantini; Monica G. Ferrini; Dolores Vernet; Thomas R. Magee; Ansha Qian; Robert A. Gelfand

(c) Analysis and Interpretation of Data
Nestor F. Gonzalez-Cadavid; Monica G. Ferrini; Liliana P. Cantini; Dolores Vernet; Thomas R. Magee; Ansha Qian; Robert A. Gelfand

Category 2

(a) Drafting the Article
Nestor F. Gonzalez-Cadavid; Jacob Rajfer; Monica G. Ferrini

(b) Revising It for Intellectual Content
Nestor F. Gonzalez-Cadavid; Jacob Rajfer; Monica G. Ferrini

Category 3

(a) Final Approval of the Completed Article
Nestor F. Gonzalez-Cadavid

References

1 Schwartz EJ, Wong P, Graydon RJ. Sildenafil preserves intracorporeal smooth muscle after radical retropubic prostatectomy. J Urol 2004;171:771–4.
2 Iacono F, Giannella R, Somma P, Manno G, Fusco F, Mirone V. Histological alterations in cavernous tissue after radical prostatectomy. J Urol 2005; 173:1673–6.
3 Nandipati KC, Raina R, Agarwal A, Zippe CD. Erectile dysfunction following radical retropubic prostatectomy: Epidemiology, pathophysiology and pharmacological management. Drugs Aging 2006;23:101–17.
4 Ostojic P, Damjanov N. The impact of depression, microvasculopathy, and fibrosis on development of erectile dysfunction in men with systemic sclerosis. Clin Rheumatol 2007;26:1671–4.
5 Kovanecz I, Rambhatla A, Ferrini M, Vernet D, Sanchez S, Rajfer J, Gonzalez-Cadavid N. Long-term continuous sildenafil treatment ameliorates corporal veno-occlusive dysfunction (CVOD) induced by cavernosal nerve resection in rats. Int J Impot Res 2007 [Epub ahead of print].
6 Burnett AL. Molecular pharmacotherapeutic targeting of PDE5 for preservation of penile health. J Androl 2008;29:3–14.
7 Collado A, Batista E, Gelabert-Mas A, Corominas JM, Arano P, Villavicencio H. Detrusor quantitative morphometry in obstructed males and controls. J Urol 2006;176:2722–8.
8 Tuygun C, Imamoglu A, Keyik B, Alisir I, Yorubulut M. Significance of fibrosis around and/or at external urinary sphincter on pelvic magnetic resonance imaging in patients with postprostatectomy incontinence. Urology 2006;68:1308–12.
9 Bercovich E, Barabino G, Pirozzi-Farina F, Deriu M. A multivariate analysis of lower urinary tract ageing and urinary symptoms: The role of fibrosis. Arch Ital Urol Androl 1999;71:287–92.

10 Liu Y. Renal fibrosis: New insights into the pathogenesis and therapeutics. Kidney Int 2006;69:213–7.
11 Eberhardt W, Pfeilschifter J. Nitric oxide and vascular remodeling: Spotlight on the kidney. Kidney Int Suppl 2007;S9–16.
12 Bella AJ, Perelman MA, Brant WO, Lue TF. Peyronie's disease (CME). J Sex Med 2007;4:1527–38.
13 Gonzalez-Cadavid NF, Rajfer J. Mechanisms of disease: New insights into the cellular and molecular pathology of Peyronie's disease. Nat Clin Pract Urol 2005;2:291–8.
14 Ruiz-Ortega M, Rodriguez-Vita J, Sanchez-Lopez E, Carvajal G, Egido J. TGF-beta signaling in vascular fibrosis. Cardiovasc Res 2007;74:196–206.
15 El-Sakka AI, Hassoba HM, Pillarisetty RJ, Dahiya R, Lue TF. Peyronie's disease is associated with an increase in transforming growth factor-beta protein expression. J Urol 1997;158:1391–4.
16 Darby IA, Hewitson TD. Fibroblast differentiation in wound healing and fibrosis. Int Rev Cytol 2007;257:143–79.
17 Henderson NC, Iredale JP. Liver fibrosis: Cellular mechanisms of progression and resolution. Clin Sci (Lond) 2007;112:265–80.
18 El-Sakka AI, Hassan MU, Nunes L, Bhatnagar RS, Yen TS, Lue TF. Histological and ultrastructural alterations in an animal model of PD disease. Br J Urol 1998;81:445–52.
19 Ferrini MG, Vernet D, Magee TR, Shahed A, Qian A, Rajfer J, Gonzalez-Cadavid NF. Antifibrotic role of inducible nitric oxide synthase. Nitric Oxide 2002;6:283–94.
20 Vernet D, Ferrini MG, Valente EG, Magee TR, Bou-Gharios G, Rajfer J, Gonzalez-Cadavid NF. Effect of nitric oxide on the differentiation of fibroblasts into myofibroblasts in the Peyronie's disease fibrotic plaque and in its rat model. Nitric Oxide 2002;7:262–76.
21 Ferrini MG, Kovanecz I, Nolazco G, Rajfer J, Gonzalez-Cadavid NF. Effects of long-term vardenafil treatment on the development of fibrotic plaques in a rat model of Peyronie's disease. BJU Int 2006;97:625–33.
22 Valente EG, Vernet D, Ferrini MG, Qian A, Rajfer J, Gonzalez-Cadavid NF. L-arginine and phosphodiesterase (PDE) inhibitors counteract fibrosis in the Peyronie's disease fibrotic plaque and related fibroblast cultures. Nitric Oxide 2003;9:229–44.
23 Davila HH, Magee TR, Zuniga FI, Rajfer J, Gonzalez-Cadavid NF. Peyronie's disease associated with increase in plasminogen activator inhibitor in fibrotic plaque. Urology 2005;65:645–8.
24 Davila HH, Ferrini MG, Rajfer J, Gonzalez-Cadavid NF. Fibrin as an inducer of fibrosis in the tunica albuginea of the rat: A new animal model of Peyronie's disease. BJU Int 2003;91:830–8.
25 Davila HH, Magee TR, Vernet D, Rajfer J, Gonzalez-Cadavid NF. Gene transfer of inducible nitric oxide synthase complementary DNA regresses the fibrotic plaque in an animal model of Peyronie's disease. Biol Reprod 2004;71:1568–77.
26 Tsuchida K. Activins, myostatin and related TGF-beta family members as novel therapeutic targets for endocrine, metabolic and immune disorders. Curr Drug Targets Immune Endocr Metabol Disord 2004;4:157–66.
27 Wang W, Koka V, Lan HY. Transforming growth factor-beta and Smad signalling in kidney diseases. Nephrology (Carlton) 2005;10:48–56.
28 Fan J, Shen H, Sun Y, Li P, Burczynski F, Namaka M, Gong Y. Bone morphogenetic protein 4 mediates bile duct ligation induced liver fibrosis through activation of Smad1 and ERK1/2 in rat hepatic stellate cells. J Cell Physiol 2006;207:499–505.
29 Parsons CJ, Takashima M, Rippe RA. Molecular mechanisms of hepatic fibrogenesis. J Gastroenterol Hepatol 2007;22(1 suppl):S79–84.
30 Lee SJ. Regulation of muscle mass by myostatin. Annu Rev Cell Dev Biol 2004;20:61–86.
31 Gonzalez-Cadavid NF, Taylor WE, Yarasheski K, Sinha-Hikim I, Ma K, Ezzat S, Shen R, Lalani R, Asa S, Mamita M, Nair G, Arver S, Bhasin S. Organization of the human myostatin gene and expression in healthy men and HIV-infected men with muscle wasting. Proc Natl Acad Sci USA 1998; 95:14938–43.
32 Gonzalez-Cadavid NF, Bhasin S. Role of myostatin in metabolism. Curr Opin Clin Nutr Metab Care 2004;7:451–7.
33 Wagner KR, McPherron AC, Winik N, Lee SJ. Loss of myostatin attenuates severity of muscular dystrophy in mdx mice. Ann Neurol 2002;52:832–6.
34 Bogdanovich S, Krag TO, Barton ER, Morris LD, Whittemore LA, Ahima RS, Khurana TS. Functional improvement of dystrophic muscle by myostatin blockade. Nature 2002;420:418–21.
35 McCroskery S, Thomas M, Platt L, Hennebry A, Nishimura T, McLeay L, Sharma M, Kambadur R. Improved muscle healing through enhanced regeneration and reduced fibrosis in myostatin-null mice. J Cell Sci 2005;118:3531–41.
36 Zhu J, Li Y, Shen W, Qiao C, Ambrosio F, Lavasani M, Nozaki M, Branca MF, Huard J. Relationships between transforming growth factor-beta1, myostatin, and decorin: Implications for skeletal muscle fibrosis. J Biol Chem 2007;282:25852–63.
37 Artaza J, Singh R, Ferrini MG, Braga M, Tsao J, Gonzalez-Cadavid NF. Myostatin promotes a fibrotic phenotypic switch in multipotent C3H 10T1/2 cells without affecting their differentiation into myofibroblasts. J Endocrinol 2008;196:235–49.
38 Artaza JN, Bhasin S, Magee TR, Reisz-Porszasz S, Shen R, Groome NP, Meerasahib MF, Gonzalez-Cadavid NF. Myostatin inhibits myogenesis and promotes adipogenesis in C3H 10T(1/2) mesenchymal multipotent cells. Endocrinology 2005;146: 3547–57.

39 Taylor WE, Bhasin S, Artaza J, Byhower F, Azam M, Willard DH Jr, Kull FC Jr, Gonzalez-Cadavid N. Myostatin inhibits cell proliferation and protein synthesis in C2C12 muscle cells. Am J Physiol Endocrinol Metab 2001;280:E221–8.
40 Magee TR, Artaza JN, Ferrini MG, Zuniga FI, Cantini L, Reisz-Porszasz S, Rajfer J, Gonzalez-Cadavid NF. Myostatin short interfering hairpin RNA gene transfer increases skeletal muscle mass. J Gene Med 2006;9:1171–81.
41 Vernet D, Nolazco G, Cantini L, Magee TR, Qian A, Rajfer J, Gonzalez-Cadavid NF. Evidence that osteogenic progenitor cells in the human tunica albuginea may originate from stem cells: Implications for Peyronie's disease. Biol Reprod 2005; 73:1199–210.
42 Qian A, Meals RA, Rajfer J, Gonzalez-Cadavid NF. Comparison of gene expression profiles between Peyronie's disease and Dupuytren's contracture. Urology 2004;64:399–404.
43 Zuk PA, Zhu M, Mizuno H, Huang J, Futrell JW, Katz AJ, Benhaim P, Lorenz HP, Hedrick MH. Multilineage cells from human adipose tissue: Implications for cell-based therapies. Tissue Eng 2001;7:211–28.
44 Calzone FJ, Britten RJ, Davidson EH. Mapping of gene transcripts by nuclease protection assays and cDNA primer extension. Methods Enzymol 1987;152:611–32.
45 Nolazco G, Kovanecz I, Vernet D, Ferrini M, Gelfand B, Tsao J, Magee T, Rajfer J, Gonzalez-Cadavid NF. Effect of muscle derived stem cells on the restoration of corpora cavernosa smooth muscle and erectile function in the aged rat. BJU Int 2008 Feb 21; [Epub ahead of print].
46 Artaza JN, Reisz-Porszasz S, Dow JS, Kloner RA, Tsao J, Bhasin S, Gonzalez-Cadavid NF. Alterations in myostatin expression are associated with changes in cardiac left ventricular mass but not ejection fraction in the mouse. J Endocrinol 2007;194:63–76.
47 Li Y, Foster W, Deasy BM, Chan Y, Prisk V, Tang Y, Cummins J, Huard J. Transforming growth factor-beta1 induces the differentiation of myogenic cells into fibrotic cells in injured skeletal muscle: A key event in muscle fibrogenesis. Am J Pathol 2004;164:1007–19.
48 Amthor H, Nicholas G, McKinnell I, Kemp CF, Sharma M, Kambadur R, Patel K. Follistatin complexes myostatin and antagonises myostatin-mediated inhibition of myogenesis. Dev Biol 2004; 270:19–30.
49 Aoki F, Kurabayashi M, Hasegawa Y, Kojima I. Attenuation of bleomycin-induced pulmonary fibrosis by follistatin. Am J Respir Crit Care Med 2005;172:713–20.
50 Yamanaka O, Ikeda K, Saika S, Miyazaki K, Ooshima A, Ohnishi Y. Gene transfer of Smad7 modulates injury-induced conjunctival wound healing in mice. Mol Vis 2006;12:841–51.
51 Liu X, Sun SQ, Hassid A, Ostrom RS. cAMP inhibits transforming growth factor-beta-stimulated collagen synthesis via inhibition of extracellular signal-regulated kinase 1/2 and Smad signaling in cardiac fibroblasts. Mol Pharmacol 2006;70:1992–2003.
52 Gressner OA, Weiskirchen R, Gressner AM. Evolving concepts of liver fibrogenesis provide new diagnostic and therapeutic options. Comp Hepatol 2007;6:7.
53 Sugimoto H, Grahovac G, Zeisberg M, Kalluri R. Renal fibrosis and glomerulosclerosis in a new mouse model of diabetic nephropathy and its regression by bone morphogenic protein-7 and advanced glycation end product inhibitors. Diabetes 2007;56:1825–33.
54 Izumi N, Mizuguchi S, Inagaki Y, Saika S, Kawada N, Nakajima Y, Inoue K, Suehiro S, Friedman SL, Ikeda K. BMP-7 opposes TGF-beta1-mediated collagen induction in mouse pulmonary myofibroblasts through Id2. Am J Physiol Lung Cell Mol Physiol 2006;290:L120–6.
55 Qi W, Chen X, Twigg S, Zhang Y, Gilbert RE, Kelly DJ, Pollock CA. The differential regulation of Smad7 in kidney tubule cells by connective tissue growth factor and transforming growth factor-beta1. Nephrology (Carlton) 2007;12:267–74.

Published in final edited form as:
Obstet Gynecol. 2009 August ; 114(2 Pt 1): 300–309. doi:10.1097/AOG.0b013e3181af6abd.

Stimulating Vaginal Repair in Rats Through Skeletal Muscle–Derived Stem Cells Seeded on Small Intestinal Submucosal Scaffolds

Matthew H. Ho, MD, PhD, **Sanaz Heydarkhan, MSc**, **Dolores Vernet, PhD**, **Istvan Kovanecz, PhD**, **Monica G. Ferrini, PhD**, **Narender N. Bhatia, MD**, and **Nestor F. Gonzalez-Cadavid, PhD**

Los Angeles Biomedical Research Institute at Harbor-UCLA Medical Center, Urology Research Laboratory, Torrance, California; the Division of Female Pelvic Medicine and Reconstructive Surgery, Department of Obstetrics and Gynecology, Harbor-UCLA Medical Center, David Geffen School of Medicine at UCLA, University of California, Los Angeles, California; the Division of Endocrinology and Molecular Medicine, Department of Internal Medicine, College of Medicine, Charles Drew University of Medicine and Science, Los Angeles, California; and the Department of Urology, David Geffen School of Medicine at UCLA, University of California, Los Angeles, California

Abstract

OBJECTIVES—Grafts are used for vaginal repair after prolapse, but their use to carry stem cells to regenerate vaginal tissue has not been reported. In this study, we investigated whether 1) muscle-derived stem cells (MDSC) grown on small intestinal submucosa (SIS) generate smooth-muscle cells (SMC) in vitro and upon implantation in a rat model of vaginal defects; 2) express markers applicable to the in-vivo detection of vaginal endogenous stem cells; and 3) stimulate the repair of the vagina.

METHODS—Mouse MDSC grown on monolayer, SIS, or polymeric mesh, were tested for cell differentiation by immunocytochemistry, Western blot and real-time polymerase chain reaction (PCR). Stem cell markers were screened by DNA microarrays followed by real-time PCR, immunocytochemistry, and Western blot. Rats that underwent hysterectomy and partial vaginectomy were left as such or implanted in the vagina with 4',6-Diamidino-2-Phenylindole (DAPI)–labeled MDSC on SIS, or SIS without MDSC, immunosuppressed, and killed at 2–8 weeks. Immunofluorescence, hematoxylin-eosin, and Masson trichrome were applied to tissue sections.

RESULTS—Muscle-derived stem cell cultures on monolayer and on scaffolds differentiate into SMC, as shown by α-smooth muscle actin (ASMA), calponin, and smoothelin markers. Muscle-derived stem cells express embryonic stem cell markers Oct-4 and nanog. Dual DAPI/ASMA fluorescence indicated MDSC conversion to SMC. Muscle-derived stem cells/SIS stimulated vaginal tissue repair, including keratin-5 positive epithelium formation and prevented fibrosis at 4 and 8 weeks. Oct-4+ putative endogenous stem cells were identified.

Corresponding author: Nestor F. Gonzalez-Cadavid, PhD, LABioMed at Harbor-UCLA Medical Center, Urology Research Laboratory, Bldg. F-6, 1124 West Carson Street, Torrance, CA 90502; ncadavid@ucla.edu.

Financial Disclosure

The authors did not report any potential conflicts of interest.

CONCLUSION—Muscle-derived stem cells/SIS implants stimulate vaginal tissue repair in the rat, thus autologous MDSC on scaffolds may be a promising approach for the treatment of vaginal repair.

Pelvic organ prolapse, and specifically vaginal prolapse, is highly prevalent and may occur in up to 50% of parous women.[1,2] Surgical cure rates vary, and recurrences are common in primary ungrafted methods of anterior vaginal repair. This has led to the use of synthetic mesh or biological grafts to provide support for the weakened fascia and musculature.[1–4] Mesh and graft reduced objective prolapse recurrence rates compared with ungrafted methods.[3–5] However, complications are frequent, particularly vaginal fibrosis, inflammation, and epithelial erosion, and the long-term durability and safety of these devices are unknown.[5,6]

In other areas of urogenital tissue repair, stem cell therapy is being investigated, particularly in the bladder and urethra for the treatment of stress urinary incontinence,[7] and in the penile corpora cavernosa, for erectile dysfunction.[8,9] Stem cells from accessible adult tissues, such as the bone marrow or skeletal muscle, pose lower risks of carcinogenesis and immunorejection than embryonic stem cells[10,11] and are also being applied for tissue repair in clinical trials of some nonurogenital conditions (http://clinicaltrials.gov). Differentiated vaginal epithelial and smooth muscle cells have been used to create a neovagina in a rabbit model.[12]

Muscle biopsies allow the isolation for autografts of muscle-derived stem cells (MDSC), which have been characterized in rodents and isolated from human muscle[13,14] and are different from the myogenically committed satellite cells studied for stress urinary incontinence.[15] Muscle-derived stem cells differentiate in vitro and in vivo into skeletal myotubes, osteoblasts, chondrocytes, and neural cells[9,13] and when implanted into the rat penile corpora cavernosa originate smooth muscle cells (SMC) replacing the cells lost during aging-related tissue fibrosis and correcting erectile dysfunction. [9] Stem cell therapy may also aim for the pharmacologic activation of "dormant" endogenous stem cells that have been found in most organs, including the penis,[9,16] ovary,[17] and testis[18] and which may express the embryonic stem cell markers Oct-4 (octamer binding transcription factor) or nanog.[19]

The purpose of this study was to investigate whether implantation in the rat vagina of MDSC grown on small intestinal submucosa (SIS) promotes tissue repair without inducing fibrosis and whether endogenous stem cells present in the vagina can induce vaginal repair.

MATERIALS AND METHODS

Hind limb muscles of C57BL/6 mice were subjected to the preplating procedure to isolate MDSC.[9,20] Mouse MDSC are the only ones prepared by this method that have been characterized as stem cells.[13] Tissues were dissociated using sequentially collagenase XI, dispase II, and trypsin, and after filtration through 60 nylon mesh and pelleting, the cells were suspended in GM-20 (Dulbecco's Modified Eagle's Medium [DMEM] with 20% fetal bovine serum). Cells were plated onto collagen I-coated flasks for 1 hour (preplate 1), and 2 hours (preplate 2), followed by sequential daily transfers of nonadherent cells and replatings for 2 to 6 days, until preplate 6. The latter is the cell population containing MDSC. Cells were maintained in GM-20 on regular culture flasks (no coating) and used in the 15th to the 25th passage, because mouse MDSC have been maintained in our laboratory for at least 40 generations with the same, or even increasing, growth rate, thus confirming their stem cell nature. The absence of SMC was verified at the initial passages by immunocytochemistry and Western blot for α-smooth muscle cell actin (ASMA) (see below).

Muscle-derived stem cells were grown also in two types of scaffolds: 1) porcine small intestinal submucosa (SIS, Cook Biotech Inc., West Lafayette, IN),[21] and 2) polymeric mesh (Vicryl mesh, Ethicon Inc., Somerville, NJ).[22] Both materials were cut in 0.5 cm^2 fragments, sterilized in alcohol and submerged in DMEM/20% fetal bovine serum. Muscle-derived stem cells were then seeded and allowed to grow until they reached more than 60% confluence on the SIS scaffold or they started to cover the small holes in the mesh of the polymeric scaffold.

Retired breeders female Fisher 344 rats (Harlan Sprague-Dawley Inc., San Diego, CA), were used. The animals were treated according to National Institutes of Health regulations with the LABioMed Institutional Animal Care and Use Committee–approved protocol. Anesthetized rats were divided in the following groups (n = 2/group/time period): 1) "intact controls," not subjected to surgery; 2) "defected vagina, untreated," subjected to hysterectomy and a partial vaginectomy to induce apical, anterior, and posterior defects. The vagina was closed with absorbable sutures; 3) "defected vagina, treated with SIS implantation," as number 2, but implanted at the moment of surgery with the SIS scaffold. The SIS scaffold was sutured into the vaginal stump with absorbable sutures. Two nonabsorbable sutures (nylon) were used to mark the ends of the scaffold; 4) "defected vagina, treated with SIS/MDSC implantation," as number 2, but implanted at the moment of surgery with the SIS scaffold that had been seeded with MDSC. In this case, the cells were grown in vitro and labeled with either the nuclear blue fluorescent stain 4',6-Diamidino-2-Phenylindole (DAPI), or with DAPI and the membrane/cytoplasmic red fluorescent stain PKH26, as detailed in each case. Tacrolimus was given daily to group 4 (1 mg/kg, subcutaneously) to avoid immunorejection of the mouse stem cells.[9] At 2, 4, or 8 weeks after implantation (and in some cases at 6 weeks), rats were killed under anesthesia, the vagina was excised and divided in approximately 2–3-mm transversal sections numbered from the more distal from 1 to 6 (according to the overall length of the vagina). Sections were cryoprotected in 25% sucrose, immersed in optimal cutting temperature compound, and subjected to cryosectioning (5 micrometers for regular microscope, or 20–30 micrometers for confocal microscope) without fixation, unless stated.

The general morphology of vaginal frozen tissue sections was evaluated with hematoxylin-eosin. For immunocytochemistry, cells grown in triplicate on collagen-coated 8-well removable chambers, or in frozen tissue sections, were reacted[9,23] with some of the primary antibodies against 1) human ASMA (mouse monoclonal in Sigma kit, 1/2, Sigma Chemical, St. Louis, MO) a marker for both SMC and myofibroblasts, or 2) Oct-4 (rabbit polyclonal, 1/500, BioVision, Mountain View, CA), a marker for embryonic stem cells; in this case frozen sections were fixed with 2% formaldehyde for 10 minutes. Immunohistochemical detection was performed by quenching in 0.3% H_2O_2-phosphate buffered saline, blocking with goat or corresponding serum, and incubating overnight at 4°C with the primary antibody. This was followed by biotinylated anti-mouse IgG (Vector Laboratories, Burlingame, CA), respectively, for 30 minutes, the avidin-biotin-peroxidase complex containing avidin-linked horse radish peroxidase (1:100; Vector Laboratories), 3,3′ diaminobenzidine, and counterstaining with hematoxylin, or no counterstaining, as indicated.

When DAPI and/or PKH26 fluorescence was detected, immunofluorescence was applied for ASMA (same antibody as above) or keratin 5, a squamous epithelial marker[24] (Monoclonal, 1/200, Vector Laboratories) using a secondary anti-mouse IgG antibody that was biotinylated (goat, 1/200, Vector Laboratories), and this complex was detected with streptavidin-Texas Red (red fluorescence), or in the case of Oct-4, also with streptavidin-FITC (green fluorescence). After washing with phosphate buffered saline, the sections were mounted with Prolong antifade (Molecular Probes, Carlsbad, CA, USA). Negative controls

for immunohistochemistry or immunofluorescence omitted the first antibodies or they were replaced by IgG isotype. Sections were viewed under an Olympus BH2 fluorescent microscope or in a confocal microscope, using regular light or blue and/or red filters and overlay.

Masson trichrome staining[23] was applied to tissue sections fixed overnight in Bouin's fixative (Sigma). For quantitative image analysis, staining intensity was determined by computerized densitometry using the ImagePro Plus 5.1 program (Media Cybernetics, Silver Spring, MD), coupled to the Olympus BH2 microscope with a Spot RT color digital camera (Diagnostic Instruments Inc., Sterling Heights, MI). Results were expressed as the ratio between the areas stained in red comprising the epithelium, lamina propria, and muscularis, divided by the area occupied by collagen fibers and extracellular matrix stained in blue. Ten nonoverlapping fields were screened per section. Three sections per tissue specimen from the groups of two rats were then used to calculate the mean ± standard error of the mean, based on 30 separate measurements per rat.

Cell homogenates were obtained in boiling lysis buffer (1% SDS, 1 mm sodium orthovanadate, 10 mm Tris pH 7.4 and protease inhibitors), and centrifuging at 16,000 g for 5 minutes.[9,23] Forty micrograms of protein were run on 7.5% or 10% polyacrylamide gels, and submitted to transfer and immunodetection with antibodies against 1) human ASMA (monoclonal, 1/1,000, Calbiochem, LA Jolla, CA); 2) human calponin-1 (basic) (mouse monoclonal, 1/25, Novocastra, Burlighame, CA), as exclusive marker for SMC; 3) proliferating cellular nuclear antigen (PCNA) (mouse monoclonal, 1:100, Chemicon, Temecula, CA) a marker for replicating cells; 4) Oct-4 (rabbit polyclonal, 1/500, BioVision, Mountain View, CA), as stem cell marker; 5) myoglobin (rabbit polyclonal 1/200, Santa Cruz Biotechnology, Inc., Santa Cruz, CA), as muscle origin marker; and 6) GAPDH (mouse monoclonal, 1/3,000, Chemicon, Temecula, CA) as a housekeeping gene.

Membranes were incubated with a secondary polyclonal horse anti-mouse IgG linked to horseradish peroxidase (1:2,000; BD Transduction Laboratories, Franklin Lakes, NJ, or 1:5,000, Amersham GE, Pittsburgh, PA), and bands were visualized with luminol (SuperSignal West Pico, Chemiluminescent, Pierce, Rockford, IL). For the negative controls, the primary antibody was omitted.

Pools of total cellular RNA from three T75 flasks for MDSC that were incubated with DMEM supplemented with fetal bovine serum at either 20% ("high serum") or 2.5% ("low serum") were isolated with Trizol-Reagent (Invitrogen, Carlsbad, CA). Quality of RNA was assessed by agarose gel electrophoresis and subjected to cDNA gene microarrays (SuperArray BioScience Corp., Frederick, MD),[25] using the following Oligo GEArray microarrays: 1) mouse stem cell (OMM-405); 2) mouse cell surface markers (OMM-055); and 3) mouse cardiovascular disease biomarkers (MM-037), which together covered potential markers for MDSC. Biotin-labeled cDNA probes were synthesized from total RNA, denatured, and hybridized overnight at 60°C in GEHybridization solution to these membranes. Chemiluminescent analysis was performed per the manufacturer's instructions. Raw data were analyzed using GEArray Expression Analysis Suite (SuperArray BioScience Corp., Frederick, MD). Expression values for each gene based on spot intensity were subjected to background correction and normalization with housekeeping genes.

Equal amounts (2 micrograms) of RNA were reverse-transcribed in duplicate using a RNA polymerase chain reaction (PCR) kit (Applied Biosystems, Foster City, CA). Forward/ reverse PCR primers for real-time PCR for smoothelin and GAPDH are as follows: nt 575–597/626–641 on BC074818.2 (67bp) and 606–626/758–738 on BC023196. Mouse gene PCR primer sets (RT2) were purchased from SuperArray Bioscience. The QIAGEN Sybr

Green PCR kit with HotStar *Taq*DNA polymerase (QIAGEN, Valencia, CA) was used with i-Cycler PCR thermocycler and fluorescent detector lid (Bio-Rad, Hercules, CA).[25]

Melting was for 15 minutes at 95°C, followed by 40 cycles of three-step PCR, including melting for 15 seconds at 95°C, annealing for 30 seconds at 58°C, elongation for 30 seconds at 72°C, with an additional detection step of 15 seconds at 81°C and amelting curve from 55–95°C (at 0.5°C per 10 seconds).[26] Inverse derivatives of melting curves showed sharp peaks for smoothelin and GAPDH 81°C and 85°C indicating correct products. We analyzed cDNAs (25 ng) in quadruplicate in parallel with GAPDH controls; standard curves (threshold cycle compared with log pg cDNA) were generated by log dilutions of from 0.1 pg to 100 ng standard cDNA (reverse-transcribed mRNA from MDSC). The mRNA starting quantities were calculated from the standard curves and averaged using i-Cycler, iQ software. The ratios of smoothelin mRNA to GAPDH mRNA were computed.

For regular real-time PCR (25), 2 micrograms of RNA were reverse-transcribed, and cDNA was amplified for 38 cycles by PCR at 94°C for 30 seconds, primer annealing at 58°C for 30 seconds, and extension at 72°C for 1 minute. Polymerase chain reaction products were analyzed in 2% agarose. Forward/reverse PCR primers in 5′-3′ nucleotide positions were are as follows: 1) Oct-4 (GenBank Accession No. NM_013633), forward: nt 830–850; and reverse: nt 1130–1150; 2) nanog (GenBank Accession No. XM_001471588) forward: nt 732–852; and reverse: nt 1032–1152; and 3) CD63 (GenBank Accession No. NM_001042580) forward: nt 478–898; and reverse: nt 778–798, 4) GAPDH (GenBank Accession No. BC059110) forward: nt 611–631; and reverse: nt 743–763.

Masson trichrome values are expressed as the mean ± standard error of the mean for 30 independent measurements per rat and 60 determinations per group. The normal distribution of the data was established using the Wilks-Shapiro test. Multiple comparisons were analyzed by a single-factor analysis of variance, followed by post-hoc comparisons with the Newman-Keuls test. Differences among groups were considered statistically significant at $P<.05$.

RESULTS

To show with specific differentiation markers that MDSC are indeed able to originate SMC in vitro, they were incubated for various periods of time (7–56 days) in DMEM with 20% fetal bovine serum. Figure 1A shows by immunocytochemistry that as early as 9 days, some of the cells express ASMA, a marker for both myofibroblasts and SMC, and that TGFβ1 (Fig. 1B) intensifies this expression. Successive periods showed similar results (not shown), and this was confirmed at 22 days by Western blot (Fig. 1C). The SMC generation was indicated with an antibody for the SMC marker calponin, not expressed in myofibroblasts, although in this case the increase of the intensity of the TGFβ1 band corrected by GAPDH was only moderate. The cells were actively replicating as shown by proliferating cell nuclear antigen (PCNA). The levels of smoothelin mRNA, another specific SMC marker, were elevated by TGFβ1, and this effect continued until at least 49 days, as shown by real-time PCR (Fig. 1D).

The MDSC may grow on scaffolds and differentiate into the desired lineage, as shown by hematoxylin-eosin staining on an epi-illumination stereomicroscope observation of the monolayer formed on the small intestinal submucosa (SIS) membrane (Fig. 1E). Because it is difficult to perform fluorescence or immunocytochemical observations on the totally opaque SIS scaffold, we opted to grow the MDSC prelabeled with the nuclear fluorescent stain DAPI onto a translucent polymeric scaffold (Vicryl mesh) and determine whether the cells transform into SMC. The MDSC rapidly proliferated onto the scaffold (Fig. 1F) and

presumably originated SMC, as detected by dual immunofluorescence for DAPI and ASMA (Fig. 1G).

Labeling with DAPI is relatively short-lived, and therefore we searched for potential markers of these cells that would not be expressed in the vagina. First, DNA microarrays representing several stem cell and related genes, as well as tissue markers, were applied to identify RNA transcripts in MDSC that were grown under either high serum (20% fetal bovine serum) to stimulate cell proliferation or low serum (2.5% fetal bovine serum) to arrest cell growth and to stimulate cell differentiation (Fig. 2A and B). Some embryonic stem cell mRNAs (nanog, Oct-4, CD63, Wnt1) and skeletal muscle or myogenic markers (myoglobin, muscle creatin kinase, notch 3) were identified, and the approximate intensity of expression was tabulated (Fig. 2C).

Real-time PCR for two of those genes, nanog and Oct-4, revealed a low expression in MDSC, as well as in the vaginal tissue, whereas CD63 was negligible in MDSC but well-expressed in the vagina. The Oct-4 and nanog were considerably expressed in the testis, as a source of germinal stem cells, and particularly in the case of nanog in the penis, as another urogenital organ. In the skeletal muscle (hind limb), where MDSC originated, Oct-4 expression was also high, whereas nanog was negligible (Fig. 3A and C, available online at http://links.lww.com/A1488). Western blotting with an Oct-4 antibody revealed a strong band in the MDSC that runs as Oct-3B and a very faint one as Oct-3A, whereas both bands were expressed similarly at high levels in the vagina, the skeletal muscle, and the penis. (Fig. 3B, available online at http://links.lww.com/A1488). Myoglobin, a skeletal muscle marker, was expressed in MDSC and the vagina, and as expected, very highly in the skeletal muscle, but not in the penis. The myoglobin band in the vaginal tissue possibly results from contamination with adjacent skeletal muscle tissue. Therefore, Oct-4, because of being an embryonic stem cell marker, was used to locate potential endogenous stem cells in the vagina, whereas due to its low expression in the MDSC, it was not useful as a tag to follow MDSC implantation in this tissue.

To study the effects of implanted MDSC on vaginal reconstruction, rats were either left intact and untreated, or were subjected to hysterectomy and partial vaginectomy to create the apical, anterior, and posterior vaginal defects. Muscle-derived stem cells grown on SIS were labeled with DAPI and implanted on the vagina at the site of vaginal defects, whereas other animal groups were implanted with SIS without cells or left untreated and killed at 2, 4, 6, and 8 weeks (n = 2/group). This time course was selected to follow up qualitatively in a preliminary “proof of concept” cell uptake, survival, differentiation, and effects on histology at several standard periods used in studies of stem cell implantation. The vaginal tissues were divided in regions numbered 1 through 6 from the one most distant to the site of implantation. The DAPI labeled MDSC on the SIS scaffolds were visualized at 4 weeks as numerous blue fluorescent nuclei in frozen unfixed tissue sections of the tissue around the site of implantation (regions 5 and 6), as shown on Figure 4A and B. These sections were immunostained with an antibody for ASMA and a red fluorescence Texas red–tagged secondary antibody that shows, in a merge of the blue and red fluorescence, that many of the implanted cells were positive for ASMA expression. Some few MDSC migrated away from the SIS implants to more distant regions (1 and 3), showing also differentiation into SMC (Fig 4C and D). Muscle-derived stem cells growing on SIS were also dually labeled with DAPI and a membrane red fluorescence tag, PKH26, and then implanted in the vagina as above. At 6 weeks (not shown) DAPI labeling became more diffuse and restricted to a small area of the field, whereas red fluorescence is still apparent and even advanced into the nuclei. This indicates that the MDSC survive for at least 6 weeks.

The other marker identified in the in vitro experiments for MDSC, the Oct-4 gene, detects the endogenous vaginal stem cells and the implanted MDSC. The vaginal tissue from intact rats (no surgery) within a region equivalent to the site of MDSC implantation displays some discrete staining in isolated regions of the muscularis, apparently in the longitudinal bundles, as well as in the stratified squamous epithelium (not shown). Staining is rather similar in hysterectomized animals with partial vaginectomy after 4 weeks of surgery and no treatment (Fig. 5A–C, available online at http://links.lww.com/A1489). Four weeks after implantation of SIS only without MDSC, there was a more extended staining, with some spreading to both longitudinal and transversal bundles in the muscularis (Fig. 5D–F, available online at http://links.lww.com/A1489). This is likely due to "activation" of endogenous stem cell replication by the combined SIS implant/tissue repair reaction. The SIS/MDSC intensified these changes with even more dissemination of Oct-4+ cells, particularly in a thicker epithelium, suggesting that many of them are derived from the implanted MDSC and others from endogenous stem cell activation (Fig. 5G–I, available online at http://links.lww.com/A1489).

The stimulatory effects of MDSC/SIS on the regeneration of vaginal tissue are seen clearly 4 weeks after surgery on hematoxylin-eosin staining of the vaginal tissue sections, where there is an apparent increase in the muscularis after receiving the implant (Fig. 6C and D) as compared with the intact vagina (no surgery) (Fig. 6A) or the untreated hysterectomized/ partially vaginectomized tissue (Fig. 6B). What is remarkable is the considerably stratified squamous epithelium that developed upon treatment with SIS and particularly with the MDSC on the SIS (Fig. 6C and D).

The stimulatory effect of MDSC on the growth of the epithelium was confirmed by immunohistodetection with Texas red fluorescence of keratin 5, a marker of squamous epithelium, compared with the respective hematoxylin-eosin staining at 4 weeks (Fig. 7). In this case, DAPI was applied after the sections were obtained as a nuclear fluorescent counterstain, not to detect the implanted MDSC. The untreated vagina from hysterectomized rats showed a disorganized and rather thin epithelium, with virtually no indentation with connective tissue papillae (Fig. 7B). Implantation of SIS without cells restored some papillae and made the epithelium thicker (Fig. 7D), but only the SIS holding the MDSC that normalized the epithelium thickness and appearance (Fig. 7F). To determine whether the MDSC themselves differentiated into epithelial cells, sections obtained from the vagina of hysterectomized/partially vaginectomized rats where the vagina had been implanted with red fluorescence PKH26-labeled MDSC growing on SIS were stained for keratin 5 but using FITC green fluorescence, and no MDSC staining was applied (Fig. 7A, C, E). Although red fluorescent implanted cells were visible in the vicinity of the green fluorescent keratin-5 positive area, there was no convincing overlapping in the overlay (not shown) that would suggest a direct conversion, thus implying that the MDSC exert a trophic effect on the epithelium more than a true differentiation.

Masson trichrome staining was applied to determine the extent of fibrosis in the tissue sections upon the different treatments at 8 weeks. Figure 8A shows in the vagina from intact animals not subjected to surgery the layer of longitudinal smooth muscle bundles in the muscularis underneath the lamina propria and the stratified squamous epithelium, stained in red, whereas virtually all the lamina propria and interstitial connective tissue in the smooth muscle is stained in blue, indicating collagen fibers. The tissue from hysterectomized and partially vaginectomized animals had a thinner but organized layer of smooth muscle (Fig. 8B). In contrast, after SIS implantation (Fig. 8C), there was very little smooth muscle and a thin epithelium, as if the scaffold would induce mainly connective tissue formation, probably from fibrosis and scar tissue formation. This may also be due, in part, to the wound healing process caused by surgery and regeneration process at longer time points. However,

when SIS with MDSC was implanted (Fig. 8D), there was a remarkably healthy smooth muscle and thicker epithelium. These results suggest that the use of MDSC on SIS scaffold regenerated vaginal smooth muscle and epithelium much faster than SIS alone. Quantitative image analysis (Fig. 8E) of the ratio between the red compared with blue areas, as a representation of the cellular/extracellular matrix ratio, was applied to 30 fields per rat. This analysis, limited by a small n imposed by the study design, indicated that MDSC seeded on the SIS generated a significantly higher amount of cellular components.

DISCUSSION

Based on a PubMed search (1980 to March 2009; key words: vagina, stem cells; all languages), this is the first article on the use of stem cells of any origin to repair defects or injury to the vagina in women or in animal models. We have shown that MDSC mounted on a biodegradable SIS scaffold implanted in the defected vagina (apical, anterior, and posterior defects) of rats survive for extended periods, differentiate into SMC in the muscularis, and promote epithelium regeneration, presumably by a trophic effect. This exploratory "proof of concept" approach was supported by finding a reduction in fibrosis and stimulation of the vaginal repair process, which seems to occur more efficiently than with SIS implants alone without cells or in the spontaneous regeneration occurring in the absence of any treatment. The current study establishes the foundation for future experimental paradigms to evaluate more precisely with a larger number of animals the effects of MDSC/SIS on vaginal tissue fibrosis at even more prolonged periods after implantation. Although we did not perform the functional study of the vaginal defects and this surgically injured vagina model is not the same as pelvic organ prolapse that has developed with time, our results show that implanted MDSC in the surgically injured vagina can survive, differentiate, and regenerate/repair the injured vagina.

In addition, we have defined the expression in MDSC of certain genes, such as Oct-4, that is a well-recognized marker of embryonic stem cells. This gene served also to identify potential endogenous stem cells in the tissue that may constitute a target for repair therapy based on their potential activation by pharmacologic interventions. Muscle-derived stem cells per se, without scaffolds, were not tested, because we considered that the physical restriction imposed by the SIS support would on one side facilitate closure of the wound and on the other side help to maintain the implanted cells around the site of repair.

One of the main limitations of the current work is that it was difficult to assess quantitatively the extent of the putative improvement of vaginal regeneration by MDSC/SIS over SIS alone or in the absence of treatment, because with the exception of the effect on fibrosis, we have based our interpretation on qualitative comparisons between vaginal tissues from each experimental group. This was prompted by the difficulty of defining markers that single-handedly or in combination represent the complexity of the coordinated repair of the different cellular compartments in the vagina and their histologic and anatomic arrangement to restore the normal tissue function. In the case of the correction of the well-defined SMC loss in the penile corpora cavernosa occurring during aging, we employed ASMA estimated by quantitative Western blot,[9] but for vaginal repair, the possibility that ASMA may also indicate generation of myofibroblasts involved in a fibrotic process[23] may complicate the interpretation. In addition, the balance between the muscularis and the squamous epithelium and lamina propria may not be well-represented by isolated markers for each tissue.

Within these constraints, the in situ estimation in tissue sections of the cellular compartment in relation to collagen and extracellular matrix is a reasonable approximation to evaluate the efficacy of MDSC/SIS, because it measures the functionally desirable restoration of the SMC/keratinocytes content compared with the noxious complication of excessive collagen

deposition, namely fibrosis. A caveat is that myofibroblasts, the main cell type in fibrosis,[27] may also be counted among the red staining area. However, the main reason for our experimental design was that as first stage, this work aimed to define the proof of concept of implanted cells surviving in the injured vagina, converting into one of the desired cell types (SMC), and stimulating the formation of the epithelium, while maintaining the proper histologic appearance. Further studies will be conducted to identify the most suitable markers for quantitative Western blots to provide a precise evaluation of the extent of repair. This would facilitate determination of the role of variables such as multiple compared with single injection sites, cell loads, pharmacologic adjuvants, influence of scaffold types, or ranges of persistence of implanted MDSC on the relative efficacy of each treatment and particularly on vaginal function.

Although in the present work we employed immunosuppression with tacrolimus because of the interspecies implantation we used (mouse MDSC into rat vagina), we envisage that this will not be needed in further animal studies or in clinical applications. First, in both cases, allografts, eg, rat MDSC donor in rat recipient and human MDSC in women, may be used, because stem cells are known to be considerably hypoimmunogenic as compared with differentiated cells.[28] Moreover, in the case of humans, autografts can easily be obtained from biopsies of the skeletal muscle that in a few weeks can generate cell cultures for reimplantation.[13] An even less invasive approach would be based on pharmacologic awakening of potential dormant endogenous stem cells from vaginal tissues similar to the Oct-4 cells identified here, which would be the ultimate goal of stem cell therapy. [27] The endogenous stem cells, which in some cases may be rudimentary embryonic stem cells,[18,19] are being increasingly identified in adult tissues as populations different from other stem cells already characterized, and in the vagina they may even be paracrinely stimulated by the implanted MDSC. In conclusion, MDSC seeded onto degradable scaffolds may constitute a promising approach for the treatment of vaginal prolapse.

Acknowledgments

Supported by an internal grant from the Division of Female Pelvic Medicine and Reconstructive Surgery of Harbor-UCLA Medical Center, University of California at Los Angeles (NGC/MH), and in part by grants NIH R21DK-070003 (NGC), DOD W81XWH-07-1-0181 (NGC), NIH 5SC2DK082388-02 MH), the Dennis W. Jahnigen Career Development Scholars Award from American Geriatrics Association (MH), the Astellas Award (MH), the June Allyson Foundation Award from the American Urogynecologic Society (MH), and the Research Grant from International Urogynecological Association (MH).

REFERENCES

1. South M, Amundsen CL. Pelvic organ prolapse: a review of the current literature. Minerva Ginecol. 2007; 59:601–612. [PubMed: 18043574]
2. Maher C, Baessler K, Glazener CM, Adams EJ, Hagen S. Surgical management of pelvic organ prolapse in women: a short version Cochrane review. Neurourol Urodyn. 2008; 27:3–12. [PubMed: 18092333]
3. Nguyen JN. The use of grafts for anterior vaginal prolapse repair: pros and cons. Curr Opin Obstet Gynecol. 2008; 20:501–505. [PubMed: 18797276]
4. Jia X, Glazener C, Mowatt G, Maclennan G, Bain C, Fraser C, et al. Efficacy and safety of using mesh or grafts in surgery for anterior and/or posterior vaginal wall prolapse: systematic review and meta-analysis. BJOG. 2008; 115:1350–1361. [PubMed: 18715243]
5. Bako A, Dhar R. Review of synthetic mesh-related complications in pelvic floor reconstructive surgery. Int Urogynecol J Pelvic Floor Dysfunct. 2008; 20:103–111. [PubMed: 18779916]
6. Huffaker RK, Muir TW, Rao A, Baumann SS, Kuehl TJ, Pierce LM. Histologic response of porcine collagen-coated and uncoated polypropylene grafts in a rabbit vagina model. Am J Obstet Gynecol. 2008; 198:582.e1–582.e7. [PubMed: 18295174]

7. Smaldone MC, Chancellor MB. Muscle derived stem cell therapy for stress urinary incontinence. World J Urol. 2008; 26:327–332. [PubMed: 18470515]
8. Bivalacqua TJ, Deng W, Kendirci M, Usta MF, Robinson C, Taylor BK, et al. Mesenchymal stem cells alone or ex vivo gene modified with endothelial nitric oxide synthase reverse age-associated erectile dysfunction. Am J Physiol Heart Circ Physiol. 2007; 292:H1278–H1290. [PubMed: 17071732]
9. Nolazco G, Kovanecz I, Vernet D, Gelfand RA, Tsao J, Ferrini MG, et al. Effect of muscle-derived stem cells on the restoration of corpora cavernosa smooth muscle and erectile function in the aged rat. BJU Int. 2008; 101:1156–1164. [PubMed: 18294308]
10. Blum B, Benvenisty N. The tumorigenicity of human embryonic stem cells. Adv Cancer Res. 2008; 100:133–158. [PubMed: 18620095]
11. Grinnemo KH, Sylvién C, Hovatta O, Dellgren G, Corbascio M. Immunogenicity of human embryonic stem cells. Cell Tissue Res. 2008; 331:67–78. [PubMed: 17846795]
12. De Philippo RE, Bishop CE, Filho LF, Yoo JJ, Atala A. Tissue engineering a complete vaginal replacement from a small biopsy of autologous tissue. Transplantation. 2008; 86:208–214. [PubMed: 18645481]
13. Urish K, Kanda Y, Huard J. Initial failure in myoblast transplantation therapy has led the way toward the isolation of muscle stem cells: potential for tissue regeneration. Curr Top Dev Biol. 2005; 68:263–280. [PubMed: 16125002]
14. Zheng B, Cao B, Crisan M, Sun B, Li G, Logar A, et al. Prospective identification of myogenic endothelial cells in human skeletal muscle. Nat Biotechnol. 2007; 25:1025–1034. [PubMed: 17767154]
15. Mitterberger M, Marksteiner R, Margreiter E, Pinggera GM, Frauscher F, Ulmer H, et al. Myoblast and fibroblast therapy for post-prostatectomy urinary incontinence: 1-year followup of 63 patients. J Urol. 2008; 179:226–231. [PubMed: 18001790]
16. Vernet D, Qian A, Nolazco G, Cantini L, Magee TR, Ferrini MG, et al. Evidence that osteogenic progenitor cells in the human tunica albuginea may originate from stem cells. Implications for Peyronie's disease. Biol Reprod. 2005; 73:1199–1210. [PubMed: 16093362]
17. Virant-Klun I, Zech N, Rozman P, Vogler A, Cvjeticanin B, Klemenc P, et al. Putative stem cells with an embryonic character isolated from the ovarian surface epithelium of women with no naturally present follicles and oocytes. Differentiation. 2008; 76:843–856. [PubMed: 18452550]
18. Zovoilis A, Nolte J, Drusenheimer N, Zechner U, Hada H, Guan K, et al. Multipotent adult germline stem cells and embryonic stem cells have similar microRNA profiles. Mol Hum Reprod. 2008; 14:521–529. [PubMed: 18697907]
19. Ratajczak MZ, Zuba-Surma EK, Shin DM, Ratajczak J, Kucia M. Very small embryonic-like (VSEL) stem cells in adult organs and their potential role in rejuvenation of tissues and longevity. Exp Gerontol. 2008; 43:1009–1017. [PubMed: 18601995]
20. Lee JY, Qu-Petersen Z, Cao B, Kimura S, Jankowski R, Cummins J, et al. Clonal isolation of muscle-derived cells capable of enhancing muscle regeneration and bone healing. J Cell Biol. 2000; 150:1085–1100. [PubMed: 10973997]
21. Chaliha C, Khalid U, Campagna L, Digesu GA, Ajay B, Khullar V. SIS graft for anterior vaginal wall prolapse repair–a case-controlled study. Int Urogynecol J Pelvic Floor Dysfunct. 2006; 17:492–497. [PubMed: 16733627]
22. Allahdin S, Glazener C, Bain C. A randomised controlled trial evaluating the use of polyglactin mesh, polydioxanone and polyglactin sutures for pelvic organ prolapse surgery. J Obstet Gynaecol. 2008; 28:427–431. [PubMed: 18604681]
23. Cantini LP, Ferrini MG, Vernet D, Magee TR, Qian A, Gelfand RA, et al. Profibrotic role of myostatin in Peyronie's disease. J Sex Med. 2008; 5:1607–1622. [PubMed: 18422491]
24. Lloyd C, Yu QC, Cheng J, Turksen K, Degenstein L, Hutton E, et al. The basal keratin network of stratified squamous epithelia: defining K15 function in the absence of K14. J Cell Biol. 1995; 129:1329–1344. [PubMed: 7539810]
25. Artaza JN, Singh R, Ferrini MG, Braga M, Tsao J, Gonzalez-Cadavid NF. Myostatin promotes a fibrotic phenotypic switch in multipotent C3H 10T1/2 cells without affecting their differentiation into myofibroblasts. J Endocrinol. 2008; 196:235–249. [PubMed: 18252947]

26. Magee TR, Kovanecz I, Davila HH, Ferrini MG, Cantini L, Vernet D, et al. Antisense and short hairpin RNA (shRNA) constructs targeting PIN (Protein Inhibitor of NOS) ameliorate aging-related erectile dysfunction in the rat. J Sex Med. 2007; 4:633–643. [PubMed: 17433082]

27. Romagnani P, Lasagni L, Mazzinghi B, Lazzeri E, Romagnani S. Pharmacological modulation of stem cell function. Curr Med Chem. 2007; 14:1129–1139. [PubMed: 17456026]

28. Le Blanc K, Ringdén O. Immunomodulation by mesenchymal stem cells and clinical experience. J Intern Med. 2007; 262:509–525. [PubMed: 17949362]

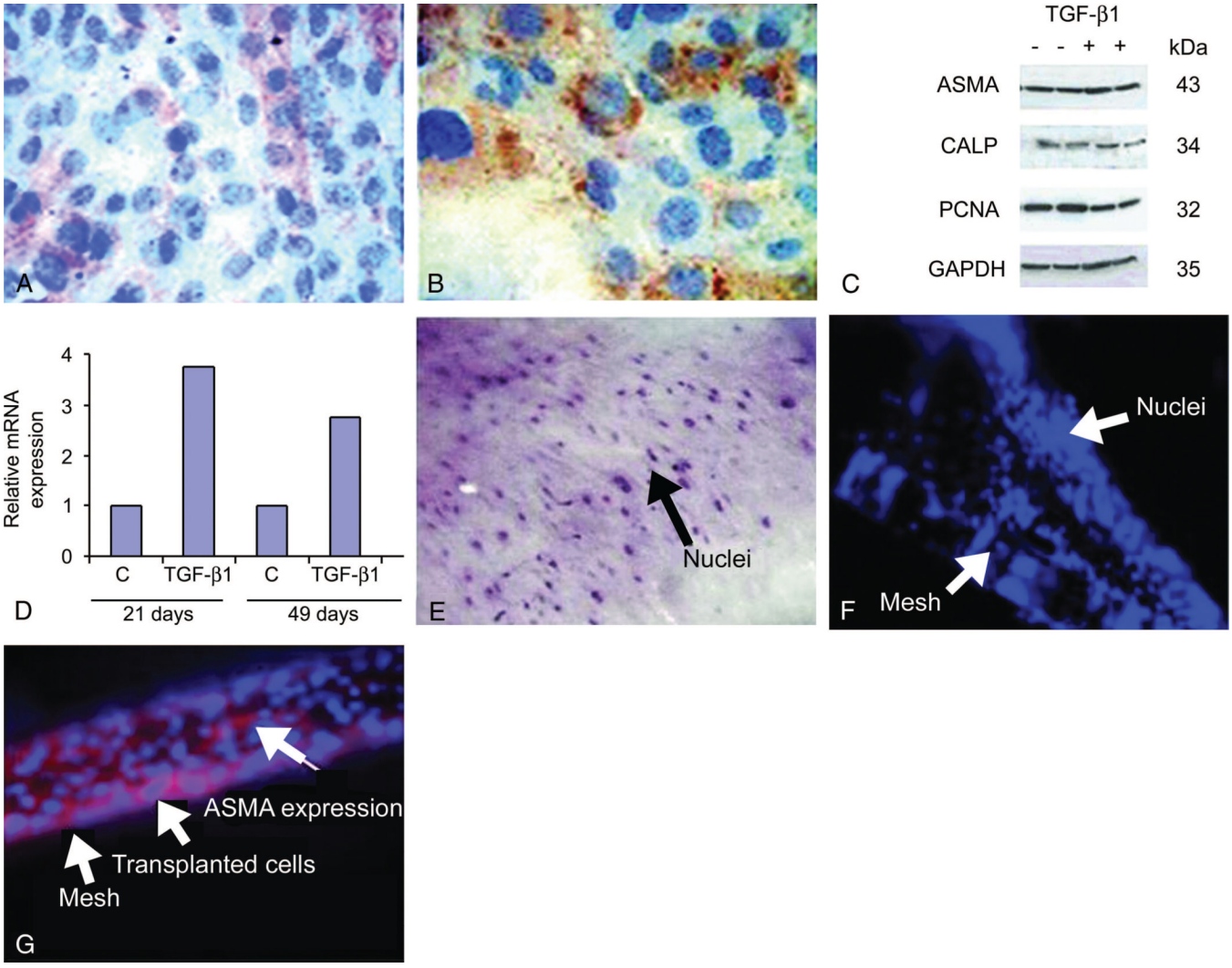

Fig. 1.

Skeletal muscle-derived stem cells (MDSC) grow in vitro on biological and synthetic scaffolds and differentiate into cells that express smooth muscle cells markers. MDSC were incubated in triplicate for up to 56 days on 6-well plates in Dulbecco's Modified Eagle's Medium (DMEM)/2.5% serum and immunostained for α-smooth muscle actin (ASMA). Panels show an early incubation (9 days) at 200X. **A.** Control; no addition made. **B.** Transforming growth factor-beta 1 (TGF-β) added; 5 ng/mL. **C.** Expression of ASMA, smooth muscle cells (SMC) marker (calponin), and cell proliferation marker (proliferating cell nuclear antigen [PCNA]) at 22 days by Western blot. **D.** Expression of messenger RNA (mRNA) for SMC marker smoothelin at 21 and 49 days by reverse transcription/real time polymerase chain reaction. Values are expressed as ratios against the respective control. **E.** MDSC were seeded on small intestinal submucosa (SIS, Cook Biotech Inc., West Lafayette, IN) on 12-well plates in DMEM/2.5% serum (with TGF-β), grown for 2 weeks, stained with hematoxylin, and examined under a reverse phase microscope (100X). **F.** MDSC were seeded on Vicryl polymeric mesh as for SIS, stained with 4',6-diamidino-2-phenylindole, and examined under a fluorescent microscope using blue fluorescence (200X). **G.** Blue/red fluorescent overlay of cells subjected to immunostaining for ASMA with a Texas red secondary antibody (200X). CALP, calponin; GADPH, glyceraldehyde-3-phosphate dehydrogenase; C, control.

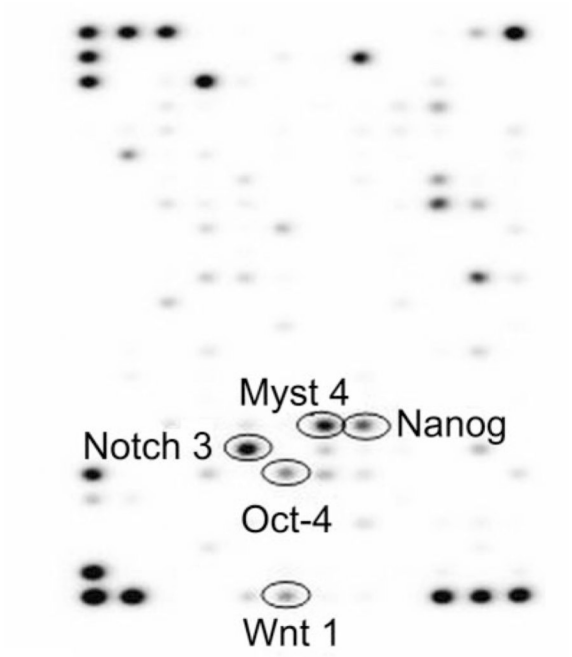

A

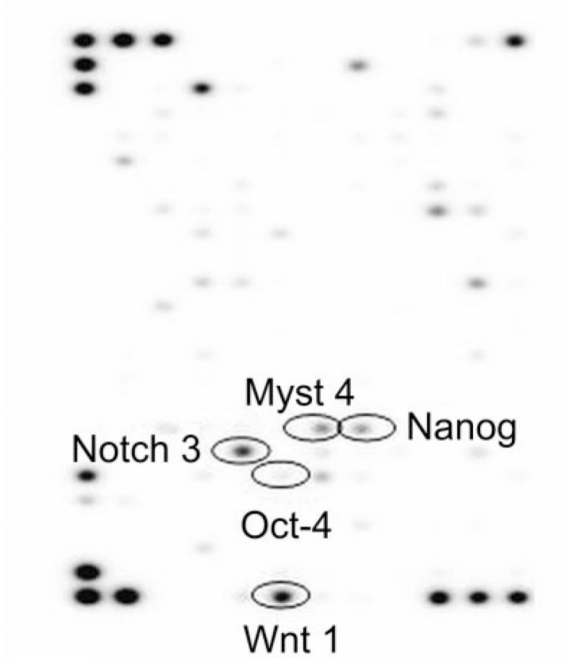

B

OMM	Number	Abbreviation	Full name	A	B
405	199	Myst 4	Myst histone acetyltransferase	45	34
	200	Nanog	Nanog homeobox	30	29
	209	Notch 3	Notch 3 gene homolog 3	53	56
	222	Pou 5 fi (Oct-4)	Pou domain, class 5	23	8
	282	Wnt 1	Wingless-related MMTV integration site 1	20	72
055	29	CD63	CD63 antigen	259	ND
037	20	Ckm	Muscle creatin kinase	ND	32
	73	Mb	Myoglobin	ND	112

C

Fig. 2.

Skeletal muscle-derived stem cells (MDSC) express messenger RNAs (mRNAs) for embryonic stem cell markers and for muscle-specific markers as detected by DNA microarrays. **A.** RNA was isolated from MDSC cultured in duplicate under low (2.5%) or **B.** high (20%) fetal bovine serum for 3 weeks and hybridized against the stem cell superarray panel (OMM-405). **C.** The mRNA levels in this specific experiment were calculated for some embryonic stem cell markers and also for other selected genes identified with two other panels (OMM-37 and OMM-055), just to confirm a given gene expression.

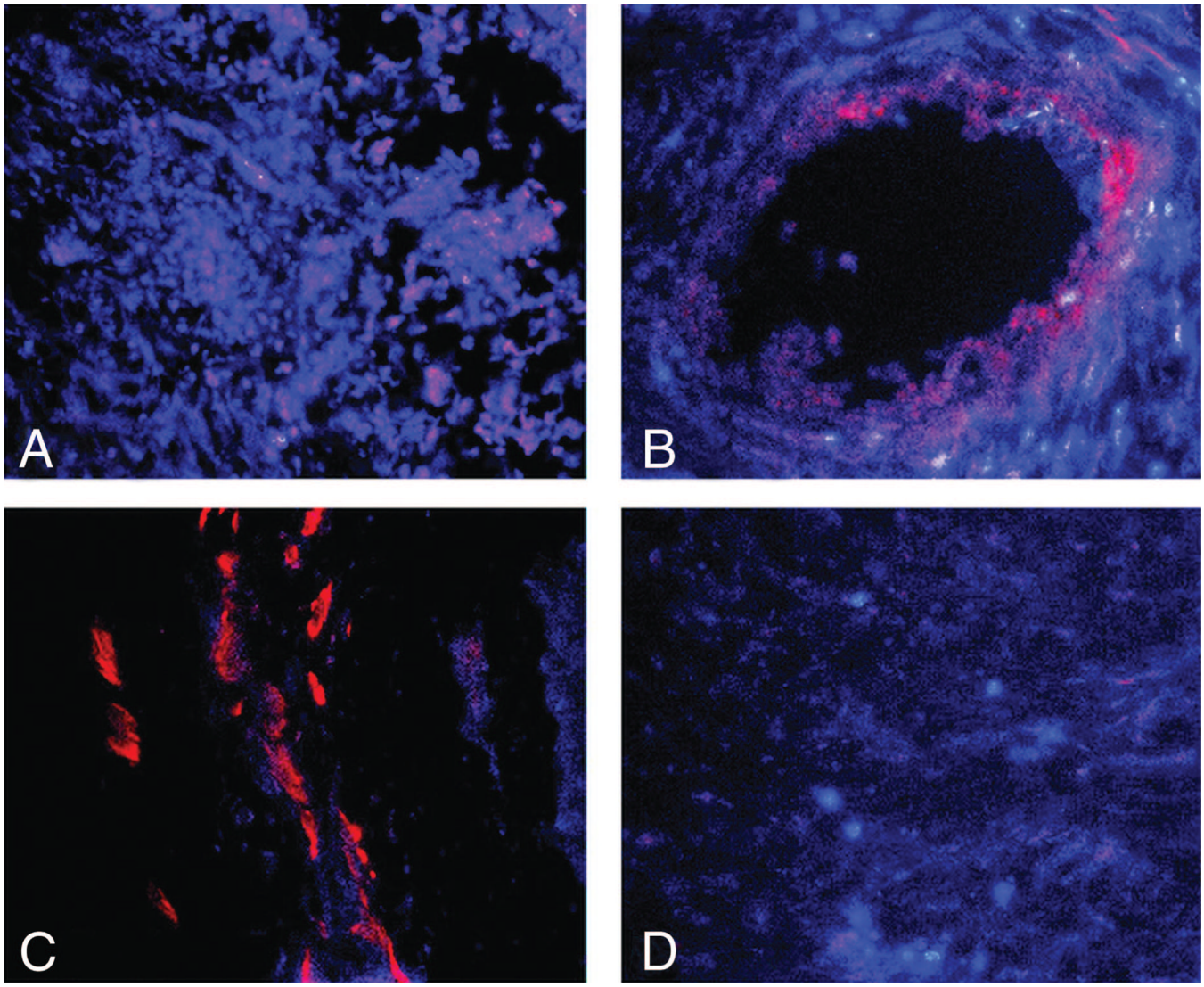

Fig. 4.

Skeletal muscle-derived stem cells (MDSC) growing on small intestinal submucosa (SIS) scaffolds differentiate into smooth muscle cells when implanted into injured vaginal tissue in the rat and spread away from the site of injection. Blue/red fluorescence overlay of vaginal tissue implanted with 4',6-diamidino-2-phenylindole (DAPI)-tagged MDSC/SIS after hysterectomy and partial vaginectomy and subjected to α-smooth muscle actin (ASMA) red-fluorescence immunodetection, focusing in the muscularis (200X). Frozen tissue sections (10% formalin-fixed) were obtained at 4 weeks after implantation. Region 5 **(A)** is immediately distal to the site of implantation, and region 6 **(B)** is directly in the site of implantation (suture site around orifice). **C and D.** Blue/red fluorescence overlay of vaginal tissue implanted with DAPI-tagged MDSC/SIS after hysterectomy and partial vaginectomy and subjected to ASMA red-fluorescence immunodetection, focusing in the muscularis (200X) but in more distal sections 1 **(C)** and 3 **(D)**.

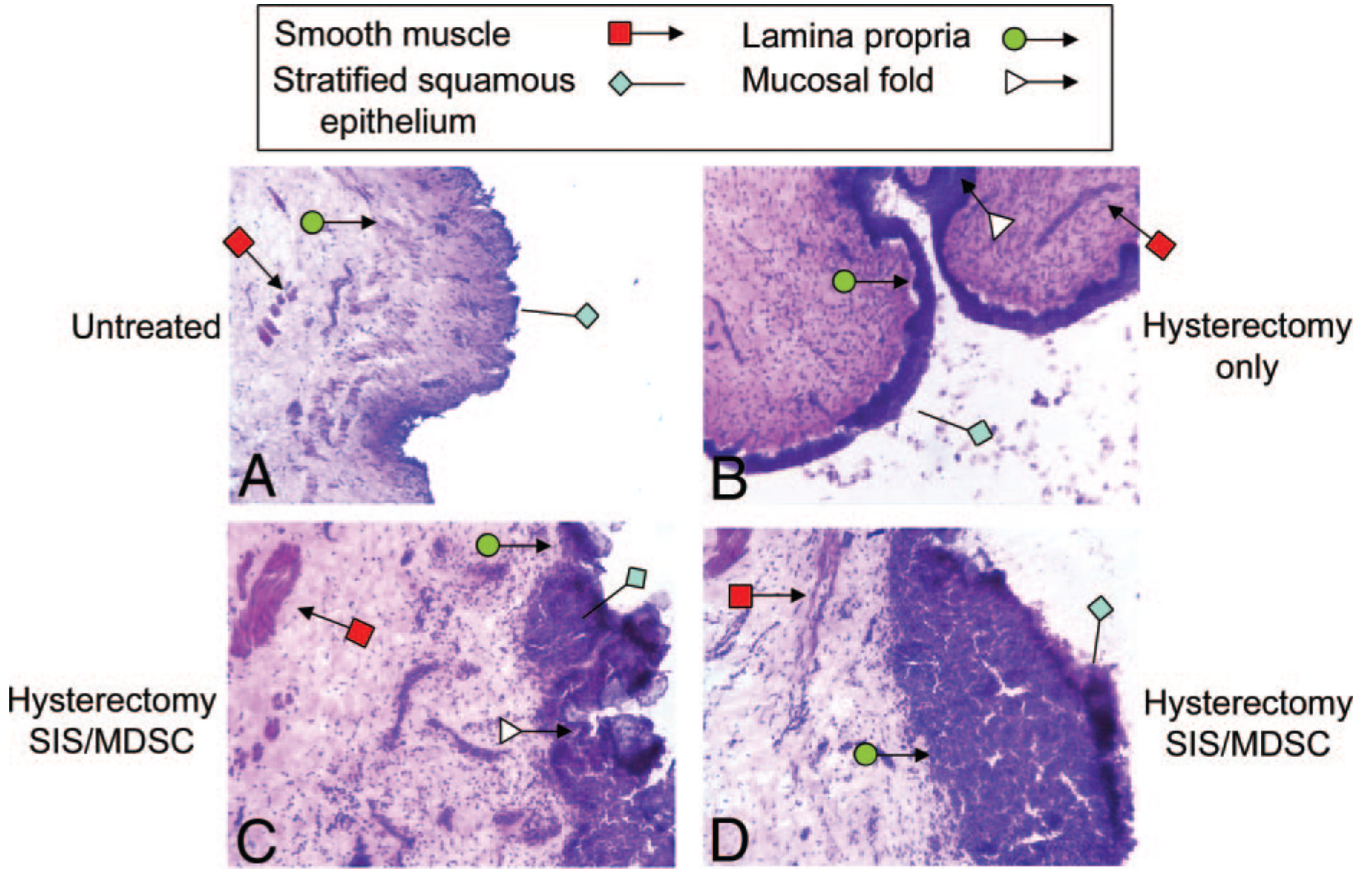

Fig. 6.

Implanted skeletal muscle-derived stem cells (MDSC)/small intestinal submucosa (SIS) induce regeneration of the stratified squamous epithelium in the vagina around the site of implantation. Frozen sections for region 5 (not fixed) were stained with hematoxylin eosin. **A.** Intact controls, 40X. **B.** Hysterectomized rats, 40X; proximal. **C and D.** Hysterectomized rats with MDSC/SIS, 200X, at two areas of the tissue section.

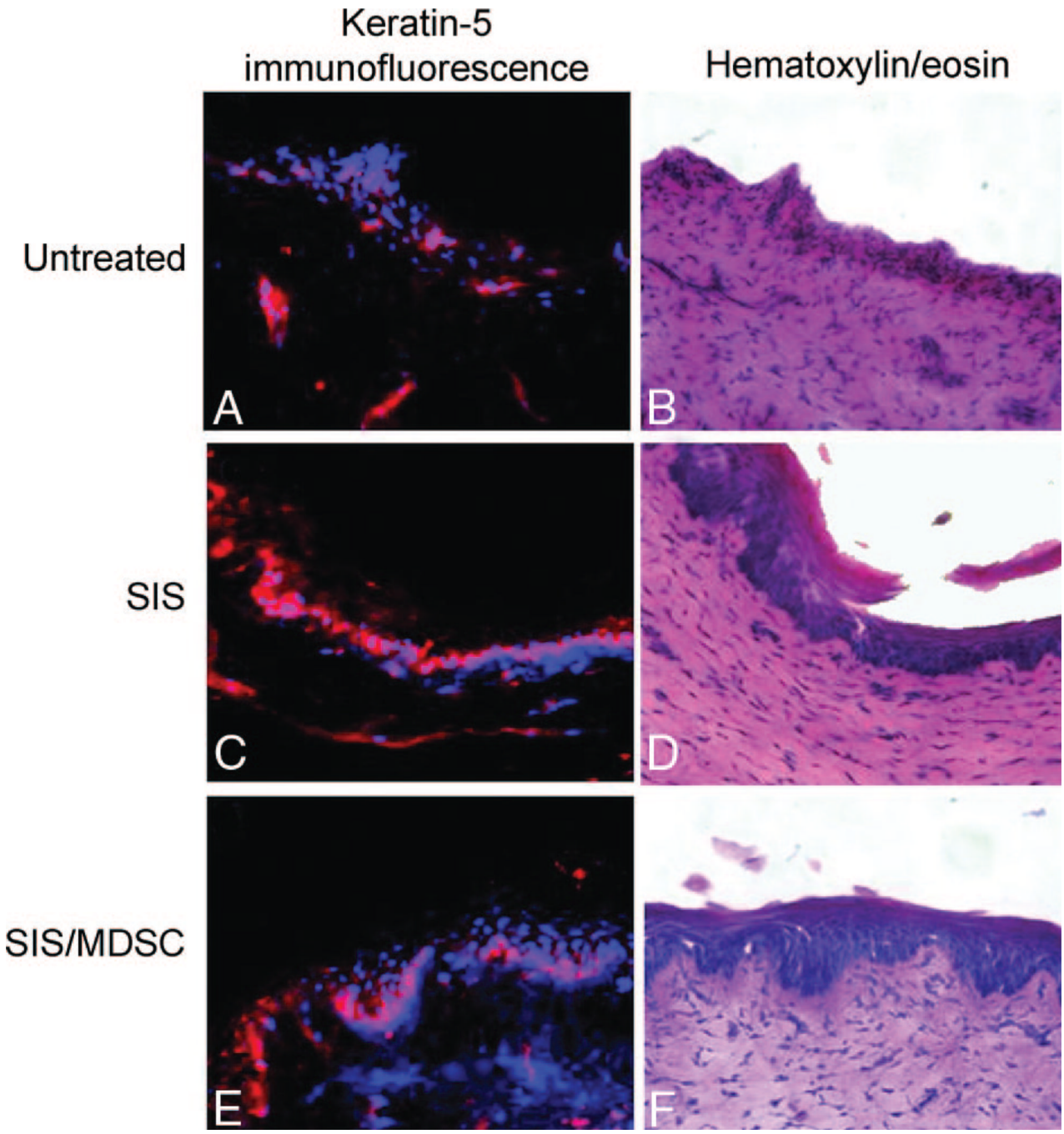

Fig. 7.

The effect exerted by muscle-derived stem cells (MDSCs) on the stratified squamous epithelium is confirm by immunohistochemistry for keratin 5. **A and B.** Untreated. **C and D.** Small intestinal submucosa (SIS). **E and F.** Small intestinal submucosa/muscle-derived stem cells. Frozen sections for region 5 (not fixed) were reacted against an antibody for keratin 5 that was detected by Texas red immunofluorescence, and nuclei were counterstained with 4′,6-diamidino-2-phenylindole (200×) **(A, C, E).** Adjacent sections were stained with hematoxylin-eosin (200×) **(B, D, E)**.

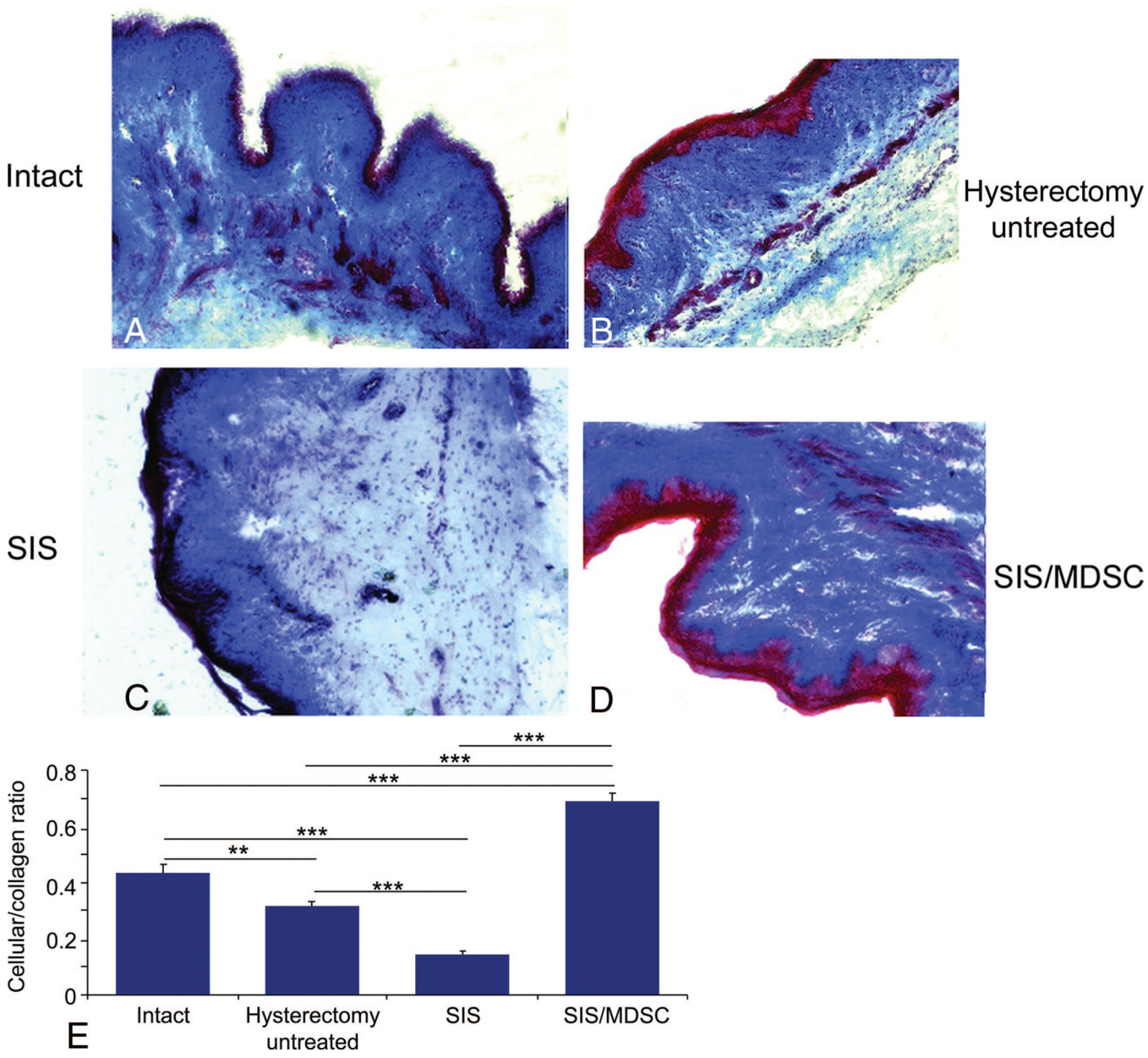

Fig. 8.

Implantation of small intestinal submucosa (SIS) with skeletal muscle-derived stem cells (MDSC) increases the cellular:extracellular ratio during vaginal regeneration. **A–D.** Representative pictures of frozen tissue sections for region 5 (fixed or not) at 8 weeks that were subjected to Masson-trichrome histochemistry (100X). **A.** Intact. **B.** Hysterectomy untreated. **C.** SIS. **D.** SIS/MDSC. **E.** Quantitative image analysis for 10 fields per specimen, three specimens per rat, and two rats per group.

Treatment of Peyronie's disease with PDE5 inhibitors: an antifibrotic strategy

Nestor F. Gonzalez-Cadavid and Jacob Rajfer

Abstract | Peyronie's disease (PD) is a localized fibrotic condition of the tunica albuginea that is associated with risk factors for corpora cavernosa fibrosis (such as advanced age and diabetes) and Dupuytren contracture, another localized fibrotic process. Most of the current pharmacological treatments for PD are not based on antifibrotic approaches that have shown promising results in animal models and clinical efficacy in other fibrotic conditions, which may explain why they are generally unsuccessful. Evidence gathered in human specimens and animal models of PD have elucidated aspects of its etiology and histopathology, showing that overexpression of transforming growth factor β1, plasminogen activator inhibitor 1, reactive oxygen species and other profibrotic factors, which are, in most cases, assumed to be induced by trauma to the tunica albuginea, leads to myofibroblast accumulation and excessive deposition of collagen. At the same time, a steady overexpression of inducible nitric oxide synthase, leading to increased nitric oxide and cGMP levels, seems to act as an endogenous antifibrotic mechanism. This process has also been reported in corporal and cardiovascular fibrosis, and has led to the demonstration that long-term continuous administration of phosphodiesterase type 5 inhibitors counteracts the development of a PD-like fibrotic plaque in a rat model, and later extended to the prevention of corporal fibrosis in animal models of erectile dysfunction.

Gonzalez-Cadavid, N. F. & Rajfer, J. *Nat. Rev. Urol.* advance online publication 9 March 2010; doi:10.1038/nrurol.2010.24

Introduction

Peyronie's disease (PD) is somewhat of a misnomer, as it is actually restricted to a small localized fibrotic plaque of the tunica albuginea of the penis.[1,2] Epidemiologic studies suggest that the disease may be present in up to 10% of all men, but primarily affects those in their sixties and seventies.[1–6] The reason PD attracts attention is that many men with the disease have some form of erectile dysfunction, and in the erect state the afflicted organ tends to curve and may be painful during intercourse. Despite its typical fibrotic histopathology, this condition is not associated with other localized or diffuse fibrotic processes, with the single exception of Dupuytren contraction, with which it shares a similar histopathology.[7–9] No satisfactory medical treatments for PD are currently available; however, experimental models have provided new insights into its pathophysiology and etiology, which have facilitated the investigation of alternative therapeutic approaches, including long-term continuous administration of phosphodiesterase type 5 (PDE5) inhibitors[10] as an antifibrotic modality. In this Review we examine the experimental evidence that forms the basis for this treatment strategy. No reports of the clinical efficacy of long-term PDE5 inhibition in patients with PD have been published, and, although the first preliminary animal study dates back to 2003,[11] this should still be considered as a novel management approach that requires future clinical validation.

Competing interests
The authors declare no competing interests.

Pathophysiology

A widely accepted hypothesis on the etiology of the PD plaque is that it originates from trauma or microtrauma to the erect penis, primarily during different types of sexual activities.[12] This hypothesis is based mainly on the demonstration of fibrin staining or immunodetection in tissue sections of human PD plaques,[13–15] findings that have been corroborated in an animal model of PD.[14] A plausible interpretation of this hypothesis is that the fibrin originates from fibrinogen that has extravasated into the interstices of the tunica albuginea during a traumatic sexual episode. Inhibition of the fibrinolytic system or an inability to degrade the intravasated fibrin would then lead to its persistence in the tunica, which initially leads to an acute inflammatory response. Because the fibrin is not degraded, the protein continues to exert a proinflammatory response, which ultimately leads to an abnormal healing process. The end result is the formation of a 'scar' that at some time evolves into a palpable plaque.[16] Indeed, injection of fibrin directly into the tunica albuginea of the rat penis elicits a PD-like plaque, resembling in many aspects the histology and evolution of the human PD plaque.[14,15,17]

The epidemiological association of PD with a history of sexually elicited trauma of the penile or pelvic surgery, which may affect the homeostasis of tissues in the penis, supports the trauma-related hypothesis for at least part of the patient population,[8,18,19] despite some contradictory evidence.[5,8,20] Considering the association of PD with Dupuytren contracture, genetic or immune-related predisposition to PD may modulate the tunical healing

Department of Urology, David Geffen School of Medicine at UCLA, and Los Angeles Biomedical Research Institute (LABioMed) at Harbor-UCLA Medical Center, Building F-6, 1124 West Carson Street, Torrance, CA 90502, USA (**N. F. Gonzalez-Cadavid**, **J. Rajfer**).

Correspondence to:
N. F. Gonzalez-Cadavid
ncadavid@ucla.edu

Key points

- Rodent models of Peyronie's disease (PD) are representative of most of the main histological and biochemical features present in human specimens
- Cell cultures obtained from the human PD plaque and its rat counterpart have added to the experimental evidence acquired in the human and in animal models
- Endogenous mechanisms of defense against tunical tissue inflammation, oxidative stress and fibrosis have been detected in the PD plaque and the rat PD-like lesion, and may be mimicked pharmacologically for treatment
- Endogenously elicited inducible nitric oxide synthase leads to sustained production of nitric oxide and cGMP, which counteract myofibroblast differentiation, accumulation of reactive oxygen species, cytokine release, and collagen deposition
- Continuous long-term administration of nitric oxide donors and phosphodiesterase 5 inhibitors has shown preventive and corrective effects in a rat model of PD: studies in patients with PD are now needed

reaction following any type of trauma to the penis, but this possibility has not been studied as intensively as is needed.[21–23]

The pathology of the PD plaque has been investigated in a variety of studies in human and animal model specimens and in related cell cultures.[1,10] Based on the results of histochemistry, immunohistochemistry and other assays performed on the human PD plaque tissues, it is clear that fibrosis—the excessive deposition of collagen and extracellular matrix (ECM) with disorganization of collagen fibers and loss of elastic fibers—is the main pathological process, combined in most cases with fibrin accumulation and different degrees of inflammation.[12–14,24,25]

Myofibroblasts (cells that share the fibroblast and smooth muscle phenotypes[26,27]) are not normally present in the tunica albuginea of the penis, but have been identified as the cells responsible for the disarrangement of the ECM in the PD plaque.[28–32] The normal process of apoptosis that eliminates myofibroblasts after they have fulfilled their role in wound healing is somehow inhibited in PD, thus leading to their persistence in the tunica albuginea. This myofibroblast accumulation is common not just to scar formation in the skin or the infarcted heart, but to most other types of fibrosis.[26,27] The PD plaque becomes harder by progressing through an intensification of fibrosis (with or without the persistence of inflammation) and, in at least 15% of the patients, through an advanced stage of calcification and ossification involving osteoblasts.[33,34] Spontaneous regression of the plaque after its initial formation occurs in rare cases.[9,34]

The scattered evidence regarding human PD plaque tissues has been considerably expanded by systematic approaches in experimental animal models, mainly in the widely used rat model of PD induced by transforming growth factor β1 (TGF-β1).[1,10] This key profibrotic factor, present in multiple tissues[35] and produced in the human PD plaque, is found at increased levels in the blood of PD patients.[36] Similarly, when a peptide derived from the TGF-β1 sequence is injected into the rat tunica, a plaque resembling that seen in human PD is found around 45 days later[11,37–41] at the injection site. Other less frequently employed but nonetheless useful animal models are based on either the successive injections of an adenoviral construct expressing a constitutively active TGF-β1 protein, leading to penile curvature during the erect state and, at times, calcification within the plaque,[42] or on a single fibrin injection that mimics the extravasation of fibrinogen, initiating acute inflammation followed by the rapid development of the PD-like plaque.[14,15,17] Both TGF-β1 and myostatin, another profibrotic factor within the TGF-β family, are involved in this process,[41] and it is quite likely that the key downstream signaling occurs via the Smad pathway, which is the mechanism common to most factors in this family.[43] A tight skin (Tsk) mouse model has been described that develops a spontaneous PD-like plaque with penile bending and areas of chondroid metaplasia with heterotypic ossification.[44]

These animal models, therefore, represent most of the histologic and biochemical features of the human PD plaque, including inflammation, myofibroblast accumulation, collagen deposition, oxidative stress, calcification, ossification and penile bending, among others. Thus, we believe that the PD-like lesion, either elicited experimentally or by spontaneous mutations in the rodent tunica, is more complex than a mere tunical fibrosis event, and, imperfect as most disease models in laboratory animals are, this experimental plaque is adequate for preclinical testing of various therapeutic strategies for PD.

Finally, the use of cell cultures from the normal, myofibroblast-free tunica albuginea or from the human PD plaque or the induced PD-like plaque from a rat, which are enriched in myofibroblasts, has allowed us to more precisely define the role of myofibroblasts in the pathophysiology of PD.[28–32,45,46] These cells have been shown to be responsible for the excessive collagen deposition seen in PD, and have even been postulated to cause penile bending by their contractile features. Moreover, pluripotent stem cells have been identified in the PD cultures. This may explain the fibrotic and osteogenic progression of the PD plaque upon the release of cytokines following microtrauma to the penis, which would stimulate stem cell commitment to this cell lineage.[31,45] PD fibroblasts are also potentially tumorigenic, or acquire this trait upon culture, but it is not known whether this is related to the presence of stem cells.[47]

There is no doubt that cell cultures derived from the human PD plaque and normal tunica albuginea closely represent their respective histologic features, notwithstanding the obvious shortcomings of any type of cell culture compared to the *in vivo* tissue. This has been tested with a multiplicity of immunocytochemical and western blot markers, as well as DNA microarrays and reverse transcription polymerase chain reaction procedures for the detection of fibroblasts, myofibroblasts and stem cells, and their respective differentiation and roles in inflammatory and fibrotic processes. The situation is similar regarding cell cultures obtained from the rat PD-like plaque, which have been shown to mimic their human counterparts. All these cultures have been useful

tools for defining therapeutic targets at the cellular and molecular level.

Cellular and molecular mechanisms

Results from experimental studies that have employed a variety of cellular and molecular biology techniques in the PD models described above, combined with the information obtained from the analysis of the human PD plaque, have made it possible to define an overall mechanistic picture of the initiation and progression of the PD plaque.[48] The mechanism resembles that seen in some other localized fibroses, including the more gradual and diffuse type that occurs in the penile corpora cavernosa of men with erectile dysfunction and many animal models of this disorder.[49] The main features of PD fibrosis are described below.

Fibrinogen extravasated into the tunica albuginea of the penis accumulates at the site of the future PD plaque owing to inhibition of the fibrinolytic and other proteolytic systems, primarily due to overexpression of plasminogen activator inhibitor 1 (PAI-1). The resulting fibrin formation, and possibly with the assistance of immunoglobulins and other extravasated proteins, triggers the release and/or activation of TGF-β1, PAI-1, and reactive oxygen species (ROS), which are recognized as key profibrotic factors in many tissues, including the kidney and vascular system. Concurrent expression of other cytokines, including monocyte chemotactic protein 1 (MCP-1; also known as CC-chemokine ligand 2 [CCL-2]), which is associated with acute inflammation that often progresses to a chronic phase, overexpression of other members of the TGF-β1 family (such as myostatin) and components of their common Smad signaling pathway, and other unknown agents combine to elicit the fibrotic process. The PD plaque then develops through excessive collagen deposition, elastin degradation, myofibroblast differentiation from fibroblasts or stem cells in the tunica, oxidative stress, and eventually calcification (Figure 1).[10,48,50,51]

The accumulation of tissue inhibitors of metalloproteinases (TIMPs) and the relative inhibition of collagenases (and/or a possible downregulation of their expression), which interferes with the normal breakdown of the accumulated collagen—and potentially, in the case of TIMPs, with therapeutic collagenase delivered to the plaque—contribute to the maintenance of the fibrotic process.[52]

One of the main findings stemming from DNA microarray analysis of the molecular profile of the PD plaque is the recognition that this tissue may be undergoing constant cellular and molecular turnover, and that spontaneous development of defense mechanisms to counteract fibrosis and oxidative stress might occur.[53,54] This transcriptional analysis detected overproduction of matrix metalloproteinases (MMPs) 2 and 9 (which contribute to collagen breakdown), decorin (which binds and neutralizes TGF-β1), and thymosins (which activate MMPs) in both PD plaques and Dupuytren nodules, as well as in cell cultures of these tissues. All these proteins seem to act as antifibrotic agents, either by combating collagen deposition or promoting its breakdown; therefore, it is plausible to postulate that they are produced in response to the fibrotic processes and that progression depends on the balance between the noxious and protective mechanisms, which in some cases may lead to spontaneous regression of the plaque.

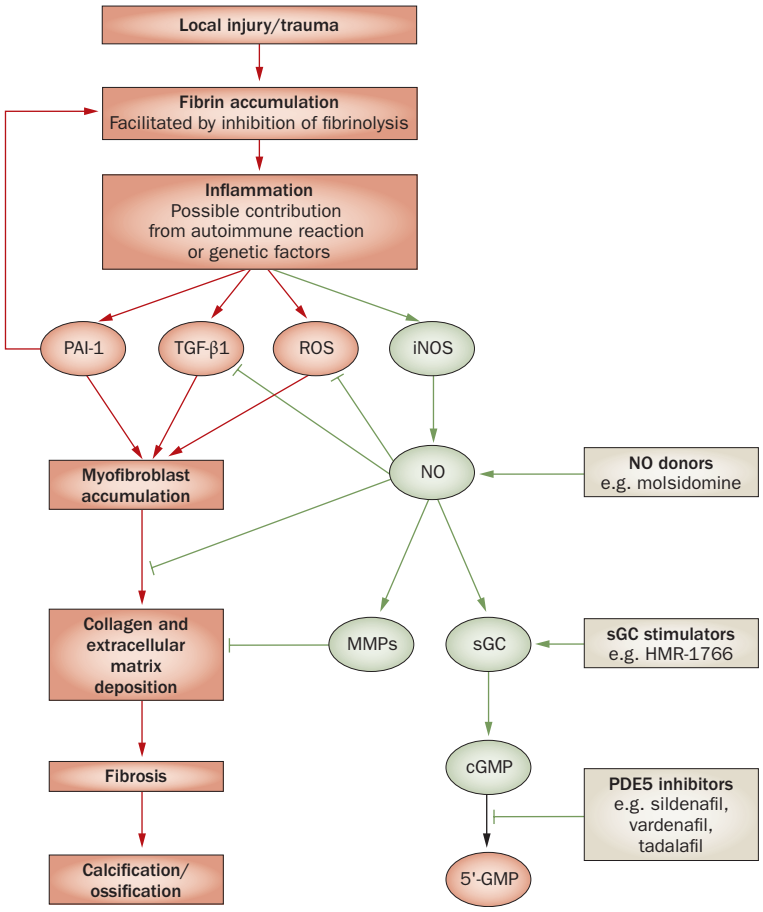

Figure 1 | Schematic representation of the etiology and pathophysiology of the fibrotic process leading to the Peyronie disease plaque (red), and the antifibrotic effects (green) of endogenous iNOS. Fibrin extravasated after injury or trauma to the penis accumulates in the tunica albuginea, which induces a local proinflammatory response. This leads to increased production of several key profibrotic factors, including PAI-1 (which inhibits fibrinolysis), TGF-β1 and ROS, which contribute to the accumulation of myofibroblasts. Myofibroblasts are responsible for the increased collagen and extracellular matrix deposition leading to fibrosis, and, owing to inhibited apoptosis of these cells, persist in the tunica albuginea. The production of iNOS seems to be an endogenous antifibrotic factor, leading to increased levels of NO in the affected tissue. NO inhibits collagen synthesis and myofibroblast differentiation and reduces oxidative stress by quenching ROS. In addition, NO increases the activity of sGC, which in turn increases levels of cGMP, which has further antifibrotic effects. Potential pharmacological interventions (gold) that might prevent or partially reverse plaque formation include NO donors, sGC stimulators and PDE5 inhibitors. Abbreviations: iNOS, inducible nitric oxide synthase; MMPs, matrix metalloproteinases; NO, nitric oxide; PAI-1, plasminogen activator inhibitor 1; PDE5, phosphodiesterase type 5; ROS, reactive oxygen species; sGC, soluble guanylate cyclase; TGF-β1, transforming growth factor β1.

Role of inducible nitric oxide synthase

Despite the experimental evidence outlined above, the current pharmacological management of PD is mostly

empirical, as it is generally based on the use of drugs targeting nonspecific or ancillary aspects of PD, such as inflammation or cell replication.[2,55] Virtually nothing has been translated from the abundant pharmacological studies in other types of fibrosis, or from preclinical studies in animal or cell culture models of PD. This renders PD a sort of orphan disease in terms of a scientifically rational approach to therapy, in contrast to the other types of fibrosis where, in general, clinical use is supported by promising preclinical studies.[48,56]

However, among the putative endogenous mechanisms of defense against fibrosis that are postulated to operate in the PD plaque, the most intensively studied and highly promising in terms of therapeutic potential is the spontaneous induction of inducible nitric oxide synthase (iNOS), a NOS isoform that is not expressed in normal penile tissue.[57] Whereas in the past it was assumed that the presence of iNOS portended a deleterious outcome to a tissue, it is now believed to in fact be a protective mechanism against tissue fibrosis in certain settings. iNOS expression produces a steady output of nitric oxide, a compound that directly inhibits collagen synthesis and myofibroblast differentiation, quenches ROS via the production of peroxynitrite, and inhibits the TGF-β/Smad signaling pathway, thus counteracting fibrosis.[11,17,25,30,41] The pro-apoptotic effects of nitric oxide might also contribute to reducing the myofibroblast population. Remarkably, iNOS production in the penis is not restricted to the tunica albuginea or to PD. For example, iNOS is detectable in the corpora cavernosa of patients with diabetes, advanced age, and even following radical prostatectomy, where fibrosis of the corpora leads to the development of corporal veno-occlusive dysfunction (CVOD). iNOS production may also been seen in the penile arteries in disease states where arteriosclerosis or arterial stiffness is present.[57–64] In all these scenarios, iNOS production, resulting in some cases from an inflammatory process, is presumed to be an antifibrotic response to the development of fibrosis within these individual tissues.

Collectively, several lines of evidence in rodent models support the antifibrotic role of iNOS in the PD plaque and in corporal and vascular tissue. Gene transfer of iNOS cDNA, which then becomes constitutively expressed, reduces fibrosis in the tunica albuginea and corpora of the penis, whereas long-term, specific inhibition of iNOS activity (by the iNOS inhibitor L-NIL) counteracts this process in both tissues, as well as in the arterial wall.[17,25,58,60] Furthermore, genetic inactivation of the iNOS gene in the iNOS knockout mouse intensifies collagen deposition in the corpora in a process exacerbated by diabetes.[64] This agrees with what has been shown in other tissues in the iNOS knockout mouse model, in which the absence of iNOS increases interstitial fibrosis after unilateral ureteral obstruction and hepatic fibrosis in animals fed a high-fat diet and in those with streptozotocin-induced diabetic nephropathy.[65–70] iNOS also has a cardioprotective role in preconditioning during ischemia reperfusion injury in mouse kidney and in granulomatous disease.[71,72]

Some evidence suggests that iNOS deletion seems to be protective rather than detrimental in certain types of fibrosis,[73–76] and that iNOS overexpression is associated with increased fibrosis, particularly in the diabetic kidney.[77] However, nitric oxide is known to inhibit myofibroblast differentiation via inhibition of the TGF-β/Smad pathway, and to have general antifibrotic effects via inhibition of collagen synthesis and ROS quenching.[78–82] The protective effects of iNOS depend, therefore, on the specific tissue type and the pathological conditions under which it is induced. In the case of the penile tissues, including the PD plaque, all the evidence so far obtained supports an antifibrotic role for iNOS.

Treatment with PDE5 inhibitors

Although some of the beneficial, antifibrotic effects of iNOS are directly attributable to nitric oxide, others may result from the increased levels of cGMP produced following stimulation of guanylate cyclase by nitric oxide, which subsequently leads to protein kinase G activation. cGMP, and in some cases PDE5 inhibitors, have been shown to inhibit myofibroblast formation in cell cultures of human and rat PD plaques[30,32] and in lung fibroblasts.[83] These antifibrotic effects are also exercised by guanylate cyclase stimulators via protein kinase G stimulation and inhibition of fibrotic mediators such as angiotensin II, or by TGF-β or Rho activation.[83–87]

An early preliminary study in the rat model of TGF-β1-induced PD demonstrated that both oral sildenafil, a PDE5 inhibitor that protects cGMP from breakdown, and oral pentoxifylline, a predominantly PDE4 inhibitor that increases cAMP synthesis, counteract the development of the PD-like plaque.[11] In the case of pentoxifylline, it was proposed that the well-known cAMP–cGMP signaling crosstalk may be responsible for its antifibrotic effects, although direct effects of cAMP or the involvement of alternative pathways modulated by pentoxifylline can not be excluded. This study revealed a completely new mechanism of action for PDE5 inhibitors, in contrast to their standard on-demand clinical administration to facilitate penile erection upon sexual stimulation, which is mediated by their short-term relaxant effect on the corporal and arterial smooth muscle produced by a transient elevation of cGMP levels. The novel concept is that PDE5 inhibitors given for a sufficiently long time can induce a sustained elevation of nitric oxide and cGMP levels that, independently of their vasorelaxant effects, which would show only during sexual stimulation, act as antifibrotic agents by reducing collagen deposition, profibrotic factor release, oxidative stress and myofibroblast numbers.

In a subsequent study in the same rat model, it was shown that another PDE5 inhibitor, vardenafil, given orally and in different dosing regimens, not only prevented but partially reversed the formation of the PD-like plaque.[40] To test the early preventive effects of vardenafil, the drug was administered to male rats either in their drinking water or as a once-daily oral instillation at either 1 or 3 mg/kg per day for 45 days following a single injection of TGF-β1 into the tunica albuginea

to induce the PD-like plaque. Other animals, in which a PD-like plaque had already been formed, received either dose of vardenafil in their drinking water for 42 days (late, therapeutic administration). Preventive treatment at the higher dose (both continuous and once-daily treatments) reduced the overall collagen content, collagen III/I ratio and the number of myofibroblasts and TGF-β1-positive cells, and selectively increased the apoptotic index of cells (presumably including myofibroblasts), in the PD-like plaque. The lower dose was less effective. When vardenafil was given continuously in the drinking water for 42 days after the PD-like plaque was formed, a partial reduction in plaque size was observed. From these two studies,[11,40] it was concluded that long-term oral treatment with a PDE5 inhibitor slows and reverses the early stages of an experimental PD-like plaque in the rat, and might ameliorate a more advanced plaque.

The optimal therapeutic regimen for discontinuous oral administration of PDE5 inhibitors was not assessed in these studies, so whether oral instillation, perhaps at a higher dose, can regress an already formed plaque is not known. However, the authors discussed the possibility of testing combinations of PDE5 inhibitors and other compounds used for the treatment of PD, such as verapamil (a calcium channel blocker), vitamin E (an antioxidant) and collagenase. An important point that was made was that, owing to the multifactorial nature of fibrosis and the difficulty of reversing established collagen crosslinking, combination therapy might be more effective than a single agent when a well-formed PD plaque is present.[40]

This first demonstration of the antifibrotic effects of long-term, continuous administration of a PDE5 inhibitor was later extended to the corpora cavernosal fibrosis that underlies CVOD, caused either by aging or by neuropraxia secondary to cavernosal nerve resection, mimicking the post-radical-prostatectomy state.[59–62] In these cases, the effects of the three PDE5 inhibitors (sildenafil, vardenafil and tadalafil) on collagen deposition in the rat corpora were similar to those seen in the PD-like plaque; however, they also seemed to provide protection against the loss of smooth muscle cells, which are responsible for normal corporal compliance and their ability to relax and achieve normal veno-occlusion. In fact, the PDE5 inhibitors decreased corporal apoptosis—specifically of smooth muscle cells in this case, as opposed to the increased apoptotic index in tunical myofibroblasts observed in the PD plaque—and oxidative stress, thus preventing or correcting CVOD. Sildenafil prevented the progression of corporal fibrosis in penile histopathology induced by cavernous neurotomy in the rat and in patients who had undergone radical prostatectomy.[88–90] These antifibrotic effects of PDE5 inhibitors, specifically the prevention of collagen deposition and the inhibition of TGF-β1 expression and oxidative stress, were also seen in rat models of diabetic nephropathy, experimental glomerulonephritis, myocardial infarction and hypertrophy, and pulmonary fibrosis;[91–95] therefore, their antifibrotic effects do not seem to be restricted to penile tissues. These effects should not be confused with the beneficial vasodilator mechanism exploited for the treatment of pulmonary hypertension.[96]

Despite the two experimental papers on the effects of continuous long-term treatment with sildenafil and vardenafil on the PD-like plaque in the TGF-β1 rat model,[11,40] the emerging literature on this modality in other types of tissue fibrosis, and the well characterized antifibrotic effects of cGMP and guanylate cyclase stimulators, no similar experimental studies have been performed in human patients with PD. An article related to the use of PDE5 inhibitors in patients with PD in fact focused on their standard "on-demand" application for treating erectile dysfunction, and not PD itself.[97] This lack of studies in humans does not seem to be due to concerns about potential adverse effects, as several trials have shown that daily administration of sildenafil or tadalafil is well tolerated.[98,99] Moreover, a 2006 case report described the beneficial effects of an antifibrotic regimen of drugs that upregulate nitric oxide (and, therefore, cGMP production) in two patients with refractory priapism (>48 h duration).[43] Based on the previous work in a rat model of PD,[11] the regimen included the PDE inhibitors pentoxifylline and sildenafil and the nitric oxide precursor L-arginine. At 1 year, both patients were found to have flexible corpora and no evidence of fibrosis.

Conclusions

Despite the strong preclinical evidence in animal models supporting the antifibrotic effects of continuous, long-term administration of PDE5 inhibitors in penile tissue, this approach has yet to be studied in patients with PD. The likelihood is that our wider experience of the on-demand use of PDE5 inhibitors for erectile dysfunction will eventually lead to the first clinical test of the antifibrotic hypothesis in the context of the relatively mild corporal fibrosis seen in patients after radical prostatectomy; only if successful in this application might its use be extended to PD. In any case, despite the promise of this novel approach, the progression of the human PD plaque to advanced fibrosis and calcification may restrict its application to the early stages of the disease. In addition, a combination regimen comprising PDE5 inhibitors and other agents that stimulate collagen breakdown may be needed to effectively reduce the size of an established plaque. We believe that a study in which the outcomes of men receiving a currently used treatment for PD plus a PDE5 inhibitor are compared with men receiving the same treatment plus placebo will help define the future role of PDE5 inhibitors in patients with PD.

Review criteria

We searched for original articles focusing on Peyronie's disease in PubMed published from 1980 onwards. The search terms we used were "Peyronie's disease" and "La Peyronie". All papers identified were full-text papers (unless indicated in the reference list) and were published in English, French or Spanish.

1. Gonzalez-Cadavid, N. F. & Rajfer, J. in *Current Clinical Urology: Peyronie's Disease, A Guide to Clinical Management* (ed. Levine, L. A.) 19–39 (Humana Press, Totowa, 2007).
2. Smith, J. F., Walsh, T. J. & Lue, T. F. Peyronie's disease: a critical appraisal of current diagnosis and treatment. *Int. J. Impot. Res.* **20**, 445–459 (2008).
3. Müller, A. & Mulhall, J. P. Peyronie's disease intervention trials: methodological challenges and issues. *J. Sex. Med.* **6**, 848–861 (2009).
4. Smith, C. J., McMahon, C. & Shabsigh, R. Peyronie's disease: the epidemiology, aetiology and clinical evaluation of deformity. *BJU Int.* **95**, 729–732 (2005).
5. Mulhall, J. P. *et al.* Subjective and objective analysis of the prevalence of Peyronie's disease in a population of men presenting for prostate cancer screening. *J. Urol.* **171**, 2350–2353 (2004).
6. Taylor, F. L. & Levine, L. A. Peyronie's disease. *Urol. Clin. North Am.* **34**, 517–534 (2007).
7. Carrieri, M. P., Serraino, D., Palmiotto, F., Nucci, G. & Sasso, F. A case–control study on risk factors for Peyronie's disease. *J. Clin. Epidemiol.* **51**, 511–515 (1998).
8. Deveci, S. *et al.* Defining the clinical characteristics of Peyronie's disease in young men. *J. Sex. Med.* **4**, 485–490 (2007).
9. Bjekic, M. D., Vlajinac, H. D., Sipetic, S. B. & Marinkovic, J. M. Risk factors for Peyronie's disease: a case–control study. *BJU Int.* **97**, 570–574 (2006).
10. Gonzalez-Cadavid, N. F. & Rajfer, J. Experimental models of Peyronie's disease. Implications for new therapies. *J. Sex. Med.* **6**, 303–313 (2009).
11. Valente, E. G. *et al.* L-Arginine and phosphodiesterase (PDE) inhibitors counteract fibrosis in the Peyronie's fibrotic plaque and related fibroblast cultures. *Nitric Oxide* **9**, 229–244 (2003).
12. Devine, C. J. Jr, Somers, K. D., Jordan, S. G. & Schlossberg, S. M. Proposal: trauma as the cause of the Peyronie's lesion. *J. Urol.* **157**, 285–290 (1997).
13. Somers, K. D. & Dawson, D. M. Fibrin deposition in Peyronie's disease plaque. *J. Urol.* **157**, 311–315 (1997).
14. Davila, H. H., Magee, T. R., Zuniga, F. I., Rajfer, J. & Gonzalez-Cadavid, N. F. Peyronie's disease associated with increase in plasminogen activator inhibitor in fibrotic plaque. *Urology* **65**, 645–648 (2005).
15. Davila, H. H., Ferrini, M. G., Rajfer, J. & Gonzalez-Cadavid, N. F. Fibrin as an inducer of fibrosis in the tunica albuginea of the rat: a new animal model of Peyronie's disease. *BJU Int.* **91**, 830–838 (2003).
16. Ehrlich, H. P. Scar contracture: cellular and connective tissue aspects in Peyronie's disease. *J. Urol.* **157**, 316–319 (1997).
17. Davila, H. H., Magee, T. R., Vernet, D., Rajfer, J. & Gonzalez-Cadavid, N. F. Gene transfer of inducible nitric oxide synthase complementary DNA regresses the fibrotic plaque in an animal model of Peyronie's disease. *Biol. Reprod.* **71**, 1568–1577 (2004).
18. Usta, M. F. *et al.* Relationship between the severity of penile curvature and the presence of comorbidities in men with Peyronie's disease. *J. Urol.* **171**, 775–779 (2004).
19. Perimenis, P., Athanasopoulos, A., Gyftopoulos, K., Katsenis, G. & Barbalias, G. Peyronie's disease: epidemiology and clinical presentation of 134 cases. *Int. Urol. Nephrol.* **32**, 691–694 (2001).
20. El-Sakka, A. I., Selph, C. A., Yen, T. S., Dahiya, R. & Lue, T. F. The effect of surgical trauma on rat tunica albuginea. *J. Urol.* **159**, 1700–1707 (1998).
21. Schiavino, D. *et al.* Immunologic findings in Peyronie's disease: a controlled study. *Urology* **50**, 764–768 (1997).
22. Noss, M. B., Day, N. S., Christ, G. J. & Melman, A. The genetics and immunology of Peyronie's disease. *Int. J. Impot. Res.* **12** (Suppl. 4), S127–S132 (2000).
23. Hauck, E. W., Hauptmann, A., Weidner, W., Bein, G. & Hackstein, H. Prospective analysis of HLA classes I and II antigen frequency in patients with Peyronie's disease. *J. Urol.* **170**, 1443–1446 (2003).
24. Anafarta, K., Bedük, Y., Uluoglu, O., Aydos, K. & Baltaci, S. The significance of histopathological changes of the normal tunica albuginea in Peyronie's disease. *Int. Urol. Nephrol.* **26**, 71–77 (1994).
25. Ferrini, M. G. *et al.* Antifibrotic role of inducible nitric oxide synthase. *Nitric Oxide* **6**, 283–294 (2002).
26. Hinz, B. *et al.* The myofibroblast: one function, multiple origins. *Am. J. Pathol.* **170**, 1807–1816 (2007).
27. Eyden, B. The myofibroblast: phenotypic characterization as a prerequisite to understanding its functions in translational medicine. *J. Cell. Mol. Med.* **12**, 2022–2037 (2008).
28. Somers, K. D. *et al.* Cell culture of Peyronie's disease plaque and normal penile tissue. *J. Urol.* **127**, 585–588 (1982).
29. Mulhall, J. P., Anderson, M. S., Lubrano, T. & Shankey, T. V. Peyronie's disease cell culture models: phenotypic, genotypic and functional analyses. *Int. J. Impot. Res.* **14**, 397–405 (2002).
30. Vernet, D. *et al.* Effect of nitric oxide on the differentiation of fibroblasts into myofibroblasts in the Peyronie's fibrotic plaque and in its rat model. *Nitric Oxide* **7**, 262–276 (2002).
31. Vernet, D. *et al.* Evidence that osteogenic progenitor cells in the human tunica albuginea may originate from stem cells: implications for peyronie disease. *Biol. Reprod.* **73**, 1199–1210 (2005).
32. Vernet, D. *et al.* Phosphodiesterase type 5 is not upregulated by tadalafil in cultures of human penile cells. *J. Sex. Med.* **3**, 84–94 (2006).
33. Vande Berg, J. S. *et al.* Mechanisms of calcification in Peyronie's disease. *J. Urol.* **127**, 52–54 (1982).
34. Kadioglu, A. *et al.* A retrospective review of 307 men with Peyronie's disease. *J. Urol.* **168**, 1075–1079 (2002).
35. Wynn, T. A. Cellular and molecular mechanisms of fibrosis. *J. Pathol.* **214**, 199–210 (2008).
36. El-Sakka, A. I., Hassoba, H. M., Pillarisetty, R. J., Dahiya, R. & Lue, T. F. Peyronie's disease is associated with an increase in transforming growth factor-beta protein expression. *J. Urol.* **158**, 1391–1394 (1997).
37. El-Sakka, A. I. *et al.* An animal model of Peyronie's-like condition associated with an increase of transforming growth factor beta mRNA and protein expression. *J. Urol.* **158**, 2284–2290 (1997).
38. El-Sakka, A. I. *et al.* Histological and ultrastructural alterations in an animal model of Peyronie's disease. *Br. J. Urol.* **81**, 445–452 (1998).
39. Bivalacqua, T. J. *et al.* A rat model of Peyronie's disease associated with a decrease in erectile activity and an increase in inducible nitric oxide synthase protein expression. *J. Urol.* **163**, 1992–1998 (2000).
40. Ferrini, M. G., Kovanecz, I., Nolazco, G., Rajfer, J. & Gonzalez-Cadavid, N. F. Effects of long-term vardenafil treatment on the development of fibrotic plaques in a rat model of Peyronie's disease. *BJU Int.* **97**, 625–633 (2006).
41. Cantini, L. P. *et al.* Profibrotic role of myostatin in Peyronie's disease. *J. Sex. Med.* **5**, 1607–1622 (2008).
42. Piao, S. *et al.* Repeated intratunical injection of adenovirus expressing transforming growth factor-β1 in a rat induces penile curvature with tunical fibrotic plaque: a useful model for the study of Peyronie's disease. *Int. J. Androl.* **31**, 346–353 (2008).
43. Rajfer, J., Gore, J. L., Kaufman, J. & Gonzalez-Cadavid, N. Case report: avoidance of palpable corporal fibrosis due to priapism with upregulators of nitric oxide. *J. Sex. Med.* **3**, 173–176 (2006).
44. Lucattelli, M. *et al.* A new mouse model of Peyronie's disease: an increased expression of hypoxia-inducible factor-1 target genes during the development of penile changes. *Int. J. Biochem. Cell Biol.* **40**, 2638–2648 (2008).
45. Nolazco, G. *et al.* Effect of muscle-derived stem cells on the restoration of corpora cavernosa smooth muscle and erectile function in the aged rat. *BJU Int.* **101**, 1156–1164 (2008).
46. Mulhall, J. P. Expanding the paradigm for plaque development in Peyronie's disease. *Int. J. Impot. Res.* **15** (Suppl. 5), S93–S102 (2003).
47. Mulhall, J. P. *et al.* Peyronie's disease fibroblasts demonstrate tumorigenicity in the severe combined immunodeficient (SCID) mouse model. *Int. J. Impot. Res.* **16**, 99–104 (2004).
48. Gonzalez-Cadavid, N. F. & Rajfer, J. Mechanisms of disease: new insights into the cellular and molecular pathology of Peyronie's disease. *Nat. Clin. Pract. Urol.* **2**, 291–297 (2005).
49. Gonzalez-Cadavid, N. F. Mechanisms of penile fibrosis. *J. Sex. Med.* **6** (Suppl. 3), 353–362 (2009).
50. Nehra, A. & Nylhall, J. Peyronie's disease. In *Standard Practice in Sexual Medicine* 1st edn (eds Porst, H. & Buvat, J.) 158–173 (Blackwell, Malden, 2006).
51. Mulhall, J. P. Expanding the paradigm for plaque development in Peyronie's disease. *Int. J. Impot. Res.* **15** (Suppl. 5), S93–S102 (2003).
52. Del Carlo, M., Cole, A. A. & Levine, L. A. Differential calcium independent regulation of matrix metalloproteinases and tissue inhibitors of matrix metalloproteinases by interleukin-1β and transforming growth factor-β in Peyronie's plaque fibroblasts. *J. Urol.* **179**, 2447–2455 (2008).
53. Magee, T. R. *et al.* Gene expression profiles in the Peyronie's disease plaque. *Urology* **59**, 451–457 (2002).
54. Qian, A., Meals, R. A., Rajfer, J. & Gonzalez-Cadavid, N. F. Comparison of gene expression profiles between Peyronie's disease and Dupuytren's contracture. *Urology* **64**, 399–404 (2004).
55. Hellstrom, W. Medical management of Peyronie's disease. *J. Androl.* **30**, 397–404 (2009).
56. Sivakumar, P. & Das, A. M. Fibrosis, chronic inflammation and new pathways for drug discovery. *Inflamm. Res.* **57**, 410–418 (2008).
57. Gonzalez-Cadavid, N. F. & Rajfer, J. The pleiotropic effects of inducible nitric oxide synthase on the physiology and pathology of penile erection. *Curr. Pharm. Des.* **11**, 4041–4046 (2005).
58. Ferrini, M. G., Davila, H., Valente, E. G., Gonzalez-Cadavid, N. F. & Rajfer, J. Aging-related induction of inducible nitric oxide synthase (iNOS) is vasculo-protective in the arterial media. *Cardiovasc. Res.* **61**, 796–805 (2004).

59. Ferrini, M. G. *et al.* Long-term continuous treatment with vardenafil prevents fibrosis and preserves smooth muscle content in the rat corpora cavernosa after bilateral cavernosal nerve transection. *Urology* **68**, 429–435 (2006).
60. Ferrini, M. G. *et al.* Long-term continuous treatment with sildenafil ameliorates aging-related erectile dysfunction and the underlying corporal fibrosis in the rat. *Biol. Reprod.* **76**, 915–923 (2007).
61. Kovanecz, I. *et al.* Long term sildenafil treatment ameliorates corporal veno-occlusive dysfunction (CVOD) induced by cavernosal nerve resection in rats. *Int. J. Impot. Res.* **100**, 867–874 (2007).
62. Kovanecz, I. *et al.* Chronic daily tadalafil prevents the corporal fibrosis and veno-occlusive dysfunction (CVOD) that occurs following cavernosal nerve resection in the rat. *BJU Int.* **101**, 203–210 (2008).
63. Ferrini, M. G. *et al.* Fibrosis and loss of smooth muscle in the corpora cavernosa precede corporal veno-occlusive dysfunction (CVOD) induced by experimental cavernosal nerve damage in the rat. *J. Sex. Med.* **6**, 415–428 (2009).
64. Ferrini, M. G. *et al.* The genetic inactivation of inducible nitric oxide synthase intensifies fibrosis and oxidative stress in the penile corpora cavernosa in type 1 diabetes. *J. Sex. Med.* (in press).
65. Hochberg, D. *et al.* Interstitial fibrosis of unilateral ureteral obstruction is exacerbated in kidneys of mice lacking the gene for inducible nitric oxide synthase. *Lab. Invest.* **80**, 1721–1728 (2000).
66. Trachtman, H., Futterweit, S., Pine, E., Mann, J. & Valderrama, E. Chronic diabetic nephropathy: role of inducible nitric oxide synthase. *Pediatr. Nephrol.* **17**, 20–29 (2002).
67. Chen, Y. *et al.* Deficiency of inducible nitric oxide synthase exacerbates hepatic fibrosis in mice fed high-fat diet. *Biochem. Biophys. Res. Commun.* **326**, 45–51 (2005).
68. Aram, G., Potter, J. J., Liu, X., Torbenson, M. S. & Mezey, E. Lack of inducible nitric oxide synthase leads to increased hepatic apoptosis and decreased fibrosis in mice after chronic carbon tetrachloride administration. *Hepatology* **47**, 2051–2058 (2008).
69. Bayir, H. *et al.* Enhanced oxidative stress in iNOS deficient mice after traumatic brain injury: support for a neuroprotective role of iNOS. *J. Cereb. Blood Flow Metab.* **25**, 673–684 (2005).
70. Park, K. M. *et al.* Inducible nitric-oxide synthase is an important contributor to prolonged protective effects of ischemic preconditioning in the mouse kidney. *J. Biol. Chem.* **278**, 27256–27266 (2003).
71. Jones, S. P. & Bolli, R. The ubiquitous role of nitric oxide in cardioprotection. *J. Mol. Cell. Cardiol.* **40**, 16–23 (2006).
72. Hesse, M., Cheever, A. W., Jankovic, D. & Wynn, T. A. NOS-2 mediates the protective anti-inflammatory and antifibrotic effects of the Th1-inducing adjuvant, IL-12, in a Th2 model 0f granulomatous disease. *Am. J. Pathol.* **157**, 945–955 (2000).
73. Zhang, P. *et al.* Inducible nitric oxide synthase deficiency protects the heart from systolic overload-induced ventricular hypertrophy and congestive heart failure. *Circ. Res.* **100**, 1089–1098 (2007).
74. Lu, L., Chen, S. S., Hassid, A. & Sun, Y. Cardiac fibrogenesis following infarction in mice with deletion of inducible nitric oxide synthase. *Am. J. Med. Sci.* **335**, 431–438 (2008).
75. Kadkhodaee, M. *et al.* Proteinuria is reduced by inhibition of inducible nitric oxide synthase in rat renal ischemia-reperfusion injury. *Transplant. Proc.* **41**, 2907–2909 (2009).
76. Kuhlencordt, P. J., Chen, J., Han, F., Astern, J. & Huang, P. L. Genetic deficiency of inducible nitric oxide synthase reduces atherosclerosis and lowers plasma lipid peroxides in apolipoprotein E-knockout mice. *Circulation* **103**, 3099–3104 (2001).
77. Toblli, J. E. *et al.* Antifibrotic effects of pioglitazone on the kidney in a rat model of type 2 diabetes mellitus. *Nephrol. Dial. Transplant.* **24**, 2384–2391 (2009).
78. Mookerjee, I. *et al.* Relaxin inhibits renal myofibroblast differentiation via RXFP1, the nitric oxide pathway, and Smad2. *FASEB J.* **23**, 1219–1229 (2009).
79. Vyas-Read, S., Shaul, P. W., Yuhanna, I. S. & Willis, B. C. Nitric oxide attenuates epithelial-mesenchymal transition in alveolar epithelial cells. *Am. J. Physiol. Lung Cell. Mol. Physiol.* **293**, L212–L221 (2007).
80. Brosius, F. C. 3rd. New insights into the mechanisms of fibrosis and sclerosis in diabetic nephropathy. *Rev. Endocr. Metab. Disord.* **9**, 245–254 (2008).
81. Kalk, P. *et al.* Pulmonary fibrosis in L-NAME-treated mice is dependent on an activated endothelin system. *Can. J. Physiol. Pharmacol.* **86**, 541–545 (2008).
82. Peters, H. *et al.* NO mediates antifibrotic actions of L-arginine supplementation following induction of anti-thy1 glomerulonephritis. *Kidney Int.* **64**, 509–518 (2003).
83. Dunkern, T. R., Feurstein, D., Rossi, G. A., Sabatini, F. & Hatzelmann, A. Inhibition of TGF-β induced lung fibroblast to myofibroblast conversion by phosphodiesterase inhibiting drugs and activators of soluble guanylyl cyclase. *Eur. J. Pharmacol.* **572**, 12–22 (2007).
84. Masuyama, H. *et al.* Pressure-independent effects of pharmacological stimulation of soluble guanylate cyclase on fibrosis in pressure-overloaded rat heart. *Hypertens. Res.* **32**, 597–603 (2009).
85. Sawada, N. *et al.* Cyclic GMP kinase and RhoA Ser188 phosphorylation integrate pro- and anti-fibrotic signals in blood vessels. *Mol. Cell. Biol.* **29**, 6018–6032 (2009).
86. Knorr, A. *et al.* Nitric oxide-independent activation of soluble guanylate cyclase by BAY 60–2770 in experimental liver fibrosis. *Arzneimittelforschung* **58**, 71–80 (2008).
87. Wang-Rosenke, Y., Neumayer, H. H. & Peters, H. NO signaling through cGMP in renal tissue fibrosis and beyond: key pathway and novel therapeutic target. *Curr. Med. Chem.* **15**, 1396–1406 (2008).
88. Iacono, F. *et al.* Histopathologically proven prevention of post-prostatectomy cavernosal fibrosis with sildenafil. *Urol. Int.* **80**, 249–252 (2008).
89. Vignozzi, L. *et al.* Effect of sildenafil administration on penile hypoxia induced by cavernous neurotomy in the rat. *Int. J. Impot. Res.* **20**, 60–67 (2008).
90. Magheli, A. & Burnett, A. L. Erectile dysfunction following prostatectomy: prevention and treatment. *Nat. Rev. Urol.* **6**, 415–427 (2009).
91. Hemnes, A. R., Zaiman, A. & Champion, H. C. PDE 5A inhibition attenuates bleomycin-induced pulmonary fibrosis and pulmonary hypertension through inhibition of ROS generation and RhoA/Rho kinase activation. *Am. J. Physiol. Lung Cell. Mol. Physiol.* **294**, L24–L33 (2008).
92. Wang, Y. *et al.* Enhancing cGMP in experimental progressive renal fibrosis: soluble guanylate cyclase stimulation vs. phosphodiesterase inhibition. *Am. J. Physiol. Renal Physiol.* **290**, F167–F176 (2006).
93. Nagayama, T. *et al.* Sildenafil stops progressive chamber, cellular, and molecular remodeling and improves calcium handling and function in hearts with pre-existing advanced hypertrophy caused by pressure overload. *J. Am. Coll. Cardiol.* **53**, 207–215 (2009).
94. Radovits, T. *et al.* The phosphodiesterase-5 inhibitor vardenafil improves cardiovascular dysfunction in experimental diabetes mellitus. *Br. J. Pharmacol.* **156**, 909–919 (2009).
95. Hohenstein, B., Daniel, C., Wittmann, S. & Hugo, C. PDE-5 inhibition impedes TSP-1 expression, TGF-β activation and matrix accumulation in experimental glomerulonephritis. *Nephrol. Dial. Transplant.* **23**, 3427–3436 (2008).
96. Steiropoulos, P., Trakada, G. & Bouros, D. Current pharmacological treatment of pulmonary arterial hypertension. *Curr. Clin. Pharmacol.* **3**, 11–19 (2008).
97. Levine, L. A. & Latchamsetty, K. C. Treatment of erectile dysfunction in patients with Peyronie's disease using sildenafil citrate. *Int. J. Impot. Res.* **14**, 478–482 (2002).
98. Porst, H. *et al.* Long-term safety and efficacy of tadalafil 5 mg dosed once daily in men with erectile dysfunction. *J. Sex. Med.* **5**, 2160–2169 (2008).
99. Bella, A. J., Deyoung, L. X., Al-Numi, M. & Brock, G. B. Daily administration of phosphodiesterase type 5 inhibitors for urological and nonurological indications. *Eur. Urol.* **52**, 990–1005 (2007).

Acknowledgments

The authors would like to primarily acknowledge the Eli and Edythe Broad Foundation, without whose initial support none of the experimental research work on PD at the UCLA group would have been possible. Additional funding was subsequently applied for some aspects of this research from NIH R01DK-53069, NIH R21DK-070003, Department of Defense PR064756, and NIH G12RR-03026.

BJUI
BJU INTERNATIONAL

Amelioration of diabetes-induced cavernosal fibrosis by antioxidant and anti-transforming growth factor-β1 therapies in inducible nitric oxide synthase-deficient mice

Monica G. Ferrini*†, Joanne Moon*, Steve Rivera‡, Jacob Rajfer‡§, Nestor F. Gonzalez-Cadavid‡§

**Department of Internal Medicine, Charles R. Drew University, †Department of Medicine, David Geffen School of Medicine at UCLA, Los Angeles, CA, ‡Department of Surgery, Los Angeles Biomedical Research Institute (LABioMed) at Harbor-UCLA Medical Center, Torrance, CA, and §Department of Urology, David Geffen School of Medicine at UCLA, Los Angeles, CA, USA*

Accepted for publication 16 March 2011

Study Type – Aetiology (case control)
Level of Evidence 1b

What's known on the subject? and What does the study add?
The development of penile fibrosis in diabetes is associated with an increase in oxidative stress and the key pro-fibrotic factor. TGFβ1 within the corpora. As a consequence, a putative compensatory expression of inducible nitric oxide synthase (iNOS) cause a steady output of nitric oxide and cGMP which act as endogenous antifibrotic agents by quenching oxidative stress and inhibiting collagen synthesis and myofibroblast formation.

This study adds to the growing body of evidence that the use of antioxidant or antifibrotic therapies may be effective in preventing and possibly ameliorating penile corporal fibrosis and therefore improving erectile function in diabetes, by targeting different pathways involved in the chronic histological damage that underlies erectile dysfunction.

OBJECTIVE

- To investigate whether sustained long-term separate treatments of diabetic inducible nitric oxide synthase knockout (iNOSKo) mice with allopurinol, an antioxidant inhibiting xanthine oxidoreductase, decorin, a transforming growth factor-β1 (TGFβ1) -binding antagonist, and molsidomine, a long-life nitric oxide donor, prevent the processes of diabetes-induced cavernosal fibrosis.

MATERIALS AND METHODS

- Eight week old male iNOS knock out (iNOSKo) mice were made diabetic by injecting 150 mg/kg B.W Streptozotocin (1P) with were either left untreated or treated with the oral antioxidant allopurinol (40 mg/kg/day), or decoin (50 mg, 1P, twice), as an anti-TGFβ1 agent (n = 8/group).
- Glycemia and oxidative stress markers were determined in blood and urine.
- Paraffin-embedded tissue sections from the penile shaft were subjected to Masson trichrome staining for the smooth muscle (smc)/collagen ratio, and imunostaining for smc content, profibrotic factors, oxidative stress, cell replication and cell death markers followed by quantitative image analysis.

RESULTS

- Eight-week treatment with either allopurinol or decorin counteracted the decrease in smooth muscle cells and the increase in apoptosis and local oxidative stress within the corpora tissue.
- Decorin but not allopurinol increased the smooth muscle cell/collagen ratio, whereas allopurinol but not decorin inhibited systemic oxidative stress.
- Molsidomine was effective in reducing both local and systemic oxidative stress, but did not prevent corporal fibrosis.

CONCLUSION

- Both allopurinol and decorin appear as promising approaches either as a single or a combined pharmacological modality for protecting the diabetic corpora from undergoing apoptosis and fibrosis although their functional effects still need to be defined.

KEYWORDS

erectile dysfunction, smooth muscle, penis, collagen, nitric oxide, decorin, allopurinol, molsidomine, apoptosis

INTRODUCTION

It is well established both in human tissue and in experimental animal models that the combination of fibrosis and oxidative stress, either localized or diffuse, is the common pathophysiological denominator of the two major disorders affecting the penis, namely Peyronie's disease [1,2] and the most common form of erectile dysfunction: corporal veno-occlusive dysfunction (CVOD) [2]. In the case of CVOD this occurs in conditions as varied as aging [3,4], types 1 and 2 diabetes mellitus [5,6], cavernosal nerve damage [7–10] and certain animal models of systemic hypertension [11]. The combined production of active TGF-β1, reactive oxygen species (ROS) and other profibrotic factors stimulates the excessive deposition of collagen and extracellular matrix by fibroblasts and myofibroblasts in the tunica albuginea and corpora cavernosa in Peyronie's disease and CVOD, respectively. In CVOD, the corporal smooth muscle cells (SMC) also undergo a switch from the contractile phenotype to the synthetic phenotype, leading to deposition of extracellular matrix components. This is compounded by a loss of SMC, which leads to an impairment in the ability of the corporal tissue to undergo relaxation by the nitric oxide/cGMP pathway and the resulting passive occlusion of the subtunical veins egressing the corpora [12].

Another common denominator of both Peyronie's disease and CVOD is the steady expression of inducible nitric oxide synthase (iNOS) by different cell types leading to the sustained generation of nitric oxide and cGMP that inhibit myofibroblast generation or SMC activation and collagen synthesis [12,13]. Nitric oxide also reduces the profibrotic effects of oxidative stress by quenching ROS, stimulates collagen degradation and protects the SMC, so in this scenario iNOS induction is considered to act as an antifibrotic mechanism. This role is supported by the inhibition of oxidative stress and fibrosis by iNOS gene transfer or long-term continuous administration of nitric oxide generators and phosphodiesterase 5 inhibitors [3,8–10,14,15] or by the exacerbation of these processes by chronic inhibition of iNOS activity by *N*-iminoethyl L-lysine [9,16,17]. Moreover, the genetic inactivation of iNOS expression in the iNOS knockout (iNOSKo) mouse leads per se to an increase in fibrosis and oxidative stress within the corporal tissue and both of these are further exacerbated in the presence of diabetes [18].

Experimental approaches to ameliorate this underlying fibrotic corporal histopathology induced by either diabetes or after a cavernosal nerve injury with phosphodiesterase 5 inhibitors [19–21] still require clinical validation. To increase the efficacy of such agents, it may be necessary to combine those that target different fibrotic pathways. One of the most obvious is the use of long half-life nitric oxide generators to mimic the effects of iNOS induction, e.g. molsidomine or SIN-10, an agent currently studied clinically as a vasodilator for the treatment of coronary artery disease and angina pectoris [22–24], and experimentally for its antifibrotic effects in the kidney and liver [25–27]. These have not been investigated so far for counteracting corporal fibrosis.

A second type of agent is an antioxidant that targets xanthine oxidoreductase (XOR), a critical enzyme involved in oxidative stress in the penis. One such example is allopurinol, widely used clinically [28,29], and having a potent experimental antifibrotic action not yet explored for erectile dysfunction [30–32]. Finally, agents that aim to inactivate TGF-β signalling, such as decorin, a proteoglycan endogenously expressed in many organs, that binds several members of the TGF-β super-family is being preclinically investigated as an antifibrotic agent in wound healing and kidney, heart and skeletal muscle fibrosis [33–38] but has not yet been used for the treatment of corporal fibrosis.

The streptozotocin-induced diabetic iNOSKo mouse model, which shows the impact of diabetes on the corpora cavernosa under conditions of iNOS deprivation, i.e. an exacerbation of corporal fibrosis [18], lends itself for the investigation of antifibrotic and antioxidant compounds with the potential for the prevention or reversal of this process. In the current study, we have tested in the diabetic iNOSKo mouse the effects of the continuous long-term separate administration of allopurinol, decorin and molsidomine on corporal fibrosis, oxidative stress and SMC turnover.

MATERIALS AND METHODS

All the experiments were approved by the Institutional Animal Care and Use Committee at our institution, and according to the National Institutes of Health Guide for the Care and Use of Laboratory Animals. Four-month-old iNOSKo B6.129P2-Nos2tm1Lau/J (iNOSKo) mice were divided into the following groups and maintained for 8 weeks before being killed ($n = 8$ mice/group): (1) iNOSKo injected once i.p. with 150 mg/kg body weight streptozotocin (iNOSKo+STZ); (2) as #1 treated with 40 mg/kg/day allopurinol in the drinking water (iNOSKo +STZ+ALLO); (3) as #1 treated with 50 μg decorin per animal; i.p. twice a day (4 mg/kg/day) (iNOSKo +STZ+DECO); (4) as #1 treated with 5 mg/kg body weight molsidomine i.p. daily (iNOSKo +STZ+MOL).

Body weights were recorded weekly. Blood for glycaemia determination was withdrawn at baseline and then weekly under 3% isofluorane anaesthesia. Urine was collected from the urinary bladder under anaesthesia before killing. Mice were killed by a bolus administration of sodium pentobarbital. Blood for the determination of the ratio of reduced to oxidized glutathione (GSH/GGSG) was collected from the heart. Penises were rapidly excised, weighed and the shaft was denuded of skin, a mid-region was fixed in 10% formalin for tissue sectioning and the rest was frozen on dry ice and stored at −80 °C for further use.

Glycaemia was determined in serum by an Accu-Chek Active blood glucose meter (Roche, Indianapolis, In.), and urinary glucose, ketone bodies, specific gravity, pH, and protein were determined using a Multistix Dip Stick (Bayer, Pittsburg, Pa).

For the measurement of GSH/GSSG ratio [16], blood was collected with or without 1-methyl-2 vinylpyridinium trifluoromethane sulphonate (M2VP) scavenger of reduced glutathione, described in the commercial kit protocol ('Bioxytech GSH/GSSG-412 kit' from Oxis Health Products, Portland, Or). The omission or addition of M2VP allows the measurement of reduced (GSH) and oxidized (GSSG) glutathione, respectively. The spectrophotometric detection was recorded at 412 nm for 3 min after the addition of 3.8 μmol NADPH. The GSH/GSSG ratio is inversely related to ROS levels.

Histochemistry and immunohistochemistry investigations used paraffin-embedded tissue sections (5 μm) for the following procedures [3,4,7–10]. (a) Masson trichrome staining for collagen (blue) and SMC (red); (b) immunodetection with: monoclonal antibody against α-smooth muscle actin (ASMA) as an SMC marker (Sigma kit, Sigma Diagnostics, St Louis, MO, USA); polyclonal antibody against TGF-β1 (1 : 200) (Promega, Madison, WI, USA), as profibrotic factor; monoclonal antibody against proliferating cell nuclear antigen (PCNA) as a marker of cell proliferation (1 : 400) (Chemicon, Temecula, CA, USA); and polyclonal antibody against XOR (1 : 5000; Abcam, Cambridge, UK), as a marker of oxidative stress. The specificity of the antibodies was validated by Western blot.

Briefly, tissue sections were treated with proteinase K (20 μg/mL), followed by quenching in 0.3% H_2O_2-PBS, blocked with goat serum (Vector Laboratories, Burlingame, CA, USA), and incubated overnight at 4 °C with the primary antibody. In the case of PCNA and XOR, antigen retrieval was performed by boiling the slides for 3 min in an antigen unmasking solution (Vector Laboratories). After the overnight incubation with the first antibodies, sections were then incubated with biotinylated anti-mouse IgG (ASMA, PCNA), or biotinylated anti-rabbit IgG (TGF-β1, XOR), respectively, followed by ABC complex (Vector Laboratories) and 3,3′-diaminobenzidine (Sigma) (PCNA and iNOS), or with the ASMA Sigma kit (ASMA) and 3-amino-9-ethylcarbazole.

Terminal deoxynucleotidyl transferase dUTP nick end labelling (TUNEL) assay was performed as described previously [3,4,7–10] by applying the Apoptag peroxidase detection assay (Chemicon), with TdT enzyme and anti-digoxigenin-conjugated peroxidase, and 3,3′-diaminobenzidine/H_2O_2. Sections were counterstained with haematoxylin QS (Vector Laboratories). Negative controls in the immunohistochemical detections were performed by replacing the first antibody with IgG isotype. The negative control for TUNEL was made by substituting buffer for the TdT enzyme. Testicular tissue sections were used as positive controls for TUNEL.

Quantitative image analysis was performed by computerized densitometry using the IMAGEPRO 4.01 program (Media Cybernetics, Silver Spring, MD, USA), coupled to a Leica B microscope equipped with a Spot RT digital camera (Diagnostic Instruments, Portland OR, USA) [1–7]. For Masson staining, 40× magnification pictures of the whole penis were analysed for SMC (stained in red) and collagen (stained in blue), and expressed as SMC/collagen ratio. For ASMA and XOR staining, only the corpora cavernosa were analysed in a computerized grid and expressed as % of positive area vs total area of the corpora cavernosa. For PCNA and TUNEL determinations, the number of positive cells at 400× was counted and results were expressed as % of positive cells/total cells in the corpora cavernosa. In all cases, four penile anatomically matched tissue sections were examined per animal at 40×, with enough fields to cover the whole corpora cavernosa, and in certain cases at 400× with eight fields per section, with eight animals per group.

Values were expressed as mean ± SEM. The normality distribution of the data was established using the Wilks–Shapiro test, followed by one-way ANOVA and post-hoc comparisons with the Bonferroni test, according to the GRAPHPAD PRISM V 4.1. Differences were considered significant at $P < 0.05$.

*FIG. 1. Long-term treatment of the diabetic inducible nitric oxide synthase knockout (iNOSKo) mice with decorin (DECO) increases the corporal smooth muscle cell (SMC)/collagen ratio. Top panel: representative pictures of Masson trichrome staining. iNOSKo+STZ; streptozotocin-injected iNOSKo mouse, untreated; iNOSKo+STZ+ALLO: iNOSKo+STZ treated with allopurinol. iNOSKo+STZ+DECO: iNOSKo+STZ treated with decorin. iNOSKo+STZ+MOL: iNOSKo+STZ treated with molsidomine. Bottom panel: quantitative image analysis for the SMC/collagen ratio expressed as means ± SEM; ***P < 0.001.*

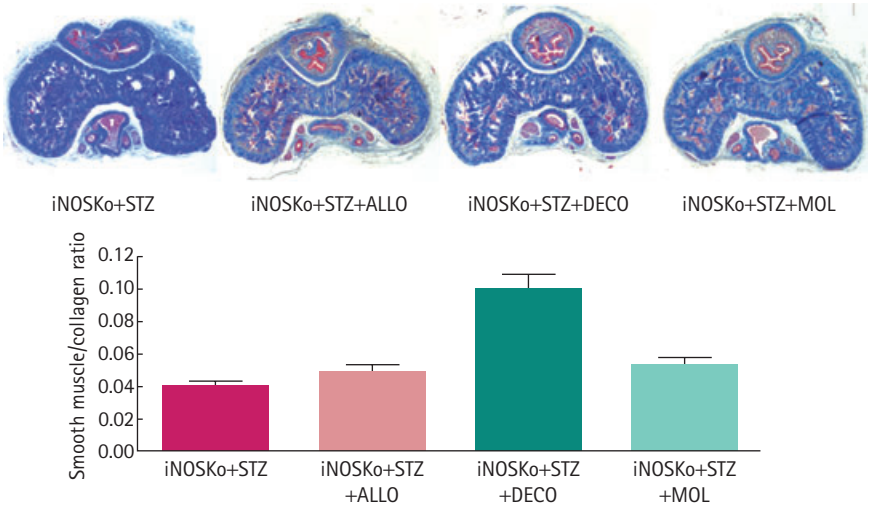

RESULTS

The effects of iNOS deletion and of diabetes induction in the streptozotocin-injected iNOSKo mice have been described previously [18]. Briefly, iNOS deletion alone causes a reduction in the corporal SMC/collagen ratio and the SMC content when compared with the normal animals (wild-type; WT). In the iNOSKo mouse that then undergoes STZ-induced diabetes, there is a further reduction in the SMC/collagen ratio which is then completely prevented by insulin in the WT mice but only partially so in the iNOSKo mice.

In the current work, as expected, 8-week treatments of this STZ-induced diabetic iNOSKo model with allopurinol, decorin and molsidomine, did not significantly affect body weight. Similarly, allopurinol and decorin did not significantly affect the streptozotocin-induced hyperglycaemia, but surprisingly in the untreated controls, molsidomine increased it to 431 ± 32 mg/dL from 354 ± 17 mg/dL ($P < 0.001$), and induced a considerable glucosuria from a basal level in the control (not shown). No ketonuria was found in any case, but the considerable proteinuria in the control (72.5 ± 33.6 mg/dL) was significantly reduced by allopurinol to 15.4 ± 5.5 mg/dL, suggesting

*FIG. 2. Long-term treatment of the diabetic inducible nitric oxide synthase knockout (iNOSKo) mice with decorin or allopurinol, increases the corporal smooth muscle cell (SMC) content. Top panel: representative pictures of α-smooth muscle actin (ASMA) immunostaining; symbols as for Fig. 1. Bottom panel: quantitative image analysis for the SMC content expressed as means ± SEM; ***P < 0.001; *P < 0.05.*

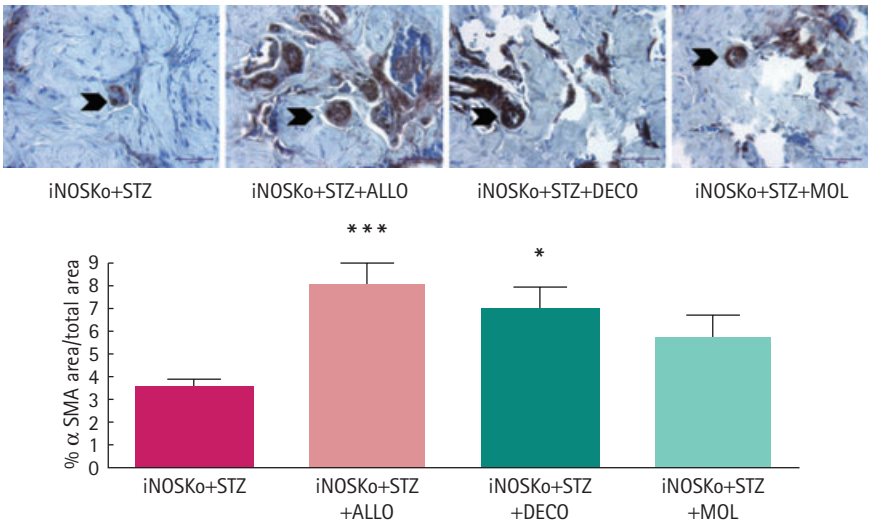

*FIG. 3. Long-term treatment of the diabetic inducible nitric oxide synthase knockout (iNOSKo) mice with decorin or allopurinol, reduces the corporal apoptotic index. Top panel: representative pictures of apoptosis by TUNEL immunostaining; symbols as for Fig. 1. Bottom panel: quantitative image analysis for the apoptotic index expressed as means ± SEM; *P < 0.05.*

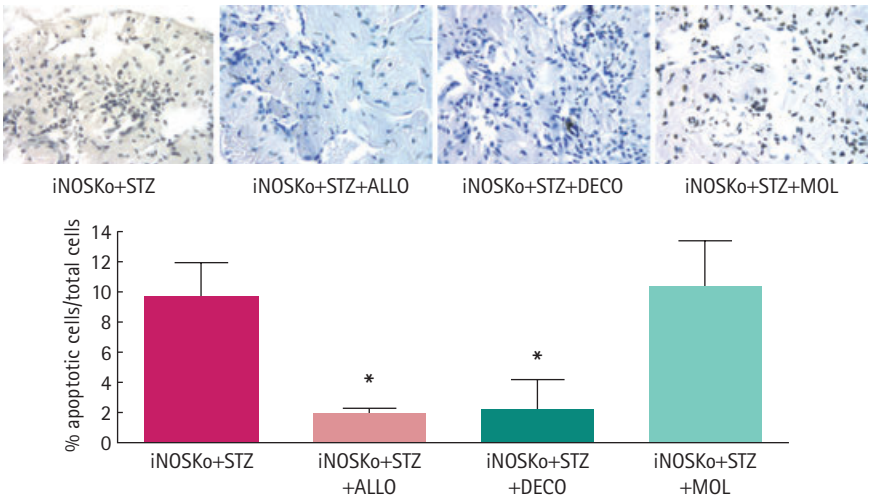

a protective effect directly on the kidney tissue independent from glycaemic control. Decorin and molsidomine did not affect proteinuria. As expected, nitrites in the urine were present in all molsidomine-treated animals

The effects of these treatments in preventing the underlying histopathology caused by diabetes and iNOS deletion in the corpora cavernosa of the iNOSKo mice were determined in paraffin-embedded corporal tissue sections. Figure 1, like the other figures, shows representative pictures for each group and bar graphs for the quantitative image analysis. Despite our initial assumption, neither allopurinol nor molsidomine affected the SMC/collagen ratio as estimated by Masson trichrome. However, decorin did increase it considerably, by 2.5-fold. In contrast, the SMC content (Fig. 2), as estimated by ASMA, was more sensitive because not only did decorin increase it by 2.0-fold but allopurinol also increased it by 2.3-fold. Although molsidomine exerted a smaller stimulation, it did not achieve statistical significance.

The protective effects of both decorin and allopurinol on the corporal SMC were reflected by a significant reduction in the apoptotic index (Fig. 3). Molsidomine did not reduce cell death (Fig. 4A). Allopurinol increased cell replication 1.5-fold whereas decorin was ineffective (Fig. 4A), but the positive cell turnovers (proliferation predominating over cell death) were increased in both cases (Fig. 4B).

The three types of treatments were uniformly effective in reducing oxidative stress in the corpora cavernosa by 46–60% as estimated by XOR (Fig. 5A). This is reflected in the expected decrease of systemic oxidative stress by allopurinol and molsidomine, represented by the nearly three-fold decrease of ROS in the blood as measured by the GSH/GSSG ratio (the higher the ratio, the lower the oxidative stress) (Fig. 5B). As expected, decorin which acts by a mechanism different from an antioxidant or a nitric oxide donor, did not reduce systemic oxidative stress.

Finally, none of the protective effects of these agents on the corporal histology seemed to be the result of a reduction in the expression of the key profibrotic factor, TGF-β1. In the case of allopurinol, *TGFB1* expression was actually stimulated 2.0-fold (not shown). The fact that decorin did not induce any significant change in *TGFB1* is as expected based on its mechanism of action of its binding to TGF-β1, and so neutralizing it, without affecting its expression.

DISCUSSION

This report is the first to compare concurrently in a mouse model of exacerbated fibrosis, the diabetic iNOSKo mouse, the potential antifibrotic, antioxidant and SMC-protective action of three pharmacological agents. They act by different mechanisms on the penile corpora cavernosa, although each one reduces

the levels of some but not all of the key profibrotic factors. Allopurinol reduces ROS and the subsequent oxidative stress through direct antioxidant activity whereas molsidomine quenches it. Decorin binds to, TGF-β1 and therefore blocks the signalling triggered by its receptor. However, although decorin and allopurinol are effective in protecting the SMC through inhibition of apoptosis, molsidomine (which theoretically should replace the effects of the absent iNOS) did not.

The critical profibrotic role of TGF-β1 expression in the diabetic iNOSKo was confirmed by the results of a long-term treatment with decorin, a small leucine-rich proteoglycan that counteracts TGF-β1 binding to its receptor and so acts as an antifibrotic agent [33–38]. The increase in the corporal SMC/collagen ratio and in SMC content while decreasing apoptosis, and the local tissue protection against oxidative stress without affecting systemic ROS, is in agreement with this mechanism. The effects of decorin have not been reported for penile tissues, other than in terms of the potentially compensatory expression of decorin observed in the human Peyronie's disease fibrotic plaque [39]. However, our results do not predict how decorin would act in a setting of normal iNOS induction, because TGF-β1 overexpression was not observed in the non-diabetic iNOSKo or in the diabetic wild-type mice in comparison with the non-diabetic wild-type animals [18]. So far, the role of TGF-β1 in corporal fibrosis induced by aging, diabetes or cavernosal damage remains elusive, in contrast to its very clear significance for Peyronie's disease [1,2], and fibrosis of other organs such as the kidney, liver and heart [33–38].

Allopurinol is perhaps the most promising agent because it was very effective in preventing corporal SMC loss in the diabetic iNOSKo mice by reducing apoptosis and oxidative stress, both systemic and local, and stimulating cell proliferation, so confirming the beneficial effects of antioxidant therapy on corporal fibrosis and erectile dysfunction in diabetes and on tissue fibrosis in general [40–42]. The lack of allopurinol effects on the corporal SMC/collagen ratio, which is in contrast to its well known effects in reducing collagen deposition in tissues such as the heart and liver [30–32], is probably related to the also unexpected increase in

*FIG. 4. Long-term treatment of inducible nitric oxide synthase knockout (iNOSKo) mice with allopurinol increases corporal cell replication and induces a positive cell turnover. (A; top panel) Representative pictures of proliferating cell nuclear antigen (PCNA) immunostaining; symbols as for Fig. 1. (A; bottom panel) Quantitative image analysis for the number of PCNA-positive cells. (B) Cell turnover determined as ratio of cell proliferation and cell death expressed as means ± SEM; *P < 0.05.*

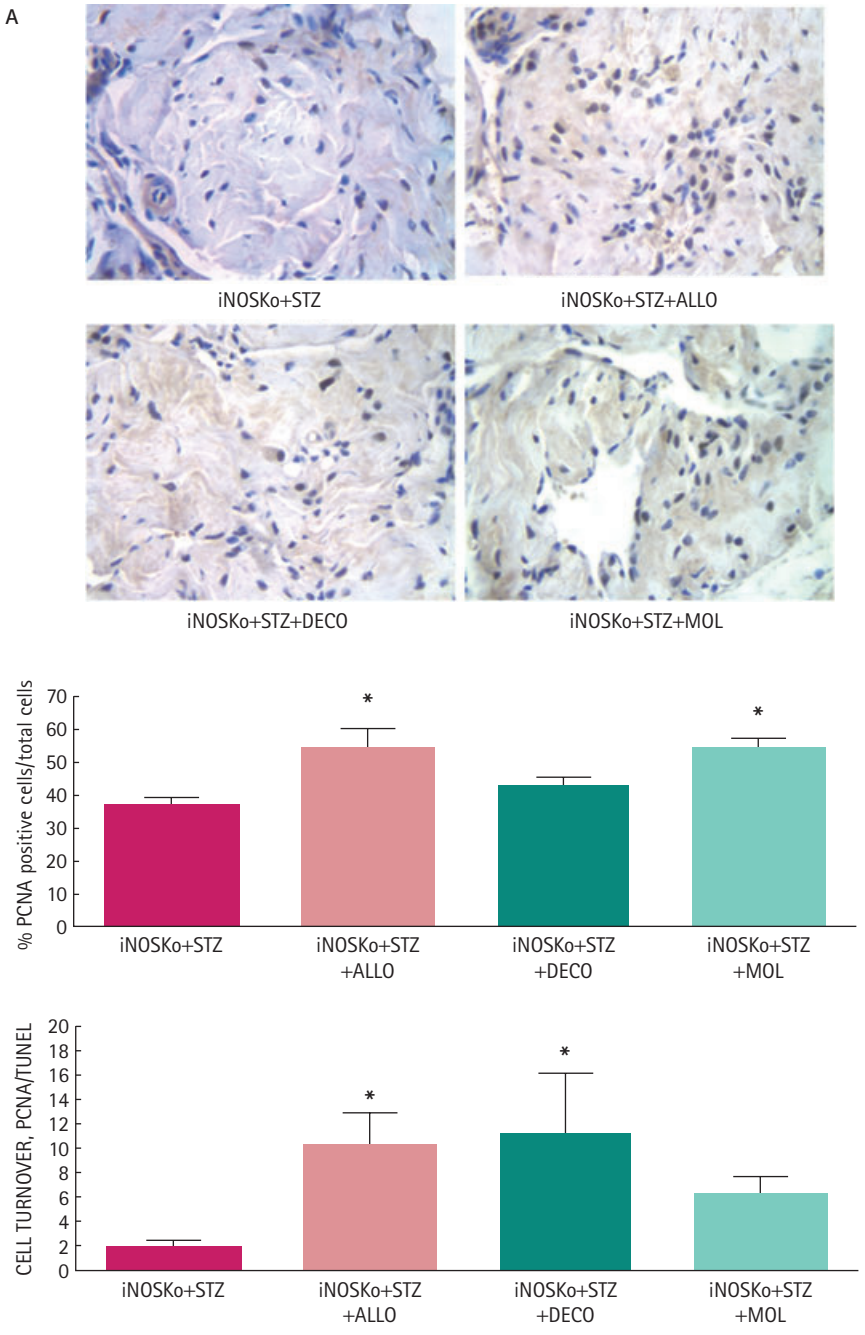

TGF-β1 expression. The systemic effects of allopurinol on ROS agree with the decrease in proteinuria that reflects an antifibrotic effect on diabetic nephropathy, previously reported for this agent, since allopurinol has been proved to be an effective antifibrotic and antioxidant in the heart and kidney [30–32]. This also confirms the pivotal role of XOR in corporal oxidative stress that has been essentially ignored in favour of NADPH oxidase [43,44], which is reflected on the absence of published reports on the effects

*FIG. 5. Long-term treatment of inducible nitric oxide synthase knockout (iNOSKo) mice with allopurinol, decorin and molsidomine reduces corporal oxidative stress and, except for decorin, decreases systemic oxidative stress. (A; top panel) Representative pictures of xanthine oxidoreductase (XOR) immunostaining; symbols as for Fig. 1. (A; bottom panel) Quantitative image analysis for the area of XOR+ staining. (B) Reduced to oxidized glutathione (GSH/GSSG) ratio in blood expressed as means ± SEM; ***P < 0.001; **P < 0.01; *P < 0.05.*

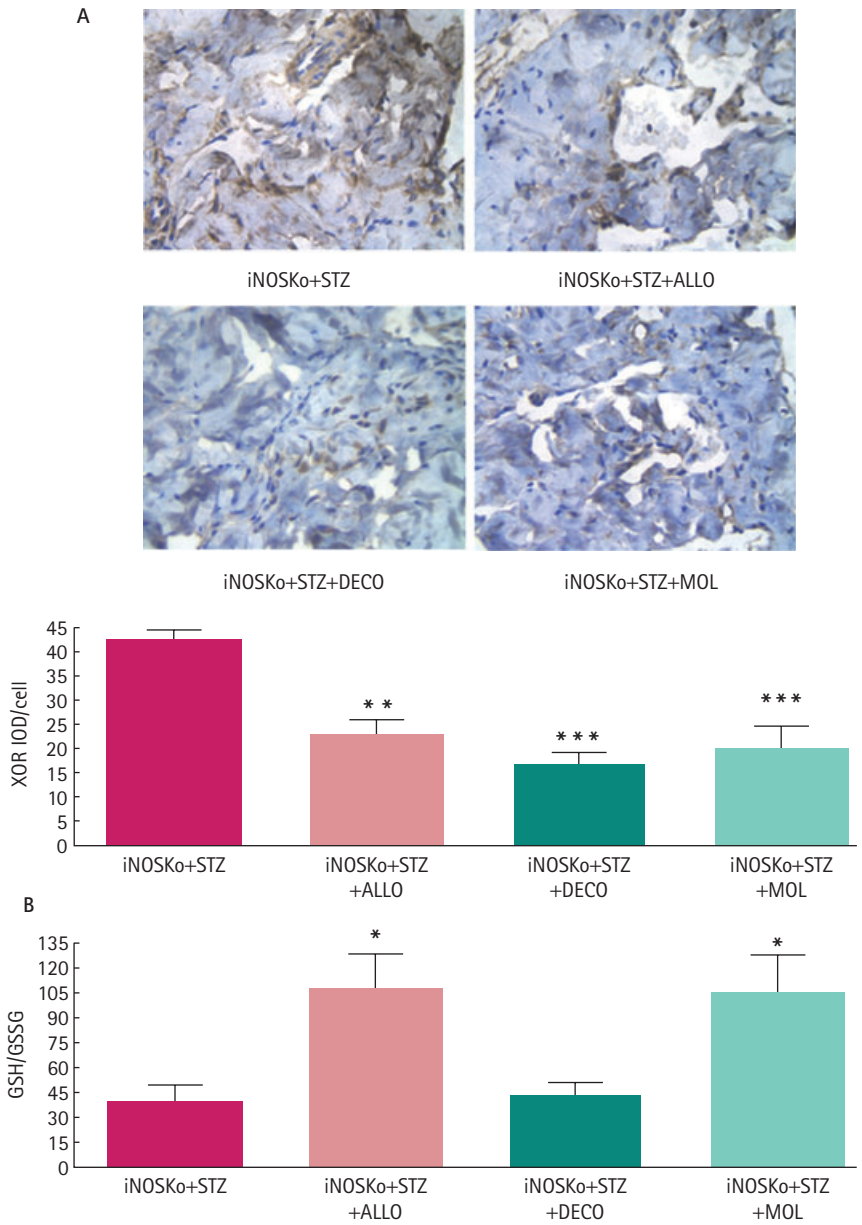

of allopurinol on erectile dysfunction or the penis. The single exception is a study that showed acute effects of allopurinol in the attenuation of ischaemia-induced and reperfusion-induced corporal injury in a rat model of veno-occlusive priapism, presumably based on the reduction of corporal lipid peroxidation [45].

Perhaps the most surprising result was the inability of the long-term administration of the long half-life exogenous nitric oxide generator, molsidomine, to affect the SMC/collagen ratio, SMC content or apoptosis, that was expected from the antifibrotic effects reported for the kidney and liver [25–27]. Linked to the vasodilating activity, but still poor efficacy of the acute administration of molsidomine or its derivative SIN-1 to induce corporal relaxation in comparison with prostaglandin E1 [46,47], this may rule out further consideration of this drug for erectile dysfunction. However, its antioxidant activity, both local and systemic, supports the view that iNOS is in fact antioxidant through a sustained production of nitric oxide in the corpora cavernosa. Nitric oxide leads to XOR downregulation in addition to ROS quenching, and is not necessarily a cause of oxidative stress because it may occur in other tissue settings. In turn, the stimulation of cell proliferation by molsidomine in the corporal tissue by nitric oxide/cGMP agrees with our previous studies [7,9,16], and again establishes an interesting divergence with the effects in general seen in the arterial wall SMC [48]. Therefore further studies may be needed to rule out any use for molsidomine for erectile dysfunction.

In summary, under conditions where the inactivation of the iNOS gene exacerbates corporal fibrosis in diabetes this histopathology is ameliorated by long-term pharmacological reduction of oxidative stress or counteracting TGF-β1, but not by simply producing nitric oxide from exogenous sources. This indicates that the use of certain antioxidant or antifibrotic agents would be effective to ameliorate corporal fibrosis and improve erectile dysfunction in diabetes, suggesting that combination therapy with some of these types of compounds, perhaps together with long-term continuous treatment with phosphodiesterase 5 inhibitors, may be beneficial by targeting different sites in the fibrosis pathways. Allopurinol, because of its long clinical use and its oral route of administration, is an interesting candidate in this respect, despite the negligible effect on corporal collagen deposition observed here. Decorin was more uniformly effective, but we are not aware of any clinical use. Further investigations in animal models are required to confirm preclinically these assumptions, particularly by measuring the penile erection response, which was not studied in the current report.

ACKNOWLEDGEMENTS

This work was funded by grants NIH 5RO1DK53069 (NGC), NIH R21DK-070003 (NGC); and DOD W81XWH-07-1-0129 (NGC).

CONFLICT OF INTEREST

None declared.

REFERENCES

1 **Gonzalez-Cadavid NF, Rajfer J.** Experimental models for Peyronie's disease. Implications for therapy. *J Sex Med* 2009; **6**: 303–13

2 **Gonzalez-Cadavid NF.** Mechanisms of penile fibrosis. *J Sex Med* 2009; **6** (Suppl. 3): 353–62

3 **Ferrini MG, Kovanecz I, Sanchez S *et al*.** Long-term continuous treatment with sildenafil ameliorates aging-related erectile dysfunction and the underlying corporal fibrosis. *Biol Reprod* 2007; **76**: 915–23

4 **Kovanecz I, Ferrini MG, Davila HH, Rajfer J, Gonzalez-Cadavid NF.** Pioglitazone ameliorates penile corpora veno-occlusive dysfunction (CVOD) in the aged rat. *BJU Int* 2007; **100**: 867–74

5 **Ahn GJ, Sohn YS, Kang KK *et al*.** The effect of PDE5 inhibition on the erectile function in streptozotocin-induced diabetic rats. *Int J Impot Res* 2005; **17**: 134–41. Erratum in: Int J Impot Res 2006; 18: 576

6 **Kovanecz I, Ferrini MG, Vernet D, Nolazco G, Rajfer J, Gonzalez-Cadavid NF.** Pioglitazone prevents corporal veno-occlusive dysfunction (CVOD) in a rat model of type 2 diabetes melittus. *BJU Int* 2006; **98**: 116–24

7 **Ferrini MG, Kovanecz I, Sanchez S *et al*.** Fibrosis and loss of smooth muscle in the corpora cavernosa precede corporal veno-occlusive dysfunction (CVOD) induced by experimental cavernosal nerve damage in the rat. *J Sex Med* 2009; **6**: 415–28

8 **Kovanecz I, Rambhatla A, Ferrini MG *et al*.** Chronic daily tadalafil prevents the corporal fibrosis and veno-occlusive dysfunction (CVOD) that occurs following cavernosal nerve resection in the rat. *BJU Int* 2008; **101**: 203–10

9 **Kovanecz I, Rambhatla A, Ferrini MG *et al*.** Long term sildenafil treatment ameliorates corporal veno-occlusive dysfunction (CVOD) induced by cavernosal nerve resection in rats. *Int J Impot Res* 2007; **100**: 867–74

10 **Ferrini MG, Davila H, Kovanecz I, Sanchez S, Gonzalez-Cadavid NF Rajfer J.** Long-term continuous treatment with vardenafil prevents fibrosis and preserves smooth muscle content in the rat corpora cavernosa after bilateral cavernosal nerve transection. *Urology* 2006; **68**: 429–35

11 **Jiang R, Chen JH, Jin J, Shen W, Li QM.** Ultrastructural comparison of penile cavernous tissue between hypertensive and normotensive rats. *Int J Impot Res* 2005; **17**: 417–23

12 **Davila HH, Rajfer J, Gonzalez-Cadavid NF.** Corporal veno-occlusive dysfunction in aging rats: evaluation by cavernosometry and cavernosography. *Urology* 2004; **64**: 1261–6

13 **Gonzalez-Cadavid NF, Rajfer J.** The pleiotropic effects of inducible nitric oxide synthase on the physiology and pathology of penile erection. *Curr Pharm Des* 2005; **11**: 4041–6

14 **Davila HH, Magee TR, Rajfer J, Gonzalez-Cadavid NF.** Gene therapy with the inducible nitric oxide synthase (iNOS) cDNA regresses the fibrotic plaque in an animal model of Peyronie's disease. *Biol Reprod* 2004; **71**: 1568–77

15 **Vernet D, Ferrini MG, Valente E *et al*.** Effect of nitric oxide on the differentiation of fibroblasts into myofibroblasts in the Peyronie's fibrotic plaque and in its rat model. *Nitric Oxide* 2002; **7**: 262–76

16 **Ferrini MG, Davila H, Valente EG.** Gonzalez-Cadavid NF*, Rajfer J*, *equal contributors) Aging-related induction of inducible nitric oxide synthase (iNOS) is vasculo-protective in the arterial media. *Cardiovasc Res* 2004; **61**: 796–805

17 **Ferrini MG, Vernet D, Magee TR *et al*.** Antifibrotic role of inducible nitric oxide synthase (iNOS). *Nitric Oxide* 2002; **6**: 283–94

18 **Ferrini MG, Rivera S, Moon J, Vernet D, Rajfer J, Gonzalez-Cadavid NF.** The Genetic Inactivation of Inducible Nitric Oxide Synthase (iNOS) Intensifies Fibrosis and Oxidative Stress in the Penile Corpora Cavernosa in Type 1 Diabetes. *J Sex Med* 2010; **7**: 3033–44

19 **Rambhatla A, Kovanecz I, Ferrini M, Gonzalez-Cadavid NF, Rajfer J.** Rationale for phosphodiesterase 5 inhibitor use post-radical prostatectomy: experimental and clinical review. *Int J Impot Res* 2008; **20**: 30–4

20 **Magheli A, Burnett AL.** Erectile dysfunction following prostatectomy: prevention and treatment. Nat. *Rev Urol* 2009; **6**: 415–27

21 **Mulhall JP.** Penile rehabilitation following radical prostatectomy. *Curr Opin Urol* 2008; **18**: 613–20

22 **Messin R, Dubois C, Famaey JP.** Comparative effects of once-daily molsidomine in coronary patients from two distinct European ethnicities. *Adv Ther* 2008; **25**: 1200–14

23 **Banasiak W, Wilkins A, Pociupany R, Ponikowski P.** Pharmacotherapy in patients with stable coronary artery disease treated on an outpatient basis in Poland. Results of the multicentre RECENT study. *Kardiol Pol* 2008; **66**: 642–9

24 **Messin R, Cerreer-Bruhwyler F, Dubois C, Famaey JP, Géczy J.** Efficacy and safety of once- and twice-daily formulations of molsidomine in patients with stable angina pectoris: double-blind and open-label studies. *Adv Ther* 2006; **23**: 107–30

25 **Oztürk H, Ya mur Y, Buyukbayram H, Dokucu AI, Gurel A.** Effects of the nitric oxide donor molsidomine on the early stages of liver damage in rats with bile duct ligation: a biochemical and immunohistochemical approach. *Eur Surg Res* 2002; **34**: 285–90

26 **Benigni A, Zoja C, Noris M *et al*.** Renoprotection by nitric oxide donor and lisinopril in the remnant kidney model. *Am J Kidney Dis* 1999; **33**: 746–53

27 **Peters H, Daig U, Martini S *et al*.** NO mediates antifibrotic actions of L-arginine supplementation following induction of anti-thy1 glomerulonephritis. *Kidney Int* 2003; **64**: 509–18

28 **McGill NW.** Management of gout: beyond allopurinol. *Intern Med J* 2010; **40**: 545–53

29 **Tsai TF, Yeh TY.** Allopurinol in dermatology. *Am J Clin Dermatol* 2010; **11**: 225–32

30 **Jia N, Dong P, Ye Y, Qian C, Dai Q.** Allopurinol Attenuates Oxidative Stress and Cardiac Fibrosis in Angiotensin II-Induced Cardiac Diastolic Dysfunction. *Cardiovasc Ther* 2011; **29**: no. doi: 10.1111/j.1755-5922.2010.00243.x

31 **Rajesh M, Mukhopadhyay P, Bátkai S *et al*.** Xanthine oxidase inhibitor allopurinol attenuates the development of diabetic cardiomyopathy. *J Cell Mol Med* 2009; **13**: 2330–41

32 **Hayashi K, Kimata H, Obata K *et al*.** Xanthine oxidase inhibition improves left

ventricular dysfunction in dilated cardiomyopathic hamsters. *J Card Fail* 2008; **14**: 238–44
33 **Järvinen TA, Ruoslahti E.** Target-seeking antifibrotic compound enhances wound healing and suppresses scar formation in mice. *Proc Natl Acad Sci USA* 2010; **107**: 21671–6
34 **Mohan RR, Gupta R, Mehan MK, Cowden JW, Sinha S.** Decorin transfection suppresses profibrogenic genes and myofibroblast formation in human corneal fibroblasts. *Exp Eye Res* 2010; **91**: 238–45
35 **Zhang Z, Wu F, Zheng F, Li H.** Adenovirus-mediated decorin gene transfection has therapeutic effects in a streptozocin-induced diabetic rat model. *Nephron Exp Nephrol* 2010; **116**: e11–21
36 **Faust SM, Lu G, Wood SC, Bishop DK.** TGFbeta neutralization within cardiac allografts by decorin gene transfer attenuates chronic rejection. *J Immunol* 2009; **183**: 7307–13
37 **Yan W, Wang P, Zhao CX, Tang J, Xiao X, Wang DW.** Decorin gene delivery inhibits cardiac fibrosis in spontaneously hypertensive rats by modulation of transforming growth factor-beta/Smad and p38 mitogen-activated protein kinase signaling pathways. *Hum Gene Ther* 2009; **20**: 1190–200
38 **Li Y, Li J, Zhu J *et al*.** Decorin gene transfer promotes muscle cell differentiation and muscle regeneration. *Mol Ther* 2007; **15**: 1616–22
39 **Qian A, Meals R, Rajfer J, Gonzalez-Cadavid NF.** Comparison of gene expression profiles between Peyronie's disease and Dupuytren's contracture. *Urology* 2004; **64**: 399–404
40 **Vicari E, La Vignera S, Condorelli R, Calogero AE.** Endothelial Antioxidant Administration Ameliorates the Erectile Response to PDE5 Regardless of the Extension of the Atherosclerotic Process. *J Sex Med* 2010; **7**: 1247–53
41 **Villalba N, Martínez P, Bríones AM *et al*.** Differential structural and functional changes in penile and coronary arteries from obese Zucker rats. *Am J Physiol Heart Circ Physiol* 2009; **297**: H696–707
42 **Shukla N, Hotston M, Persad R, Angelini GD, Jeremy JY.** The administration of folic acid improves erectile function and reduces intracavernosal oxidative stress in the diabetic rabbit. *BJU Int* 2009; **103**: 98–103
43 **Tziomalos K, Hare JM.** Role of xanthine oxidoreductase in cardiac nitroso-redox imbalance. *Front Biosci* 2009; **14**: 237–62
44 **Jeremy JY, Jones RA, Koupparis AJ *et al*.** Reactive oxygen species and erectile dysfunction: possible role of NADPH oxidase. *Int J Impot Res* 2007; **19**: 265–80
45 **Evliyaoglu Y, Kayrin L, Kaya B.** Effect of allopurinol on lipid peroxidation induced in corporeal tissue by veno-occlusive priapism in a rat model. *Br J Urol* 1997; **80**: 476–9
46 **Sazova O, Kadio lu A, Gürkan L *et al*.** Intracavernous administration of SIN-1+VIP in an in vivo rabbit model for erectile function. *Int J Impot Res* 2002; **14**: 44–9
47 **von Heyden B, Brock GB, Martinez-Piñeiro L, Lue TF.** Intracavernous injection of linsidomine chlorhydrate in monkeys: lack of toxic effect with long-term use. *Eur Urol* 1996; **30**: 502–5
48 **Ahanchi SS, Tsihlis ND, Kibbe MR.** The role of nitric oxide in the pathophysiology of intimal hyperplasia. *J Vasc Surg* 2007; **45** (Suppl. A): A64–73

Correspondence: Monica Ferrini, Department of Internal Medicine, Charles Drew University (CDU), Los Angeles, CA 90059, USA.
e-mail: monicaferrini@cdrewu.edu

Abbreviations: **ALLO**, allopurinol; **ASMA**, α-smooth muscle actin; **CVOD**, corporal veno-occlusive dysfunction; **DECO**, decorin; **GSH/GSSG**, reactive glutathione/oxidized glutathione; **iNOS**, NOS II, inducible nitric oxide synthase; **iNOSKo**, iNOS knockout mouse; **PCNA**, proliferating cell nuclear antigen; **ROS**, reactive oxygen species; **SMC**, smooth muscle cells; **STZ**, streptozotocin; **TUNEL**, terminal deoxynucleotidyl transferase dUTP nick end labelling; **XOR**, xanthine oxidoreductase.

Effects of sildenafil and/or muscle derived stem cells on myocardial infarction

Judy S-C Wang[1], Istvan Kovanecz[1,3], Dolores Vernet[1,2], Gaby Nolazco[1,2], George E Kopchok[1], Sheryl L Chow[4], Rodney A White[1], Nestor F Gonzalez-Cadavid[1-3]*

[1]Department of Surgery, Los Angeles Biomedical Research Institute (LABioMed) at Harbor-UCLA Medical Center, Torrance, CA, USA

[2]Department of Internal Medicine, Charles Drew University, Los Angeles, CA, USA

[3]Department of Urology, David Geffen School of Medicine at UCLA, Los Angeles, CA, USA

[4]Western University, Pomona, CA, USA

***Corresponding author**

Email addresses:

JSCW: swang@ucla.edu

IK: ikovanecz@labiomed.org

DV: dovernet@aol.com

GN: gnolazco@labiomed.org

GEK: gkopchok@labiomed.org

SLC: SChow@westernu.edu

RAW: rawhite@ucla.edu

NFGC: ncadavid@ucla.edu

Abstract

Background: Previous studies have shown that long-term oral daily PDE 5 inhibitors (PDE5i) counteract fibrosis, cell loss, and the resulting dysfunction in tissues of various rat organs and that implantation of skeletal muscle-derived stem cells (MDSC) exerts some of these effects. PDE5i and stem cells in combination were found to be more effective in non-MI cardiac repair than each treatment separately. We have now investigated whether sildenafil at lower doses and MDSC, alone or in combination are effective to attenuate LV remodeling after MI in rats.

Methods: MI was induced in rats by ligature of the left anterior descending coronary artery. Treatment groups were: "Series A": 1) untreated; 2) oral sildenafil 3 mg/kg/day from day 1; and "Series B": intracardiac injection at day 7 of: 3) saline; 4) rat MDSC (10^6 cells); 5) as #4, with sildenafil as in #2. Before surgery, and at 1 and 4 weeks, the left ventricle ejection fraction **(LVEF)** was measured. LV sections were stained for collagen**,** myofibroblasts, apoptosis, cardiomyocytes, and iNOS, followed by quantitative image analysis**.** Western blots estimated angiogenesis and myofibroblast accumulation, as well as potential sildenafil tachyphylaxis by PDE 5 expression. Zymography estimated MMPs 2 and 9 in serum.

Results: As compared to untreated MI rats, sildenafil improved LVEF, reduced collagen, myofibroblasts, and circulating MMPs, and increased cardiac troponin T. MDSC replicated most of these effects and stimulated cardiac angiogenesis. Concurrent MDSC/sildenafil counteracted cardiomyocyte and endothelial cells loss, but did not improve LVEF or angiogenesis, and increased myofibroblasts and upregulated PDE 5.

Conclusions: Long-term oral sildenafil, or MDSC given separately, reduce the MI fibrotic scar and improve left ventricular function in this rat model. The failure of the treatment combination

may be due to inducing overexpression of PDE5 and some MDSC differentiation into myofibroblasts.

Keywords: stem cells, myocardial infarction, heart failure, PDE5 inhibitors, fibrosis

Background

Cardiac fibrosis is a major factor of tissue remodeling during myocardial infarction (MI) recovery, heart failure, ischemia reperfusion injury, and in most cardiomyopathies [1]. The excessive extracellular matrix, together with the activated fibroblasts and particularly myofibroblasts responsible for its deposition during tissue remodeling, impair the contractile function of the surviving cardiomyocytes. Fibrosis may even affect the normal ECM/fibroblast interaction in force networking around myocytes and putative electrical coupling of both cell types. The etiology, molecular/cellular pathology, progression, and impact on contractile tissue compliance of cardiac tissue fibrosis, resemble the fibrosis occurring in the arterial bed wall [2,3] and in vascular tissues such as the kidney, skeletal muscle, urogenital organs [4-6], and others, except for the cells that are affected and the functional outcomes.

The current conventional therapy of MI, the modulators of the renin-angiotensin-aldosterone system (RAAS), counteracts fibrosis induced by angiotensin II in parallel to other beneficial effects [7]. A novel antifibrotic and cardiomyocyte protective therapy complementing hemodynamic effects is emerging, i.e., the long-term continuous use of phosphodiesterase 5 inhibitors (PDE5i) [8,9], based initially on the cardiac preconditioning exerted by nitric oxide and its main effector cGMP, presumably through inducible nitric oxide synthase (iNOS) [10,11].

A recent study showed that the PDE 5 inhibitor sildenafil given intraperitoneally daily for 4 weeks after permanent left anterior descending (LAD) coronary artery ligation attenuated the increase in left ventricular end-diastolic diameter in the mouse, and improved fractional shortening, overall survival, infarct size, and apoptotic index [12]. The induction of eNOS and iNOS and reduction of apoptosis by this sildenafil treatment mediated by cGMP-dependent protein kinase (PKG) was abrogated in isolated mouse hearts by the inhibition of ERK phosphorylation [13].

Other studies demonstrated that sildenafil blunted interstitial cardiac fibrosis in MI in the rat [14], that the long-term sildenafil or vardenafil regimen exerted similar effects after ischemia reperfusion injury in rabbits [15], and that tadalafil, a long acting PDE 5 inhibitor, improved left ventricular function and survival during doxorubicin-induced cardiotoxicity [16]. However, it is difficult to compare most ischemia/reperfusion studies, performed with single bolus treatment that exerts transient vasodilation, with chronic treatments modifying the underlying cardiac histopathology. For instance, sildenafil in rats reduced infarct size at 24 hrs and cardiomyocyte/endothelial apoptosis while increasing fractional shortening and ejection fraction at 45 days [17]. The same acute treatment in ischemia reperfusion/injury was applied with tadalafil in mice and rats [18,19].

However, despite sildenafil is an approved treatment for pulmonary hypertension in humans, some results with PDE 5 inhibitors in animal models are inconsistent, apparently dependent on the degree of experimental cardiac stress and remodeling [20].

The antifibrotic effects of chronic treatment with PDE5i that may occur on experimental left ventricle remodeling after MI, resembling the process in non cardiac tissues. Long-term, daily treatment with any one of the three PDE 5 inhibitors, as opposed to sporadic administration

to induce penile corporal vasorelaxation and thus erection, prevents and even reverses corporal fibrosis in rat models of vasculogenic erectile dysfunction, a sentinel of cardiovascular disease [21-23]. Clinical application of this chronic PDE 5 inhibitor modality is being considered [24]. The antifibrotic action of PDE 5 inhibitors also operates in rat models of bleomycin-induced pulmonary vascular fibrosis [25], diabetic nephropathy [26], and the Peyronie's fibrotic plaque [27].

PDE5i may be concurrently administered with stem cells to increase the efficacy of adult stem cell therapy for MI [28]. The combination of sildenafil and adipocyte derived stem cells implanted into the left ventricle of rats with dilated cardiomyopathy increased LVEF and angiogenesis while decreasing cardiac oxidative stress, apoptosis and fibrosis, as compared to the stem cells alone [29]. In vitro pre-conditioning of the same stem cells by sildenafil improved their cardiac repair efficacy in mice with MI [30]. It is possible that PDE5i modulate, through cGMP and PKG, stem cell lineage commitment towards cardiomyocytes [31,32].

Mouse and human skeletal muscle derived stem cells (MDSC) induce angiogenesis, reduce scar formation, and improve LVEF, mainly through VEGF expression, in mouse models of MI [33-35]. In rat models of MI, MDSC were therapeutically superior to myoblasts and comparable to bone marrow stem cells, although it is unclear whether MDSC convert into cardiomyocytes [36]. Skeletal myoblasts have a controversial experimental and clinical efficacy, whereas MDSC by being truly pluripotent, and non-myogenically committed cells, are more promising. However, there are no reports on PDE5i modulation of MDSC.

In this study we aimed to investigate whether: a) chronic daily treatment with oral sildenafil at low dose in rats subjected to MI by permanent ligature of the LAD coronary artery improves LVEF, and reduces collagen deposition, myofibroblast accumulation, and loss of

cardiomyocytes in the left ventricle; b) intracardiac implantation of MDSC affects similarly cardiac function and remodeling, and sildenafil stimulates these effects.

Methods

Ethics

The investigation conforms to the Guide for the Care and Use of Laboratory Animals published by the US National Institutes of Health (NIH Publication No. 85-23, National Academy Press, Washington, DC, USA, revised 1996) and was approved by the IACUC at LABioMed.

Animal procedures

Male Fisher 344 rats were either 3-4 months old (MDSC isolation), or retired breeders (MI treatments), from Harlan Sprague-Dawley Inc., San Diego, CA, USA under aseptic conditions were anesthetized with isoflurane, intubated, and ventilated to perform a left thoracotomy to expose the heart. MI was induced by permanent ligation of the LAD coronary artery, about 2 mm from the tip of the left auricle, using a 6/0 polypropylene suture (Ethicon, Inc). The chest, muscle, and skin were closed with standard procedures. Rats were allowed to recover from anesthesia, subjected to procedures below and then sacrificed at 4 weeks. Mortality during surgery or for the following 2-3 days was about 30%, and only a couple of deaths occurred thereafter. Replacement rats were added to the study as deaths occurred, so the desired final n=7-8/group was maintained, unless specified.

Rats (final n=8/group) were randomly divided into five groups: series A: untreated control (group 1); sildenafil (3 mg/kg/day) in the drinking water from day 1 (group 2); series B: aseptic intracardiac injection into the penumbra at day 7, by repeating surgery to expose the

heart, of: 0.1 ml saline (group 3); rat MDSC (10^6 cells in 0.1 ml saline) labeled with the nuclear fluorescent stain 4',6-diamidino-2-phenylindole (DAPI) (group 4); MDSC as group #4, complemented with sildenafil given from day 7 as group #2 (group 5) (Figure 1)

Left ventricular ejection fraction (LVEF) was measured at three stages: a) basal (before surgery); b) 1 week after surgery; and c) before sacrifice, at 4 weeks. Anesthetized animals in the supine or lateral decubitus position were subjected to 2D and M-mode echocardiography (15-MHz linear-array transducer system) under acoustic coupling gel.

MDSC isolation and culture

MDSC were prepared from the hind limb muscles from the rat [33-36], using the preplating procedure, a validated standardized method for MDSC isolation [37], as in our previous reports [38-40]. Tissues were dissociated using sequentially collagenase XI, dispase II and trypsin, and after filtration through 60 nylon mesh and pelleting, the cells were suspended in Dulbecco's Modified Eagle's Medium (DMEM) with 20% fetal bovine serum. Cells were plated onto collagen I-coated flasks for 1 hr (preplate 1 or pP1), and 2 hrs (preplate 2 for pP2), followed by sequential daily transfers of non-adherent cells and re-platings for 2 to 6 days, until preplate 6 (pP6). The latter is the cell population containing MDSC. Cells were then selected using magnetic beads coated with the Sca 1 antibody. Cells were replicated on regular culture flasks (no coating) and used in the 5^{th}-10^{th} passage, since the mouse counterparts have been maintained in our laboratory for at least 40 passages with the same, or even increasing, growth rate**.** Flow cytometry was performed to determine whether they were Sca 1+/CD34+/CD44+/Oct 4 cells [40].

Detection and estimation in tissue sections

At 4 weeks, blood was extracted from anesthetized rats and the animals were sacrificed. The right ventricle and great vessels were trimmed from the heart and the left ventricles were sliced transversally from apex to base into 4 similar height slices numbered from 1 through 4. Slices #2 contained the infarction area and site of MDSC injection and its top ½ region was cryoprotected, embedded in OCT, and used for cryosectioning around the site of cell implantation. The remainder was fixed in 10% formaldehyde fixation for paraffin embedding. In both cases, transverse sections were obtained from apex to base (8 μm). The other left ventricular slices were frozen in liquid nitrogen and stored at -80°C.

The MI area was determined by staining frozen sections with Picro Sirius red, using computerized planimetry for the calculation of the % of infarcted left ventricle [17]. Immunohistochemistry in paraffin-embedded sections was performed [17,28,38-40] for: a) myofibroblasts by α-smooth muscle actin (ASMA) with anti human mouse monoclonal in Sigma kit, 1:2 (Sigma Chemical, St Louis, MO, USA)**;** b) apoptotic index by the TUNEL reaction with the Apoptag kit (Millipore, Billerica, MA, USA); and c) rabbit polyclonal anti-iNOS (Calbiochem/EMD, Brookfield, WI, USA). Cardiomyocyte loss was estimated with a monoclonal antibody against Troponin T-C (Santa Cruz Biotechnology, Santa Cruz, CA, USA)**.** The primary antibodies were detected by the biotinylated anti-mouse IgG (Vector Laboratories, Burlingame, CA, USA), the ABC complex containing avidin-linked horseradish peroxidase (1:100; Vector Laboratories), and 3,3' diaminobenzidine, and counterstaining with hematoxylin. For detecting the implanted DAPI-labeled MDSC, frozen sections were stained for Troponin T, but following with a biotinylated secondary anti-mouse IgG antibody (goat, 1:200, Vector Laboratories) and streptavidin-Texas Red.

The sections were viewed under an Olympus BH2 fluorescent microscope, and quantitative image analysis was performed with ImagePro-Plus 5.1 software (Media Cybernetics, Silver Spring, MD, USA) coupled to a Leica digital bright field/fluorescence microscope/VCC video camera. After images were calibrated for background lighting, integrated optical density (IOD=area x average intensity) was calculated. 6-7 fields were measured per tissue section, with 3-4 sections per specimen, and 8 specimens per group.

Protein detection and estimations in tissue homogenates

Homogenates from left ventricular region #3 below the infarcted area were obtained in boiling lysis buffer (1% SDS, 1mM sodium orthovanadate, 10 mM Tris pH 7.4 and protease inhibitors), and centrifuging at 16,000 *g* for 5 min [38-40]. 5-30 µg of protein were run on 4-15% polyacrylamide gels, and submitted to transfer and immunodetection with the antibodies against Troponin T as above, and the additional ones: calponin, mouse monoclonal (Santa Cruz); ASMA, mouse monoclonal (Calbiochem, EMD, San Diego, CA, USA); Von Willebrand factor, rabbit polyclonal (Abcam Inc, Cambridge, MA); PDE5, rabbit polyclonal (Calbiochem); GAPDH, mouse monoclonal (Chemicon, Temecula, CA, USA). Membranes were incubated with secondary polyclonal horse anti-mouse or anti-rabbit IgG linked to horseradish peroxidase (1:2000; BD Transduction Laboratories, Franklin Lakes, NJ, or 1:5000, Amersham GE, Pittsburgh, PA, USA) and bands were visualized with luminol (SuperSignal West Pico, Chemiluminescent, Pierce, Rockford, IL, USA). Quantitative estimation was performed by densitometry, establishing the ratio between the band intensities of each protein against the reference GAPDH value.

Zymography for MMPs

A serum dilution (5 µg protein) was mixed with equal volumes of zymography sample buffer (125 mM Tris-HCl, pH 6.8, 50% glycerol, 8% SDS, 0.02% bromophenol blue), loaded onto 10% polyacrylamide zymogram gels containing gelatin or casein (BioRad), and electrophoresed with 2.5 mM Tris-HCl, 19.2 mM glycine, 0.01% SDS, pH 8.3, at 100 V [41]. The gels were then equilibrated for 30 min at room temperature with renaturing buffer (2.5% Triton). Zymograms were developed overnight at 37° C in developing buffer, 50 mM Tris-HCl, pH 7.5, 200 mM NaCl, 5 mM $CaCl_2$, 0.02% Brij-35. Gels were stained with 0.5% Coomassie Blue for 1 hr, destained with methanol/glacial acetic acid/water (50:10:40), rehydrated in the 5:7:88 mix, and dried. Areas of MMP activity appeared as clear bands. Zymograms intensities were analyzed using NIH Image J.

Drugs

The following drugs were used: buprenorphine (Reckitt &Colman Products, England) and carprofen (Pfizer, USA) for postoperative pain relief; and sildenafil (Pfizer, USA) dissolved in the drinking water [21-23].

Statistical analysis

All results are expressed as mean ± standard error of the mean (SEM). The normality distribution of the data was established using the Wilk–Shapiro test. Multiple comparisons were analyzed by a single factor ANOVA, followed by Newman–Keuls multiple comparison test. Differences among groups were considered statistically significant at $P < 0.05$.

Results

Effects of chronic sildenafil

We first tested the effects of sildenafil on MI in the rat, at a 3 mg/kg/day given in the drinking water. Figure 2 top shows that this dose moderately (30%) improved the LVEF over the one in the untreated rats (36.6 ± 3.5 vs. 47.8 ± 4.1), and reduced to the same extent the infarction size measured at 4 weeks by quantitative immunohistochemistry for collagen fibers with Picro Sirius red (16.4 ± 0.66 vs. 11.32 ± 1.07), in a region corresponding to the area mainly affected by the LAD occlusion (region #2) (Figure 2 bottom).

The antifibrotic effects of this dose of sildenafil in the rat were confirmed by the considerable 73% reduction of myofibroblasts (13.8 ± 1.5 vs. 3.9 ± 0.4), in the same left ventricular region denoted by ASMA immunostaining (Figure 3 top). iNOS was expressed in this region, as it occurs in most fibrotic processes, but its levels remained unchanged after sildenafil treatment (not shown). There was a non-significant increase by sildenafil on the troponin T content in the same region of the left ventricle (604 ± 152 vs. 979 ± 372), (Figure 3 bottom).

Effects of MDSC implantation, alone or in combination with sildenafil

The intracardiac implantation of homologous (rat) MDSC into the infarcted heart, one week after LAD, improved considerably (50%) LVEF over the value in the saline injected rats (34.6 ± 3.8 vs. 51.9 ± 9.1), (Figure 4 top). However, contrary to expectations, the combination of this treatment with sildenafil at the time of MDSC implantation abrogated the beneficial effects of the cell therapy against the same control (32.6 ± 4.2). This was paralleled by the contrast between a 34% reduction in collagen deposition in the infarcted area in the region around cell implantation exerted by MDSC (15.2 ± 1.7 vs. 9.9 ± 0.7), and the essential disappearance against the same control of this beneficial effect when sildenafil was given concurrently (13.2 ± 1.6), (Figure 4 bottom).

The DAPI-labeled nuclei of the implanted MDSC persisted after 4 weeks in the infarction region and were mostly from cells engrafted in the interstitial connective tissue. A few appeared to overlap the cardiomyocytes identified by troponin T immunofluorescence staining, but this is insufficient to ascertain whether MDSC converted into cardiomyocytes (Figure 5 top). There was a non-significant increase in troponin T in the left ventricle by MDSC, and a higher (30%) and significant increase by the combination of MDSC and sildenafil, as measured by quantitative immunohistochemistry in comparison to the saline injected control (347 ± 99 and 474 ± 27 vs. 227 ± 24) (Figure 5 middle). Matching this cardiomyocyte protection, the apoptotic index was reduced by MDSC by 49% and to virtually negligible levels by the combination with sildenafil (2.5 ± 0.2 and 0.2 ± 0.1 vs. 4.9 ± 0.2) (Figure 5 bottom).

The modest increase in troponin seen in the infarction area (region #2) by the treatment with MDSC or MDSC + sildenafil was accompanied by an approximately 25% increase in the expression of the 41 kDa troponin band estimated by western blot in the adjacent non infarcted region closer to the base (1.6 ± 0.2 and 1.5 ± 0.2 vs. 1.3 ± 0.1), (#3) but the change was non-significant (Figure 6). In contrast, there was a significant increase by MDSC of the smooth muscle cells (SMC) (1.0 ± 0.1 vs. 0.35 ± 0.1), and endothelial cells (0.9 ± 0.1 vs. 0.8 ± 0.1), represented respectively by calponin and von Willebrand proteins, as an indication of angiogenesis (Figure 6). Although MDSC + sildenafil treatment increased endothelial content, it did not affect calponin. In turn, ASMA expression, a marker of myofibroblasts also shared by SMC was not affected by MDSC (1.0 ± 0.2 vs. 1.0 ± 0.2), thus suggesting that the myofibroblasts and fibrosis were reduced, since part of this expression is due to the increased SMC shown by calponin which is not present in myofibroblasts. Sildenafil supplementation not

only abrogated this antifibrotic effect of the MDSC but actually increased ASMA expression in comparison to the control (1.6 ± 0.1 vs. 1.0 ± 0.2), and hence myofibroblast number.

To investigate whether some of the effects exerted by concurrent sildenafil could be due to an increase in PDE 5 protein that would counteract the inhibition of its activity by the drug, PDE 5 was also estimated (Figure 6). That this was the case was shown by the significant increase of PDE 5 levels by MDSC + sildenafil, but not by MDSC alone in comparison to the saline injected rats (0.9 ± 0.1 and 1.2 ± 0.2 vs. 0.6 ± 0.1). PDE 5 expression was also detected in the MDSC. The magnitude of all the observed changes by western blot assays in the area adjacent to the infarct is likely to be lower than in region #2 used for histochemical evaluation of the infarct area.

The relative effects of sildenafil or MDSC alone, or in combination, on left ventricle remodeling were also assessed by determining the release of MMPs to the circulation, using zymography to estimate the levels of the pro-enzymes and processed MMPs. Only the gelatinases MMP-2 and -9 were detected in serum. MDSC reduced significantly the levels of serum pro-MMP-2 (7.0 ± 1.6 vs. 14.8 ± 1.6) and -9 (1.7 ± 1.7 vs. 8.9 ± 2.6) and of active MMP-9 (1.7 ± 1.1 vs. 8.7 ± 2.5) in comparison to the saline injection, but the concurrent administration of sildenafil did not alter these effects (Figure 7).

Discussion

This study aimed to address the issue on whether concurrent long-term daily administration of low doses of oral PDE 5 inhibitors, compatible with standard on demand clinical use, can stimulate the potential antifibrotic and antiapoptotic effects of stem cells, in this case MDSC, on MI repair, thus extending to this condition prior similar studies with PDE 5 inhibitors alone on

the vascular bed and in urological organs, and even in avascular tissues [6,16,21-23,27]. First, we have shown that oral sildenafil given alone (no MDSC) to the rat for 4 weeks post-MI, acts as expectedly, by moderately increasing the LVEF and troponin recovery in tissue sections in the left ventricular region around the infarction, and reducing the fibrotic area and myofibroblast infiltration. Second, MDSC given alone (no sildenafil) acted similarly, while also reducing apoptosis measured by TUNEL, enhancing angiogenesis (SMC content) assayed by western blot, and lowering tissue remodeling as indicated by pro-MMP 2 and 9 and active MMP 9 levels in serum. Third, the concurrent long-term administration of MDSC + sildenafil to rats with MI intensified as expected the antiapoptotic, and cardiomyocyte and endothelial protective effects of the separate MDSC and sildenafil treatments, and preserved the serum MMP pattern of the rats receiving MDSC.

However, unexpectedly the MDSC + sildenafil combination treatment inhibited the improvement of the LVEF and the reduction of the fibrotic area by MDSC or sildenafil alone, and the increased angiogenesis (measured by SMC content) by MDSC, while increasing the abundance of the profibrotic myofibroblasts. We postulate that this abrogation by the combination treatment of some of the beneficial effects on cardiac tissue and function exerted by each independent treatment is due in part to the observed upregulation of PDE 5 expression (that would counteract the inhibition of PDE 5 enzyme activity by sildenafil alone), and also speculatively to the shift of MDSC differentiation towards myofibroblast generation, as discussed below.

The dose of oral sildenafil for the current rat study, 3 mg/kg/day, was selected to be clinically translatable to humans, and also to be compatible with the goal of modulate the differentiation of stem cells given concurrently [42[. It is double the daily dose given for 4 weeks

either IP for MI in the mouse [12], or orally, concurrent with MDSC, as antifibrotic in the rat corpora cavernosa [43]. This dose comparison is likely to be reflected in the respective sildenafil blood concentrations, since neither the oral vs. IV or IP administration [44] nor the small difference in rat/mouse surface/weight ratios [45] are expected to affect considerably the proportional pharmacokinetics. Translated to the human based on the rat/human surface correction factor [21,23,45], our oral dose would be roughly equivalent to about 30-40 mg/day, or slightly less than the usual oral dose given sporadically on demand to induce penile erection through corpora cavernosal vasodilation. Other studies on MI in the rat [14] have used much higher doses of sildenafil (100mg/kg/day), but when they are translated to human treatment they exceed considerably (more than tenfold) the clinical doses.

The beneficial effects of PDE5is for experimental ischemia/reperfusion, cardiac hypertrophy, and heart failure [9-19,46] have been ascribed to mechanisms as varied as nitric oxide generation by upregulation of iNOS or eNOS, protein kinase C activation, opening of mitochondrial ATP-sensitive potassium channels, or inhibition of the RhoA-Rho kinase pathway in cardiac tissue, or even distal effects reducing peripheral resistance and aortic and large artery stiffness. However, we believe that the improvement of the LVEF by our selected chronic daily dose of sildenafil resulted from the expected antifibrotic action of PDE5is that replicated the inhibition of collagen deposition, myofibroblast accumulation, and the preservation of key functional cells under various tissue damage conditions previously described in non cardiac tissues [4,6,21-23,27]. This is essentially due to the inhibition of collagen synthesis, and myofibroblast differentiation, and in certain cases, of apoptosis that by counteracting fibrosis not only helps to protect the normal cardiac tissue composition, but also the normal ECM/fibroblast interaction in force networking around the myocytes and putative electrical coupling of both cell types [1].

Our results on the reduction of MI scar size coincide with the two long-term experimental studies of cardioprotection in mice and rats after permanent LAD occlusion by PDE5i given IP [12,17]. The caveat is that in the latter studies measurements were done at 24 hrs when the effects are due to rapid vasodilation and related mechanisms instead of the long-term antifibrotic action. Myofibroblast accumulation, troponin T loss, angiogenic markers, or MMPs in serum were not reported in those papers.

The lack of intensification of iNOS expression in the rat post-MI cardiac tissue by sildenafil does not agree with what was observed in the mouse in this condition and in ischemia reperfusion injury [12,13], and even in other organs [21-23], suggesting that studies on the time course of iNOS blockade or overexpression on the cardioprotective effects of chronic sildenafil in MI are needed to clarify these discrepancies. This is of interest, considering that although in other tissues fibrosis was exacerbated by blocking iNOS by long-term administration of the iNOS inhibitor L-NIL or by its genetic inactivation in the iNOS ko mouse [4,46,47], in MI the role of iNOS in fibrosis, vis-à-vis eNOS, is confusing, as evidenced by various reports claiming deleterious, protective, or no effects [47]. This may result from the opposite actions of iNOS in the early inflammatory remodeling phase as compared to the subsequent fibrogenesis.

The improvement of cardiac function, reduction of fibrotic scar, and cardiomyocyte preservation by MDSC implantation into the MI area are in agreement with previous results in mice [33-35] and in rats [36], although it is not clear whether there is some conversion of the engrafted cells into cardiomyocytes that does occur with myoblasts or satellite cells, or this is exclusively due to trophic effects such as the stimulation of angiogenesis. The latter seems to have occurred in the present work, as judged by the observed increase in SMC and endothelial markers.

The common denominator of these effects of sildenafil is the expression of PDE5 in both the human left and right ventricle, specifically in smooth muscle and endothelial cells, and in the cardiomyocytes themselves, which is considerably increased in end-stage ischemic cardiomyopathy, and the assumption that this may contribute to at least right ventricular heart failure [20]. The observed upregulation of PDE5 in the MDSC/long-term sildenafil combination may explain the loss of efficacy of MDSC in improving LVEF and reducing scar size, since this may cause tachyphylaxis [20,48]. This PDE5 upregulation has been postulated to occur in the penile smooth muscle due to the presence of cGMP-responsive elements in the PDE5 gene promoter [49], but has not been observed in vivo [50]. Our assumption would require on one side that sildenafil modulates MDSC lineage commitment towards a fibrotic phenotype and myofibroblast formation, and on the other side that the PDE5 upregulation itself occurs in the MDSC or their differentiation, since in the absence of MDSC sildenafil was moderately effective. The MDSC myofibroblast differentiation was suggested previously [51], assuming that the release of local environmental stimuli after muscle injury triggers the differentiation of MDSC into fibrotic cells, thus illustrating the importance of controlling the local environment within the injured tissue to optimize regeneration via the transplantation of stem cells. We have shown this differentiation in vitro [40]. This process also occurs with mesenchymal cells, even in the absence of injury [53]. Moreover, endogenous cardiac stem cells originate fibroblasts, which are essential for proper tissue repair, but also myofibroblasts whose accumulation may lead to inadequate scar formation [54]. In turn, sustained high cGMP levels induced by PDE5is, in the absence of PDE5 upregulation, reduced myoblast formation [55], so that the reverse, i.e. the decrease of cGMP by high PDE5, may trigger this differentiation. It is of interest that sildenafil was effective in potentiating the efficacy of adipose-derived mesenchymal stem cells on cardiac

repair in rat dilated cardiomyopathy [29], but it reduced the efficacy of MDSC in tissue repair, in this case in corporal penile fibrosis and loss of SMC subsequent to nerve damage [43], suggesting that various types of stem cells may react differently to PDE5i in terms of their repair capacity.

Altogether our results confirm in the rat that daily oral sildenafil at low dose and MDSC exert separately a modest cardioprotection post-MI by ameliorating the infarction scar formation and remodeling, but the in vivo combination of these treatments, at least in the rat, is counteractive. Further research is needed to identify sildenafil regimens that may not induce the PDE5 upregulation, or alternatively by overriding the higher PDE5 levels by an efficient inhibition of enzyme activity. In vitro preconditioning of stem cells with PDE5i prior to implantation has just been shown, in this case with sildenafil and adipose-derived stem cells, to reduce in the mouse post-MI cardiomyocyte apoptosis and fibrosis, possibly by improving stem cell survival and paracrine effects by secretion of growth factors [30] . This strategy would avoid the in vivo sildenafil/stem cell interaction in the host cardiac tissue setting, while preserving the beneficial effects on stem cell trophic effects and/or lineage commitment, even in the absence of a direct protective action by sildenafil on cardiac tissue.

The design of the current work was restricted to the five arms already described, in order to simplify it. However, once the sildenafil dosages and times of administration are optimized, the selected treatment should be compared with the conventional RAAS therapy [7,56,57]. This may involve an angiotensin II type I receptor blocker or a type 2 receptor stimulator, or an angiotensin-converting enzyme inhibitor, based on their well known antifibrotic, anti-inflammatory, and cardiomyocyte protection effects, and also in combination with MDSC. In fact, it is known that RAAS modulators can inhibit or stimulate cardiovascular progenitor

functions, even if the overall picture is not yet clear [58]. For instance, although AT(1) receptor blockade and ACE inhibition stimulate proliferation and differentiation of endothelial progenitor cells (EPC) and angiogenesis, Ang-(1-7) that behaves similarly towards EPC may either inhibit or stimulate angiogenesis according to dosages**.** There are no reports on the modulation of implanted stem cells by these agents. Similarly, no studies with a RAAS/PDE5i combination have been reported, even if combo approaches in the absence of stem cells with AT(1) blockers and ACE inhibitors are being tested [59]. Therefore, the optimal MDSC/sildenafil combination should also be tested against an MDSC/RAAS combination to assess which antifibrotic/pro-differentiation approach may be more efficacious.

Acknowledgements

This study was supported by the Department of Defense [W81XWH-07-1-0181 to N.G.C.], and partially by the National Institutes of Health [R21DK070003 to N.G.C; M01-RR00425, Harbor-UCLA General Clinical Research Center to N.G.C. and J.W.] and seed grants from LABioMed/Norris Foundation (N.G.C./R.W.) and Western/Drew Collaboration [12304P to S.C. and N.G.C.). The invaluable advice of Dr. Robert A. Kloner and cooperation of Drs. Wangde Dai and Arash Keyhani for the LAD permanent occlusion training are gratefully acknowledged. Brian Leung and Jacques Busquet efficiently assisted in some experiments.

Competing interests

The authors declare that they have no competing interests.

Authors' contributions

All authors read and approved the final manuscript.

Experiment design and manuscript drafting: NFCG with the assistance of RAW.

Animal experiments: JSCW, IK, SLC. Ejection fraction measurements: JSCW, GEK, IK, SLC. Laboratory assays: JSCW, IK, DV, GN, SLC.

References

1. Porter KE, Turner NA. **Cardiac fibroblasts: at the heart of myocardial remodeling**. *Pharmacol Ther* 2009, **123:**255-278.

2. Forte A, Della Corte A, De Feo M, Cerasuolo F, Cipollaro M. **Role of myofibroblasts in vascular remodeling: focus on restenosis and aneurysm.** *Cardiovasc Res* 2010, [Epub ahead of print]

3. Kovanecz I, Nolazco G, Ferrini MG, Toblli JE, Heydarkhan S, Vernet D, Rajfer J, Gonzalez-Cadavid NF. **Early onset of fibrosis within the arterial media in a rat model of type 2 diabetes mellitus with erectile dysfunction.** *BJU Int* 2009, **103:**1396-1404.

4. Toblli JE, Ferrini MG, Cao G, Vernet D, Angerosa M, Gonzalez-Cadavid NF. **Antifibrotic effects of pioglitazone on the kidney in a rat model of type 2 diabetes mellitus.** *Nephrol Dial Transplant* 2009, **24:**2384-2391.

5. Serrano AL, Muñoz-Cánoves P. **Regulation and dysregulation of fibrosis in skeletal muscle.** *Exp Cell Res* 2010, [Epub ahead of print]

6. Gonzalez-Cadavid NF. **Mechanisms of penile fibrosis.** *J Sex Med* 2009, **3**:353-362.

7. Gajarsa JJ, Kloner RA. **Left ventricular remodeling in the post-infarction heart: a review of cellular, molecular mechanisms, and therapeutic modalities.** *Heart Fail Rev* 2011, **16**:13-21.

8. Kukreja RC, Salloum FN, Das A, Koka S, Ockaili RA, Xi L. **Emerging new uses of phosphodiesterase-5 inhibitors in cardiovascular diseases**. *Exp Clin Cardiol* 2011;**16**:e30-35.

9. Kukreja RC. **Cardiovascular protection with sildenafil following chronic inhibition of nitric oxide synthase**. *Br J Pharmacol* 2007; **150**:538-40.

10. Ovize M, Baxter GF, Di Lisa F, Ferdinandy P, Garcia-Dorado D, Hausenloy DJ, Heusch G, Vinten-Johansen J, Yellon DM, Schulz R; Working Group of Cellular Biology of Heart of European Society of Cardiology. **Postconditioning and protection from reperfusion injury: where do we stand?** Position paper from the Working Group of Cellular Biology of the Heart of the European Society of Cardiology. *Cardiovasc Res* 2010, **87:**406-423.

11. Kumar P, Francis GS, Tang WH. **Phosphodiesterase 5 inhibition in heart failure: mechanisms and clinical implications.** *Nat Rev Cardiol* 2009, **6:**349-355.

12. Salloum FN, Abbate A, Das A, Houser JE, Mudrick CA, Qureshi IZ, Hoke NN, Roy SK, Brown WR, Prabhakar S, Kukreja RC. **Sildenafil (Viagra) attenuates ischemic cardiomyopathy and improves left ventricular function in mice.** *Am J Physiol Heart Circ Physiol* 2008, **294:**H1398-406. .

13. Das A, Salloum FN, Xi L, Rao YJ, Kukreja RC. **ERK phosphorylation mediates sildenafil-induced myocardial protection against ischemia-reperfusion injury in mice.** *Am J Physiol Heart Circ Physiol* 2009, **296:**H1236-1243.

14. Pérez NG, Piaggio MR, Ennis IL, Garciarena CD, Morales C, Escudero EM, Cingolani OH, Chiappe de Cingolani G, Yang XP, Cingolani HE. **Phosphodiesterase 5A inhibition induces Na+/H+ exchanger blockade and protection against myocardial infarction.** *Hypertension* 2007, **49:**1095-1103.

15. Salloum FN, Takenoshita Y, Ockaili RA, Daoud VP, Chou E, Yoshida K, Kukreja RC. **Sildenafil and vardenafil but not nitroglycerin limit myocardial infarction through opening of mitochondrial K(ATP) channels when administered at reperfusion following ischemia in rabbits.** *J Mol Cell Cardiol* 2007, **42:**453-458.

16. Koka S, Kukreja RC. **Attenuation of Doxorubicin-induced Cardiotoxicity by Tadalafil: A Long Acting Phosphodiesterase-5 Inhibitor**. *Mol Cell Pharmacol* 2010, **2:**173-178.

17. Koneru S, Varma Penumathsa S, Thirunavukkarasu M, Vidavalur R, Zhan L, Singal PK, Engelman RM, Das DK, Maulik N. **Sildenafil-mediated neovascularization and protection against myocardial ischaemia reperfusion injury in rats: role of VEGF/angiopoietin-1.** *J Cell Mol Med* 2008, **12:**2651-2664.

18. Sesti C, Florio V, Johnson EG, Kloner RA. **The phosphodiesterase-5 inhibitor tadalafil reduces myocardial infarct size.** *Int J Impot Res* 2007, **19:**55-61.

19. Salloum FN, Chau VQ, Hoke NN, Abbate A, Varma A, Ockaili RA, Toldo S, Kukreja RC. **Phosphodiesterase-5 inhibitor, tadalafil, protects against myocardial ischemia/reperfusion through protein-kinase g-dependent generation of hydrogen sulfide.** *Circulation* 2009, **120**:S31-36. Erratum in: *Circulation* 2009, **120:**e139.

20. Shan X, Quaile MP, Monk JK, French B, Cappola TP, Margulies KB. **Differential Expression of PDE5 in Failing and Non-Failing Human Myocardium.** *Circ Heart Fail* 2011, [Epub ahead of print] PubMed PMID: 22135403.

21. Kovanecz I, Rambhatla A, Ferrini M, Vernet D, Sanchez S, Rajfer J, Gonzalez-Cadavid N. **Long-term continuous sildenafil treatment ameliorates corporal veno-occlusive dysfunction (CVOD) induced by cavernosal nerve resection in rats.** *Int J Impot Res* 2008, **20:**202-212.

22. Kovanecz I, Rambhatla A, Ferrini MG, Vernet D, Sanchez S, Rajfer J, Gonzalez-Cadavid N. **Chronic daily tadalafil prevents the corporal fibrosis and veno-occlusive dysfunction that occurs after cavernosal nerve resection.** *BJU Int* 2008, **101:**203-210.

23. Ferrini MG, Kovanecz I, Sanchez S, Vernet D, Davila HH, Rajfer J, Gonzalez-Cadavid NF. **Long-term continuous treatment with sildenafil ameliorates aging related erectile dysfunction and the underlying corporal fibrosis in the rat.** *Biol Reprod* 2007, **76**:915-923.

24. Magheli A, Burnett AL; Medscape. **Erectile dysfunction following prostatectomy: prevention and treatment.** *Nat Rev Urol* 2009, **6:**415-427.

25. Hemnes AR, Zaiman A, Champion HC. **PDE 5A inhibition attenuates bleomycin-induced pulmonary fibrosis and pulmonary hypertension through inhibition of ROS generation and RhoA/Rho kinase activation.** *Am J Physiol Lung Cell Mol Physiol* 2008, **294:**L24-33.

26. Jeong KH, Lee TW, Ihm CG, Lee SH, Moon JY, Lim SJ. **Effects of sildenafil on oxidative and inflammatory injuries of the kidney in streptozotocin-induced diabetic rats.** *Am J Nephrol* 2009, **29:**274-282.

27. Gonzalez-Cadavid NF, Rajfer J. **Treatment of Peyronie's disease with PDE 5 inhibitors: an antifibrotic strategy.** *Nat Rev Urol* 2010, **7:**215-221.

28. Mazo M, Pelacho B, Prósper F. **Stem cell therapy for chronic myocardial infarction.** *J Cardiovasc Transl Res* 2010, **3:**79-88.

29. Lin YC, Leu S, Sun CK, Yen CH, Kao YH, Chang LT, Tsai TH, Chua S, Fu M, Ko SF, Wu CJ, Lee FY, Yip HK. **Early combined treatment with sildenafil and adipose-derived mesenchymal stem cells preserves heart function in rat dilated cardiomyopathy.** *J Transl Med* 2010, **8:**88.

30. Hoke NN, Salloum FN, Kass DA, Das A, Kukreja RC. **Preconditioning by Phosphodiesterase-5 Inhibition Improves Therapeutic Efficacy of Adipose Derived Stem Cells Following Myocardial Infarction in Mice**. *Stem Cells* 2011, doi: 10.1002/stem.789. [Epub ahead of print]

31. Mujoo K, Sharin VG, Bryan NS, Krumenacker JS, Sloan C, Parveen S, Nikonoff LE, Kots AY, Murad F. **Role of nitric oxide signaling components in differentiation of embryonic stem cells into myocardial cells.** *Proc Natl Acad Sci USA* 2008, **105:**18924-18929.

32. Ybarra N, del Castillo JR, Troncy E. **Involvement of the nitric oxide-soluble guanylyl cyclase pathway in the oxytocin-mediated differentiation of porcine bone marrow stem cells into cardiomyocytes.** *Nitric Oxide* 2011, **24:**25-33.

33. Oshima H, Payne TR, Urish KL, Sakai T, Ling Y, Gharaibeh B, Tobita K, Keller BB, Cummins JH, Huard J. **Differential myocardial infarct repair with muscle stem cells compared to myoblasts.** *Mol Ther* 2005, **12:**1130-1141.

34. Payne TR, Oshima H, Okada M, Momoi N, Tobita K, Keller BB, Peng H, Huard J. **A relationship between vascular endothelial growth factor, angiogenesis, and cardiac repair after muscle stem cell transplantation into ischemic hearts.** *J Am Coll Cardiol* 2007, **50:**1677-1684.

35. Okada M, Payne TR, Zheng B, Oshima H, Momoi N, Tobita K, Keller BB, Phillippi JA, Péault B, Huard J. **Myogenic endothelial cells purified from human skeletal muscle improve cardiac function after transplantation into infarcted myocardium.** *J Am Coll Cardiol* 2008, **52:**1869-1880.

36. Tamaki T, Akatsuka A, Okada Y, Uchiyama Y, Tono K, Wada M, Hoshi A, Iwaguro H, Iwasaki H, Oyamada A, Asahara T. **Cardiomyocyte formation by skeletal muscle-derived**

multi-myogenic stem cells after transplantation into infarcted myocardium. *PLoS One* 2008, **3:**e1789.

37. Gharaibeh B, Lu A, Tebbets J, Zheng B, Feduska J, Crisan M, Péault B, Cummins J, Huard J. **Isolation of a slowly adhering cell fraction containing stem cells from murine skeletal muscle by the preplate technique.** *Nat Protoc* 2008, **3:1501**-1509.

38. Nolazco G, Kovanecz I, Vernet D, et al. **Effect of muscle-derived stem cells on the restoration of corpora cavernosa smooth muscle and erectile function in the aged rat.** *BJU Int* 2008, **101:**1156-1164.

39. Ho MH, Heydarkhan S, Vernet D, Kovanecz I, Ferrini MG, Bhatia NN, Gonzalez-Cadavid NF. **Stimulating vaginal repair in rats through skeletal muscle-derived stem cells seeded on small intestinal submucosal scaffolds.** *Obstet Gynecol* 2009, **114:**300-309.

40. Tsao J, Vernet D, Gelfand R, Kovanecz I, Nolazco G, Gonzalez-Cadavid NF. **Myostatin inactivation affects myogenesis by muscle derived stem cells in vitro and in the mdx mouse.** *Military Health Research Forum* 2009, Kansas City, Missouri, USA

41. Brown RD, Jones GM, Laird RE, Hudson P, Long S. **Cytokines regulate matrix metalloproteinases and migration in cardiac fibroblasts.** *Biochem Biophys Re Commun* 2007, **362:**200-235.

42. Gómez-Pinedo U, Rodrigo R, Cauli O, Herraiz S, Garcia-Verdugo JM, Pellicer B, Pellicer A, Felipo V. **cGMP modulates stem cells differentiation to neurons in brain in vivo.** *Neuroscience* 2010, **165**:1275-1283.

43. Kovanecz I, Rivera S, Nolazco G, Vernet D, Rajfer J, Gonzalez-Cadavid NF **Long term daily molsidomine and low dose sildenafil, and corporal implantation of muscle derived**

stem cells (MDSC), alone or in combination, prevent corporal venooclusive dysfunction (CVOD) in a rat model of cavernosal nerve damage. *J Urol* 2011, **185**:e452

44. Muirhead GJ, Rance DJ, Walker DK, Wastall P. **Comparative human pharmacokinetics and metabolism of single-dose oral and intravenous sildenafil.** *Br J Clin Pharmacol* 2002, **53**:13S-20S.

45. Freireich EJ, Gehan EA, Rall DP, Schmidt LH, Skipper HE. **Quantitative comparison of toxicity of anticancer agents in mouse, rat, hamster, dog, monkey, and man.** *Cancer Chemother Rep* 1966, **50**:219-244.

46. Chau VQ, Salloum FN, Hoke NN, Abbate A, Kukreja RC. **Mitigation of the progression of heart failure with sildenafil involves inhibition of RhoA/Rho-kinase pathway.** *Am J Physiol Heart Circ Physiol* 2011, **300:**H2272-2279.

47. Ferrini MG, Rivera S, Moon J, Vernet D, Rajfer J, Gonzalez-Cadavid NF. **The Genetic Inactivation of Inducible Nitric Oxide Synthase (iNOS) Intensifies Fibrosis and Oxidative Stress in the Penile Corpora Cavernosa in Type 1 Diabetes.** *J Sex Med* 2010, **7:**3033-3044.

48. Zhang M, Takimoto E, Hsu S, Lee DI, Nagayama T, Danner T, Koitabashi N, Barth AS, Bedja D, Gabrielson KL, Wang Y, Kass DA. **Myocardial remodeling is controlled by myocyte-targeted gene regulation of phosphodiesterase type 5.** *J Am Coll Cardiol* 2010, **56:**2021-2030.

49. Lin G, Xin ZC, Lue TF, Lin CS. **Up and down-regulation of phosphodiesterase-5 as related to tachyphylaxis and priapism.** *J Urol* 2003, **170:**S15-18;

50. Musicki B, Champion HC, Becker RE, Kramer MF, Liu T, Sezen SF, Burnett AL. **In vivo analysis of chronic phosphodiesterase-5 inhibition with sildenafil in penile erectile tissues: no tachyphylaxis effect.** *J Urol* 2005, **174:**1493-1496.

51. Li Y, Huard J**. Differentiation of muscle-derived cells into myofibroblasts in injured skeletal muscle.** *Am J Pathol* 2002, **161**:895-907.

52. Anjos-Afonso F, Siapati EK, Bonnet D. **In vivo contribution of murine mesenchymal stem cells into multiple cell-types under minimal damage conditions.** *J Cell Sci* 2004, **117**:5655-5664

53. Ono Y, Sensui H, Okutsu S, Nagatomi R. **Notch2 negatively regulates myofibroblastic differentiation of myoblasts.** *J Cell Physiol* 2007, **210**:358-369.

54. Carlson S, Trial J, Soeller C, Entman ML. **Cardiac mesenchymal stem cells contribute to scar formation after myocardial infarction.** *Cardiovasc Res* 2011, **91**:99-107.

55. Vernet D, Magee T, Qian A, Nolazco G, Rajfer J, Gonzalez-Cadavid N. **Phosphodiesterase type 5 is not upregulated by tadalafil in cultures of human penile cells.** *J Sex Med* 2006, **3**:84-94; discussion 94-95.

56. Dorn GW 2nd. **Novel pharmacotherapies to abrogate postinfarction ventricular remodeling.** *Nat Rev Cardiol* 2009, **6**:283-291.

57. Ludwig M, Steinhoff G, Li J. **The regenerative potential of angiotensin AT(2) receptor in cardiac repair.** *Can J Physiol Pharmacol* 2012, Feb 24. [Epub ahead of print]

58. Qian C, Schoemaker RG, van Gilst WH, Roks AJ. **The role of the rennin angiotensin-aldosterone system in cardiovascular progenitor cell function.** *Clin Sci (Lond)* 2009, **116**:301-314.

59. Ma TK, Kam KK, Yan BP, Lam YY. **Renin-angiotensin-aldosterone system blockade for cardiovascular diseases: current status.** *Br J Pharmacol* 2010, **160**:1273-1292.

Figure legends

Figure 1 Experimental protocol. Myocardial infarction **(MI)** was induced in rats by left anterior descending coronary artery **(LAD)** ligation. Arrows indicate the time points for treatments with sildenafil alone, MDSC, and MDSC+sildenafil, performance of surgical procedure, and measurement of various parameters (listed under each arrow), and final sacrifice.

Figure 2 Long-term oral sildenafil improved left ventricular function and reduced infarction size after LAD occlusion. Sildenafil was given continuously for 4 weeks in the drinking water (3 mg/kg/day) (n=8/group). ***Top:*** The LVEF was measured before MI (basal), and at 1 and 4 weeks. UT: untreated control; S: sildenafil. ***Middle:*** representative micrographs (4 X) for the histochemical detection of collagen by Picrosirius red in paraffin-embedded sections. ***Bottom:*** quantitative image analysis of infarction area. Statistical differences are stated for untreated versus basal, and sildenafil versus untreated *p<0.05; ***p<0.005

Figure 3 Long-term oral sildenafil reduced myofibroblast accumulation in the infarction area, but did not significantly counteract the cardiomyocyte loss in this region. (n=8/group). Paraffin-embedded sections were used. ***Top:*** quantitative image analysis of myofibroblasts by immunohistochemistry for ASMA. ***Middle:*** representative micrographs for the immunohistochemical detection of troponin T. ***Bottom:*** quantitative image analysis of troponin T. UT: untreated control; S: sildenafil; ***p<0.005

Figure 4 Intracardiac implantation of MDSC improved the LVEF and reduced infarction size after LAD, but concurrent chronic sildenafil abrogated these effects. Intracardiac injection of saline or MDSC was conducted at 1 week (n=7/group). Sildenafil was then given continuously in the drinking water until sacrifice at 4 weeks. ***Top:*** Ejection fraction before MI (basal), and at 1 and 4 weeks. NaCl: control injected with saline; MDSC: injection with MDSC;

MDSC+S: MDSC with sildenafil. ***Bottom:*** quantitative image analysis of infarction area by Picrosirius red histochemistry. Statistical differences are stated for untreated versus basal, and MDSC, and MDSC+sildenafil versus untreated *p<0.05

Figure 5 MDSC implanted in the MI area survived after 4 weeks and reduced the apoptotic index, in a process stimulated by sildenafil that also partially counteracted the cardiomyocyte loss. (n=7/group). ***Top:*** representative picture of frozen sections from MI regions that received DAPI-labeled MDSC, visualized with blue (DAPI) and red (Texas red) fluorescence filters for implanted nuclei and troponin-T stained cardiomyocytes, respectively. Arrows: cardiomyocyte/MDSC nuclei overlapping. ***Middle and lower panels:*** quantitative image analysis by Troponin T and TUNEL (apoptosis) immuno-histochemistry in paraffin-embedded sections, respectively. Abbreviations as in Figure 4. Statistical differences are stated for untreated versus basal, and MDSC, and MDSC+sildenafil versus untreated *p<0.05; **p<0.01;***p<0.005

Figure 6 Implanted MDSC stimulated angiogenesis and reduced myofibroblasts, without affecting PDE 5 expression, while concurrent sildenafil protected the endothelium but increased myofibroblasts and upregulated PDE5. (n=7/group). Protein extracts were obtained from region #3 adjacent to the infarction area and subjected to western blot analysis. ***A:*** representative immunoblots (n=8), indicating band sizes. ***B:*** PDE 5 assayed in MDSC cultures in duplicate. ***C:*** Densitometric values corrected by GAPDH. Statistical differences are stated for untreated versus basal, and MDSC, and MDSC+sildenafil versus untreated *p<0.05; **p<0.01;***p<0.005

Figure 7 Implanted MDSC reduced left ventricular remodelling, as indicated by the decrease of both pro MMP-2 and 9 in serum, and concurrent long-term oral sildenafil, did

not modified these effects. MMPs were analyzed by zymography (n=7/group). The Y axes indicate relative densitometric intensities. Abbreviations as in Figures 1 and 3 *$p<0.05$

Figure 1

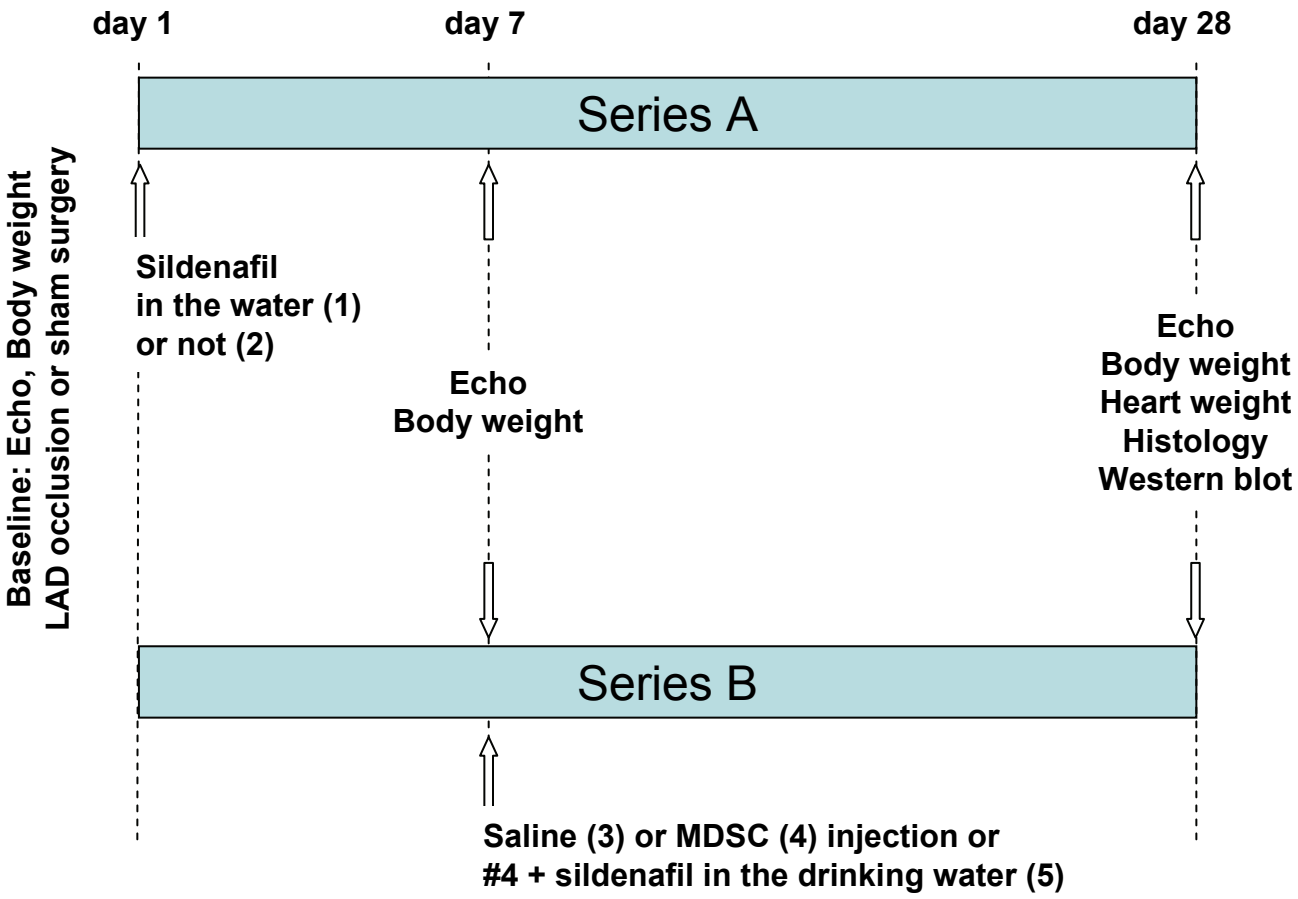
day 1
day 7
day 28
Series A
Baseline: Echo, Body weight
LAD occlusion or sham surgery
Sildenafil
in the water (1)
or not (2)
Echo
Body weight
Echo
Body weight
Heart weight
Histology
Western blot
Series B
Saline (3) or MDSC (4) injection or
#4 + sildenafil in the drinking water (5)

Figure 2

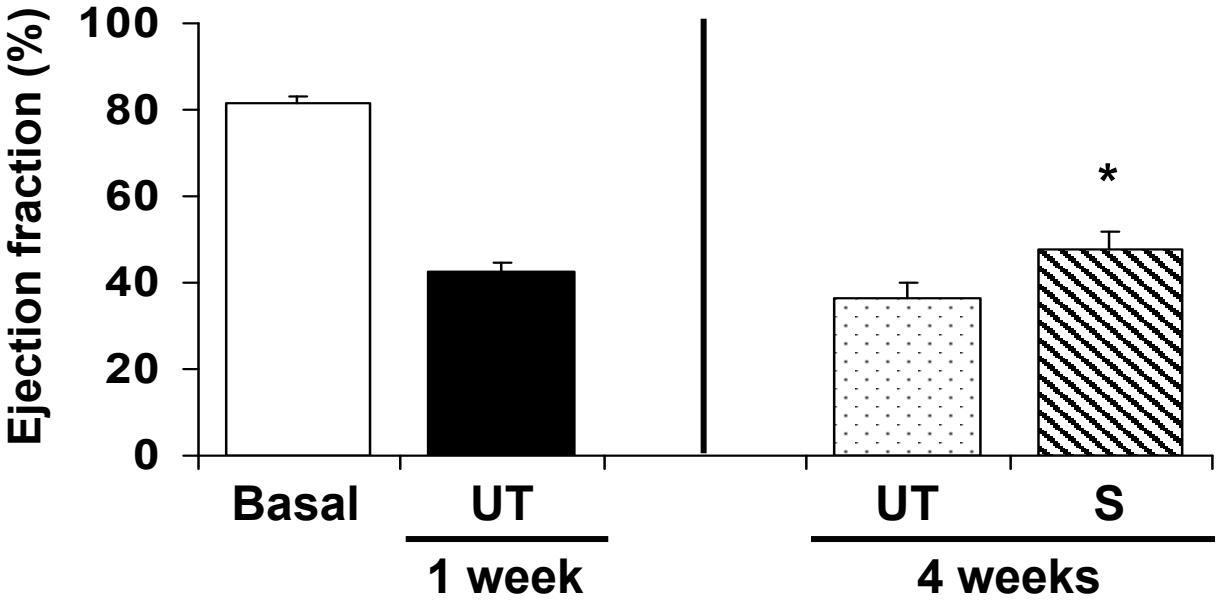
Ejection fraction (%)
100
80
60
40
20
0
*
Basal
UT
UT
S
1 week
4 weeks

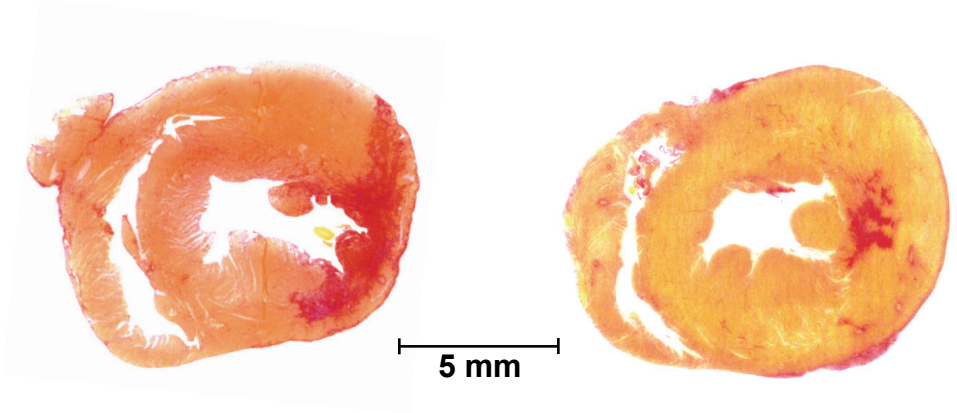
5 mm

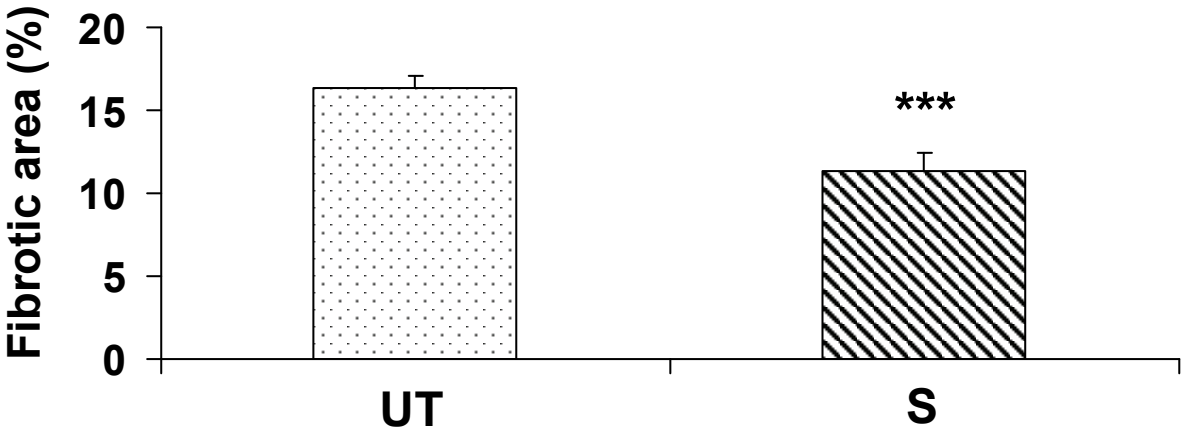
Fibrotic area (%)
20
15
10
5
0
***
UT
S

Figure 3

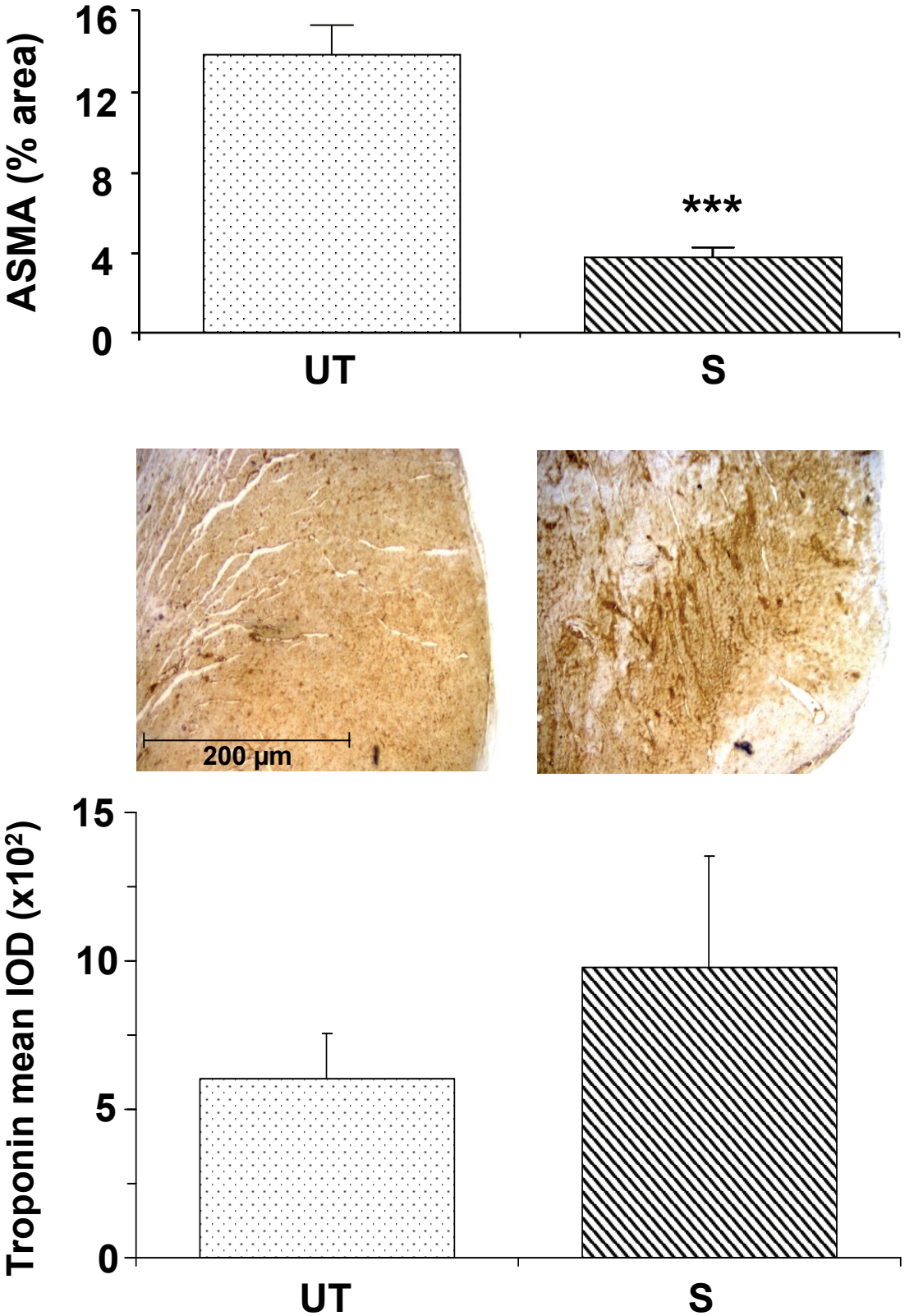
ASMA (% area)
16
12
8
4
0
***
UT
S
200 µm
Troponin mean IOD (x10²)
15
10
5
0
UT
S

Figure 4

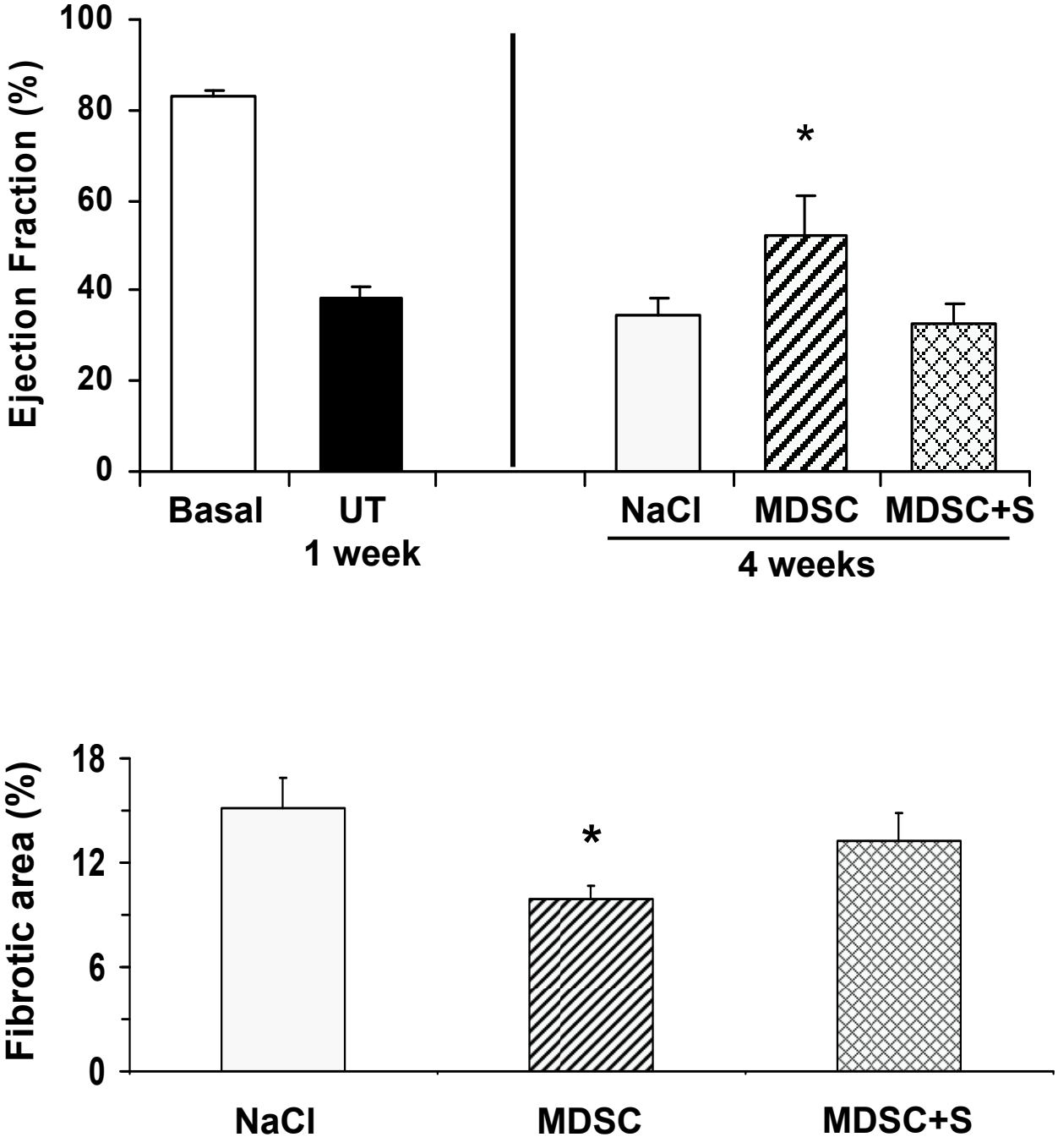
Ejection Fraction (%)
100
80
60
40
20
0
*
Basal
UT
1 week
NaCl
MDSC
MDSC+S
4 weeks
Fibrotic area (%)
18
12
6
0
*
NaCl
MDSC
MDSC+S

Figure 5

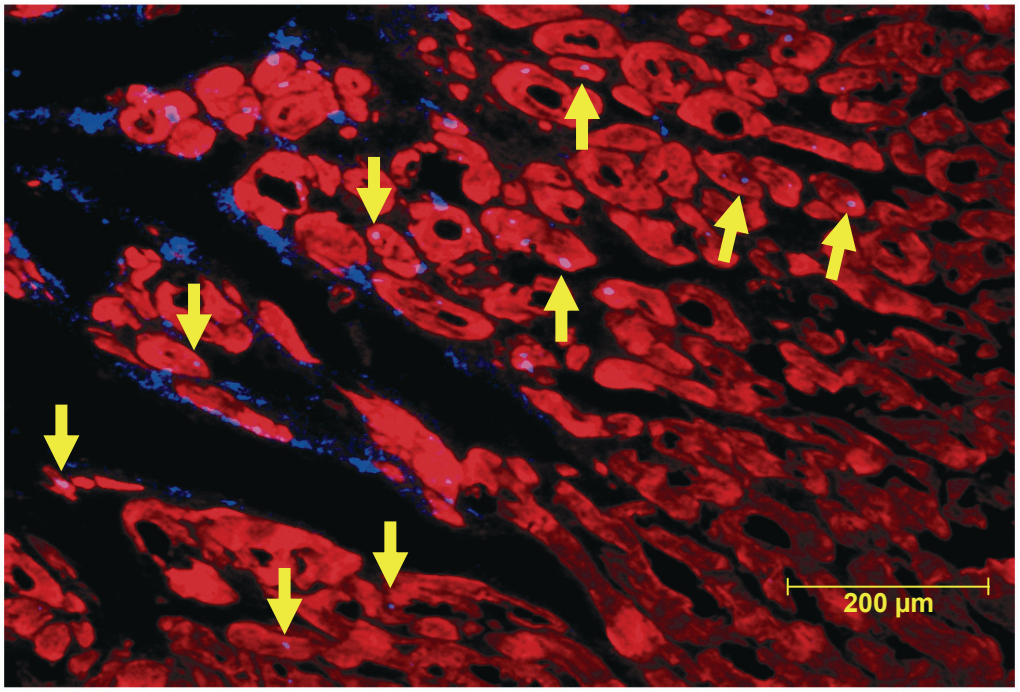
200 µm

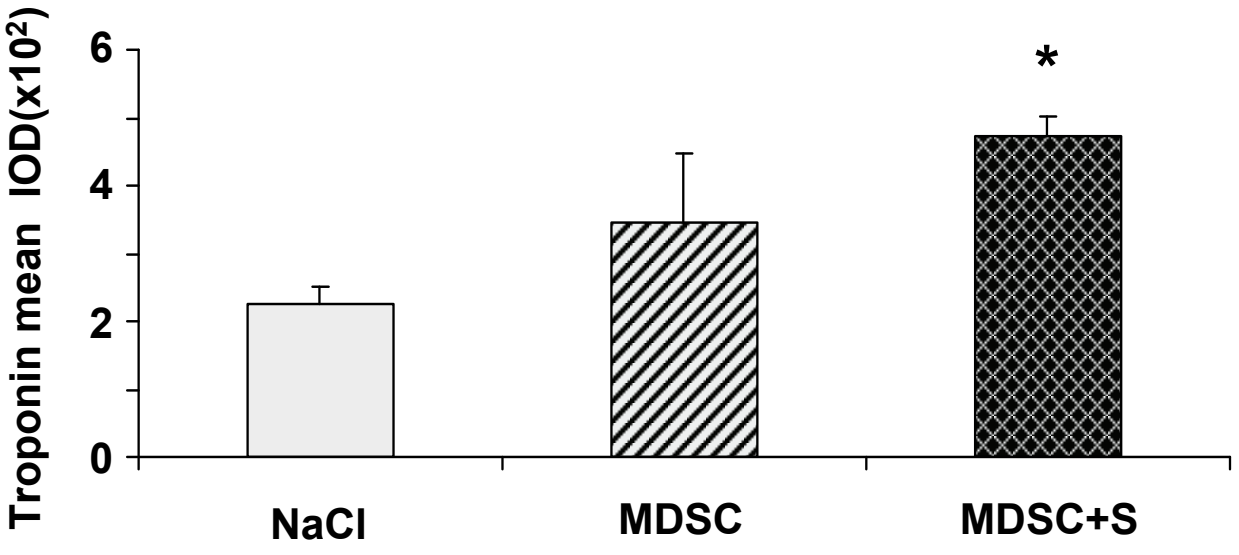
Troponin mean IOD(x10²)
6
4
2
0
*
NaCl
MDSC
MDSC+S

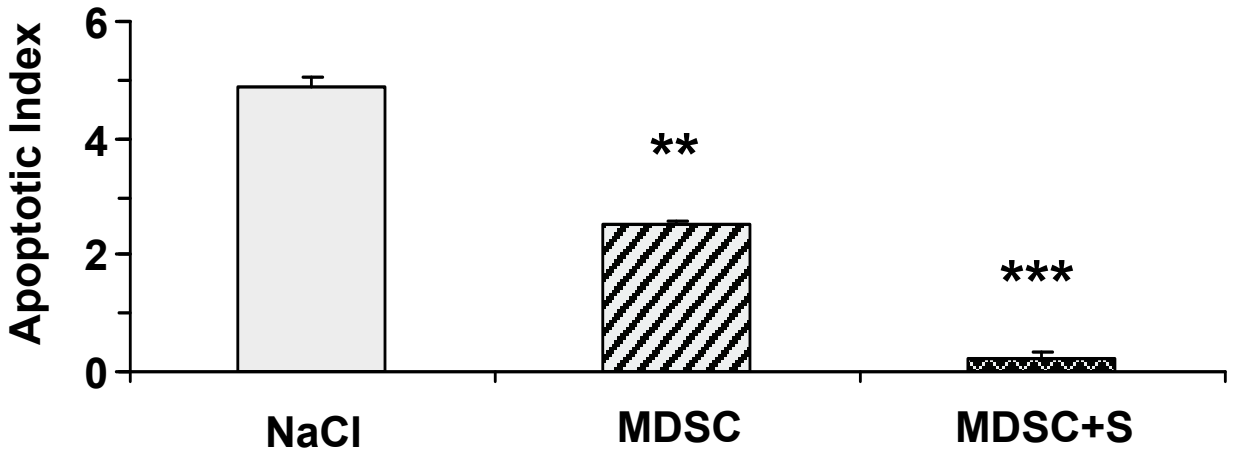
Apoptotic Index
6
4
2
0
**
***
NaCl
MDSC
MDSC+S

Figure 6

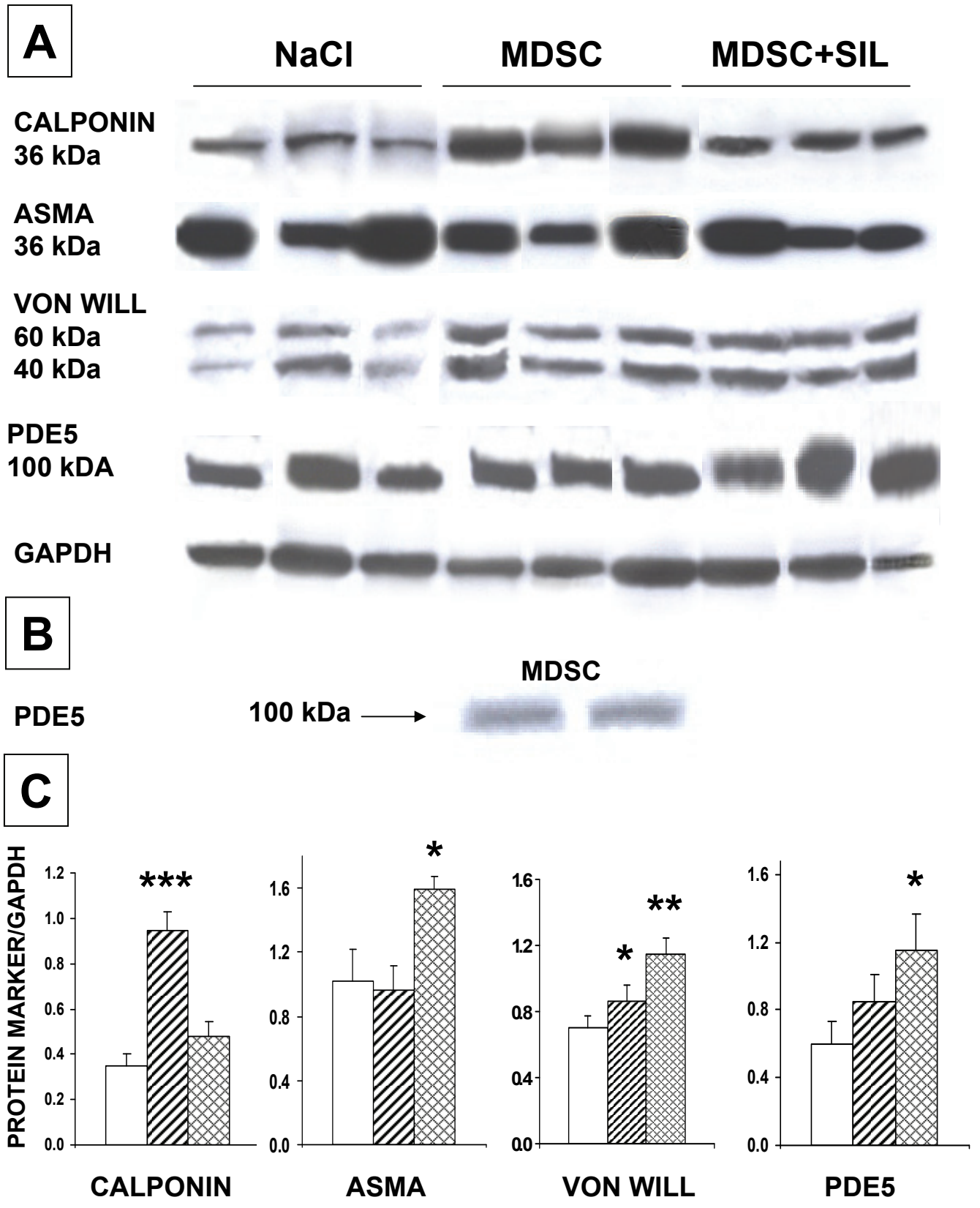
A
NaCl
MDSC
MDSC+SIL
CALPONIN
36 kDa
ASMA
36 kDa
VON WILL
60 kDa
40 kDa
PDE5
100 kDA
GAPDH
B
MDSC
PDE5
100 kDa
C
PROTEIN MARKER/GAPDH
***
*
**
*
*
CALPONIN
ASMA
VON WILL
PDE5

Figure 7

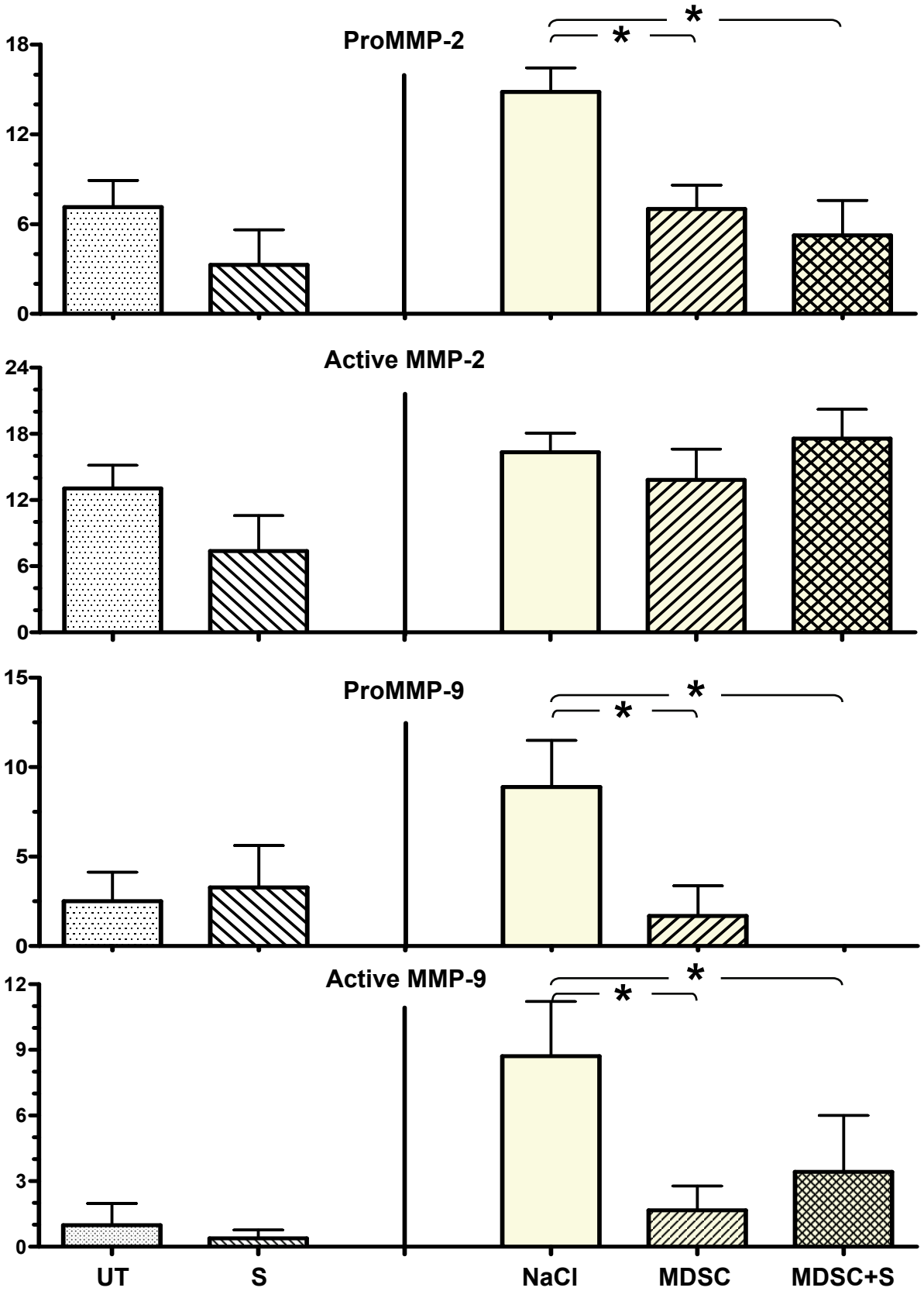
ProMMP-2
18
12
6
0
*
*
Active MMP-2
24
18
12
6
0
ProMMP-9
15
10
5
0
*
*
Active MMP-9
12
9
6
3
0
*
*
UT
S
NaCl
MDSC
MDSC+S

MYOSTATIN GENETIC INACTIVATION INHIBITS MYOGENESIS BY MUSCLE DERIVED STEM CELLS IN VITRO BUT NOT WHEN IMPLANTED IN THE mdx MOUSE MUSCLE

Tsao J[1], Vernet D[1,3], Gelfand R[1,3], Kovanecz I[2,3], Nolazco G[1], Bruhn KW[3], Gonzalez-Cadavid NF#[1,2,3]

[1]Department of Internal Medicine, Charles Drew University (CDU), Los Angeles, CA, [2]Department of Urology, David Geffen School of Medicine at UCLA, Los Angeles, CA, [3]Los Angeles Biomedical Research Institute (LABioMed) at Harbor-UCLA Medical Center, Torrance, CA,

#Corresponding author: Nestor F. Gonzalez-Cadavid, Ph.D., Charles Drew University, Department of Internal Medicine, Hawkins Building, Room #3071D, 1731 East 120th Street, Los Angeles, CA, 90059

Telephone: 323-563-9330; **fax:** 323-563-9352; **e-mail**: ncadavid@ucla.edu

Running Title: Myostatin/dystrophin silencing and muscle stem cells

Submitted: March 29, 2012

Abstract

Introduction: Stimulating the commitment of implanted dystrophin+ muscle derived stem cells (MDSC) into myogenic, as opposed to lipofibrogenic lineages, is a promising therapeutic strategy for Duchenne muscular dystrophy (DMD).

Methods: To examine whether counteracting myostatin, a negative regulator of muscle mass and a pro-lipofibrotic factor, would help this process, we compared the in vitro myogenic and fibrogenic capacity of MDSC from wild type (WT) and myostatin knockout (Mst KO) mice under various modulators, the expression of key stem cell and myogenic genes, and the capacity of these MDSC to repair the injured gastrocnemius in aged dystrophic mdx mice with exacerbated lipofibrosis.

Results: Surprisingly, the potent in vitro myotube formation by WT MDSC was refractory to modulators of myostatin expression or activity, and the Mst KO MDSC failed to form myotubes under various conditions, despite both MDSC expressed Oct-4 and various stem cell genes and differentiated into non-myogenic lineages. The genetic inactivation of myostatin in MDSC was associated with silencing of critical genes for early myogenesis (Actc1, Acta1, and MyoD). WT MDSC implanted into the injured gastrocnemius of aged mdx mice significantly improved myofiber repair and reduced fat deposition and, to a lesser extent, fibrosis. In contrast to their in vitro behavior, Mst KO MDSC in vivo also significantly improved myofiber repair, but had little effects on lipofibrotic degeneration.

Conclusions: While WT MDSC are considerably myogenic in culture and stimulate muscle repair after injury in the aged mdx mouse, myostatin genetic inactivation blocks myotube formation in vitro but the myogenic capacity is recovered in vivo under the influence of the myostatin+ host tissue environment, presumably by reactivation of key genes originally silenced in the Mst KO MDSC.

Key words: dystrophin, muscle dystrophy, muscle injury, mdx mouse, Duchenne, fibrosis

Introduction

The lipofibrotic degeneration of skeletal muscle, i.e. excessive deposition of endomysial collagen, other extracellular matrix, and fat, characterizes muscle dystrophy, and in particular Duchenne muscular dystrophy (DMD) [1,2], as seen also in its animal model, the mdx mouse [3-5]. This process, associated with inflammation and oxidative stress [6], is partially responsible for the severe muscle contractile dysfunction in DMD and the mdx mouse, mainly caused by the bouts of myofiber necrosis caused by dystrophin genetic inactivation, that in the gastrocnemius are rather mild in young animals but become particularly severe after 8-10 months of age [4]. Dystrophic muscle fibrosis is not only a major factor for DMD mortality, but also hampers the uptake and survival of cells implanted for potential therapeutic approaches [7], and/or may drive their differentiation into myofibroblasts [4]. Therefore, trying to ameliorate this process while stimulating myogenesis constitutes an ancillary strategy to favor repair and regeneration of dystrophic muscle tissue, even under ineffective or absent dystrophin replacement.

Although pharmacological approaches to combat muscle lipofibrotic degeneration and the underlying chronic inflammation are being widely investigated, biological factors such as myostatin, the main negative regulator of muscle mass [8], are also potential key targets. Myostatin, a member of the TGFβ family, aggravates muscle dystrophy not only as an anti-myogenic agent but also as a pro-fibrotic and adipogenic factor [9-14]. Inhibition of myostatin by using its propeptide, shRNA, or specific antibodies, improves myogenesis and reduces fibrosis in the mdx mouse. The same effects are generated in response to genetic deletion of myostatin in the myostatin knock-out (Mst KO) mouse, where myofiber hypertrophy is associated with less fat and reduced fibrosis [15-20].

It is assumed that in the dystrophic or injured muscle, tissue repair and the opposite process of lipofibrotic degeneration involve not only the differentiation of progenitor satellite cells and fibroblasts into myofibers and myofibroblasts, respectively, but also the modulation of lineage commitment by stem cells present in the adult muscle [21-23]. These stem cells have been isolated from the rodent and human skeletal muscle and named in general as muscle-derived stem cells (MDSC), because they have the ability to differentiate in vitro into multiple cell lines, and to generate myofibers, osteoblasts, cardiomyocytes, or smooth muscle cells after implantation into the skeletal muscle, bone, heart, corpora cavernosa, or vagina, respectively [21-27]. They are not satellite cells and may act also by secreting paracrine growth factors that are believed to modulate the differentiation of endogenous stem cells or the survival of differentiated cells in the tissue. However, the roles of MDSC in the biology and pathophysiology of the skeletal muscle are largely unknown.

Myostatin modulates the differentiation of pluripotent cells in vitro, albeit in some cases with conflicting outcomes [14,28-30]. It also inhibits the proliferation and early differentiation of both satellite cells from the skeletal muscle and cultured myoblasts, and blocking its expression improves the success of their in vivo transplantation [31-33]. To our knowledge, no reports are available on myostatin effects on MDSC differentiation, either in vitro or in the context of repairing the exacerbated lipofibrosis in the injured muscle of aged mdx mice.

MDSC obtained from wild type (WT) mice have been tested experimentally aiming to trigger repair of the mdx muscle with variable results [34-38], but they appear to be superior in this respect to myoblasts or satellite cells [39]. However, some of the main limitations of myoblast therapy when translated from the murine models into DMD and other human muscle dystrophies may also affect the MDSC and other types of stem cells [40]. Therefore, it is a therapeutic goal to enhance the repair capacity of WT MDSC by in vitro or in vivo modulation of their multilineage potential, and to stimulate or even awake endogenous stem cells of dystrophic muscle to regenerate myofibers while avoiding differentiation into cells responsible for lipofibrotic degeneration. Such an approach may be provided by the use of MDSC where myostatin is genetically inactivated, i.e., obtained from the Mst KO mouse, under the assumption that myogenesis would be stimulated and the undesired lineage commitment reduced, even when implanted into a host tissue environment with normal myostatin expression. No reports are available on the in vitro and in vivo differentiation of these MDSC and how this affects, even paracrinely, muscle repair. Potential in vitro modulation of MDSC, or the effects that myostatin or dystrophin gene inactivation exert on this balance.

In the current study we have investigated the in vitro myogenic versus fibrogenic and adipogenic differentiation of Mst KO MDSC vis-à-vis the WT counterpart, and the effects of manipulation of these processes by modulating myostatin expression or activity, and by other putative regulators of muscle mass and fibrosis. Their differential in vitro features in terms of the expression of some key stem cell and myogenic genes, and the repair ability of Mst KO MDSC in the injured mdx muscle, were also studied. The ultimate goal is to gain a preliminary insight on how in vitro preconditioning of MDSC by pharmacological or gain of function approaches may modulate their capacity to repair dystrophic skeletal muscle, to design in vivo pharmacological interventions that may mimic these processes, and even myostatin blockade in the host muscle to activate myogenesis in the endogenous dystrophin negative MDSC. .

Methods

MDSC isolation

Mst knock-out mice (C57BL/6J/Mst-/-), referred to here as "Mst KO", are regularly maintained and bred in our vivarium on a BL/6 background [41], derived from the original strain on a Balb/c background. Aged-matched wild type control mice (C57BL/6J), referred to here as "WT", were from Jackson Laboratories. Hind limb muscles from the WT and Mst KO male mice (12-16 weeks old) were subjected to the preplating procedure to isolate MDSC , a well validated method that has led to extensively characterized stem cell populations [5,24-27,39,42]. Tissues were dissociated using sequentially collagenase XI, dispase II and trypsin, and after filtration through 60 μm nylon mesh and pelleting, the cells were suspended in Dulbecco's Modified Eagle's Medium (DMEM), with 10% fetal bovine serum (FBS), 10% horse serum, and 0.5% chick embryo extract. Cells were plated onto collagen I-coated flasks for 1 hr (preplate 1 or pP1), and 2 hrs (preplate 2 for pP2), followed by sequential daily transfers of non-adherent cells and re-platings for 2 to 6 days, until preplate 6 (pP6). The latter is the cell population containing MDSC. Sca1+ cells were selected with immunobeads (Milteny) coated with antibody against Sca1 as small size cells with large nucleus that easily form clusters/spheroids [24-27]. Cells were subjected to flow cytometry as below for the MDSC standard markers Sca1, CD34, and CD44, and for the key stem cell gene, Oct 4 [43], maintained in GM-20 (DMEM, with 20% FBS) on regular culture flasks (no coating) and used in the 14th-28th passage. WT MDSCs have been maintained in our laboratory for at least 40 generations with the same, or even increasing, growth rate**.**

Flow Cytometry

MDSC and KO cells were grown in GM-20, washed twice with Hanks, disaggregated by repeated pipeting in Cell Stripper (Mediatech, Manassas VA), pelleted, and resuspended in staining buffer consisting of PBS, 3% FBS, 0.01% Na azide (SB). Cells were incubated in the presence of antibodies for 30 min. on ice, washed twice with SB, and finally resuspended in SB for flow cytometry on an LSR II (BD Biosciences). Data analysis and plotting were done using FACSDiva Version 6.1.1 software. All fluorophore-conjugated antibodies and isotype controls were from eBioscience (San Diego, CA), as follows: CD44-APC-eFluor 780; CD34-eFluor 660; Sca1-PE; Oct 4-PE (performed separately, following cell permeabilization with BD

CytoFix/CytoPerm Kit), and the appropriate rat isotype controls IgG2b-APC-eFluor 780, IgG2a-eFluor 660, and IgG2a-PE. BD CompBeads (rat) were used for compensation.

Stem cell characterization, differentiation, and modulation

MDSC cultures were analyzed for the expression of stem cell markers below, on collagen-coated 6-well plates and 8-removable chamber plates. Multipotency was analyzed in 2-week incubations with GM-20 or GM-10 (GM with 10% FBS) supplemented or not with 10 nM DMSO or 5 ng/ml TGFβ1, or, to induce myofiber formation, after reaching confluence, for 2-3 weeks with Hedrick's medium (Dulbecco modified Eagle medium, 10% FBS-5% horse serum and 50 μm hydrocortisone to promote proliferation, a key event in myogenic differentiation) [44,45], or as described. In certain cases, cultures were treated with or without 20 μM 5'-azacytidine (AZCT) in GM-20 for 3 days to induce multipotency, prior to switching them to the appropriate medium [11,14,44].

For the tests on the modulation of MDSC skeletal myotube formation by various factors, cells were allowed to reach confluence, switched to Hedrick's medium, and incubated for 2 weeks with 2 μg/ml recombinant 113 amino acid myostatin protein (R-Mst), a recombinant 16 kDa protein containing 113 amino acid residues of the human myostatin protein (BioVendor Laboratory Medicine Inc., Palackeho, Czech Republic) [14], or with a recombinant mouse follistatin protein (RD Systems, Minneapolis, MN) at 0.2 μg /ml [11,14], changing medium twice a week. In other experiments, incubations with the monoclonal (Chemicon International, Temecula, CA) and polyclonal (Millipore Corp, Billerica, MA) antibodies against myostatin (1:20) were substituted for the previous treatments Alternatively, the adenoviruses expressing the mouse myostatin full-length cDNA under the CMV promoter (AdV-CMV-Mst375) and an shRNA, which targets myostatin RNA and inhibits more than 95% of myostatin gene expression [11,14,17] (AdV-Mst shRNA) were transduced into MDSC at 80% confluence. Then cells were switched to Hedrick's medium as above.

Implantation of MDSC into skeletal muscle

Male mdx mice (C57BL/6/10ScSn-Dmd^{mdx}), referred to here as "mdx", obtained from Jackson Laboratories (Bar Harbor, ME) were allowed to reach 10 months of age, in order to allow lipofibrotic degeneration to become more evident, not only in the diaphragm but also in the gastrocnemius. In contrast, in young animals (12-16 weeks of age) the first round of muscle necrosis and regeneration has already subsided ("stable phase").

Mice were treated according to National Institutes of Health (NIH) regulations with an Institutional Animal Care and Use Committee-approved protocol. In one experiment, the WT and mdx MDSCs (0.5–1.0 × 10^6 cells/50 µL saline) were labeled with the nuclear fluorescent stain 4',6-diamidino-2-phenylindole (DAPI) [24-27], and implanted aseptically under anesthesia into the surgically exposed tibialis anterior. The muscle had been cryoinjured by pinching it for 10 seconds with a forceps cooled in liquid nitrogen immediately prior to implantation. Control mice with the same cryoinjury received saline. Mice were euthanized after 2 weeks, the tibialis excised and subjected to cryoprotection in 30% sucrose, embedding in OCT and cryosectioned.

In another experiment, the DAPI-labeled WT and Mst KO MDSCs (0.5 × 10^6 cells/50 µL GM) were implanted into the central region of the surgically exposed left gastrocnemius of 10 month old mdx mice, which four days earlier had been injured with two injections of notexin in both tips of the muscle (total: 0.2 µg in 10 µL saline). Control muscle injured mice were injected with saline (n=5/group). Mice were euthanized at 3 weeks, the gastrocnemius excised and a section around the site of notexin injection was used for cryosectioning. The remainder tissue was kept frozen at -80 °C.

Immunocytochemistry and dual immunofluorescence

Cells on collagen-coated eight-well removable chambers, fixed in 2% p-formaldehyde, and 10 µm unfixed frozen tissue sections, were reacted [10,11,14,17,24-27] with some of the following primary antibodies against: (1) human myosin heavy chain fast, detecting both MHC-IIa and MHC-IIb); monoclonal, 1:200 Vector Laboratories, Burlingame, CA, USA), a marker for skeletal myotubes and myofibers; (2) human αSMA (mouse monoclonal in Sigma kit, 1:2, Sigma Chemical, St Louis, MO, USA), a marker for both SMC and myofibroblasts; (3) neurofilament 70 (NF70; mouse monoclonal, 1:10, Millipore, Billerica, Massachusetts, USA); (4) Dystrophin (rabbit polyclonal, 1:200 Abcam, Cambridge, Massachusetts, USA); (5) Sca-1 (mouse monoclonal, 1:100, BD Pharmingen, San Jose, CA) and M.O.M blocking kit (Vector, Burlingame, CA), and 6) Oct-4 (rabbit polyclonal, 1:500, BioVision, Mountain View, CA). When MDSC on 8-well chambers were not previously tagged with DAPI, all nuclei were stained with coverslips with DAPI anti-fading emulsion

Cultures or tissue sections not involving DAPI labeling were subjected to immuno-histochemical detection by quenching in 0.3% H_2O_2, blocking with goat (or corresponding serum), and incubated overnight at 4 °C with the primary antibody. This was followed by biotinylated anti-mouse IgG (Vector Laboratories), respectively, for 30 min, the ABC complex containing avidin-linked horseradish peroxidase (1:100; Vector Laboratories), 3,3'

diaminobenzidine, and counterstaining with hematoxylin, or no counterstaining. For cells labeled with DAPI, fluorescent detection techniques were used. The secondary anti-mouse IgG antibody was biotinylated (goat, 1:200, Vector Laboratories) and this complex was detected with streptavidin-Texas Red. After washing with PBS, the sections were mounted with Prolong antifade (Molecular Probes, Carlsbad, CA, USA). Negative controls in all cases omitted the first antibodies or were replaced by IgG isotype. In the case of Oct-4, streptavidin-FITC was used (green fluorescence).

In tissue cryosections for experiments involving DAPI-labeled cells (10 μm), tissue sections were processed in regions where the DAPI + cells could be detected. Muscle fibers were either stained with hematoxylin/eosin, or by MHC-II antibody, either by Texas red fluorescence as above, or with the diaminobenzidine tetrahydrochloride-based detection method (Vectastain-Elite ABC kit; Vector Labs), counterstaining with Harris hematoxylin. Tissue sections that were incubated with mouse IgG instead of the primary antibody served as negative controls. The sections were viewed under an Olympus BH2 fluorescent microscope, and cell cultures under an inverted microscope. In some cases, the cytochemical staining was quantitated by image analysis using ImagePro-Plus 5.1 software (Media Cybernetics, Silver Spring, MD, USA) coupled to a Leica digital microscope bright field light fluorescence microscope/VCC video camera. After images were calibrated for background lighting, integrated optical density (IOD=area x average intensity) was calculated.

Gene transcriptional expression profiles

Pools of total cellular RNA from three T25 flasks for each MDSC cultured in DM-20 were isolated with Trizol-Reagent (Invitrogen, Carlsbad, CA), and subjected to DNAse treatment, assessing RNA quality by agarose gel electrophoresis. cDNA gene microarrays (SuperArray BioScience Corp., Frederick, MD) [11,24,41] were applied, using the mouse stem cell (OMM-405), Oligo GEArray microarray: Biotin-labeled cDNA probes were synthesized from total RNA, denatured, and hybridized overnight at 60 $^{\circ}$C in GEHybridization solution to these membranes. Chemiluminescent analysis was performed per the manufacturer's instructions. Raw data were analyzed using GEArray Expression Analysis Suite (SuperArray BioScience Corp., Frederick, MD). Expression values for each gene based on spot intensity were subjected to background correction and normalization with housekeeping genes, and then fold changes in relative gene expression were calculated

The expression of some of the down- or up-regulated genes detected above was examined on 1 μg RNA isolated from consecutive similar incubations performed in triplicate by

reverse transcription (RT) using a 16-mer oligo(dT) primer, as previously described [11,24], and the resulting cDNA was amplified using PCR in a total volume of 20 µl. The locations of the primers utilized for the quantitative estimation of mouse myostatin mRNA were nts 136–156 (forward) and 648–667 (reverse), numbering from the translation initiation codon (later called F2/R2) as previously described. For mouse GAPDH primers, sequences were from the mRNA sequence NM_008084.2, using a forward primer spanning nts 778-797 and reverse primer spanning nts 875-852, with a product length of 98 nt.

Additional primers were designed using the NCBI Primer Blast program applied to mRNA sequences and synthesized by Sigma-Aldrich. Numbering refers to the length in NT from the 5' end of the mRNA: Acta1 (skeletal muscle actin) NM_009606.2 (forward 501-520 and reverse 841-822, product length 341); Actc1 (cardiac actin) NM_009608.3 (forward 38-58 and reverse 554-530, product length 517); 4) MyoD NM_010866.2 (forward 515-534 and reverse 1013-994, product length 499); and 5) Pax3 NM_008781.4 (forward 1164-1183 and reverse 1893-1874, product length 730). The number of PCR cycles used for each primer set is stated in Figure 6. All primers were designed to include an exon-exon junction in the forward primer except for GAPDH and MyoD1. Negative controls omitted the reverse transcriptase.

Protein expression by western blots

Cells were homogenized in boiling lysis buffer (1% SDS, 1mM sodium orthovanadate, 10 mM Tris pH 7.4 and protease inhibitors, followed by centrifugation at 16,000 *g* for 5 min [10,11,14,17,24-27). 40 µg of protein were run on 7.5% or 10% polyacrylamide gels, and submitted to transfer and immunodetection with antibodies against: 1) human αSMA (monoclonal, 1:1000, Calbiochem, La Jolla, CA); 2) Oct-4, as for immunohistochemistry; 3) MyoD (rabbit polyclonal 1:200, Santa Cruz Biotechnology, Inc., Santa Cruz, CA); 4) MHC (fast), as for immunohistochemistry; 5) TGF-β1 (rabbit polyclonal 1:1000; Promega Corporation); 6) myostatin (rabbit polyclonal 1:1000; Chemicon International Inc, Temecula, CA), 7) ActRIIb (monoclonal, 1:1000, Abcam, Cambridge, MA); and 8) GAPDH (mouse monoclonal, 1:3000, Chemicon). Membranes were incubated with secondary polyclonal horse anti-mouse or anti-rabbit IgG linked to horseradish peroxidase (1:2000; BD Transduction Laboratories, Franklin Lakes, NJ, or 1:5000, Amersham GE, Pittsburgh, PA), and bands were visualized with luminol (SuperSignal West Pico, Chemiluminescent, Pierce, Rockford, IL). For the negative controls the primary antibody was omitted.

Statistics

Values are expressed as the mean (SEM). The normality distribution of the data was established using the Wilk–Shapiro test. Multiple comparisons were analyzed by a single factor ANOVA, followed by *post hoc* comparisons with the Newman–Keuls test. Differences among groups were considered statistically significant at $P < 0.05$.

Results

MDSC cultures from the Mst KO resemble their counterparts from WT mice in morphology, replication, cell markers and multipotent differentiation

WT MDSC (pP6 fraction) formed in vitro the most robust skeletal myotubes (see next section) at about passage 13, and both types of MDSC were compared from passages 10-28. The morphology of the proliferating cultures was similar but the replication times for the Mst KO MDSC were slower than for the WT MDSC (27.0 vs. 19.8 hrs, respectively) This morphology and replication pattern continued throughout the 13-28 passages period of study.

The WT MDSC culture was previously shown to be Sca 1+ [30], Sca1 selection was used for both cultures, and flow cytometry confirmed its expression in subconfluent cultures in DM-10 of both the WT and Mst KO MDSC (Figure 1A), with negligible isotype reaction. The similarity of both types of cells was evident as well for the expression of two MDSC markers CD34, CD44, and the key embryonic stem cell marker, Oct-4, even if the cell populations show some heterogeneity in the expression of these markers., Oct 4 in both MDSC cultures is similarly and considerably expressed mainly in the nuclei (the Oct-4A isoform) with some additional cytoplasmic staining (B). That MDSC have some embryonic stem cell features is also suggested by a mild alkaline phosphatase reaction, a feature of embryonic stem cells (C).
The stem cell nature of the nuclear Okt 4A expression was confirmed by the detection of the 45 kDa Okt 4A transcriptionally active protein accompanied in a lower extent by the 33 kDa Oct 4B of cytoplasmic origin (B bottom).

The similarity of the Mst KO and WT MDSC in term of the expression of other stem cell related genes was demonstrated by a DNA microarray analysis of a panel of 260 stem cell-related genes. Table 1 shows that there are not substantial differences in the expression of most well known embryonic stem cell genes such as c-Myc, Oct-4 (Pou5), alkaline phosphatase 2 and 5, telomerase reverse transcriptase, leukemia inhibitory factor (LIF), and mastermind like 1, among the other related genes. This agrees with the fact that the multilineage differentiation

capacity of these MDSC seems to be qualitatively similar among the three types, as shown by the generation in neurogenic medium of cells expressing the neuronal marker NF70 (Figure 2), and in fibrogenic medium of cells, presumably myofibroblasts, expressing α-smooth muscle actin (ASMA). However, the proportion of positive cells was lower in Mst KO MDSC and the cells expressing NF-70 lacked the more apparent neuronal morphology of the differentiated WT MDSC. Both MDSC cultures also differentiated similarly into cells expressing calponin as smooth muscle cell marker and von Willebrand factor as endothelial cell marker (not shown).

The genetic inactivation of myostatin is however associated with the loss of the ability of MDSC to form myotubes in vitro, and with the down-regulation of key myogenic genes

The WT MDSC form large polynucleated myotubes expressing MHC II in confluent cultures upon incubation for 1 to 2 weeks in the Hedrick's myogenic medium (Figure 3A,B). However, remarkably the Mst KO MDSC (C) were unable to generate any myotube under these conditions, even after 4 weeks. Immunofluorescence detected high MHC II expression in the robust myotubes from WT MDSC (D), but again no MHC II or myotubes were found in the Mst KO confluent cultures (not shown). This is also illustrated in the western blot analysis where the strong MHC II 210 kDa band in the WT MDSC extract is not seen in the confluent Mst KO MDSC (E). The early myogenic marker MyoD is expressed as expected in the non-confluent WT MDSC in GM-20 (non-myogenic medium), but very little in the Mst KO MDSC.

That this was not an artifact of poor myogenesis in the Hedrick's medium, was shown by the fact that although robust myotube formation in the WT MDSC occurred in GM-10 or GM-20 even if of smaller size (Figure 4B,C compared with A), not a single myotube was observed with confluent Mst KO MDSC in these media (not shown). WT MDSC myogenic differentiation in medium with high concentration of FBS indicates that cell to cell contact is sufficient to trigger MDSC myogenesis, and does not require growth factor depletion. No adipogenesis was detected with Oil red O in Hedrick's medium (not shown). Western blots of parallel confluent cultures of WT MDSC showed that MHC-II was expressed in all media (triplicate cultures), although more intensively in Hedrick's (D). There was no difference in MyoD expression among the different media.

The inability of confluent Mst KO in several media to form myotubes was irrespective of passage. Myotube formation by WT MDSC cultures persisted for up to 40 passages, although the size and number of the myotubes started to decline as the passage number increased. Cultures of pP5 or pP5 from Mst KO mice obtained during the pre-plating procedure also failed to generate skeletal myotubes. Despite the drastic obliteration of MHC II+ myotube formation in

confluent Mst MDSC, the transcriptional expression of most myogenesis related genes in the respective proliferating cells was, as in the case of the stem cell genes in Table 1, very similar. For instance, expression of BMPRs (bone morphogenic protein receptors), the Wnt signaling receptors frizzled and jag, IGF1, Notch 1, and Notch 3, was not reduced in Mst KO MDSC as compared with the WT MDSC (Table 2). However, six notable differences were noticed in which each gene was substantially down-regulated in the Mst KO MDSC, versus a strong expression in the WT MDSC. They are Spp1 (secreted phosphoprotein 1, or osteopontin), Actc 1 (cardiac α-actin), MyoD1, cadherin 15, Myf 5, and Notch 2 (see discussion). In contrast, other cadherins (11 and 6), related to neuromuscular development, were up-regulated by 9 and 4-fold, respectively, in the Mst KO MDSC. Other than these, there was a virtual 98% similarity among the three MDSC types in terms of the 260 genes investigated. There was an excellent correlation between MyoD mRNA expression in both cultures and the previously detected MyoD protein levels shown on Figure 3.

These results were corroborated by RT/PCR for some of the mRNAs described on the tables. Figure 5A shows the gel electrophoretic pattern after staining with ethidium bromide, and Figure 5B presents the densitometric values of each band from triplicate determinations corrected by the housekeeping gene values. These ratios are comparable between both MDSC cultures for each gene, but not among the different genes for each culture, because of the different number of cycles applied for the respective transcript amplification. Actc1, Acta1, and MyoD are significantly down-regulated in Mst KO as compared with WT MDSC, and Pax 3 is overexpressed, in good agreement with the DNA microarrays.

Myotube formation cannot be turned on in Mst KO MDSC by stem cell reactivating agents, and the WT MDSC are also refractory to positive or negative modulation of myostatin expression.

Incubation of Mst KO MDSC for 3 days with 5-azacytidine, a demethylating agent and potent inducer of myogenic capacity in pluripotent cell lines [11,14] prior to their reaching confluency and switching to myogenic medium, failed to induce myotube formation, but it also failed to stimulate it in the WT MDSC (not shown). Follistatin, that should upregulate myotube formation by binding myostatin, was also virtually ineffective on WT MDSC, and the same resistance to modulation was observed under recombinant myostatin that should exert the opposite effects, Figure 6A-D shows that the area occupied by MHC II + myotubes was not reduced in the cultures treated from the start of myotube induction with 2 μg/ml myostatin (B), or increased by 0.5 μg/ml follistatin (C), as compared to untreated controls (A). Changes were not

significant (D). This failure of myostatin and follistatin to affect myogenesis in any type of MDSC occurred despite these cells express the myostatin receptor ActRIIb, in both cultures, as shown by western blot (F), implying that they should be responsive to exogenous myostatin. Endogenous myostatin expression was not detected in any untreated culture (not shown), even if TGFβ1, another key member of the TGFβ family was expressed (E). Finally, neither the monoclonal nor the polyclonal antibodies against myostatin affected myogenesis in the WT MDSC as compared to the respective cultures incubated with control IgG (not shown).

This suggests that the WT MDSC ability to form myotubes is refractory to the modulation by myostatin, and this was confirmed by transfection with the AdV Mst cDNA construct, or alternatively with the AdV Mst shRNA which also expresses beta galactosidase, which did not inhibit or stimulate this process despite myostatin and beta galactosidase were respectively expressed. (not shown). The suppression of myotube formation in the Mst KO MDSC by myostatin genetic inactivation and the lack of response to demethylating agents, suggests that this is a complex imprinting process occurring during their embryological generation, of a different nature than the resistance to paracrine and autocrine myostatin modulators observed in the WT MDSC.

Mst KO MDSC stimulate myofiber repair in the injured aged gastrocnemius of the aged mdx mouse, but the absence of myostatin in these cells does not confer them a distinctive advantage over the WT MDSC

To test the persistence of MDSC after implantation into the muscle, DAPI-labeled cells were implanted into the cryolacerated gastrocnemius of the aged mdx mouse and frozen tissue was examined by immunocytofluorescence for MHC II after 2 weeks. Figure 7A shows that the blue fluorescent WT MDSC nuclei are detected in many of the red fluorescent myofibers and many of these nuclei are central, as may be expected from regenerating myofibers (yellow arrows). Other nuclei are seen in the interspersed connective tissue among the fibers. The Mst KO MDSC were not tested in this model. The MDSC implantation was then repeated into the notexin-injured muscle of aged mdx mice, using either WT or Mst KO cells, or vehicle, and sacrificing at 3 weeks. WT MDSC significantly stimulated by 54.5% the appearance of central nuclei on hematoxylin/eosin stained frozen tissue sections in comparison to control injured muscle receiving vehicle, as shown on a representative field (B). When the central nuclei were counted in tissue sections from the three mouse groups by quantitative image analysis, the Mst KO MDSC, that had failed to convert into myotubes in vitro, were now able in vivo to increase significantly by 42.4% the number of central nuclei in the myofibers in comparison to the vehicle

injected mice (C). However, this stimulation of myofiber repair did not surpass the efficacy of the WT MDSC, in contrary to what was originally expected from the absence of myostatin in the Mst KO MDSC.

These results were supported by the fact that Mst KO MDSC significantly increased the expression of MCH-II in the notexin-injured mdx aged muscle estimated by western blot, as compared to the vehicle-injected muscle, and this was slightly more effective than WT MDSC (Figure 8 left). It should be emphasized that this measurement was conducted in the central region of the muscle, distant from the notexin-injured sites at both ends of the muscle used for the tissue section studies, suggesting that the stimulatory effect on MHC-II expression by MDSC may have been even higher in the injured tissue. However, Mst KO MDSC did not reduce ASMA expression, an indicator of myofibroblast generation, and hence fibrosis, whereas the WT MDSC did decrease by 23% this expression (right)

Both WT and Mst KO skeletal muscles show dystrophin expression on frozen sections by the sarcolemma immunofluorescence around the myofibers (Figure 9A), a gene that is carried by their respective MDSC. Some of the myofibers in the mdx muscle, negative for dystrophin, which were implanted with either Mst KO MDSC or WT MDSC show a partial dystrophin+ staining of the sarcolemma in one of the areas of some sections and not in others (B) that however do contain myofibers (C). This suggests that there is some conversion or fusion of the implanted MDSC into myofibers, but that this process may be much less frequent than the stimulation of myofiber differentiation or fusion.

As expected, fat infiltration is visible in the injured aged gastrocnemius from vehicle-injected aged mdx mice, mainly interstitially but also as Oil Red O+ small regions around or inside myofibers (Figure 10A,B). WT MDSC were effective in reducing significantly this fat infiltration by 68%, and Mst KO MDSC also induced a decrease, although it was not significant (Figure 10C).

Discussion

To our knowledge this is the first report testing the myogenic capacity of MDSC isolated from transgenic mice with inactivation of the myostatin gene, in comparison to the WT MDSC, both in vitro and in the injured muscle of the aged mdx mice in vivo [23,39]. Our main findings were: a) in contrast to WT MDSC, Mst KO MDSC were unable to form myotubes in vitro, despite no major differences were found between both MDSC cultures in terms of morphology,

replication rates, expression of most members of a subset of key embryonic-like stem cell and other markers, and non-myogenic multi-lineage differentiation; b) however, a fundamental difference is that the expression of key genes in myogenesis seen in WT MDSC such as actc1, acta1, and myoD, was virtually obliterated in Mst KO; c) surprisingly, both types of MDSC were refractory in vitro to the modulation or induction of myotube formation by well known regulators of this process, or of myofiber number in vivo, such as demethylating agents, myostatin inhibition or overexpression, or follistatin, despite myostatin receptors are expressed in MDSC cultures; d) the myofiber regeneration and anti-lipofibrotic, capacities of WT MDSC were evident even in the environment of a severely injured mdx gastrocnemius at an age where lipofibrotic degeneration is considerable; e) in turn, these capacities, blocked in cell culture, were recovered in Mst KO MDSC when they were implanted in the injured mdx aged muscle setting, even if not at the level expected from the supposed paracrine effects triggered in the MDSC by the absence of myostatin.

The WT MDSC used here as control, fulfill all the criteria that have been extensively defined as potential tools for skeletal muscle, cardiac, and osteogenic repair upon implantation into the target organs [29,34]. In the current work, MDSC were isolated as the pP6 fraction using the extensively validated preplating procedure on collagen-coated flasks and Sca1 selection, and shown to have the expected morphology, rapid replication for at least 50 passages, express MDSC markers such as Sca1, CD24 and CD34, and the stem cell gene Oct 4, and the ability differentiate in vitro into multiple cell lineages. The latter capability includes a robust formation of multinucleated and branched myotubes that is assumed to translate in vivo into their ability to donate their nuclei to injured skeletal myofibers or at least to paracrinely stimulate their regeneration. This is evidenced by a much higher number of centrally located nuclei, and even some central location of the DAPI-labeled implanted nuclei. In previous studies we had shown that WT MDSC generate at least smooth muscle and epithelial cells when implanted into urogenital tissues [24,25], adding up to the extensive demonstration of their stem cell nature [7,12,23,46] related to their putative origin as myoendothelial stem cells in the muscle and other tissues [47] Another novel finding here is that WT MDSC have some embryonic-like stem cell features, mainly the expression of nuclear Oct-4 A, myc, LIF, and other embryonic stem cell genes. Okt 4 is a key not only for embryonic stem cell programming, but also for iPS generation, where it can act virtually by itself [48]. Our MDSC cultures contain some tiny rounded cells similar to the very small embryonic-like stem cells (VSEL) described in many adult organs [49], and other larger ones.

An important finding is the unexpected observation that myotube formation by the WT MDSC in vitro is refractory to modulation by agents that are well known to affect this process, or skeletal muscle mass in vivo. The fact that myotube formation by WT MDSC was not influenced by: a) demethylating agents like azacytidine that stimulate 'stemness" in cell lines [44]; b) downregulation or overexpression of myostatin, despite the detectable expression of its receptor (ActIIb); b) counteracting myostatin activity by the respective antibodies or follistatin, that in vivo stimulate myofiber growth [18-20]; poses questions related to the role of MDSC during normal myogenesis. A study showing that myostatin stimulated fibroblast proliferation in vitro and induced its differentiation into myofibroblasts, while increasing TGFβ1 expression in C2C12 myoblasts, did not examine MDSC differentiation [12]. The claim of a small inhibitory effect of myostatin on the fusion index in MDSC [46] may indicate less fusion efficiency but might not entirely reflect the actual effects on the number and size of myotubes, as determined here. This question requires further clarification in terms of the actual modulation of MDSC differentiation.

It may be speculated that satellite cells rather than MDSC are the only myogenic progenitors during normal myofiber growth, as opposed to repair of damaged fibers [50]. Therefore the selected in vitro conditions may not mimic the repair process, or alternatively unknown in vivo paracrine or juxtacrine modulators may modify the response of MDSC to the better characterized agents tested in this work. Another possibility is that myostatin and other modulators investigated here would stimulate in vivo satellite cell replication and fusion to the adjacent myofibers to induce hypertrophy, without truly affecting MDSC differentiation or fusion.

We are unaware of any report on the isolation or characterization of MDSC from the Mst KO. Therefore, it is also both novel and unexpected to find that these cells obtained from the same skeletal muscles as the WT MDSC, using identical procedures, and displaying rather similar non-myogenic pluripotency and stem cell marker features, are however completely unable to form myotubes in vitro. In fact, our prediction was that the Mst KO MDSC should be more myogenic than the WT MDSC because of the absence of the myogenic inhibitor myostatin, The fact that Mst replenishment, either as recombinant protein or as cDNA does not counteract the unexpected myogenic blockade found in the Mst KO MDSC, suggests speculatively that these cells have been imprinted in the embryo by the myostatin genetic inactivation through down-stream pathways that have become unresponsive to the invitro myostatin modulation that we explored here. This may involve genes in other myogenic pathways whose expression may be altered as we observed in Mst KO MDSC However, validation of this assumption requires further investigation.

An interesting corollarium is the activation of the in vitro-suppressed myogenesis in Mst KO MDSC, and/or their ability to fuse with preexisting myofibers, after their implantation into the notexin-injured mdx gastrocnemius. At the age selected (10 month-old), this muscle experiences the considerable damage that occurs in the diaphragm much earlier [3,4], and this is compounded by injury. It may be speculated that the restoration of myotube (myofiber) formation by Mst KO MDSC in this setting occurs by paracrine or juxtacrine modulation, possibly of some of the key genes silenced in these cells. Estimation of their products and proof-of-function approaches may elucidate this issue. The fact that despite Mst KO MDSC being able to fuse with or differentiate into new myofibers, they do not increase the muscle repair process in a clearly more efficient way than WT MDSC, may possibly result from the persistent myostatin expression in the fibers that may counteract its absence in Mst KO MDSC. This suggests the need to block systemically myostatin in the host muscle, not just in the implanted MDSC.

One of the genes that may be involved in the silencing of Mst KO MDSC myogenesis in vitro and its reactivation in vivo is the cardiac α-actin (Actc) the major striated actin in fetal skeletal muscle and in adult cardiomyocytes, but strongly down-regulated in adult skeletal muscle to 5% of the total striated actin [51], whose mRNA is highly expressed in the proliferating (non-differentiating) WT MDSC but at very low level in the Mst KO MDSC. The same applies to the α1-actin (Acta1) mRNA, the adult protein encoding thin filaments [52]. Since actins are so crucial for cell division, motility, cytoskeleton, and contraction, and mutations are associated with severe myopathies, it would not be surprising that their down-regulation could cause to the lack of myogenic commitment in vitro in Mst KO.

Similarly, the striking transcriptional down-regulation of myoD, a critical early gene in skeletal myogenesis [53], confirmed at the protein level, and of secreted phosphoprotein 1, or osteopontin, a gene mostly involved in ossification, inflammation, and fibrosis, but postulated recently to participate in early myogenesis and skeletal muscle regeneration [54], may also trigger the absence of myogenic capacity in Mst KO. Interestingly, the fact that Pax 3 mRNA, upstream of MyoD in the myogenic signaling [55] is expressed in Mst KO MDSC at higher levels than in WT MDSC, suggests that the myogenic commitment of Mst KO and mdx MDSC is arrested at some point in between these genes. Since a critical regulator of skeletal muscle development, Mef2a (Myocyte enhancer factor 2a) [56], is expressed similarly in both MDSC (as Pax 3 is), albeit at very low levels, the silencing may occur at the level of the satellite cell marker, Pax 7. Therefore, it is not surprising that expression of a member of the cadherin family (cadherin-15) that is involved in later stages such as myoblast differentiation and fusion [57] is so down-regulated in Mst KO MDSC.

Conclusions

Our results show that MDSC obtained from wild type and transgenic mice lacking myostatin express Oct-4 and other embryonic like stem cell genes and appear similar in most features, except for the null or poor expression in Mst KO MDSC of some critical early genes. These genes encode factors critical for myogenesis and for maintaining the integrity of myotubes and myofibers, thus possibly leading to their inability to form myotubes in vitro. The cross-talk of Mst KO MDSC with myofibers and other cell types in the host injured mdx muscle may release the pertinent gene silencing and restore the typical myogenic ability of the MDSC. Although our results do not prove the initial working hypothesis that myostatin inactivation would enhance the myogenic capacity of MDSC, this possibility still needs further in vivo testing by blocking myostatin not just in the implanted MDSC but in the host muscle with follistatin, shRNA, antibodies, or other procedures. Finally, systemic muscle-targeted WT MDSC implantation that was previously shown as a promising approach to stimulate repair in the adult dystrophic muscle [5,12,38,39], may be even effective in the setting of an injured aged dystrophic skeletal muscle with severe bouts of necrosis [4].

Abbreviations: AdV-CMV-Mst375: adenovirus construct expressing the mouse myostatin full-length cDNA under the CMV promoter**; AdV-Mst shRNA:** shRNA against myostatin RNA; **ASMA:** α-smooth muscle actin; **MDSC**: muscle derived stem cells; **Mst KO**: myostatin knock out mouse; **QIA:** quantitative image analysis**; TGF β1**: transforming growth factor β1. **VSEL:** very small embryonic-like stem cells. **WT:** wild type mouse.

Competing interests

None.

Authors' contributions

GCNF conceived, designed and coordinated the study and wrote the article. TJ and KI performed the animal studies and participated in the immunoassays. VD and NG carried out the in vitro cell culture studies and performed the protein assays. GR performed the molecular genetic studies, RNA isolation and flow cytometry, and participated in the immunoassays. KI

participated in the histochemistry and immunoassays and edited the article. BKW helped carried out the flow cytometry studies. All authors performed statistical analyses, read and approved the final manuscript.

Acknowledgements

This work was supported by DOD W81XWH-07-1-0181 grant, and partially by NIH R21DK-070003 grant, to NGC

References

1. Desguerre I, Mayer M, Leturcq F, Barbet JP, Gherardi RK, Christov C. **Endomysial fibrosis in Duchenne muscular dystrophy: a marker of poor outcome associated with macrophage alternative activation.** *J Neuropathol Exp Neurol* 2009, **68**:762-773.

2. Sun G, Haginoya K, Wu Y, Chiba Y, Nakanishi T, Onuma A, Sato Y, Takigawa M, Iinuma K, Tsuchiya S. **Connective tissue growth factor is overexpressed in muscles of human muscular dystrophy.** *J Neurol Sci* 2008, **267**:48-56.

3. Ishizaki M, Suga T, Kimura E, Shiota T, Kawano R, Uchida Y, Uchino K, Yamashita S, Maeda Y, Uchino M. **Mdx respiratory impairment following fibrosis of the diaphragm.** *Neuromuscul Disord* 2008, **18**:342-348.

4. Alexakis C, Partridge T, Bou-Gharios G. **Implication of the satellite cell in dystrophic muscle fibrosis: a self-perpetuating mechanism of collagen overproduction.** Am J Physiol *Cell Physiol* 2007, **293**:C661-669.

5. Huang P, Zhao XS, Fields M, Ransohoff RM, Zhou L. **Imatinib attenuates skeletal muscle dystrophy in mdx mice.** *FASEB J* 2009, **23**:2539-2548.

6. Whitehead NP, Yeung EW, Allen DG. **Muscle damage in mdx (dystrophic) mice: role of calcium and reactive oxygen species.** *Clin Exp Pharmacol Physiol* 2006, **33**:657-662.

7. Deasy BM, Feduska JM, Payne TR, Li Y, Ambrosio F, Huard J. **Effect of VEGF on the regenerative capacity of muscle stem cells in dystrophic skeletal muscle.** *Mol The*. 2009, **17**:1788-1798.

8. Tsuchida K. **Targeting myostatin for therapies against muscle-wasting disorders.** *Curr Opin Drug Discov Devel* 2008, **11**:487-494.

9. Li ZB, Kollias HD, Wagner KR. **Myostatin directly regulates skeletal muscle fibrosis.** *J Biol Chem* 2008, **283**:19371-19378.

10. Cantini LP, Ferrini MG, Vernet D, Magee TR, Qian A, Gelfand RA, Rajfer J, Gonzalez-Cadavid NF. **Profibrotic role of myostatin in Peyronie's disease.** *J Sex Med* 2008, **5**:1607-1622.

11. Artaza JN, Singh R, Ferrini MG, Braga M, Tsao J, Gonzalez-Cadavid NF. **Myostatin promotes a fibrotic phenotypic switch in multipotent C3H 10T1/2 cells without affecting their differentiation into myofibroblasts.** *J Endocrinol* 2008, **196**:235-249.

12. Zhu J, Li Y, Shen W, Qiao C, Ambrosio F, Lavasani M, Nozaki M, Branca MF, Huard J. **Relationships between transforming growth factor-beta1, myostatin, and decorin: implications for skeletal muscle fibrosis**. *J Biol Chem* 2007, **282**:25852-25863.

13. Guo T, Jou W, Chanturiya T, Portas J, Gavrilova O, McPherron AC. **Myostatin inhibition in muscle, but not adipose tissue, decreases fat mass and improves insulin sensitivity.** *PLoS One* 2009, **4**:e4937.

14. Artaza JN, Bhasin S, Magee TR, Reisz-Porszasz S, Shen R, Groome NP, Meerasahib MF, Gonzalez-Cadavid NF. **Myostatin inhibits myogenesis and promotes adipogenesis in C3H 10T(1/2) mesenchymal multipotent cells.** *Endocrinology* 2005, **146**:3547-3557.

15. Morine KJ, Bish LT, Pendrak K, Sleeper MM, Barton ER, Sweeney HL **Systemic myostatin inhibition via liver-targeted gene transfer in normal and dystrophic mice.** *PLoS One* 2010, **5**:e9176.

16. Dumonceaux J, Marie S, Beley C, Trollet C, Vignaud A, Ferry A, Butler-Browne G, Garcia L. **Combination of Myostatin Pathway Interference and Dystrophin Rescue Enhances Tetanic and Specific Force in Dystrophic mdx Mice.** *Mol Ther* 2010, **18**:881-887.

17. Magee TR, Artaza JN, Ferrini MG, Vernet D, Zuniga FI, Cantini L, Reisz-Porszasz S, Rajfer J, Gonzalez-Cadavid NF. **Myostatin short interfering hairpin RNA gene transfer increases skeletal muscle mass.** *J Gene Med* 2006, **8**:1171-1181.

18. Tsuchida K. **Myostatin inhibition by a follistatin-derived peptide ameliorates the pathophysiology of muscular dystrophy model mice.** *Acta Myol* 2008, **27**:14-18.

19. Colussi C, Gaetano C, Capogrossi MC **AAV-dependent targeting of myostatin function: follistatin strikes back at muscular dystrophy.** *Gene Ther* 2008, **15**:1075-1076.

20. Nakatani M, Takehara Y, Sugino H, Matsumoto M, Hashimoto O, Hasegawa Y, Murakami T, Uezumi A, Takeda S, Noji S, Sunada Y, Tsuchida K. **Transgenic expression of a myostatin inhibitor derived from follistatin increases skeletal muscle mass and ameliorates dystrophic pathology in mdx mice.** *FASEB J* 2008, **22**:477-487.

21. Tedesco FS, Dellavalle A, Diaz-Manera J, Messina G, Cossu G. **Repairing skeletal muscle: regenerative potential of skeletal muscle stem cells.** *J Clin Invest* 2010, **120**:11-19.

22. Relaix F, Marcelle C. **Muscle stem cells.** *Curr Opin Cell Biol* 2009, **21**:748-753.

23. Quintero AJ, Wright VJ, Fu FH, Huard J. **Stem cells for the treatment of skeletal muscle injury.** *Clin Sports Med* 2009, **28**:1-11.

24. Ho MH, Heydarkhan S, Vernet D, Kovanecz I, Ferrini MG, Bhatia NN, Gonzalez-Cadavid NF. **Stimulating vaginal repair in rats through skeletal muscle-derived stem cells seeded on small intestinal submucosal scaffolds**. *Obstet Gynecol* 2009, **114**:300-309.

25. Nolazco G, Kovanecz I, Vernet D, Gelfand RA, Tsao J, Ferrini MG, Magee T, Rajfer J, Gonzalez-Cadavid NF. **Effect of muscle-derived stem cells on the restoration of corpora cavernosa smooth muscle and erectile function in the aged rat.** *BJU Int* 2008, **101**:1156-1164.

26. Kovanecz I Rivera S, Nolazco G, Vernet D, Rajfer J, Gonzalez-Cadavid NF. **Long- term daily low doses of sildenafil, molsidomine and corporal inplantation of muscle derived stem cells (MDSC) alone or in combination, prevent corporal veno-oclusive dysfunction (CVOD) in a rat model of cavernosal nerve damage** [abstract]**.** *J Urol* 2011, **185**:e452-453.

27. Wang JS-C, Kovanecz I, Vernet D, Nolazco G , Kopchok GE, Chow SL, White RA, Gonzalez-Cadavid N. **Effects of sildenafil and/or muscle-derived stem cells on myocardial infarction.** *J Translat Med* 2012, revision after preliminary acceptance

28. Manceau M, Gros J, Savage K, Thomé V, McPherron A, Paterson B, Marcelle C. **Myostatin promotes the terminal differentiation of embryonic muscle progenitors.** *Genes Dev* 2008, **22**:668-681.

29. Guo W, Flanagan J, Jasuja R, Kirkland J, Jiang L, Bhasin S. **The effects of myostatin on adipogenic differentiation of human bone marrow-derived mesenchymal stem cells are mediated through cross-communication between Smad3 and Wnt/beta-catenin signaling pathways.** *J Biol Chem*, 2008, **283**:9136-9145.

30. Hamrick MW, Shi X, Zhang W, Pennington C, Thakore H, Haque M, Kang B, Isales CM, Fulzele S, Wenger KH. **Loss of myostatin (GDF8) function increases osteogenic differentiation of bone marrow-derived mesenchymal stem cells but the osteogenic effect is ablated with unloading.** *Bone* 2007, **40**:1544-1553.

31. Yamada M, Tatsumi R, Yamanouchi K, Hosoyama T, Shiratsuchi S, Sato A, Mizunoya W, Ikeuchi Y, Furuse M, Allen RE. **High concentrations of HGF inhibit skeletal muscle satellite cell proliferation in vitro by inducing expression of myostatin: a possible mechanism for**

reestablishing satellite cell quiescence in vivo. *Am J Physiol Cell Physiol* 2010, **298**:C465-476.

32. Trendelenburg AU, Meyer A, Rohner D, Boyle J, Hatakeyama S, Glass DJ. **Myostatin reduces Akt/TORC1/p70S6K signaling, inhibiting myoblast differentiation and myotube size.** *Am J Physiol Cell Physiol* 2009, **296**:C1258-1270.

33. Benabdallah BF, Bouchentouf M, Rousseau J, Bigey P, Michaud A, Chapdelaine P, Scherman D, Tremblay JP. **Inhibiting myostatin with follistatin improves the success of myoblast transplantation in dystrophic mice.** *Cell Transplant* 2008, **17**:337-350.

34. Motohashi N, Uezumi A, Yada E, Fukada S, Fukushima K, Imaizumi K, Miyagoe-Suzuki Y, Takeda S. **Muscle CD31(-) CD45(-) side population cells promote muscle regeneration by stimulating proliferation and migration of myoblasts.** *Am J Pathol* 2008, **173**:781-791.

35. Cerletti M, Jurga S, Witczak CA, Hirshman MF, Shadrach JL, Goodyear LJ, Wagers AJ. **Highly efficient, functional engraftment of skeletal muscle stem cells in dystrophic muscles.** *Cell* 2008, **134**:37-47.

36. Quenneville SP, Chapdelaine P, Skuk D, Paradis M, Goulet M, Rousseau J, Xiao X, Garcia L, Tremblay JP. **Autologous transplantation of muscle precursor cells modified with a lentivirus for muscular dystrophy: human cells and primate models.** *Mol Ther* 2007, **15**:431-438.

37. Bachrach E, Perez AL, Choi YH, Illigens BM, Jun SJ, del Nido P, McGowan FX, Li S, Flint A, Chamberlain J, Kunkel LM. **Muscle engraftment of myogenic progenitor cells following intraarterial transplantation.** *Muscle Nerve* 2006, **34**:44-52.

38. Lavasani M, Lu A, Peng H, Cummins J, Huard J. **Nerve growth factor improves the muscle regeneration capacity of muscle stem cells in dystrophic muscle.** *Hum Gene Ther* 2006, **17**:180-192.

39. Urish K, Kanda Y, Huard J. **Initial failure in myoblast transplantation therapy has led the way toward the isolation of muscle stem cells: potential for tissue regeneration.** Curr *Top Dev Biol* 2005, **68**:263-280.

40. Mouly V, Aamiri A, Périé S, Mamchaoui K, Barani A, Bigot A, Bouazza B, François V, Furling D, Jacquemin V, Negroni E, Riederer I, Vignaud A, St Guily JL, Butler-Browne GS. **Myoblast transfer therapy: is there any light at the end of the tunnel?** *Acta Myol* 2005, **24**:128-133.

41. Reisz-Porszasz S, Bhasin S, Artaza JN, Shen R, Sinha-Hikim I, Hogue A, Fielder TJ, Gonzalez-Cadavid NF. **Lower skeletal muscle mass in male transgenic mice with muscle-specific overexpression of myostatin.** *Am J Physiol Endocrinol Metab* 2003, **285**:E876-888.

42. Gharaibeh B, Lu A, Tebbets J, Zheng B, Feduska J, Crisan M, Péault B, Cummins J, Huard J. **Isolation of a slowly adhering cell fraction containing stem cells from murine skeletal muscle by the preplate technique.** *Nat Protoc* 2008, **3**:1501-1509.

43. Liedtke S, Stephan M, Kögler G. **Oct4 expression revisited: potential pitfalls for data misinterpretation in stem cell research.** *Biol Chem* 2008, **389**:845-850.

44. Singh R, Artaza JN, Taylor WE, Gonzalez-Cadavid NF, Bhasin S. **Androgens stimulate myogenenic differentiation and inhibit adipogenesis in C3H 10T1/2 pluripotent stem cells through an androgen receptor-mediated pathway.** *Endocrinology* 2003, **144**:5081-5088.

45. Mizuno H, Zuk PA, Zhu M, Lorenz HP, Benhaim P, Hedrick MH. **Myogenic differentiation by human processed lipoaspirate cells.** *Plast Reconstr Surg* 2002, **109**:199-209.

46. Nozaki M, Li Y, Zhu J, Ambrosio F, Uehara K, Fu FH, Huard J. **Improved muscle healing after contusion injury by the inhibitory effect of suramin on myostatin, a negative regulator of muscle growth.** Am J Sports Med 2008, **36**:2354-2362.

47. Crisan M, Yap S, Casteilla L, Chen CW, Corselli M, Park TS, Andriolo G, Sun B, Zheng B, Zhang L, Norotte C, Teng PN, Traas J, Schugar R, Deasy BM, Badylak S, Buhring HJ, Giacobino JP, Lazzari L, Huard J, Péault B. **A perivascular origin for mesenchymal stem cells in multiple human organs.** *Cell Stem Cell* 2008, **3**:301-313.

48. Ratajczak MZ, Zuba-Surma EK, Shin DM, Ratajczak J, Kucia M. **Very small embryonic-like (VSEL) stem cells in adult organs and their potential role in rejuvenation of tissues and longevity.** *Exp Gerontol* 2008, **43**:1009-1017.

49 Giorgetti A, Montserrat N, Rodriguez-Piza I, Azqueta C, Veiga A, Izpisúa Belmonte JC. **Generation of induced pluripotent stem cells from human cord blood cells with only two factors: Oct4 and Sox2.** *Nat Protoc* 2010, **5**:811-820.

50. Pallafacchina G, François S, Regnault B, Czarny B, Dive V, Cumano A, Montarras D, Buckingham M. **An adult tissue-specific stem cell in its niche: a gene profiling analysis of in vivo quiescent and activated muscle satellite cells.** *Stem Cell Res* 2010, **4**:77-91.

51. Nowak KJ, Ravenscroft G, Jackaman C, Filipovska A, Davies SM, Lim EM, Squire SE, Potter AC, Baker E, Clément S, Sewry CA, Fabian V, Crawford K, Lessard JL, Griffiths LM, Papadimitriou JM, Shen Y, Morahan G, Bakker AJ, Davies KE, Laing NG. **Rescue of skeletal muscle alpha-actin-null mice by cardiac (fetal) alpha-actin.** *J Cell Biol* 2009, **185**:903-915.

52. Ochala J. **Thin filament proteins mutations associated with skeletal myopathies: defective regulation of muscle contraction.** *J Mol Med* 2008, **86**:1197-1204.

53. Rudnicki MA, Le Grand F, McKinnell I, Kuang S. **The molecular regulation of muscle stem cell function.** *Cold Spring Harb Symp Quant Biol* 2008, **73**:323-31.

54. Uaesoontrachoon K, Yoo HJ, Tudor EM, Pike RN, Mackie EJ, Pagel CN. **Osteopontin and skeletal muscle myoblasts: association with muscle regeneration and regulation of myoblast function in vitro.** *Int J Biochem Cell Biol* 2008, **40**:2303-2314.

55. Lagha M, Kormish JD, Rocancourt D, Manceau M, Epstein JA, Zaret KS, Relaix F, Buckingham ME. **Pax3 regulation of FGF signaling affects the progression of embryonic progenitor cells into the myogenic program.** *Genes Dev* 2008, **22**:1828-1837.

56. Liu N, Williams AH, Kim Y, McAnally J, Bezprozvannaya S, Sutherland LB, Richardson JA, Bassel-Duby R, Olson EN. **An intragenic MEF2-dependent enhancer directs muscle-specific expression of microRNAs 1 and 133.** *Proc Natl Acad Sci USA* 2007, **104**:20844-2089.

57. Hsiao SP, Chen SL. **Myogenic regulatory factors regulate M-cadherin expression by targeting its proximal promoter elements.** *Biochem J* 2010, **428**:223-233

Tables

TABLE 1. Some stem cell-related genes are transcribed similarly in MDSC irrespective of myostatin or dystrophin genetic inactivation RNA from the three MDSC types at 80% confluence (not undergoing myogenesis) were treated by DNAse and submitted to DNA microarrays. Some key stem cell genes are selected. Values are relative expression levels normalized by housekeeping genes. GAPDH expression was 98-102.

GENE	FUNCTION	WT	KO
Myc	**Myelocytomatosis oncogene**	**12.4**	**18.1**
Pou5F1	**Pou domain (Oct4)**	**10.1**	**16.7**
Akp 2	**Alkaline Phosphatase 2**	**6.4**	**6.9**
Akp 5	**Alkaline Phosphatase 5**	**1.2**	**1.6**
Tert	**Telomerase reverse transcriptase**	**1.0**	**1.0**
Utf 1	**Undifferentiated embryonic cell TP1**	**1.0**	**0.8**
Man 1	**Mastermind like 1**	**13.1**	**16.7**
Lif	**Leukemia inhibitory factor**	**1.5**	**0.9**
PPARγ	**Peroxisome proliferating ARγ**	**1.1**	**1.8**

TABLE 2. Some key skeletal myogenesis-related genes are downregulated in MDSC by myostatin or dystrophin genetic inactivation, whereas others remain unchanged. See Table 1 for further description.

GENE	FUNCTION	WT	KO
Spp1	Secreted phosphoprotein 1 (osteopontin)	70.8	20.3
Actc 1	α actin (cardiac)	39.9	6.5
Myo D1	Myogenic differentiation 1	17.5	2.7
Cadherin 15	Cadherin 15	8.7	1.7
Myf 5	Myogenic factor 5	4.2	2.7
Notch 2	Notch gene homolog 2	4.2	2.8
BMPR 2	Bone morphogenetic receptor 2	23.3	20.3
BMPR 1a	Bone morphogenetic receptor 1a	8.1	10.4
BMPR 1b	Bone morphogenetic receptor 1b	0.8	0.8
BMPR 4	Bone morphogenetic protein 4	2.7	2.7
IGF 1	Insulin-like growth factor 1	5.1	4.2
Jag 1	Jagged 1	2.8	3.4
Fzd 1	Frizzled homolog 1	2.7	2.8
Notch 1	Notch gene homolog 1	2.6	2.7
Notch 3	Notch gene homolog 3	2.8	2.6

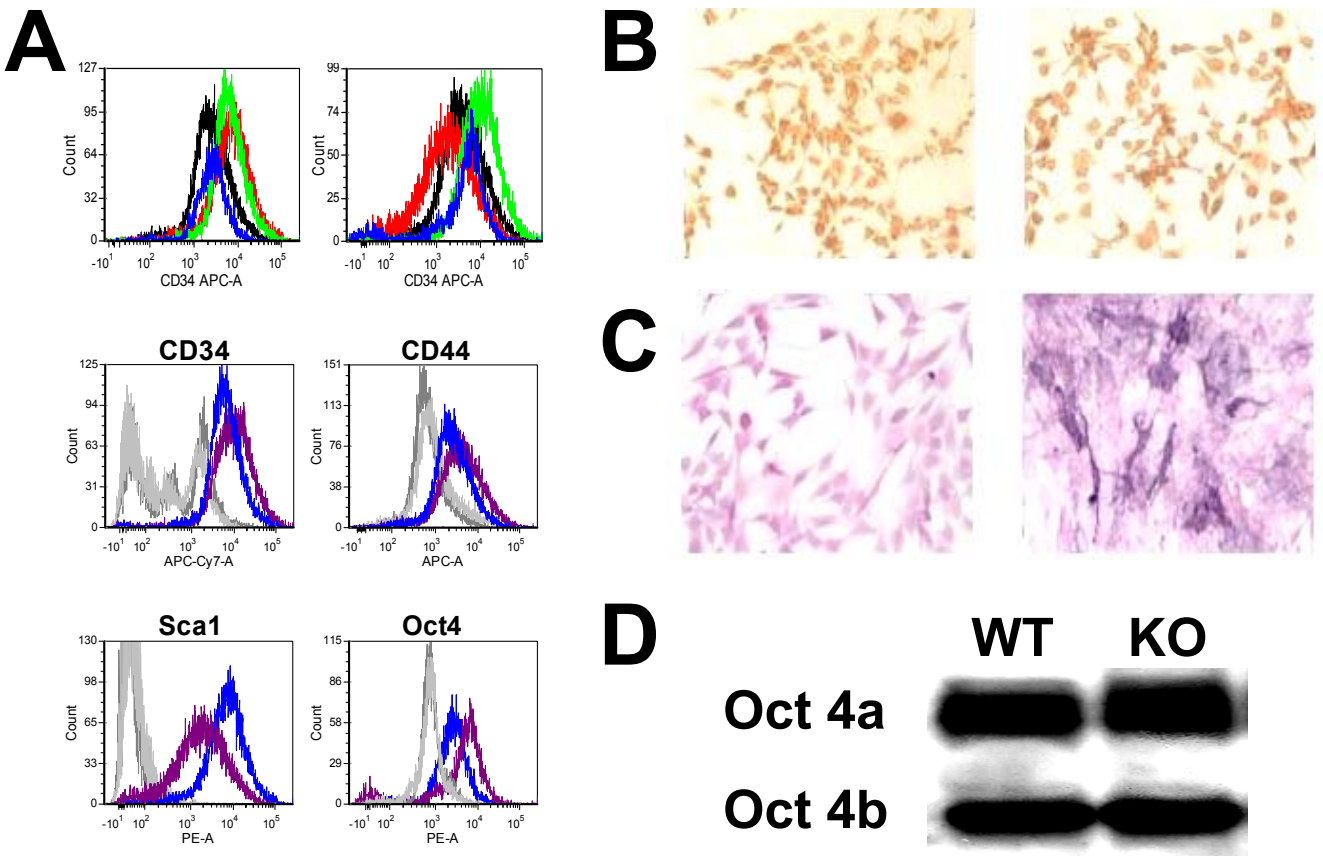

Figure 1. Effect of genetic inactivation of myostatin on the expression of key stem cell marker genes in MDSC. (**a**) Flow cytometry (no gate) was conducted for Sca1 (red), CD34 (black), CD44 (green) and Okt4 (blue) in WT MDSC (blue) and Mst KO MDSC (purple), against the respective isotypes (not shown). Top panels Left: WT MDSC; Right: Mst KO MDSC. Bottom panels: each antigen is compared separately for WT (blue) and Mst KO (purple), with the corresponding isotypes (WT: dark gray; Mst KO: light gray). (**b**) representative pictures of proliferating MDSC were subjected to immunocytochemistry for Oct-4, showing nuclear location in most cells (200X). (**c**) proliferating MDSC were subjected to cytochemistry for alkaline phosphatase (200 X). (d) homogenates from the same cell cultures were subjected to western blot for Oct-4 (nuclear: 45 kDa; cytoplasmic:33 kDa).

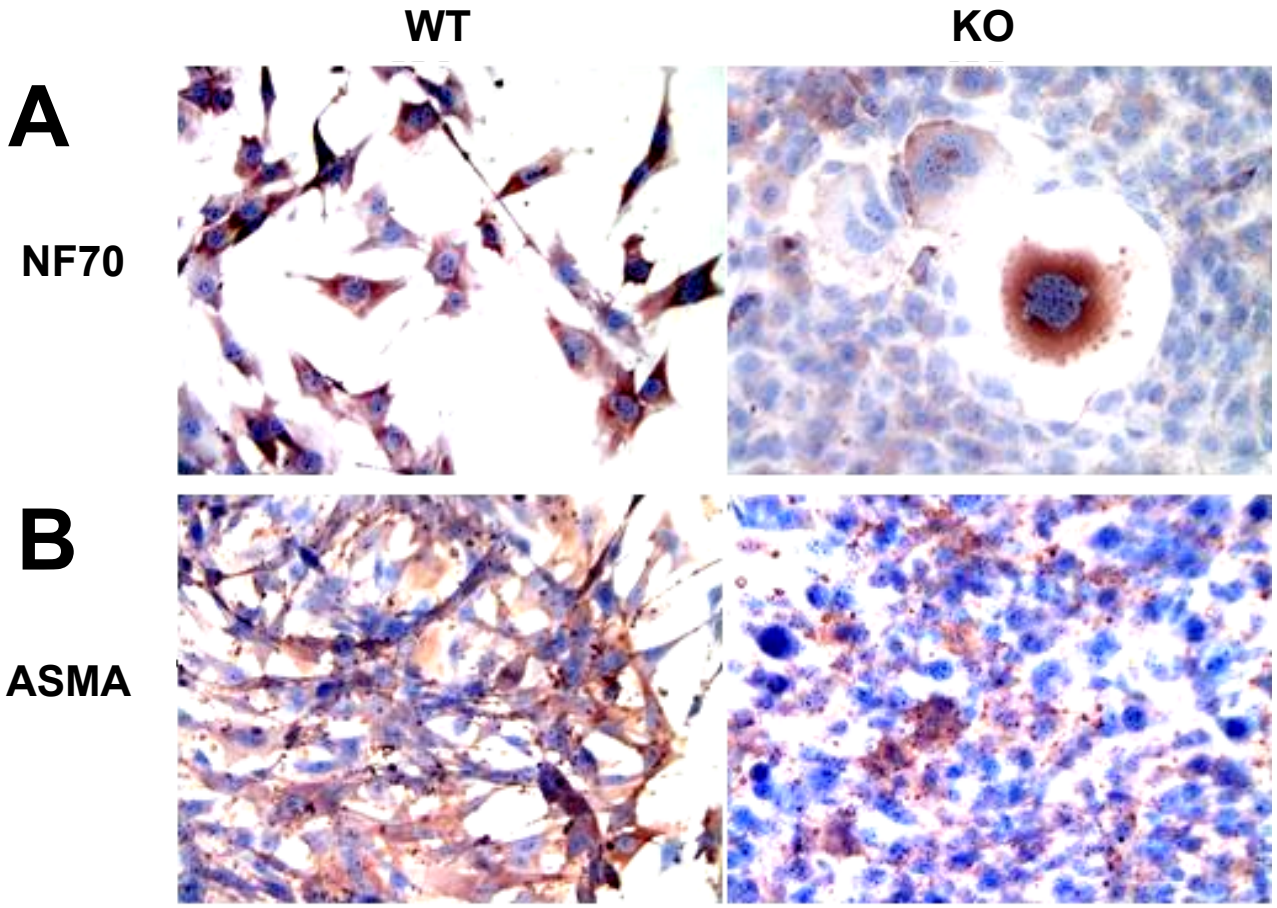

Figure 2. Myostatin genetic inactivation does not block the multipotent non-myogenic differentiation capacity of MDSC. Representative pictures of proliferating MDSC treated for 2 weeks in differentiation media and subjected to immunocytochemistry for NF-70 (**a**) and ASMA (**b**) to detect marker expression of neural cells and myofibroblasts (200 X).

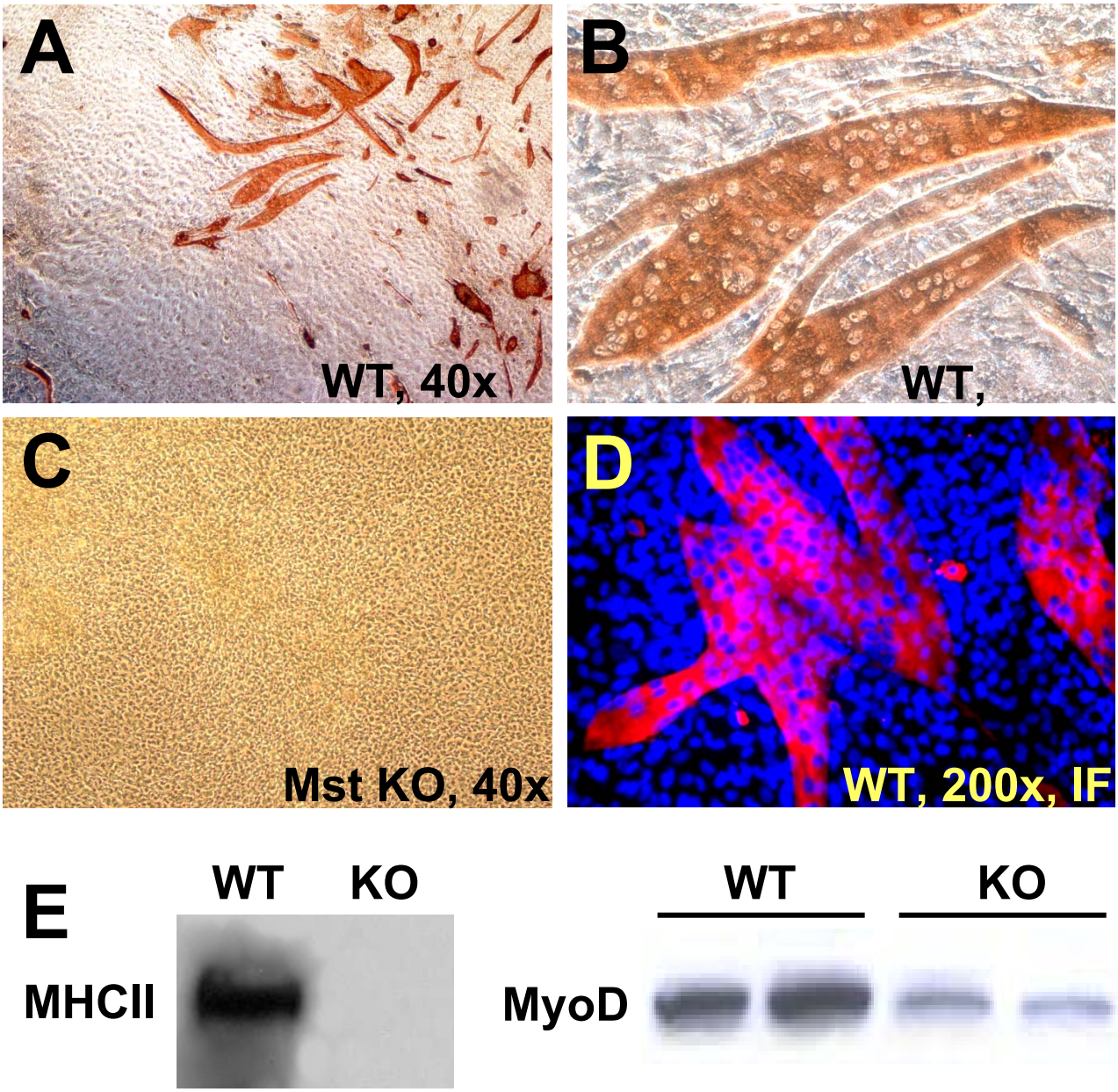

Figure 3. Myostatin genetic inactivation blocks the myogenic differentiation capacity of MDSC. (**a-c**) representative pictures of confluent MDSC from the WT MDSC and Mst KO maintained for 2 weeks in myogenic medium ("Hedrick's") and subjected to immuno-cytochemistry for MHC II to detect differentiation into polynucleated myotubes (magnifications as indicated). (**d**) blue/red merge of confluent MDSC in myogenic medium labeled with DAPI and submitted to immunofluorescent detection of MHC (200X); (**e**) western blot for MHC II (210 kDa) in the confluent cultures undergoing myogenesis, and MyoD (45 kDa) in the non-confluent cultures in non-myogenic medium.

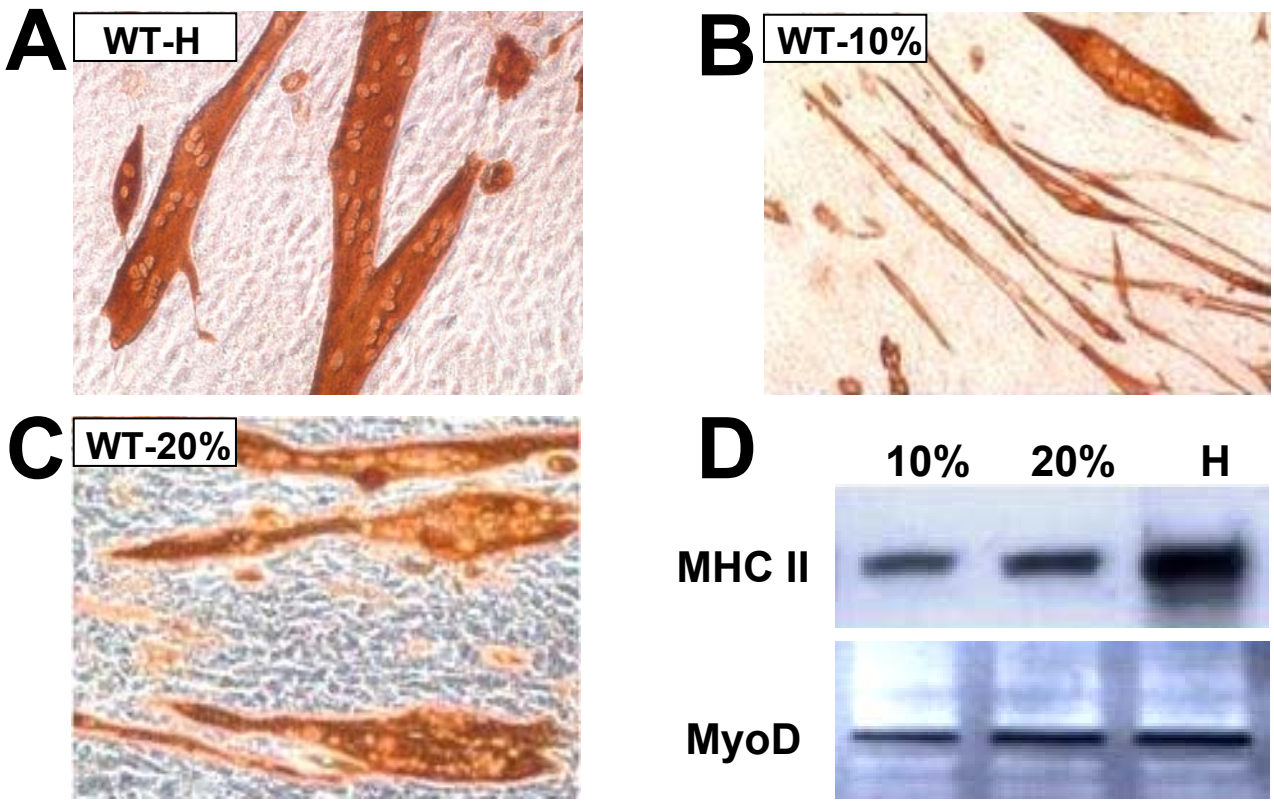

Figure 4. The potent myotube forming capacity of WT MDSC in myogenic medium is decreased but still maintained under high serum concentrations, in the presence of steady MyoD expression. (**a**) representative micrographs of myotubes generated in confluent WT MDSC maintained for 2 weeks in Hedrick's medium as evidenced by immunocytochemistry for MHC II (200 X).; (**b**) and (**c**) as (**a**) but in PM with 20% or 10% serum (200X). (**d**) Representative western blots for WT MDSC incubated in triplicate in each one of the above cultures in the three types of media subjected to immunodetection for MHC II (210 kDa) and MyoD (44 kDa). 10: 10% PM; 20: 20% PM; H: Hedrick's medium

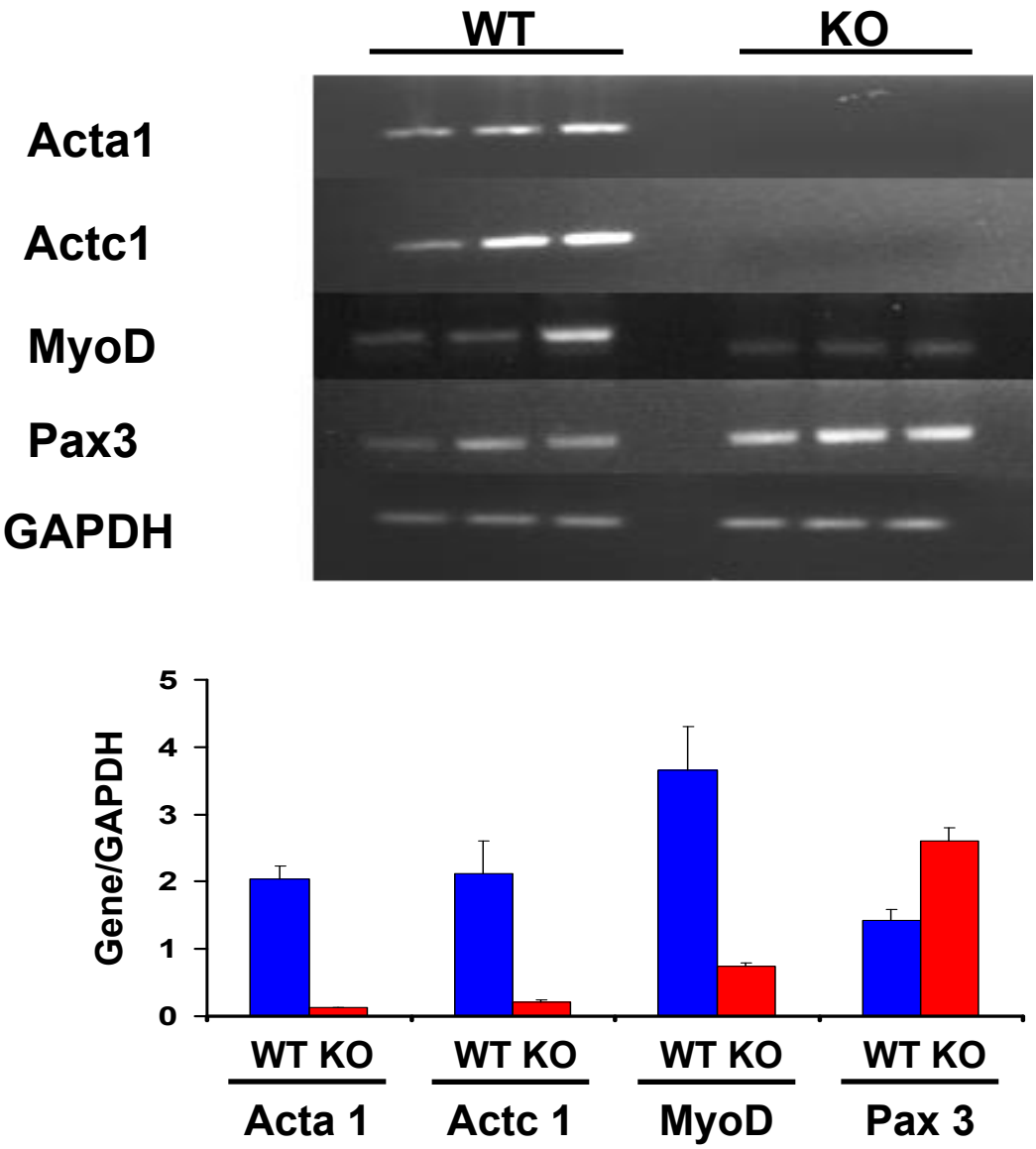

Figure 5. RT/PCR confirmation of selected differences in the transcriptional expression of undifferentiated WT and Mst KO MDSC, detected by DNA microarrays. RNAs obtained from triplicate cultures of proliferating MDSC, consecutive to those used for DNA microarrays on Tables 1 and 2, were subjected to RT/PCR with specific primers spanning an intron for the number of PCR cycles stated in parenthesis, as follows: Actc1 (30), Acta1 (30), MyoD1 (33), Pax3 (28), and GAPDH (26). (**a**) ethidium bromide-stained agarose gels; (**b**) densitometry of relative band intensities referred to housekeeping gene for the indicated number of PCR cycles. Controls without reverse transcriptase were blank. * $p < 0.05$ ** $p < 0.01$; *** $p < 0.001$.

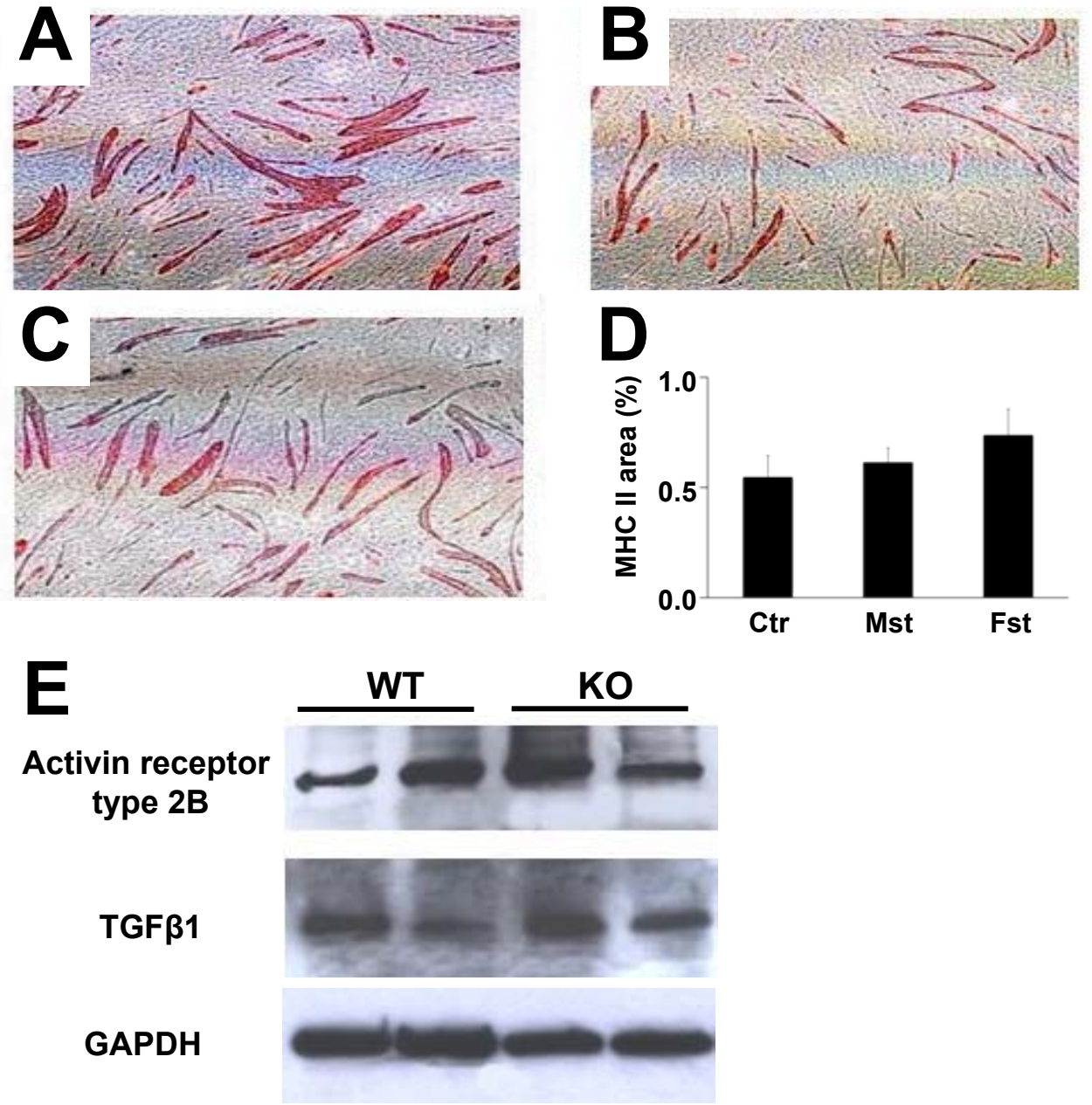

Figure 6. Myostatin and follistatin fail to modulate the myogenic differentiation of MDSC, despite the myostatin receptor is expressed. (**a-d**) confluent WT MDSC in myogenic medium were incubated in triplicate on 6-well plates for 1 week with recombinant myostatin (**b**) or follistatin (**c**) or with no addition (**a**), and subjected to immunocytochemistry for MHC II (40X). The relative area occupied by the MHC II + myotubes was estimated by quantitative image analysis (15 fields/well/3 wells) (**d**). Cont: control; Mst: myostatin; Fst: follistatin. No myotubes were formed in confluent Mst KO under any treatment (not shown). (**e-f**) western blot detection in confluent MDSC from both mice strains of the expression of the ActRIIb (**e**) and TGFβ1 (**f**). Myostatin was not detected.

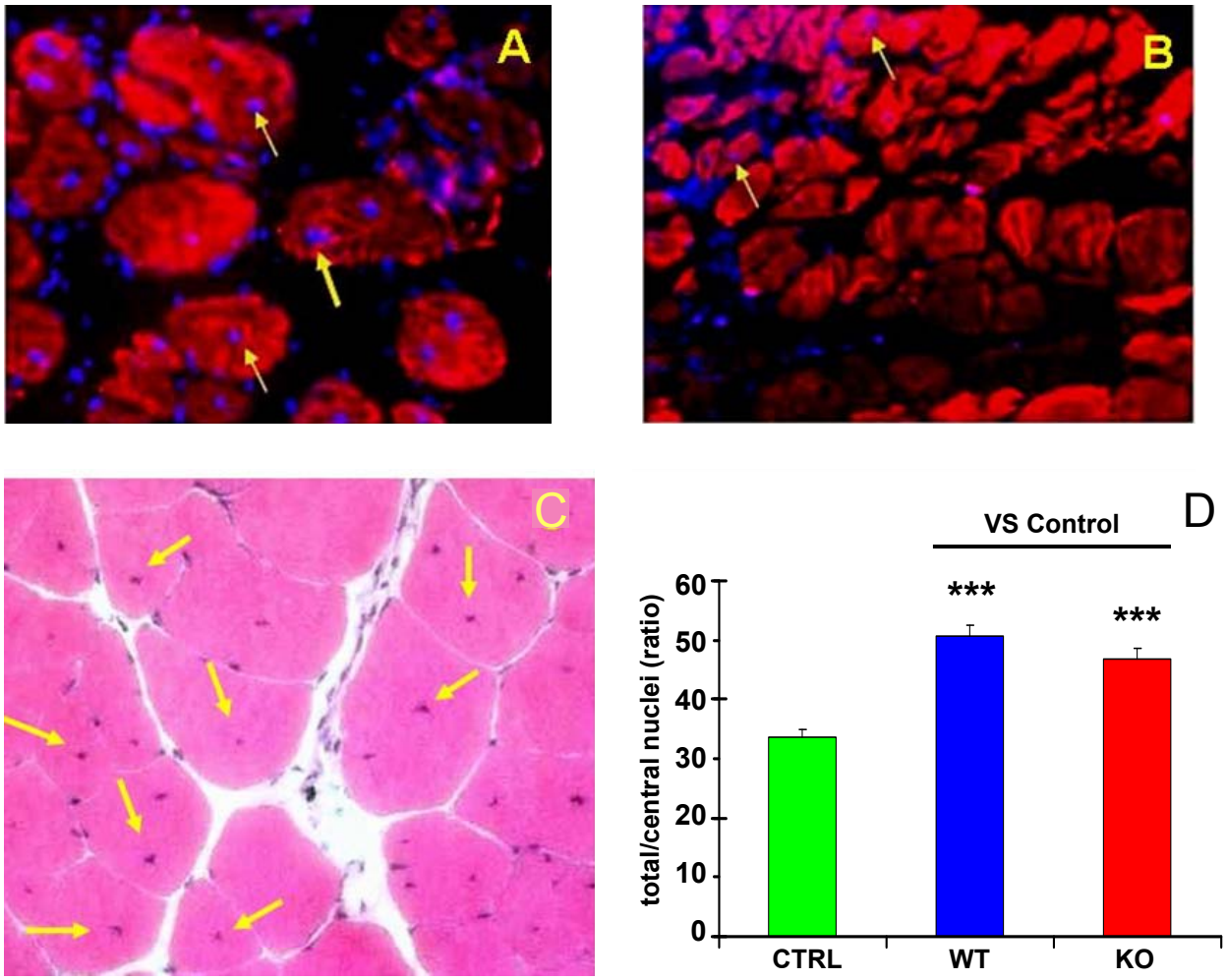

Figure 7. Mst KO MDSC failed to generate myotubes in vitro, but in vivo stimulate tissue repair comparable to the WT MDSC . Aged (10-month old) mdx mice were used to maximize myofiber loss and lipofibrotic degeneration in the gastrocnemius. (**a**) Muscles were cryoinjured and implanted with 0.5 x 106 DAPI-labeled WT MDSC, and allowed to undergo repair for 10 days. Frozen muscle sections were stained for MHC-II with Texas red streptavidin, and the merge of blue and red fluorescence was obtained (200X). MDSC nuclei centrally located within myofibers are indicated with yellow arrows. (**b**) Gastrocnemius injury in the aged mdx mice was performed in the two apexes of the muscle with notexin, and muscles were injected 4 days later with saline or with 1.0 x 106 WT MDSC or Mst KO MDSC in saline (n=5/group). Repair was allowed to proceed for 3 weeks. Hematoxylin eosin staining was performed in frozen sections and a representative picture shows myofibers from the gastrocnemius implanted with WT MDSC with arrows pointing to abundant central nuclei (200X). (**c**) quantitative image analysis of these tissue sections (WT), in comparison to tissue sections from Mst KO MDSC-implanted mice (KO) and saline-injected controls, based on 12 fields per section, 3 sections per animal. * $p < 0.05$

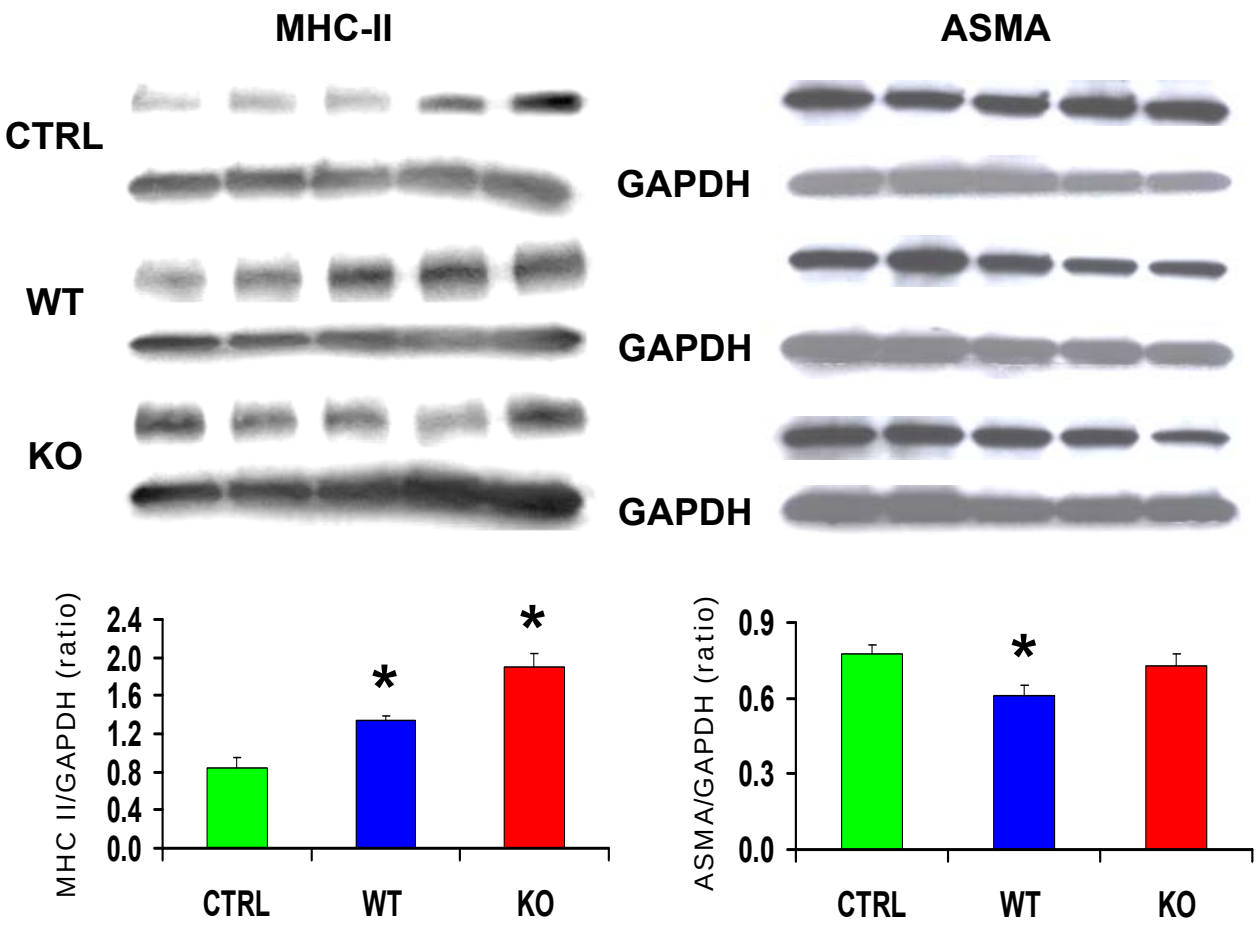

Figure 8. Implanted Mst KO MDSC stimulate more effectively than WT MDSC the expression of MHC-II in the muscle, but does not reduce ASMA. **Top:** Western blot analysis for MHC II, ASMA, and GAPDH (reference gene) in homogenates of skeletal muscle tissue from the central region adjacent to area examined histochemically in Figure 7B. Each lane corresponds to an individual mouse homogenate (n=5/group), and the three gels were run simultaneously. **Bottom:** Densitometric evaluation of the relative intensity expressed as ratios of the MCH-II or ASMA and GAPDH bands. * $p < 0.05$

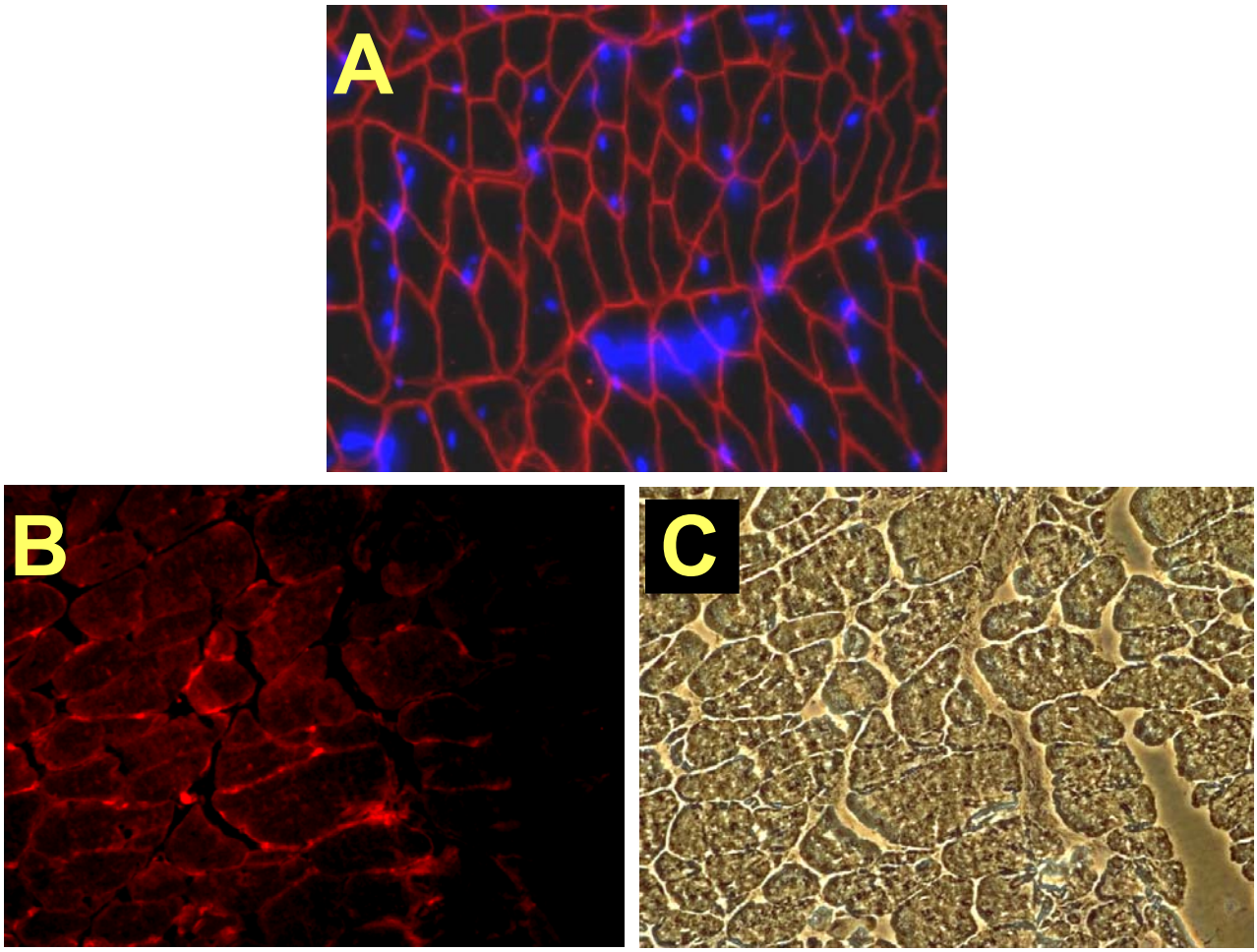

Figure 9. The dystrophin+ MDSC restore some dystrophin expression in the injured mdx gastrocnemius. (**a**) Myofibers from the intact gastrocnemius from the WT mouse, the source of WT MDSC, show positive immunofluorescence for dystrophin (nuclei stained with DAPI) (200X). (**b**) in other tissue sections, MDSC appear to have fused with the mdx myofibers showing dystrophin+ staining in a small area; (**c**) the same field as in (**b**) examined under visible light confirming the integrity of the myofibers including the dystrophin– area.

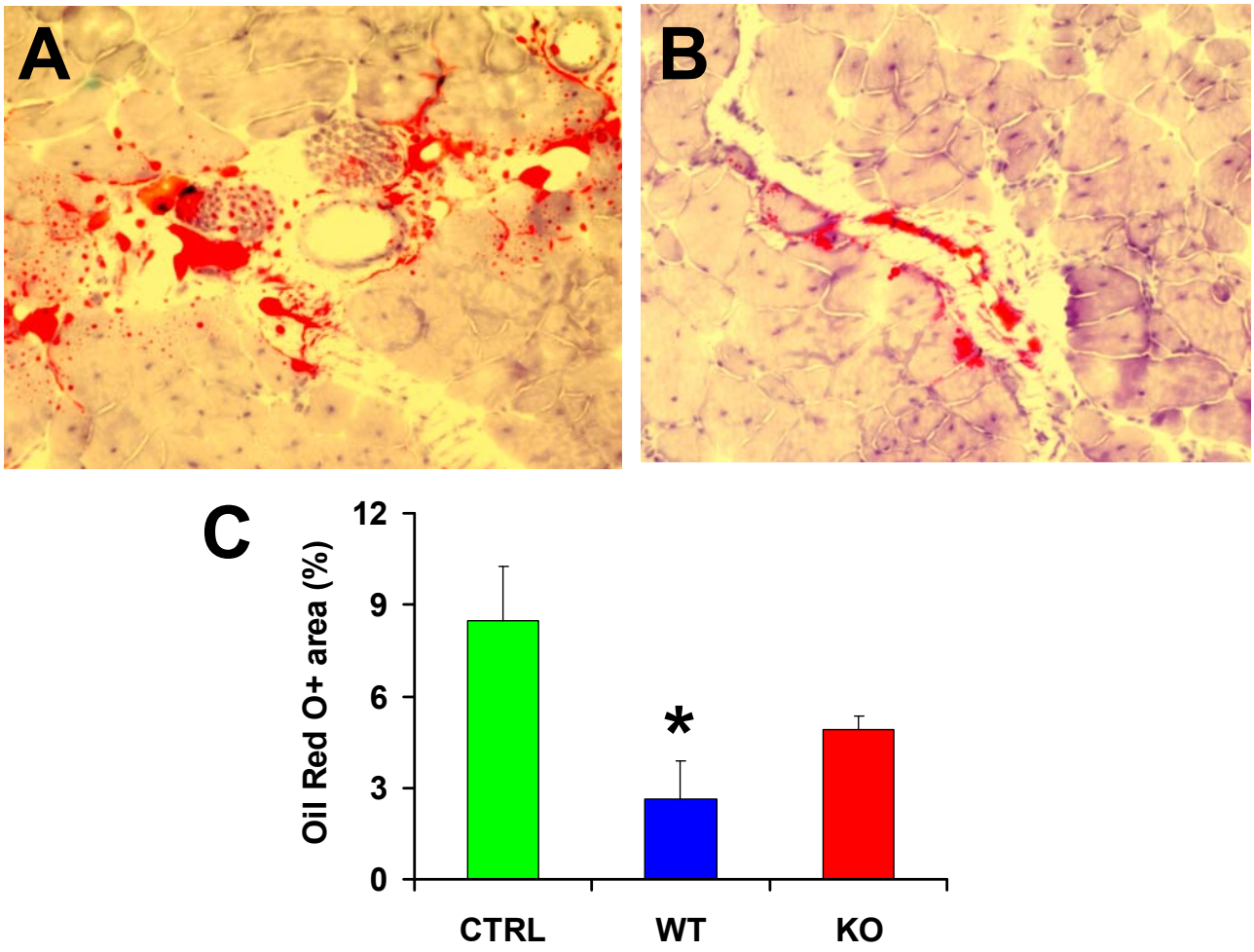

Figure 10. The Mst KO MDSC are less effective than the WT MDSC in reducing fat deposit in the injured mdx mouse gastrocnemius. (**a,b**) Representative picture of a positive field from frozen tissue sections from the untreated mdx injured gastrocnemius, adjacent to the ones shown on Figure 8C, fixed in formalin and stained with Oil Red O, showing mostly interstitial fat and occasional myofiber fat infiltration (200X). Staining in the sections from the muscle implanted with WT and Mst KO MDSC was similar, but in sparser locations. (**c**) quantitative image analysis of the tissue sections from the three rat groups, based on 12 fields per tissue section and the total positive area per section (%), calculated as a mean for 3 adjacent sections per rat, and 5 mdx mice/group. * $p < 0.05$

Separate or combined treatments with muscle derived stem cells, daily sildenafil, or molsidomine prevent erectile dysfunction in a rat model of cavernosal nerve damage

Kovanecz I[1,2], Rivera S[1], Nolazco G[1,3], Vernet D[1], Segura D[1,4], Gharib S[1,4], Rajfer J[1,2], Gonzalez-Cadavid NF[1-3]

[1]Division of Urology, and Los Angeles Biomedical Research Institute (LABioMed) at Harbor-UCLA Medical Center, Torrance, CA, [2]Department of Urology, David Geffen School of Medicine at UCLA, Los Angeles, CA, [3]Department of Internal Medicine, Charles Drew University (CDU), Los Angeles, CA, [4]California State University at Dominguez Hills.

***Corresponding author**: Nestor F. Gonzalez-Cadavid, Ph.D., LABioMed at Harbor-UCLA Medical Center, Bldg. C-3, 1124 West Carson Street, Torrance, CA 90502, USA

Telephone: 310-222-3810; **fax:** 310-222-1914; **e-mail**: ncadavid@ucla.edu

Running Title: Sildenafil/muscle stem cells on CVOD in nerve damage

Key words: Stem cells, corporal veno-occlusive dysfunction, fibrosis, corpora cavernosa, PDE 5 inhibitors

ABSTRACT

Objectives: Long-term daily administration of PDE5 inhibitors **(PDE5i)** in the rat prevents or reverses corporal smooth muscle cell **(SMC)** loss, fibrosis and the resulting CVOD in both aging and bilateral cavernosal nerve resection **(BCNR)** models for erectile dysfunction **(ED)**. In the aging rat model, corporal implantation of skeletal muscle derived stem cells **(MDSC)** reverses CVOD. Nitric oxide **(NO)** and cGMP can modulate stem cell lineage. We have now investigated in the BCNR model the effects of sildenafil **(S)** at different doses, alone or in combination with MDSC or the NO donor molsidomine, on CVOD and the underlying corporal histopathology,

Methods: Rats subjected to BCNR were maintained for 45 days either untreated or given sildenafil in the drinking water at 10, 2.5, and 1.25 mg/kg/day (medium, low, and very low doses), or retrolingually, or with additional intraperitoneal molsidomine as NO donor or MDSC implanted into the corpora cavernosa, or received molsidomine or MDSC alone. Dynamic infusion cavernosometry evaluated CVOD. The underlying histopathology was assessed on penile sections by Masson trichrome, immunohistochemistry for α-smooth muscle actin **(ASMA),** or dual immunofluorescence for nNOS and NF-70, and in fresh tissue by western blot for calponin, SHP-2. Bax, NF70, nNOS, and BDNF, and also by picrosirius red for collagen.

Results: All treatments normalized erectile function (drop rate), and most increased the SMC/ collagen ratio and ASMA expression in corporal tissue sections, and reduced collagen content in the penile shaft tissue (PST). MDSC also increased calponin, nNOS and BDNF in the PST. The combination treatments were not superior to the different agents given alone.

Conclusions: Lowering the dose of a continuous long term sildenafil administration from 10 to 1.25 mg/kg/day still maintained the prevention of CVOD in the BCNR rat previously observed with 20 mg/kg/day, but the prevention of the underlying histopathology was much less effective. As in the aging rat model, MDSC also counteracted CVOD, but supplementation with sildenafil did not improve the outcome.

INTRODUCTION

Erectile dysfunction **(ED)** is the most prevalent complication of prostate cancer treatment (radical prostatectomy **(RP),** radiotherapy, cryoablation and androgen deprivation). In post-RP, ED can occur in up to 70% of these patients even in centers of excellence that apply nerve sparing techniques **[1-3]**, and severely affects the quality of life of patients, posing a heavy burden on health care costs **[4-6]**. The fear of this complication is often a deterrent for the patient to opt for RP even when it is the treatment of choice.

In post-RP/radiotherapy, and possibly cryotherapy **[8,9]**, cavernosal nerve damage causes first an acute neurogenic ED by interfering with the nitrergic neurotransmission originated from the brain, mediated by nitric oxide **(NO) [10]**, and then a neuropraxia of the corpora cavernosa leading to fibrosis, apoptosis and loss of corporal smooth muscle cells **(CSMC) [11]**. This impairs the compliance of the tissue and its ability to retain blood during erection causing corporal veno-occlusive dysfunction **(CVOD) [11-13]**. This is a form of vasculogenic ED that is the prevalent type of ED **[14]**. Frequent resistance to oral PDE 5 inhibitors or intracorporal injections applied “on demand” to induce erections were observed in post-RP CVOD, because vasodilation by the oral PDE 5 inhibitors requires the integrity of both the cavernosal nerve to transmit the sexual stimulus and the CSMC to respond, and local vasodilators are ineffective when the corporal tissue is injured **[9]**.

There is therefore a considerable clinical interest in finding new strategies for penile regeneration and this has spurred experimental studies in animal models of post-RP, essentially in rats and mice where the cavernosal nerve damage is induced by either: a) bilateral cavernosal nerve resection **(BCNR) [12-16]** or transsection **(BCNT) [17]**, where a small fragment of the cavernosal nerve is resected or the nerve cut close to the prostate, respectively, mimicking a severe injury that may occur under standard surgical conditions, or b) controlled bilateral cavernosal nerve crush **(BCNC) [18]**, possibly resembling the milder damage induced

by bilateral nerve sparing techniques. Although BCNR is the most severe form of damage that may exceed the one induced in men in nerve sparing procedures, it has two advantages over BCNC, i.e., absolute reproducibility of the extent of injury, and the fact that interventions ameliorating its impact on both the nerves and the corpora cavernosa will obviously be more successful in repairing the milder BCNC damage.

Using BCNR procedures in the rat we have shown that long-term continuous administration of the three PDE 5 inhibitors **(PDE 5i)**, sildenafil, tadalafil, and vardenafil, partially prevent CVOD by counteracting the underlying corporal histopathology by an antifibrotic mechanism **[12,15,16,19]**. This is different from the vasodilator mechanism that operates in the conventional “on demand” palliative interventions to facilitate penile erection upon sexual stimulation. The BCNC model basically confirmed these results **[18]**, and on the other hand it is known that chronic PDE 5i protects selectively endothelium-dependent relaxations of strips of corpus cavernosum in vitro **[20]**. Long-term sildenafil reversed CVOD and improved the underlying corporal histology in a rat model of aging **[21]**. No studies are available on whether the same effects can be elicited by long-term nitric oxide donors or soluble guanyl cyclase stimulators, through the elevation of cGMP levels.

However, since the daily doses of PDE 5i in these BCNR studies were, when translated from rats to humans, about 2-3 fold higher than the usual ones used on demand, and so far only a few clinical studies with non-conclusive results have been performed on this modality with standard doses **[22,23]**, further experimental studies with lower doses are needed to validate this approach. In the case of sildenafil, the effective dose previously tested in rats **[15,21]** was 20 mg/kg/day, which, when corrected for differences in total body surface area, **[24,25]** is equivalent to about 200 mg/day in men. In addition to this pharmacological therapy, alternative strategies, such as the use of stem cells by themselves or in combination with long-term continuous administration of PDE 5i need to be examined. Despite the promising results in several studies with different stem cell types in animal models of ED associated with aging and

diabetes **[17,26-32]**, only a few reports are available for ED post-RP models, and they share some limitations **[33]**.

The field of stem cell therapy of ED was opened in the BCNC model by applying embryonic stem cells **[34]**, which suffer from the fact that the clinical use of embryonic stem cells for non-life threatening conditions is unlikely**.** These cells failed to be detected at late stages, the correction of ED by EFS was partial, and no studies on corporal damage or CVOD were performed. Some of these experimental concerns apply to a study using skeletal muscle derived stem cells **(MDSC)** in a BCNT model **[17]**, and more recently in a short report on the amelioration of CVOD in the BCNR model, compounded by questions on the "MDSC" population employed **[35]**. MDSC were effective in reversing an impaired EFS response in aged rats and to convert to SMC and other differentiated cells in the corpora cavernosa and in the injured vagina **[32,36]**. To our knowledge, no combination of PDE 5i and stem cell treatments or with NO donors has been tested for ED in animal models, even if this modality was studied for myocardial infarction with some inconclusive results **[37]**.

In the present work we have investigated whether sildenafil given for 45 days to BCNR rats at 1/2 through 1/16 the doses previously tested, and the NO donor molsidomine, in combination or not with sildenafil, could prevent CVOD and improve the underlying corporal histopathology, and whether similar or better effects could be obtained with MDSC alone or in the presence of a chronic very low dose of sildenafil.

MATERIALS AND METHODS

MDSC isolation and culture

MDSC were prepared from the hind limb muscles from the mouse **[38-40]**, using the preplating procedure, a validated standardized method for MDSC isolation **[41]**, as in our previous reports **[32,36,42]**. Tissues were dissociated using sequentially collagenase XI,

dispase II and trypsin, and after filtration through 60 μm nylon mesh and pelleting, the cells were suspended in Dulbecco's Modified Eagle's Medium **(DMEM)** with 20% fetal bovine serum. Cells were plated onto collagen I-coated flasks for 1 hr (preplate 1 or pP1), and 2 hrs (preplate 2 for pP2), followed by sequential daily transfers of non-adherent cells and re-platings for 2 to 6 days, until preplate 6 **(pP6)**. The latter is the cell population containing MDSC. Cells were then selected using magnetic beads coated with the Sca 1 antibody. Cells were replicated on regular culture flasks (no coating) and used in the 5th-10th passage, since the mouse counterparts have been maintained in our laboratory for at least 40 passages with the same, or even increasing, growth rate**.** Flow cytometry was performed to show that these cultures were Sca 1+/CD34+/CD44+ cells **[42]**.

BCNR procedure

Five month-old male Fisher 344 rats (Charles River, Wilmington, MA) were subjected to BCNR as previously described **[13,15,16,19]**. All animal experiments were approved by the IACUC at our institution. Essentially, animals were operated under aseptic conditions and isoflurane anesthesia. In supine position, a midline incision was done, the pelvic cavity was opened, and the bladder and prostate were located. Under an operating microscope, the major pelvic ganglion and its inbound and outbound nerve fibers were identified after removing the fascia and fat on the dorsolateral lobe of the prostate. The main branch of the cavernosal nerve is the largest efferent nerve, which runs along the surface of the prostatic wall. Above the main branch there are another four to six small efferent fibers, which also run towards the membranous urethra, considered as ancillary branches of the CN. In order to recognize the main cavernosal nerve, stimulation with an electrode to induce penile erection was applied. In the sham-operated group both cavernosal nerves were identified but not resected. In BCNR, the main cavernosal nerves and ancillary branches were resected by removing a 3-mm segment. This procedure mainly eliminates the nitrergic NANC stimulation to the CSM that elicits its

relaxation during penile erection, while also interrupting some vasoconstrictor neurotransmission through coalescent adrenergic fibers in the cavernosal nerve.

Animal treatments

Animals *(total: 80 rats; n=8/group) were treated as follows*: **SH:** sham-operated, untreated; Series I: **LS:** BCNR, low dose sildenafil, in water: 2.5 mg/kg/day**; LS(RL):** BCNR, low dose sildenafil, retrolingual**; MS:** BCNR, medium dose sildenafil, in water: 10 mg/kg/day; **M:** BCNR, molsidomine, IP, 10 mg/kg/day**; M+LS:** BCNR, molsidomine IP, with low dose sildenafil in water**; M+MS:** BCNR, molsidomine IP, with medium dose sildenafil in water**;** Series II: **SC:** MDSC (10^6 cells) injected in 0.05 ml Hanks, intracorporal **[32]**; the MDSC were labeled with the nuclear fluorescent stain 4′,6-diamidino-2-phenylindole **(DAPI)** and implanted aseptically into two different sites in the mid-part of the shaft in anaesthetized rats; tacrolimus was given daily (1 mg/kg, s.c.) to avoid immuno-rejection of the mouse stem cells; **SC+VLS:** MDSC (10^6 cells) injected, with tacrolimus, as in #8, and supplemented with very low dose sildenafil, in water: 1.25 mg/kg/day**;** and 10) very low dose sildenafil, in water**.**

Treatments were interrupted at 42 days, and the experiment was finalized 3 days later (washout). The drinking volumes were determined daily, and body weights were recorded weekly. The daily sildenafil doses given to these animals were as stated above. They are estimated at approximately equivalent to doses 10-fold higher in men when expressed in mg/day (i.e., 1.25 mg/kg/day in rats equivalent to 12.5 mg/day in men), based on differences in total body surface area between the rat and the human **[24,25]**.

Dynamic Infusion Cavernosometry (DIC)

Cavernosometry was performed as previously described **[13,15,16,19]**. Briefly, basal intracavernosal pressure **(ICP)** was recorded, and 0.1 ml papaverine (20 mg/ml) was administered through a cannula into the corpora cavernosa. The ICP during tumescence was

recorded as “ICP after papaverine”. Saline was then infused through another cannula, increasing infusion rate by 0.05 ml/min every 10 seconds, until the ICP reached 100 mmHg (“maintenance rate”). The “drop rate” was determined by recording the fall in ICP within the next 1 minute after the infusion was stopped.

Determinations in tissue sections

After cavernosometry, animals were sacrificed and the skin-denuded penile shafts were fixed overnight in 10% buffered formalin, transferred into ethanol (70%) and stored at 4°C until processed for paraffin embedded tissue sections (6-8 μm). Adjacent tissue sections were used for: a) Masson trichrome staining for collagen (blue) and SMC (red); and b) immunodetection with monoclonal antibodies against α-smooth muscle actin **(ASMA)** as a SMC marker (Sigma kit, Sigma Diagnostics, St Louis, MO). For immunodetection sections were then incubated with biotinylated anti-Mouse IgG, followed by ABC complex (Vector labs, Temecula, CA) and 3,3'diaminobenzidine (Sigma) (PCNA and iNOS). Sections were counterstained with hematoxylin. Negative controls in the immunohistochemical detections were done by replacing the first antibody with IgG isotype.

Quantitative image analysis **(QIA)** was performed by computerized densitometry using the ImagePro 4.01 program (Media Cybernetics, Silver Spring, MD), coupled to an Olympus BHS microscope equipped with an Olympus digital camera **[13,15,16,19]**. For Masson staining, 40× magnification pictures of the penis comprising half of the corpora cavernosa were analyzed for SMC (stained in red) and collagen (stained in blue), and expressed as SMC/collagen ratio. For ASMA, only the corpora cavernosa were analyzed in a computerized grid and expressed as % of positive area vs. total area of the corpora cavernosa. In all cases, three fields at 40x (both sides of the corpora cavernosa) or 8 fields at 400x, were analyzed per tissue section, with at least 4 matched sections per animal and 8 animals per group.

Qualitative dual immunofluorescence determinations were also performed in frozen tissue sections (8-10 μm) for neurofilament 70 **(NF70)** with an antibody clone DA2, mouse monoclonal (Millipore, Billerica, MA), and for neuronal nitric oxide synthase (nNOS) using a rabbit monoclonal (ABCAM, Cambridge, MA).

Determinations in tissue homogenates

1. Penile tissue homogenates (80-100 mg tissue) were obtained in T-PER (PIERCE, Rockford, IL) and protease inhibitors (3 μM leupeptin, 1 μM pepstatin A, 1mM phenyl methyl sulfonyl fluoride), and centrifuged at 10,000 g for 5 min. Supernatant proteins (30-50 μg) were subjected to western blot analyses (13,15,16,19) by 7-10 % Tris-HCl polyacrylamide gel electrophoresis (PAGE) (Bio-Rad, Hercules, CA) in running buffer (Tris/Glycine/SDS). Proteins were transferred overnight at 4°C to nitrocellulose membranes in transfer buffer (Tris/glycine/methanol) and the next day, the non-specific binding was blocked by immersing the membranes into 5% non-fat dried milk, 0.1% (v/v) Tween 20 in PBS for 1hour at room temperature. After several washes with washing buffer (PBS Tween 0.1%), the membranes were incubated with the primary antibodies for 1 hour at room temperature monoclonal antibodies were as follows: a) calponin 1 **(Calp 1)** mouse monoclonal (Santa Cruz Biotechnology, Inc. Santa Cruz, CA); b) Src homology region 2-containing protein tyrosine phosphatase **(SHP-2)** rabbit polyclonal (Santa Cruz Biotechnology, Inc); c) BAX rabbit polyclonal (Santa Cruz Biotechnology, Inc); d) NF70, as for immunofluorescence ; e) nNOS, as for immunofluorescence; f) brain-derived neurotrophic factor **(BDNF),** rabbit monoclonal ABCAM, Cambridge, MA and g) mouse glyceraldehyde 3-phosphate dehydrogenase **(GAPDH)** mouse monoclonal (Millipore, Billerica, MA), as a reference housekeeping protein.

The washed membranes were incubated for 1 hour at room temperature with 1:3,000 dilution (anti-mouse), followed by a secondary antibody linked to horseradish peroxidase. After several washes, the immunoreactive bands were visualized using the ECL plus western blotting

chemiluminescence detection system (Amersham Biosciences, Piscataway, NJ). The densitometric analyses of the bands were performed with Image J (NIH, Bethesda, MD). A positive control was run throughout all gels for each antibody to standardize for variations in exposures and staining intensities. Negative controls were performed omitting the primary antibody. Band intensities were determined by densitometry and corrected by the respective intensities for GAPDH, upon reprobing.

Collagen was estimated by the picrosirius red procedure **[43]**, using an aliquot of the tissue homogenates prepared for western blotting, mixing it with Sirius Red saturated in picric acid incubated for 30 min, and centrifuged at 15,000 x g for 5 min, to pellet the collagen. This pellet is rinsed once with 0.1M HCl to remove excess dye, centrifuged again, and the pellet is extracted in 0.5M NaOH, clarified, and measured spectrophotometrically at 550 nm. The standard curve is Type I Collagen, acid soluble, (Sigma Chemical Corp) from 0-80 µg. Values are expressed as micrograms of collagen per milligram of tissue.

Statistical analysis

Values were expressed as mean ± SEM. For Series I, the normality distribution of the data was established using the Wilk-Shapiro test. Multiple comparisons were analyzed by a two factor (time and treatment) analysis of variance (two way ANOVA), followed by post-hoc comparisons with Tukey post test, according to the GraphPad Prism V 4.1. For Series II-IV, comparisons between a single group and the respective control group (as indicated in each figure) were done with the unpaired t-test. Differences were considered significant at $p < 0.05$.

RESULTS

A sustained administration of sildenafil at median and low doses prevents CVOD after BCNR and reduces collagen deposition in the corpora cavernosa, but combination with molsidomine is not more effective than the drugs alone

In order to determine whether long-term continuous sildenafil given to BCNR rats in the drinking water could prevent CVOD at doses lower than the previously used high dose of 20 mg/kg/day **[15]**, rats were treated with ½ (MS) and 1/8 (LS) of this dose for 45 days. **Fig. 1 top** shows that the very high drop rate measured by cavernosometry in the UT rats, an indication of CVOD, was reduced by MS and even by LS to a normal level, as compared to our standard values in sham operated animals**.** The same effect was achieved by LS(RL) a once daily retrolingual administration of low dose sildenafil. However, unexpectedly, the LS and LS(RL) virtually did not modify the corporal SMC/collagen ratio measured histochemically by Masson trichrome, in contrast to the MS dose that did increase it and normalized the value **(bottom)**.

The effects of all treatments on the penile shaft collagen content, measured by a colorimetric Sirius red procedure **(Fig. 2)** were the expected ones, since it was reduced even below the sham rats value used as reference.

The increase in cGMP levels induced by long-term daily IP molsidomine was sufficient to also normalize the drop rate in the cavernosometry **(Fig. 3 top)**, and therefore the supplementation with LS or MS was in fact unnecessary and both treatments acted similarly. However, the small increase in the Masson trichrome estimate of the corporal SMC/collagen by M and M+MS is non significant and much lower than expected **(bottom),** despite MS by itself did improve this ratio as shown on **Fig. 1**.

Implantation of MDSC also prevents CVOD and reduces collagen, but supplementation with sildenafil does not substantially enhance these effects

Since MDSC counteracted ED measured by EFS in a rat model of aging **[32]**, we examined whether these stem cells can prevent CVOD measured by cavernosometry in the BCNR rat model, in order to investigate whether the effects can be enhanced by sildenafil supplementation **Fig. 4 top** shows that MDSC did normalize the drop rate in the cavernosometry determination and that this was also achieved by a very low dose of sildenafil,

1.25 mg/kg/day (VLS), which is half of the lowest dose tested in the previous experiments. Therefore, it was not surprising that the combination of both treatments, SC+VLS, was not different from the individual treatments. However, only the MDSC increased significantly the low SMC/collagen ratio by Masson trichrome seen in the UT rats **(bottom)**.

The corporal SMC content identified by immunohistochemistry for the ASMA marker in the trabecular region was also marginally increased by the MDSC, alone or in combination with VLS , but not by VLS alone **(Fig. 5 top)**. In the case of collagen, estimated by sirius red in the whole penile corporal shaft, its content was reduced by VLS alone or in combination with MDSC, but MDSC failed to change the levels seen in the UT rats **(bottom)**.

MDSC preserve the SMC relaxation/contraction phenotype and enhance nitrergic nerve content, but a very low dose of sildenafil has little effect

The previous results show that despite the clear effect of the separate MDSC and low or very low sildenafil (or molsidomine at normal doses) treatments in improving the CVOD, these agents only moderately prevented the underlying corporal fibrosis that sildenafil exerts at higher doses **[15]**. Therefore, ancillary mechanisms are likely to cooperate with these mild beneficial effects on the histopathology by acting on other targets that help to maintain corporal compliance and thus counteract CVOD. One of them would be the enhancement of SMC calponin I, and of SHP-2, a protein that inactivates the anti-SMC relaxation Rho-A kinase by dephosphorylating Vav **[44]**. **Fig. 6** presents the quantitative western blot determination in the penile shaft homogenates, showing that MDSC, but not sildenafil, increased calponin in penile shaft homogenates, albeit non-significantly, and reduced the proapoptotic Bax, in agreement to the effects on ASMA, but there were no changes in SHP-2 expression. The latter was stimulated by VLS. An unexpected result was the upregulation of Bax by VLS

The well known neurotrophic effects of MDSC alone **[45]** and sildenafil alone **[46]** may lead to an amelioration of neural damage and hence of the impact of the neuropraxia on the

corporal histology and erectile function. However, neither VLS nor MDSC or their combination increased the expression measured by western blot of the neural marker NF-70 **(Fig. 7)**, but very interestingly, MDSC was the only treatment that did upregulate nNOS and BDNF, thus suggesting a neural trophic effect. At least part of this nNOS expression is in the nerves, specifically in cavernosal nerve terminals, in addition to the dorsal nerve**,** as shown by dual fluorescence for both proteins **(Fig. 8)**. This suggests that some improvement in nitrergic nerves and hence nitrergic neurotransmission with NO release impacts both the overall erectile response per se and specifically the contractile machinery of the corporal smooth muscle.

To facilitate an overall comparison of the different groups the general results are summarized in **Tables 1** and **2**.

DISCUSSION

In this work we investigated whether reducing the dose of sildenafil in the continuous long-term treatment at 20 mg/kg/day (roughly equivalent to 200 mg daily in men) of ED after BCNR, that prevented the CVOD and the corporal fibrosis and loss of SMC **[15]**, remained effective at ½, 1/8 and 1/16 lower doses, and whether the intraperitoneal injection of molsidomine, or the intracorporeal injection of MDSC are also able to prevent the development of CVOD and the impairment of smooth muscle compliance caused by the neuropraxia **[13]**. Our results show that in terms of the functional effect this is the case, and that single daily retrolingual sildenafil, mimicking the clinical administration as tablets, was also effective. So were the combinations of molsidomine or MDSC with sildenafil, but no additive effect was observed, possibly because the drop rates estimated by cavernosometry were already normalized by the individual treatments alone. Although these treatments exerted some antifibrotic and SMC-protective effects in the corpora, they were surprisingly much lower than with the previous 20 mg/kg dose **[15]**, and the sildenafil combinations failed to improve them. At

least for the single treatments, it is likely that their observed beneficial effects on the SMC relaxation phenotype and nitrergic nerves may contribute to the antifibrotic effects. Of all treatments, the MDSC intracorporal implantation was the one with more coherent effects on the corporal histopathology, except for the lack of reduction in collagen content in the penile shaft that is unexplained.

Irrespective of the mechanism, it is clear that the beneficial effects of long-term continuous PDE 5i on erectile function were not strictly dependent on sustained high cGMP levels induced by the high doses previously applied, so that now the lower continuous doses are more clinically relevant and may give a window in men from perhaps daily 15 to 50 mg sildenafil. Obviously, considering the long-active features of tadalafil **[16]** doses and frequency may be even lower. In contrast, molsidomine at the safe, but relatively high dose used alone or in combination (about daily 100 mg), was not better than sildenafil alone. It is unlikely that molsidomine may have any advantage over PDE 5i , based on its modest performance in the diabetic mouse **[52]**. However, the potential of NO stimulation of cGMP levels through other longer lasting NO donors **[47]** should be tested, as well as guanyl cyclase stimulators **[48]**, perhaps in combination with PDE5i at low doses.

In the case of the MDSC intracorporal implantation, the current work has shown that they can prevent CVOD after cavernosal nerve damage, a condition that was not studied in a previous BCNT report using MDSC **[18]**, where only the EFS response was tested and no effects on the corpora SMC were studied. The fast recovery of the EFS to about 60 mmHg at 2 weeks after MDSC (pP6 fraction in the preplating procedure) implantation, and the subsequent decay of this response at 4 weeks is difficult to reconcile with a successful BCNT that initially should interrupt completely nitrergic neurotransmission and hence the EFS response, so this may need reassessment. A clarification regarding the nature of the MDSC that in a recent short communication normalized the drop rate and stimulated the papaverine response 4 weeks after BCNR is also required, since here the pP4 fraction was employed, a fraction enriched in satellite

cells but not MDSC **[35]**. Satellite cells are committed to skeletal myofiber formation and are not strictly stem cells. In any case, in the absence of Sca 1 selection, flow cytometry, and assessment of differentiation capacity, this cell fraction is undefined. As no evaluation of the impact on corporal SMC and fibrosis was performed, in contrast to the current and other reports with MDSC **[32,36,37,39]** it is not possible to draw a conclusion as to why the CVOD was ameliorated by the non-stem cell pP4 fraction.

The upregulation of corporal nNOS by MDSC is promising and may be derived from the neurogenic potential of these stem cells **[45]**, and may help to counteract the neuropraxia, and release NO that would also assist in overcoming the CVOD. The increase in BDNF, also by the MDSC, is a logical candidate for triggering some type of neural repair, since it is widely recognized as a key factor in this process and specifically in the corpora after cavernosal nerve damage **[50]**. The evaluation of how effective this process may be in the BCNR model, where the nerves are resected, would then require not just the measurement of erectile function by cavernosometry, but also by EFS, similarly to what is done in the much milder damage of the BCNC models. Contrary to our expectations a concurrent sildenafil administration at 1.25 mg/kg/day obliterated these beneficial effects, similarly to what we have reported for the low dose sildenafil/MDSC combination in the fibrotic process of myocardial infarction **[37]**. In the latter case PDE 5 was upregulated by the combination (but not by MDSC or sildenafil alone), either in the MDSC themselves or in the corporal tissue, probably resulting from a sildenafil effect on MDSC differentiation.

In summary, although both low and very low dose sildenafil, MDSC, and their combination ameliorate CVOD post-cavernosal nerve damage, more work is needed to define the optimal drug dose and cell input as well as their optimal proportion, that may require higher sildenafil doses to compensate for the PDE 5 upregulation that may not be dose-dependent, and thus saturate the enzyme activity to inhibit it. Also, with MDSC, as well as with the other stem cells main hurdles affecting stem cell therapy in ED need to be resolved in experimental

models, such as poor differentiation efficacy and uncontrolled lineage commitment, spontaneous senescence of the stem cells, deleterious environment of the corporal tissue affected by the neuropraxia, and the inefficient repair of cavernosal nerves. Although a clinical trial for post-RP ED has started in France **[51]** with bone marrow stem cells, it is advisable to go more in depth pre-clinically into the biology of stem cells within the paracrine hues of the corporal tissue, and the optimization of their pharmacological modulation.

ACKNOWLEDGEMENTS

This work was supported by DOD W81XWH-07-1-0181 and W81XWH-07-1-0129 grants, and partially by NIH R21DK-070003 grant, to NGC

REFERENCES

1. Mazzola C, Mulhall JP. Penile rehabilitation after prostate cancer treatment: outcomes and practical algorithm. Urol Clin North Am. 2011;38:105-18.

2. Magheli A, Burnett AL; Medscape. Erectile dysfunction following prostatectomy: prevention and treatment. Nat Rev Urol. 2009;6:415-27.

3. Tal R, Valenzuela R, Aviv N, Parker M, Waters WB, et al. Persistent erectile dysfunction following radical prostatectomy: the association between nerve-sparing status and the prevalence and chronology of venous leak. J Sex Med. 2009;6:2813-9.

4 Miller DC, Saigal CS, Litwin MS. The demographic burden of urologic diseases in America. Urol Clin North Am. 2009 Feb;36(1):11-27

5. Wilke DR, Krahn M, Tomlinson G, Bezjak A, Rutledge R, Warde P. Sex or survival: short-term versus long-term androgen deprivation in patients with locally advanced prostate cancer treated with radiotherapy. Cancer. 2010; 116:1909-17.

6. Giannakopoulos X, Charalabopoulos K, Charalabopoulos A, Golias C, Peschos D, Sofikitis N. Quality of life survey in patients with advanced prostate cancer. Exp Oncol. 2005; 27:13-7.

7. Hatzimouratidis K, Burnett AL, Hatzichristou D, McCullough AR, Montorsi F, Mulhall JP. Phosphodiesterase type 5 inhibitors in postprostatectomy erectile dysfunction: a critical analysis of the basic science rationale and clinical application. Eur Urol. 2009;55:334-47.

8. Mendenhall WM, Henderson RH, Indelicato DJ, Keole SR, Mendenhall NP. Erectile dysfunction after radiotherapy for prostate cancer. Am J Clin Oncol. 2009 Aug;32(4):443-7.

9. Kimura M, Yan H, Rabbani Z, Satoh T, Baba S, Yin FF, Polascik TJ, Donatucci CF, Vujaskovic Z, Koontz BF. Radiation-induced erectile dysfunction using prostate-confined modern radiotherapy in a rat model. J Sex Med. 2011 Aug;8(8):2215-26.

10. Nangle MR, Keast JR. Reduced efficacy of nitrergic neurotransmission exacerbates erectile dysfunction after penile nerve injury despite axonal regeneration. Exp Neurol. 2007 Sep;207(1):30-41.

11. Gonzalez-Cadavid NF. Mechanisms of penile fibrosis. J Sex Med. 2009; Suppl 3:353-62.

12. Rambhatla A, Kovanecz I, Ferrini M, Gonzalez-Cadavid NF, Rajfer J. Rationale for phosphodiesterase 5 inhibitor use post-radical prostatectomy: experimental and clinical review. Int J Impot Res. 2008; 20:30-4.

13. Ferrini MG, Kovanecz I, Sanchez S, Umeh C, Rajfer J, Gonzalez-Cadavid NF. Fibrosis and loss of smooth muscle in the corpora cavernosa precede corporal veno-occlusive dysfunction (CVOD) induced by experimental cavernosal nerve damage in the rat. J Sex Med. 2009;6:415-28.

14. Kendirci M, Trost L, Sikka SC, Hellstrom WJ. The effect of vascular risk factors on penile vascular status in men with erectile dysfunction. J Urol. 2007 Dec;178(6):2516-20

15. Kovanecz I, Rambhatla A, Ferrini M, Vernet D, Sanchez S, et al Long-term continuous sildenafil treatment ameliorates corporal veno-occlusive dysfunction (CVOD) induced by cavernosal nerve resection in rats. Int J Impot Res. 2008; 20:202-12.

16. Kovanecz I, Rambhatla A, Ferrini MG, Vernet D, Sanchez S, et al Chronic daily tadalafil prevents the corporal fibrosis and veno-occlusive dysfunction that occurs after cavernosal nerve resection. BJU Int, 2008;101:203-10.

17. Kim Y, de Miguel F, Usiene I, Kwon D, Yoshimura N, Huard J, Chancellor MB. Injection of skeletal muscle-derived cells into the penis improves erectile function. Int J Impot Res 2006; 18:329-34

18. Müller A, Tal R, Donohue JF, Akin-Olugbade Y, Kobylarz K, Paduch D, Cutter SC, Mehrara BJ, Scardino PT, Mulhall JP. The effect of hyperbaric oxygen therapy on erectile function recovery in a rat cavernous nerve injury model. J Sex Med. 2008 Mar;5(3):562-70.

19. Ferrini MG, Davila HH, Kovanecz I, Sanchez SP, Gonzalez-Cadavid NF, Rajfer J. Vardenafil prevents fibrosis and loss of corporal smooth muscle that occurs after bilateral cavernosal nerve resection in the rat. Urology. 2006 Aug;68(2):429-35.

20. Behr-Roussel D, Gorny D, Mevel K, Caisey S, Bernabé J, Burgess G, Wayman C, Alexandre L, Giuliano F. Chronic sildenafil improves erectile function and endothelium-dependent cavernosal relaxations in rats: lack of tachyphylaxis. Eur Urol. 2005 Jan;47(1):87-91

21. Ferrini MG, Kovanecz I, Sanchez S, Vernet D, Davila HH, Rajfer J, Gonzalez-Cadavid NF. Long-term continuous treatment with sildenafil ameliorates aging-related erectile dysfunction and the underlying corporal fibrosis in the rat. Biol Reprod. 2007 May;76(5):915-23.

22. Hatzimouratidis K, Burnett AL, Hatzichristou D, McCullough AR, Montorsi F, Mulhall JP. Phosphodiesterase type 5 inhibitors in postprostatectomy erectile dysfunction: a critical analysis of the basic science rationale and clinical application. Eur Urol. 2009 Feb;55(2):334-47.

23. Fusco F, Razzoli E, Imbimbo C, Rossi A, Verze P, Mirone V. A new era in the treatment of erectile dysfunction: chronic phosphodiesterase type 5 inhibition. BJU Int. 2010 Jun;105(12):1634-9.

24. Freireich EJ, Gehan EA, Rall DP, Schmidt LH, Skipper HE. Quantitative comparison of toxicity of anticancer agents in mouse, rat, hamster, dog, monkey, and man. *Cancer Chemother Rep* 1966, 50:219-244.

25. Valente EG, Vernet D, Ferrini MG, Qian A, Rajfer J, Gonzalez-Cadavid NF. L-arginine and phosphodiesterase (PDE) inhibitors counteract fibrosis in the Peyronie's fibrotic plaque and related fibroblast cultures. Nitric Oxide. 2003 Dec;9(4):229-44.

26. Huang YC, Ning H, Shindel AW, Fandel TM, Lin G, Harraz AM, Lue TF, Lin CS. The Effect of Intracavernous Injection of Adipose Tissue-Derived Stem Cells on Hyperlipidemia-Associated Erectile Dysfunction in a Rat Model. J Sex Med. 2010 Feb 5. [Epub ahead of print]

27. Song YS, Lee HJ, Park IH, Kim WK, Ku JH, Kim SU. Potential differentiation of human mesenchymal stem cell transplanted in rat corpus cavernosum toward endothelial or smooth muscle cells. Int J Impot Res. 2007 Jul-Aug;19(4):378-85.

28. Bivalacqua TJ, Deng W, Kendirci M, Usta MF, Robinson C, Taylor BK, Murthy SN, Champion HC, Hellstrom WJ, Kadowitz PJ. Mesenchymal stem cells alone or ex vivo gene modified with endothelial nitric oxide synthase reverse age-associated erectile dysfunction. Am J Physiol Heart Circ Physiol. 2007 Mar;292(3):H1278-90.

29. Qiu X, Sun C, Yu W, Lin H, Sun Z, Chen Y, Wang R, Dai Y. Combined Strategy of Mesenchymal Stem Cells Injection with VEGF Gene Therapy for the Treatment of Diabetes Associated Erectile Dysfunction. J Androl. 2011 Feb 10. [Epub ahead of print]

30. Qiu X, Lin H, Wang Y, Yu W, Chen Y, Wang R, Dai Y. Intracavernous transplantation of bone marrow-derived mesenchymal stem cells restores erectile function of streptozocin-induced diabetic rats. J Sex Med. 2011 Feb;8(2):427-36.

31. Deng W, Bivalacqua TJ, Champion HC, Hellstrom WJ, Murthy SN, Kadowitz PJ. Superoxide dismutase - a target for gene therapeutic approach to reduce oxidative stress in erectile dysfunction. Methods Mol Biol. 2010;610:213-27.

32. Nolazco G, Kovanecz I, Vernet D, Ferrini M, Gelfand B, et al Effect of muscle derived stem

cells on the restoration of corpora cavernosa smooth muscle and erectile function in the aged rat. BJU Int, 101:1156-64

33. Albersen M, Kendirci M, Van der Aa F, Hellstrom WJ, Lue TF, Spees JL. Multipotent stromal cell therapy for cavernous nerve injury-induced erectile dysfunction. J Sex Med. 2012 Feb;9(2):385-403.

34. Bochinski D, Lin GT, Nunes L, Carrion R, Rahman N, et al. The effect of neural embryonic stem cell therapy in a rat model of cavernosal nerve injury. BJU Int. 2004 Oct;94(6):904-9.

35. Woo JC, Bae WJ, Kim SJ, Kim SD, Sohn DW, Hong SH, Lee JY, Hwang TK, Sung YC, Kim SW. Transplantation of muscle-derived stem cells into the corpus cavernosum restores erectile function in a rat model of cavernous nerve injury. Korean J Urol. 2011 May;52(5):359-63.

36. Ho MH, Heydarkhan S, Vernet D, Kovanecz I, Ferrini MG, Bhatia NN, Gonzalez-Cadavid NF. Stimulating vaginal repair in rats through skeletal muscle-derived stem cells seeded on small intestinal submucosal scaffolds. Obstet Gynecol. 2009 Aug;114(2 Pt 1):300-9.

37. Wang J S-C, Kovanecz I, Vernet D, Nolazco G, Kopchok GE, Chow, SL, White RA, Gonzalez-Cadavid NF. Effects of sildenafil and/or muscle derived stem cells on myocardial infarction. J Transl Medic, preliminary acceptance

38. Oshima H, Payne TR, Urish KL, Sakai T, Ling Y, Gharaibeh B, Tobita K, Keller BB, Cummins JH, Huard J. Differential myocardial infarct repair with muscle stem cells compared to myoblasts. *Mol Ther* 2005, 12:1130-1141.

39. Payne TR, Oshima H, Okada M, Momoi N, Tobita K, Keller BB, Peng H, Huard J. A relationship between vascular endothelial growth factor, angiogenesis, and cardiac repair after muscle stem cell transplantation into ischemic hearts. *J Am Coll Cardiol* 2007, 50:1677-1684.

40. Okada M, Payne TR, Zheng B, Oshima H, Momoi N, Tobita K, Keller BB, Phillippi JA, Péault B, Huard J. Myogenic endothelial cells purified from human skeletal muscle improve cardiac function after transplantation into infarcted myocardium. *J Am Coll Cardiol* 2008, 52:1869-1880.

41. Gharaibeh B, Lu A, Tebbets J, Zheng B, Feduska J, Crisan M, Péault B, Cummins J, Huard J. Isolation of a slowly adhering cell fraction containing stem cells from murine skeletal muscle by the preplate technique. *Nat Protoc* 2008, 3:1501-1509.

42. Tsao J, Vernet D, Gelfand R, Kovanecz I, Nolazco G, Bruhn KW, Gonzalez-Cadavid NF Myostatin genetic inactivation inhibits myogenesis by muscle derived stem cells in vitro but not when implanted in the mdx mouse muscle. Stem Cells Res Ther, 2012, submitted

43. Keira SM; Ferreira LM; Gragnani A; Duarte IS, Barbosa J. Experimental model for collagen estimation in cell culture. Acta Cir. Bras. 2004; 19 suppl 1:17-22

44. Kovanecz I, Ferrini MG, Davila HH, Rajfer J, Gonzalez-Cadavid NF (2007) Ageing related corpora veno-occlusive dysfunction in the rat is ameliorated by pioglitazone. BJU Int. 2007 Oct;100(4):867-74.

45. Ii M, Nishimura H, Sekiguchi H, Kamei N, Yokoyama A, Horii M, Asahara T. Concurrent vasculogenesis and neurogenesis from adult neural stem cells. Circ Res. 2009 Oct 23;105(9):860-8.

46. Gómez-Pinedo U, Rodrigo R, Cauli O, Herraiz S, Garcia-Verdugo JM, Pellicer B, Pellicer A, Felipo V. cGMP modulates stem cells differentiation to neurons in brain in vivo. Neuroscience. 2010 Feb 17;165(4):1275-83.

47. Hemmrich K, Gummersbach C, Paul NE, Goy D, Suschek CV, Kröncke KD, Pallua N. Nitric oxide and downstream second messenger cGMP and cAMP enhance adipogenesis in primary human preadipocytes. Cytotherapy. 2010 Jul;12(4):547-53.

48. Mujoo K, Sharin VG, Bryan NS, Krumenacker JS, Sloan C, Parveen S, Nikonoff LE, Kots AY, Murad F. Role of nitric oxide signaling components in differentiation of embryonic stem cells into myocardial cells. Proc Natl Acad Sci U S A. 2008 Dec 2;105(48):18924-9.

49. Lu SH, Lin AT, Chen KK, Chiang HS, Chang LS. Characterization of smooth muscle differentiation of purified human skeletal muscle-derived cells. J Cell Mol Med. 2011 Mar;15(3):587-92.

50. Zhang HY, Jin XB, Lue TF. Three important components in the regeneration of the cavernous nerve: brain-derived neurotrophic factor, vascular endothelial growth factor and the JAK/STAT signaling pathway. Asian J Androl. 2011 Mar;13(2):231-5.

51. Clinical trial NCT01089387. Intracavernous Bone Marrow Stem-cell Injection for Post Prostatectomy Erectile Dysfunction. http://clinicaltrials.gov

52. Ferrini MG, Moon J, Rivera S, Rajfer J, Gonzalez-Cadavid NF. Amelioration of diabetes-induced fibrosis by antioxidant and anti-TGFβ1 therapies in the penile corpora cavernosa in the absence of iNOS expression. Br J Urol, 2011, in press

LEGENDS TO FIGURES

Fig. 1. Effects of sustained low and medium dose sildenafil on CVOD and the corporal SMC/collagen ratio after BCNR. Sildenafil was given continuously for 45 days in the drinking water, except as stated. Top: drop rate values during cavernosometry, as a measure of CVOD; Bottom: corporal SMC/collagen ratios as a measure of tissue fibrosis. UT: BCNR rats, untreated; LS: BCNR rats with low dose sildenafil, 2.5 mg/kg/day; MS: BCNR rats with medium dose sildenafil, 10 mg/kg/day LS(RL): as LS, but once a day, retrolingual. SH: sham animals are taken from another series of animals and used as reference, but not for the statistical comparisons. *: $p<0.05$; **: $p<0.01$; ***: $p<0.001$.

Fig. 2. Effects of sustained low and medium dose sildenafil on the corporal collagen content after BCNR. Sildenafil was given as in Fig. 1. Penile shaft collagen content estimated from penile shaft homogenates by a spectrophotometric picrosirius red elution method. UT: BCNR rats, untreated; LS: BCNR rats with low dose sildenafil, 2.5 mg/kg/day; MS: BCNR rats with medium dose sildenafil, 10 mg/kg/day LS(RL): as LS, but once a day, retrolingual. SH: sham animals are taken from another series of animals and used as reference, but not for the statistical comparisons. *: $p<0.05$; **: $p<0.01$; ***: $p<0.001$.

Fig. 3. Effects of sustained molsidomine and sildenafil combination on CVOD and the corporal SMC/collagen ratio after BCNR. Molsidomine was given daily IP and continuous sildenafil supplementation was done in the drinking water for 45 days. Top: drop rate values during cavernosometry, as a measure of CVOD; Bottom: corporal SMC/collagen ratios as a measure of tissue fibrosis; UT: BCNR rats, untreated; M: BCNR rats, molsidomine 10 mg/kg/day; M+LS: as M plus low dose sildenafil 2.5 mg/kg/day; M+MS: as M plus medium dose sildenafil 10 mg/kg/day. SH: sham animals are taken from another series of animals and used as reference, but not for the statistical comparisons. *: $p<0.05$; **: $p<0.01$; ***: $p<0.001$.

Fig. 4. Effects of MDSC implantation and sildenafil supplementation on CVOD and the corporal SMC/collagen ratio after BCNR. MDSC were implanted intracorporally and sildenafil supplementation was done continuously in the water for 45 days. Top: drop rate values during cavernosometry, as a measure of CVOD; Bottom: corporal SMC/collagen ratios as a measure of tissue fibrosis; UT: BCNR rats, untreated; VLS: BCNR rats, very low sildenafil, 1.25 mg/kg/day; SC: BCNR rats, stem cells (10^6) alone; SC+VLS: as SC plus very low sildenafil 1.25 mg/kg/day. SH: sham animals are taken from another series of animals and used as reference, but not for the statistical comparisons. *: $p<0.05$; **: $p<0.01$; ***: $p<0.001$.

Fig. 5. Effects of MDSC implantation and sildenafil supplementation on the corporal SMC and collagen contents after BCNR. MDSC and sildenafil were given as in Fig. 4. Top: corporal SMC content estimated by immunohistochemistry for ASMA; Bottom: penile shaft collagen content estimated by from penile shaft homogenates by a spectrophotometric picrosirius red elution method. UT: BCNR rats, untreated; VLS: BCNR rats, very low sildenafil, 1.25 mg/kg/day; SC: BCNR rats, stem cells (10^6) alone; SC+VLS: as SC plus very low sildenafil 1.25 mg/kg/day. SH: sham animals are taken from another series of animals and used as reference, but not for the statistical comparisons. *: $p<0.05$; **: $p<0.01$; ***: $p<0.001$.

Fig. 6. Effects of MDSC implantation and sildenafil supplementation on the contractile phenotype and apoptosis in the corporal SMC after BCNR. MDSC and sildenafil were given as in Figs. 4 and 5. Top A-C: Representative immunoblots for each group from n=8/group and for each antibody, with the respective GAPDH. UT: BCNR rats, untreated**;** LS: BCNR rats, very low sildenafil 1.25 mg/kg/day; SC: BCNR rats, stem cells (10^6) alone; SC+LS; as SC plus very low sildenafil 1.25 mg/kg/day; Bottom A-C: densitometric ratios of each antibody value corrected by GAPDH. .Each treatment group was run against the UT specimens, and then the statistical comparison of each group was performed separately against the UT. *: $p<0.05$; **: $p<0.01$; ***: $p<0.001$.

Fig. 7. Effects of intracorporal MDSC implantation and sildenafil supplementation on neural content in the corpora cavernosa after BCNR. MDSC and sildenafil were given as in Figs. 4 and 5. Top A-C: Representative immunoblots for each group from n=8/group and for each antibody, with the respective GAPDH. UT: BCNR rats, untreated**;** LS: BCNR rats, very low sildenafil 1.25 mg/kg/day; SC: BCNR rats, stem cells (10^6) alone; SC+LS; as SC plus very low sildenafil 1.25 mg/kg/day; Bottom A-C: densitometric ratios of each antibody value corrected by GAPDH. .Each treatment group was run against the UT specimens, and then the statistical comparison of each group was performed separately against the UT. *: $p<0.05$; **: $p<0.01$; ***: $p<0.001$.

Fig. 8. Immunofluorescent identification of nitrergic nerve generation stimulated by stem cell implantation. Fresh tissue sections were subjected to dual immunofluorescence and nuclei stained with DAPI. Pictures were taken at 200X at the dorsal nerve and corporal areas of the penile shaft. Left: DAPI staining (blue) and nNOS (red); right: merge of left panel with NF-70 (green). SC: BCNR rats, stem cells (10^6) alone; SC+VLS: as SC with VLS.

Figure 1

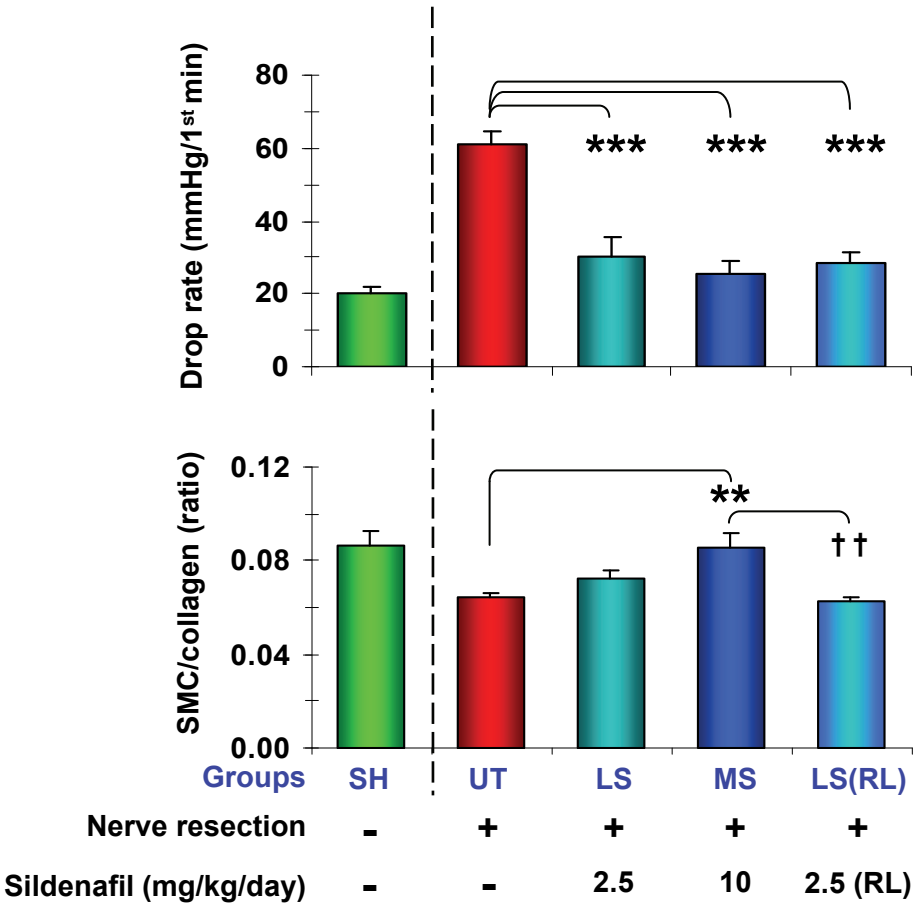
Drop rate (mmHg/1st min)
80
60
40
20
0
***
***
***
SMC/collagen (ratio)
0.12
0.08
0.04
0.00
**
††
Groups
SH
UT
LS
MS
LS(RL)
Nerve resection
-
+
+
+
+
Sildenafil (mg/kg/day)
-
-
2.5
10
2.5 (RL)

Figure 2

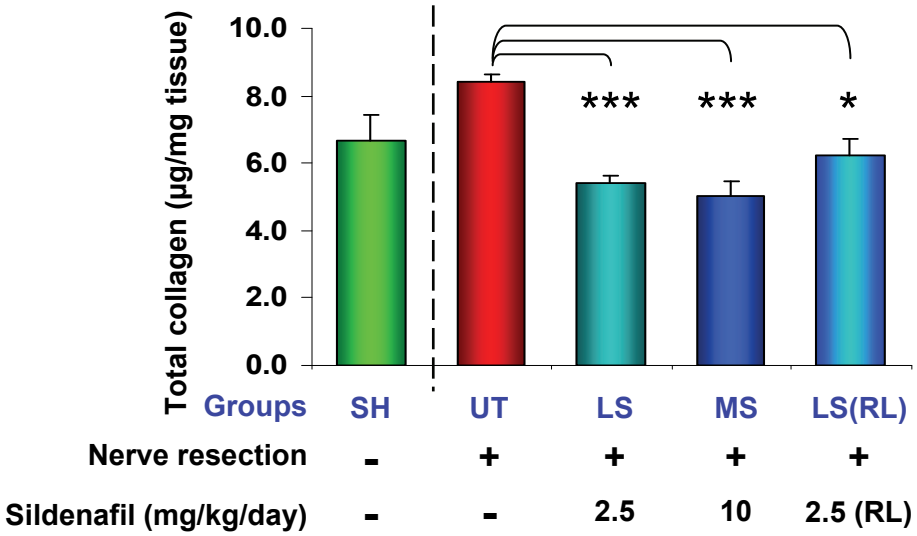
Total collagen (µg/mg tissue)
10.0
8.0
6.0
4.0
2.0
0.0
***
***
*
Groups
SH
UT
LS
MS
LS(RL)
Nerve resection
-
+
+
+
+
Sildenafil (mg/kg/day)
-
-
2.5
10
2.5 (RL)

Figure 3

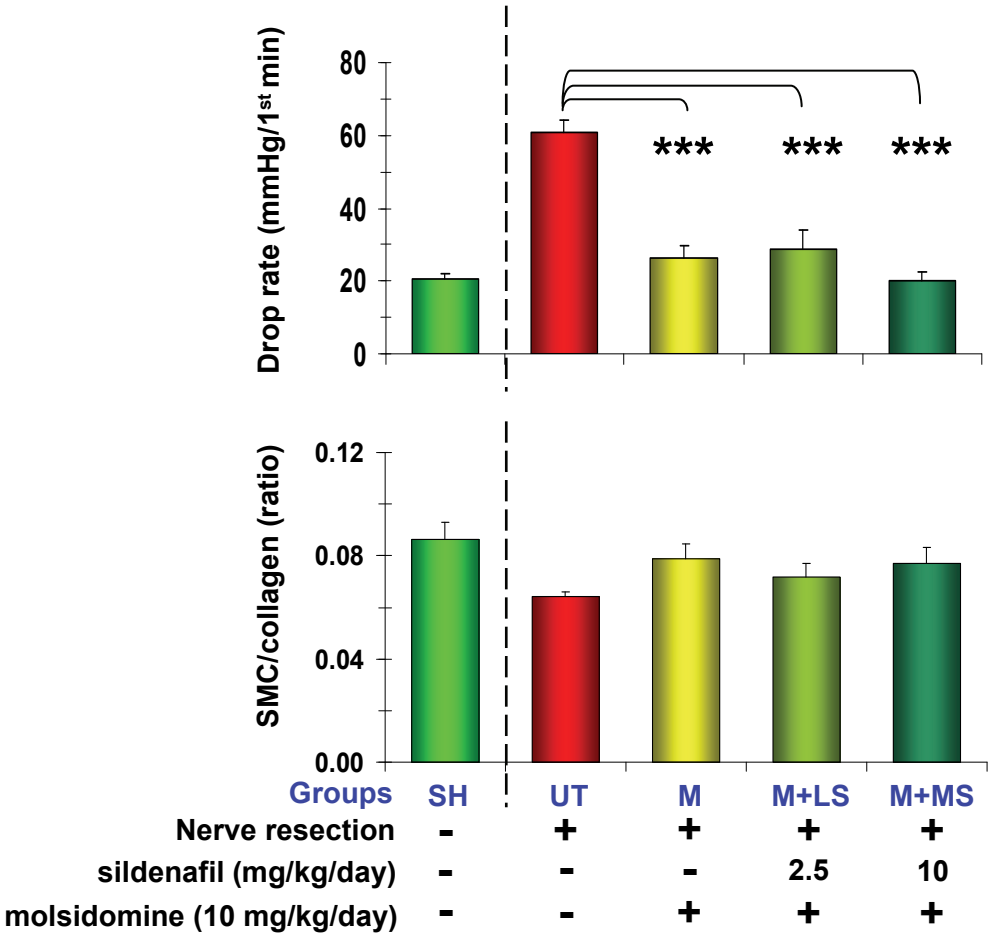
Drop rate (mmHg/1st min)
80
60
40
20
0
***
***
***
SMC/collagen (ratio)
0.12
0.08
0.04
0.00
Groups SH UT M M+LS M+MS
Nerve resection - + + + +
sildenafil (mg/kg/day) - - - 2.5 10
molsidomine (10 mg/kg/day) - - + + +

Figure 4

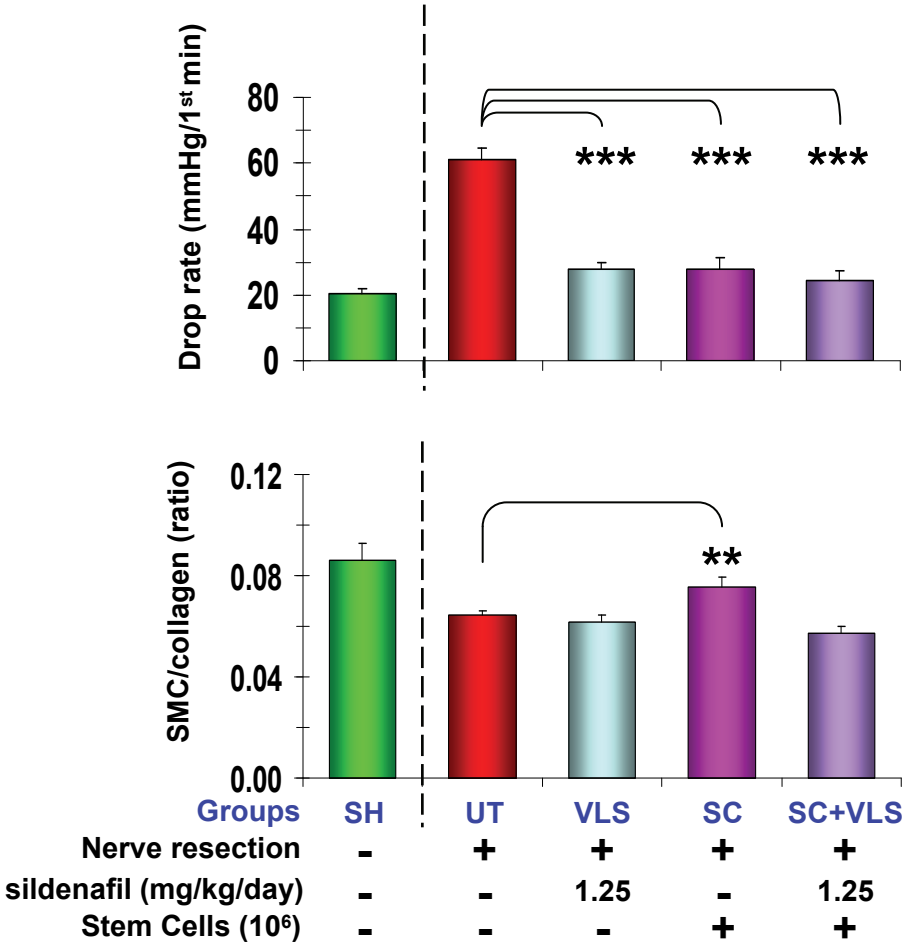
Drop rate (mmHg/1st min)
80
60
40
20
0
***
***
***
SMC/collagen (ratio)
0.12
0.08
0.04
0.00
**
Groups
SH
UT
VLS
SC
SC+VLS
Nerve resection
- + + + +
sildenafil (mg/kg/day)
- - 1.25 - 1.25
Stem Cells (10⁶)
- - - + +

Figure 5

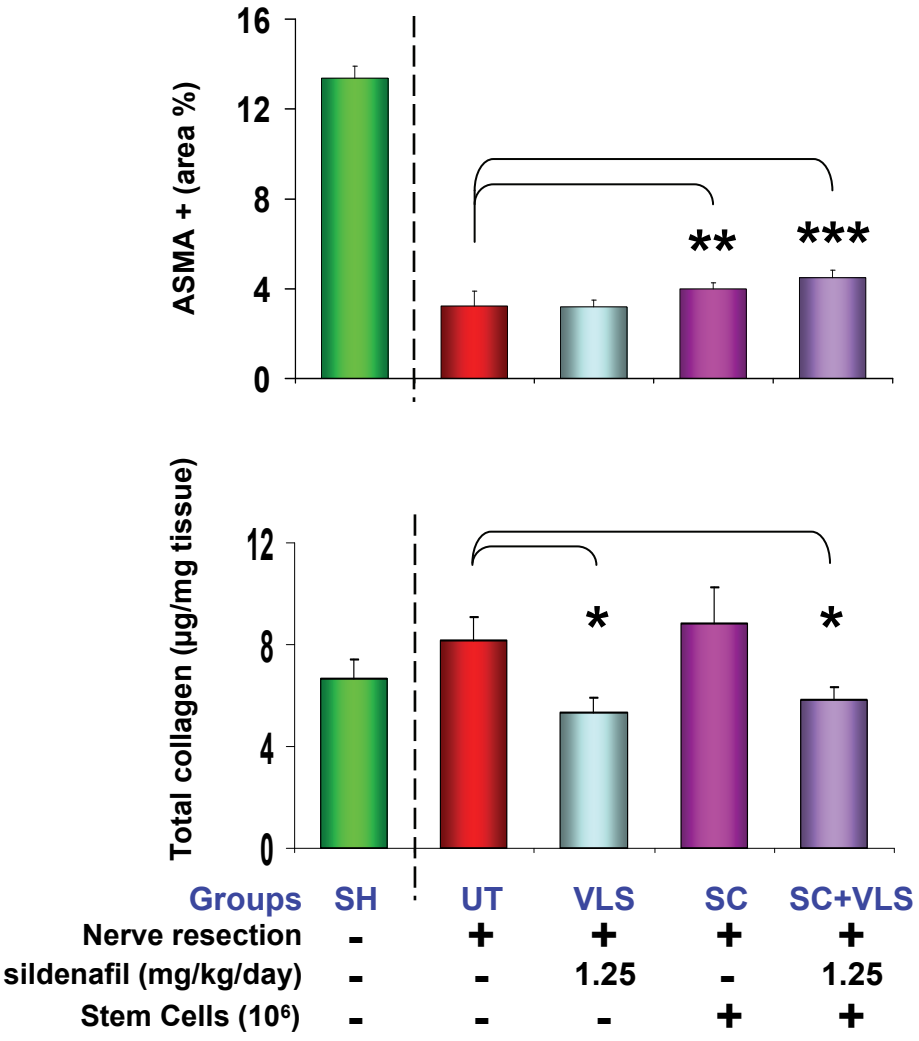
ASMA + (area %)
16
12
8
4
0
**
***
Total collagen (µg/mg tissue)
12
8
4
0
*
*
Groups SH UT VLS SC SC+VLS
Nerve resection - + + + +
sildenafil (mg/kg/day) - - 1.25 - 1.25
Stem Cells (10⁶) - - - + +

Figure 6

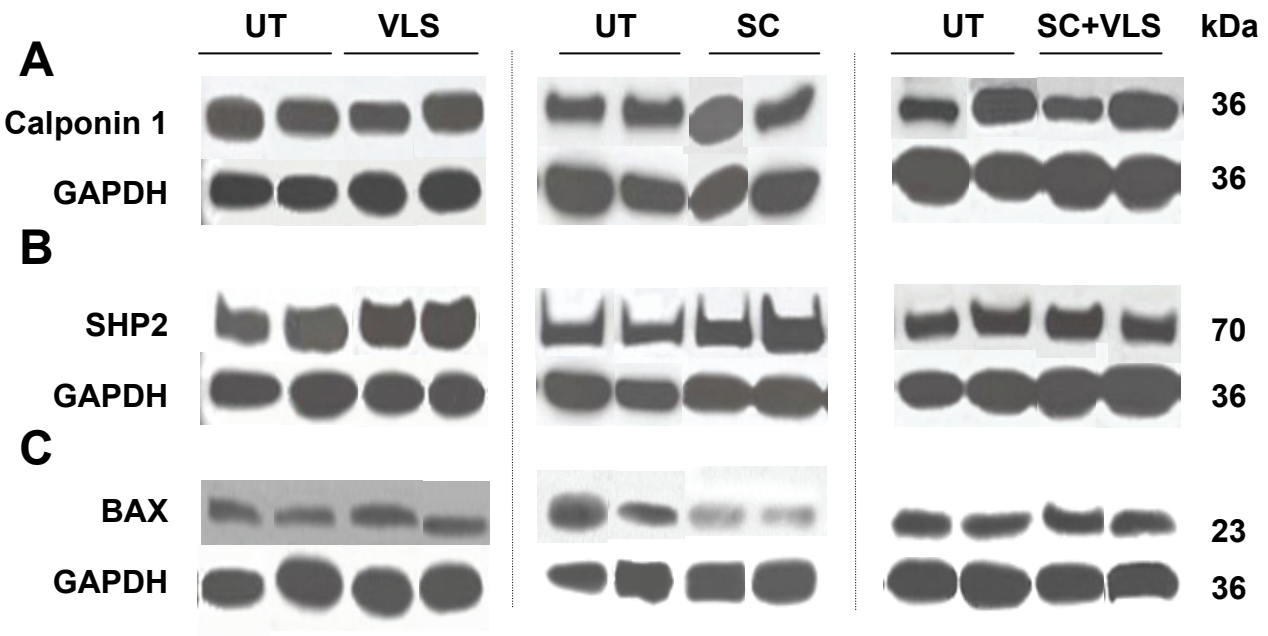
UT
VLS
UT
SC
UT
SC+VLS
kDa
A
Calponin 1
GAPDH
36
36
B
SHP2
GAPDH
70
36
C
BAX
GAPDH
23
36

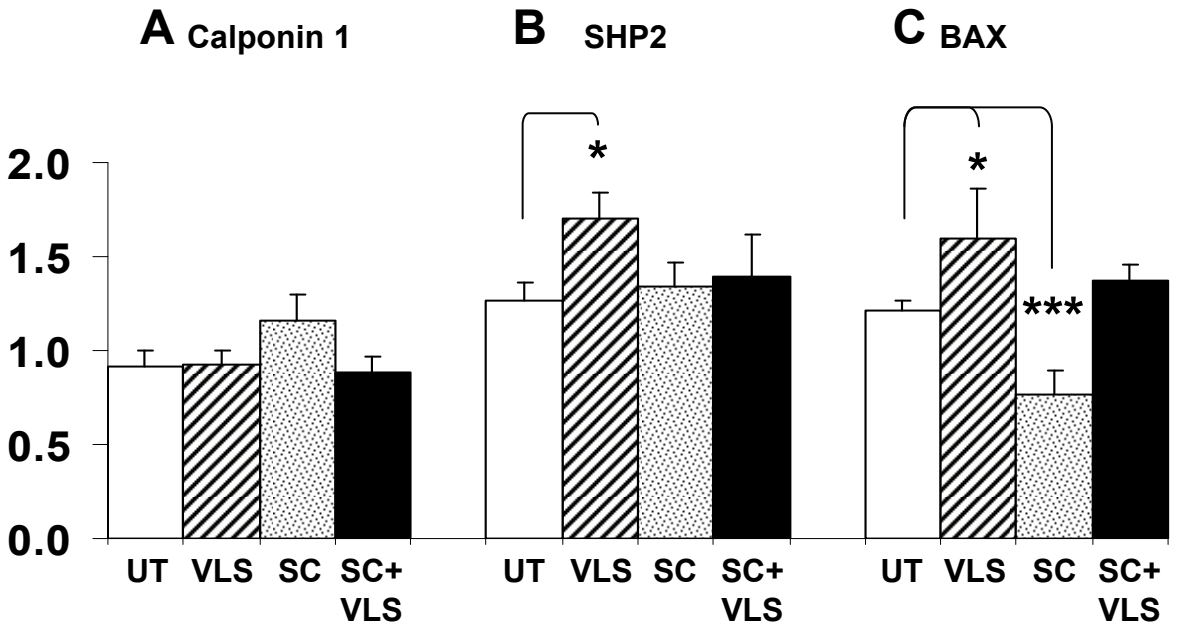
A Calponin 1
B SHP2
C BAX
2.0
1.5
1.0
0.5
0.0
*
*
***
UT
VLS
SC
SC+ VLS
UT
VLS
SC
SC+ VLS
UT
VLS
SC
SC+ VLS

Figure 7

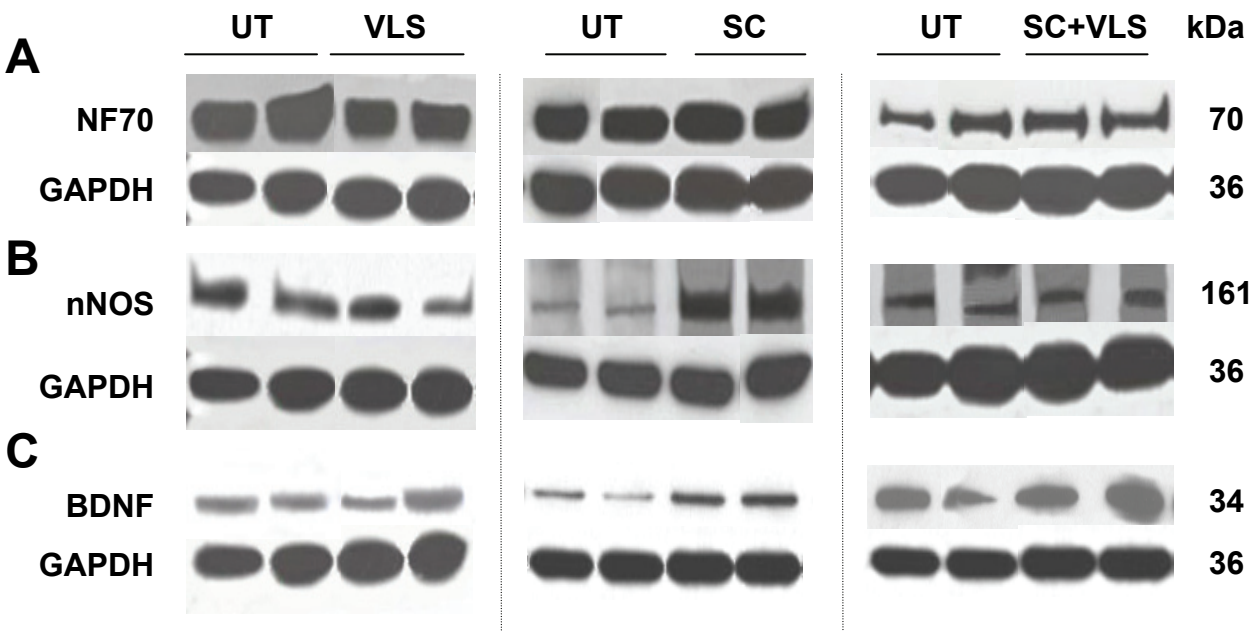
A
B
C
UT
VLS
UT
SC
UT
SC+VLS
kDa
NF70
GAPDH
nNOS
GAPDH
BDNF
GAPDH
70
36
161
36
34
36

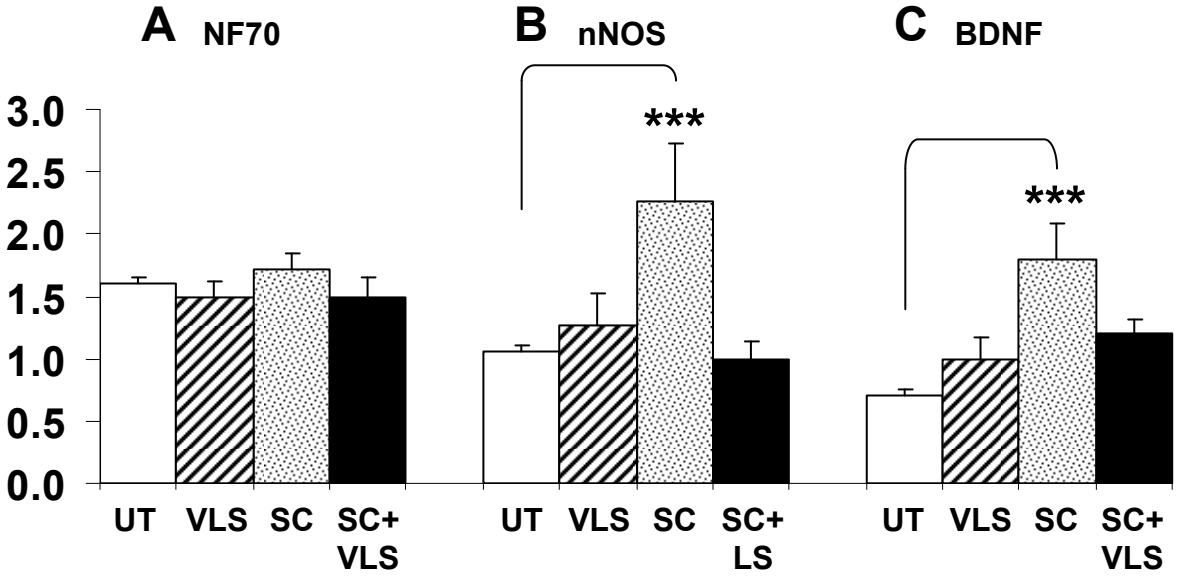
A NF70
B nNOS
C BDNF
3.0
2.5
2.0
1.5
1.0
0.5
0.0
***
***
UT
VLS
SC
SC+ VLS
UT
VLS
SC
SC+ LS
UT
VLS
SC
SC+ VLS

Figure 8

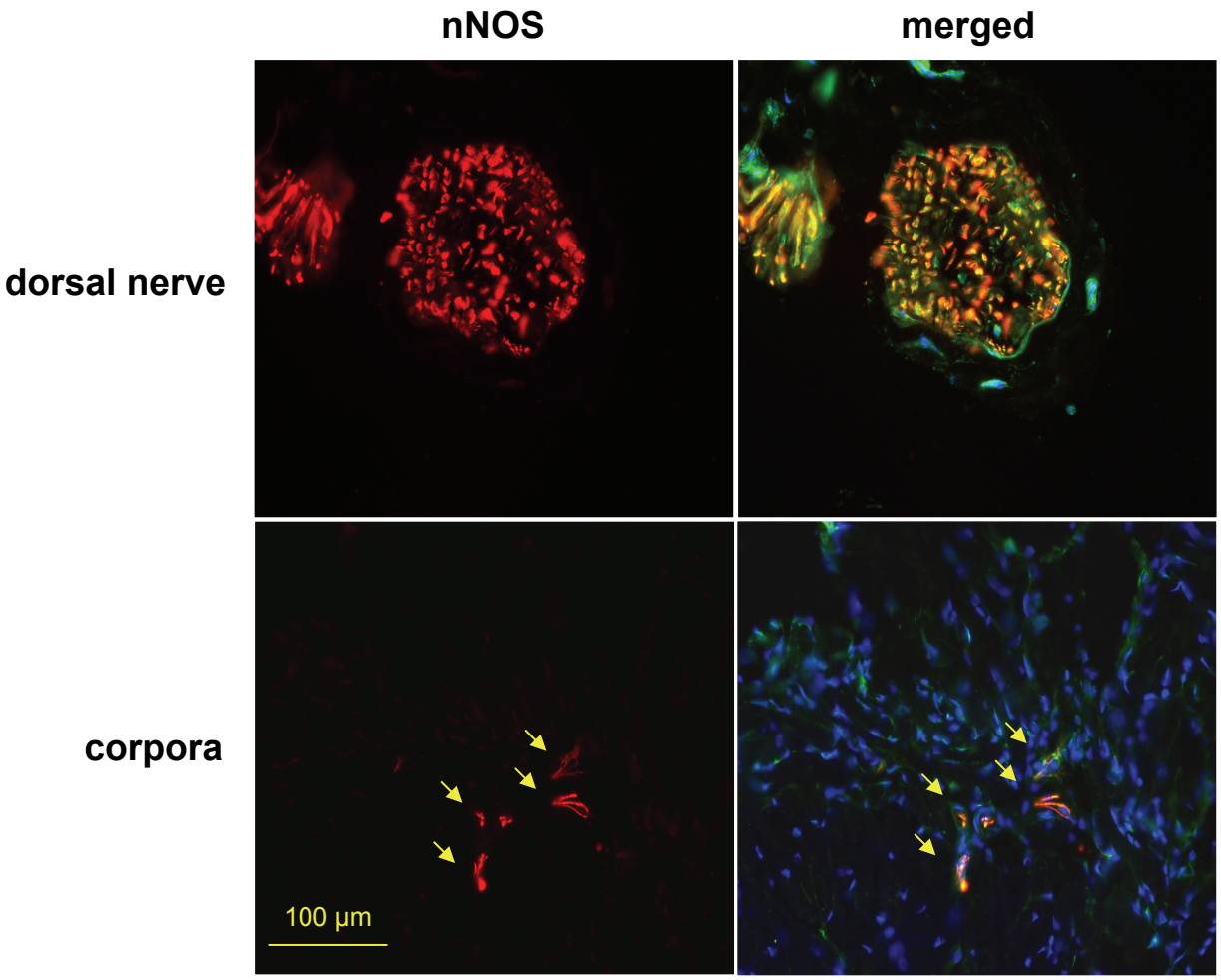

Table 1. Comparative summary of effects of sildenafil and molsidomine on ED and the underlying histopathology in BCNR rats.

		sildenafil			molsidomine		
Effects on	**Endpoint**	**LS**	**MS**	**LS(RL)**	**M**	**M+LS**	**M+MS**
Function	**Drop rate**	↓↓↓	↓↓↓	↓↓↓	↓↓↓	↓↓↓	↓↓↓
Corporal	**SMC/collagen**	-	↑	-	↑	-	-
Shaft	**collagen**	↓↓↓	↓↓↓	↓	ND	ND	ND

↑: increase; ↓ : decrease; -: no change; ND: not determined The number of arrows reflects the significance levels (p) for the bar graph values on Figures 1-8.

LS: low sildenafil; MS:medium sildenafil; LS(RL): low sildenafil retrolingual; M: molsidomine

Table 2. Comparative summary of effects of sildenafil and MDSC on ED and the underlying histopathology in BCNR rats.

Effects on	Endpoint	VLS	SC	SC+VLS
Function	Drop rate	↓↓↓	↓↓↓	↓↓↓
Corporal	SMC/collagen	-	↑	-
	ASMA	-	↑	↑
Shaft	collagen	↓	-	↓
	Calponin 1	-	↑NS	-
	SHP-2	↑	-	-
	BAX	↑	↓↓↓	-
	NF 70	-	-	-
	nNOS	-	↑↑↑	-
	BDNF	-	↑↑↑	-

↑: increase; ↓ : decrease; -: no change; NS: not significant. The number of arrows reflects the significance levels (p) for the bar graph values on Figures 1-8.

VLS: very low sildenafil; SC:MDSC